Department of Veterinary Biosciences, Faculty of Veterinary Medicine
Department of Medical and Clinical Genetics, Faculty of Medicine
University of Helsinki
Folkhälsan Research Center

Genetics of three canine eye disorders

Maria Kaukonen

Dissertatines Scholae Doctoralis Ad Sanitatem Investigandam
Universitatis Helsinkiensis

Integrative Life Sciences Doctoral Program

Academic Dissertation
To be presented, with the permission of the Faculty of Veterinary Medicine of the University of Helsinki, for public examination in lecture room Suomen Laki, Porthania, Yliopistonkatu 3,
on December 5th, 2019, at 12 noon.

Helsinki 2019

Supervisor

Professor Hannes Lohi
University of Helsinki, Finland
The Folkhälsan Research Center, Finland

Reviewers

Professor Danika Bannasch
University of California, Davis, USA

Adjunct Professor Soile Nymark
Tampere University, Finland

Opponent

Professor Alison Hardcastle
University College London, UK

Cover image: Tiina Salmivuori

ISSN 2342-3161 (print)
ISSN 2342-317X (online)

ISBN 978-951-51-5595-5 (paperback)
ISBN 978-951-51-5596-2 (PDF)
http://ethesis.helsinki.fi

Unigrafia
Helsinki 2019

The Faculty of Veterinary Medicine uses the Urkund system (plagiarism recognition) to examine all doctoral dissertations.

Abstract

The genetic background of three canine hereditary eye diseases, namely microphthalmia, open-angle glaucoma and progressive retinal atrophy, were addressed in this thesis. Currently, no standardized curative treatment options are available for these diseases. Gene defects behind each of them were identified using modern genome-wide approaches followed by functional validations.

In study I, the genetic analyses revealed that a 3-bp deletion in the *RBP4* gene is associated with microphthalmia in Irish Soft-Coated Wheaten Terriers. Simultaneously, a new mode of maternal inheritance was discovered as the disease manifests only if both the dam and the offspring were homozygous for the variant. During gestation, RBP4 transfers vitamin A from maternal liver stores to the developing puppy. The defective protein is not secreted into serum, causing vitamin A deficiency, a known risk factor for microphthalmia.

In study II, a recessive missense variant in *ADAMTS10* was associated with open-angle glaucoma in Norwegian Elkhounds. The disease was found to be bilateral, unresponsive to medical treatment and led to irreversible blindness by the age of six years.

In study III, a recessive variant in a putative silencer region fully segregated with progressive retinal atrophy in Miniature Schnauzers. The breed was also found to suffer from another genetic form of the disease, for which a tentative locus was identified.

The results of this study have led to novel scientific insights and practical applications and have translational implication to human medicine with similar conditions and gene associations. Three gene tests have been developed to aid veterinary diagnostics and breeding programs. The new mode of maternal inheritance discovered in study I could be a more common phenomenon in developmental disorders across species and should be taken into consideration in all genetic studies.

Tiivistelmä

Tässä väitöstutkimuksessa selvitettiin kolmen perinnöllisen, koirilla spontaanisti ilmenevän silmäsairauden geneettisiä aiheuttajia. Sairauksien taustalla vaikuttavat geenivirheet tunnistettiin hyödyntämällä perimän laajuisia tutkimusmenetelmiä ja erilaisia toiminnallisia kokeita.

Ensimmäisessä osatyössä paikannettiin vehnäterriereillä ilmenevän silmän alikehittyneisyyden eli mikroftalmian todennäköiseksi syyksi virhe *RBP4*-geenissä. Samalla löytyi uudenlainen äidistä riippuvainen periytymistapa, sillä sairaus ilmeni vain, jos sekä emä että pentu olivat geenivirheen suhteen samaperintäisiä. RBP4 kuljettaa tiineyden aikana A-vitamiinia emältä pennulle, mutta geenivirheen vuoksi proteiinia ei pystytä tuottamaan ja pentu kärsii A-vitamiinin puutteesta. A-vitamiini on tärkeä useiden elinten normaalille kehittymiselle, ja silmä on sen puutokselle herkin.

Toisessa osatyössä tutkittiin harmailla norjanhirvikoirilla ilmenevää avokulmaglaukoomaa. Taudin edetessä silmänsisäinen paine kohoaa ja koirat sokeutuvat pysyvästi noin kuusivuotiaina. Geneettiset analyysit paikansivat sairautta aiheuttavan geenivirheen *ADAMTS10*-geeniin, joka on aiemmin liitetty beagleilla tavattuun avokulmaglaukoomaan.

Kolmannessa osatyössä tutkittiin kääpiösnautsereilla ilmenevää etenevää verkkokalvorappeumaa. Nuorilla aikuisilla sokeuteen johtavan muodon todennäköiseksi aiheuttajaksi paljastui säätelyalueella sijaitseva geenivirhe. Rodussa ilmenee toistakin muotoa taudista, jonka aiheuttaja paikantui alustavasti X-kromosomiin.

Väitöstyön tuloksena on voitu kehittää tutkituille sairauksille geenitestit jalostuksen ja diagnostiikan tueksi. Tuloksia voidaan hyödyntää myös lääketieteessä, sillä samat sairaudet ilmenevät ihmisilläkin. *ADAMTS10*- ja *RPB4*-geenit on liitetty aiemmin vastaaviin ihmissairauksiin, mutta verkkokalvorappeumaan liittyvä lokus on uusi ja sen roolia tulisi selvittää myös ihmispotilailla. Ensimmäisessä osatyössä löydetty uudenlainen periytymistapa on todennäköisesti luultua yleisempi muillakin lajeilla kehityksellisissä sairauksissa, ja tulee ottaa huomioon tulevaisuudessa kaikessa genetiikan tutkimuksessa.

Table of contents

Abstract 3
Tiivistelmä 4
Table of contents 5
List of original publications 8
Author's contribution 9
Abbreviations 10
1 Review of the literature 11
1.1 Canine genetics 11
1.1.1 Unique genome architecture facilitates gene mappings 11
1.1.2 Development of genomic tools and resources 13
1.2 Healthy canine eye 16
1.2.1 Anatomy of the canine eye 16
1.2.2 Development of the ocular globe 22
1.2.3 Vision 23
1.3 Canine hereditary eye diseases 26
1.3.1 Microphthalmia 26
1.3.2 Glaucoma 30
1.3.3 Progressive retinal atrophy 34
2 Study aims and hypothesis 42
3 Materials and methods 43
3.1 Ethical statement 43
3.2 Study cohorts 43
3.2.1 Recruitment, pedigrees and sampling 43
3.2.2 Clinical phenotyping 44
3.3 Genetic analyses 45
3.3.1 Genome-wide association studies 45
3.3.2 Identification and validation of candidate variants 46
3.4 Functional experiments 49
3.4.1 Serum biochemistry 49
3.4.2 Western blotting 50
3.4.3 Nuclear magnetic resonance 52
3.4.4 Dual luciferase reporter assay 53
3.4.5 RT-qPCR 54
4 Results 55

4.1 Single-residue deletion in RBP4 with unique maternal transmission causes congenital eye disease in Irish Soft-Coated Wheaten Terriers 55
4.1.1 Bilateral microphthalmia and other ocular findings in four closely-related litters of ISCWTs 55
4.1.2 Microphthalmia locus maps to canine chromosome 28 56
4.1.3 Whole-genome sequencing reveals an in-frame deletion in *RBP4* 56
4.1.4 Segregation analysis indicates unique maternal inheritance effect 57
4.1.5 Dose-dependent decrease in circulating RBP4 and vitamin A *in vivo* 59
4.1.6 K12del RBP4 circulates as a homodimer *in vivo* 60
4.1.7 K12del RBP4 forms dimers and is poorly secreted from cultured HeLa cells 61
4.1.8 K12del protein forms monomers and binds vitamin A *in vitro* 61
4.2 A novel missense mutation in *ADAMTS10* is associated with primary open-angle glaucoma in Norwegian Elkhounds 62
4.2.1 Eye examinations reveal severe POAG in NEs 62
4.2.2 GWAS maps the disease to a known canine POAG locus 63
4.2.3 Candidate gene approach reveals a fully-penetrant missense variant in *ADAMTS10* 63
4.3 Two new loci and a putative regulatory variant in Miniature Schnauzers affected with progressive retinal atrophy 64
4.3.1 Clinical examinations suggest multiple different types of PRA in MSs 64
4.3.2 GWAS confirms that MSs are affected with at least two genetically distinct types of PRA 65
4.3.3 Whole-genome sequencing approach indicates a recent origin for type 1 PRA –specific variant 67
4.3.4 Type 1 PRA-associated variant lies within a putative silencer with HAND1::TCF3 transcription factor binding motif 69

4.3.5 Two predicted HAND1::TCF3 target genes, *COL9A2* and *EDN2*, are overexpressed in the case retina.....70
5 Discussion.....71
5.1 New mode of maternal inheritance and a novel candidate gene in canine congenital eye disease.....71
5.2 A novel missense variant in *ADAMTS10* is associated with canine primary open-angle glaucoma.....73
5.3 Multiple genetically distinctive types of PRA affect Miniature Schnauzers – a putative silencer variant associated with type 1 disease.....76
6 Conclusions and future prospects.....80
Acknowledgments.....82
References.....83

List of original publications

This thesis is based on the following publications:

I **Kaukonen M,** Woods S, Ahonen S, Lemberg S, Hellman M, Hytönen MK, Permi P, Glaser T, Lohi H. Maternal Inheritance of a Recessive RBP4 Defect in Canine Congenital Eye Disease. *Cell Reports*. 2018 May 29;23(9):2643–2652.

II Ahonen SJ, **Kaukonen M,** Nussdorfer FD, Harman CD, Komáromy AM, Lohi H. A Novel Missense Mutation in *ADAMTS10* in Norwegian Elkhound Primary Glaucoma. *PLoS One*. 2014 Nov 5;9(11):e111941.

III **Kaukonen M,** Quintero IB, Mukarram AK, Marjo K. Hytönen, Saila Holopainen, Wickström K, Kyöstilä K, Arumilli M, Jalomäki S, Daub CO, Kere J, DoGA consortium, Lohi H. A putative regulatory variant in a spontaneous canine model of retinitis pigmentosa. *PLoS Genetics*. 2019, in revision.

The publications are referred to in the text by their Roman numerals.

Author's contribution

Author's contribution to each publication:

I **Maternal Inheritance of a Recessive RBP4 Defect in Canine Congenital Eye Disease.**
Apart from the Western blotting and NMR experiments (whose planning and sample collection the author participated in), the author designed and performed the experiments, analyzed the data and wrote the paper under the supervision of Professor Lohi.

II **A Novel Missense Mutation in *ADAMTS10* in Norwegian Elkhound Primary Glaucoma.**
The author designed and conducted the experiments together with PhD Ahonen under the supervision of Professor Lohi: PhD Ahonen and the author conducted sample selection and phenotype grouping based on clinical examinations. PhD Ahonen conducted pedigree analysis and genome-wide association study. The author planned primers for candidate gene sequencing, planned and tested the PCR assay, conducted segregation analysis in the initial and breed screening cohorts (including 596 dogs altogether) and analyzed variant pathogenicity *in silico*. The author participated in writing the article, while the main responsibility belonged to PhD Ahonen.

III **A putative regulatory variant in a spontaneous canine model of retinitis pigmentosa.**
Apart from the silencer *in silico* analyses, the STRT experiment and luciferase assay (for which the author participated in planning, collecting samples and analyzing data), the author designed and performed the experiments, analyzed the data and wrote the paper under the supervision of Professor Lohi.

Abbreviations

ADAMTS	A disintegrin and metalloproteinase domain with thrombospondin type-1 motifs) family
ADAMTS -10	ADAM metallopeptidase with thrombospondin type 1 motif 10
bHLH	Basic helix-loop-helix
CEA	Collie eye anomaly
CFA	Canine chromosome
GWAS	Genome-wide association study
ECM	Extracellular matrix
ER	Endoplasmic reticulum
ERG	Electroretinogram
HAND1	Heart and neural crest derivatives expressed 1
HIVEP3	Human immunodeficiency virus type I enhancer binding protein 3
ICA	Iridocorneal angle
IOP	Intra-ocular pressure
ISCWT	Irish Soft-Coated Wheaten Terrier
MAC	Microphthalmia, anophthalmia and coloboma
MS	Miniature Schnauzer
NE	Norwegian Elkhound
NMR	Nuclear magnetic resonance
OCT	Optical coherence tomography
PCAG	Primary closed-angle glaucoma
PCG	Primary congenital glaucoma
PLA	Pectinate ligament abnormality
POAG	Primary open-angle glaucoma
PRA	Progressive retinal atrophy
RBP4	Retinol binding protein 4
RP	Retinitis pigmentosa
RPE	Retinal pigment epithelium
RT-qPCR	Real-time quantitative PCR
SNP	Single nucleotide polymorphism
TCF3	Transcription factor 3
TFBS	Transcription factor binding site
WES	Whole-exome sequencing
WGS	Whole-genome sequencing

1 Review of the literature

1.1 Canine genetics

1.1.1 Unique genome architecture facilitates gene mappings

Two genetic bottlenecks, an old one and a recent one, have made the domestic dog (*Canis lupus familiaris*) genetically unique (Figure 1A). Around 15,000–100,000 years (Vila et al., 1997, Savolainen et al., 2002) (7,000–50,000 generations (Lindblad-Toh et al., 2005)) ago, the dog was domesticated from the grey wolf (*Canis lupus lupus*). Attempts to localize the origin of domestication have produced controversial results (Vila et al., 1997, Sablin, Khlopachev, 2002, Germonpré et al., 2009, Thalmann et al., 2013, Frantz et al., 2016), possibly reflecting the available sample material in the studies or the actual fact that there have been several domestication events in different geographical locations. During domestication, only a fraction of genetic diversity present in wolves remained in dogs. Another more recent, bottleneck occurred, when the modern dog breeds were created some hundred years (around 50–100 generations (Lindblad-Toh et al., 2005)) ago by allowing only dogs with desired morphological or behavioral traits to mate. This kind of aggressive artificial selection often included inbreeding and the use of popular sires (Calboli et al., 2008), which fixated the desired traits to the breeds but also led to decreased genetic diversity, later demonstrated by genetic analyses. Currently, the Federation Cynologique Internationale recognizes 349 dog breeds, each of which forms its own genetic isolate as pure-bred dogs are allowed to be bred only with same-breed individuals according to breed-barrier rules.

The normal dog karyotype has 38 pairs of acrocentric autosomes and two metacentric sex chromosomes. The first draft version of the dog genome was published in 2003, when the genome of a male standard poodle was sequenced (Kirkness et al., 2003). In 2005, a female boxer was sequenced to produce the CanFam 1.0 and 2.0 annotations and to report the haplotype structure in several dog breeds (Lindblad-Toh et al., 2005). Within-breeds and between-breeds comparisons indicated that, as suspected from the evolutionary history of pure-bred dogs, there is less genetic diversity between individual dogs from the same breed than between individuals from different breeds (Lindblad-Toh et al., 2005). Approximately 1 per 1,600 bp was polymorphic within any of

the studied 10 breeds, whereas between breeds, the number was almost double (Lindblad-Toh et al., 2005). The similarity of the breeds is interesting, as individual breeds also have specific additional

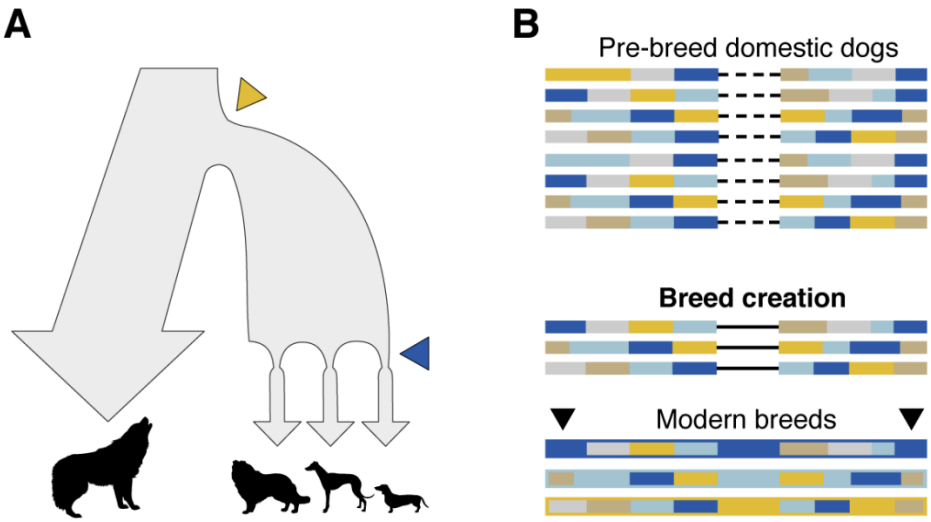

Figure 1 *The dog has a unique genomic architecture resulting from its evolutionary history. [A] During domestication from the grey wolf, only a fraction of the genetic diversity present in the grey wolf remained in the domestic dog, accounting for an old bottleneck (yellow arrow). The creation of modern breeds some hundred years ago represents another recent bottleneck (blue arrow), as aggressive selection was done to establish the breeds with desired morphological or behavioral traits. [B] The two bottlenecks have resulted in a specific haplotype structure in dogs, where long-range LD is observed within breeds and short-range LD across breeds. Different colors represent distinct haplotypes. Image source (wolf and dog shapes): www.Pixabay.com.*

bottlenecks (e.g., due to catastrophes such as the World Wars) and very different population sizes, but their importance seems minor in comparison to the two common bottlenecks (Lindblad-Toh et al., 2005).

Because of the evolutionary history, dogs have a specific haplotype structure. Long-range linkage disequilibrium (LD) regions extending over multiple megabases are seen within dog breeds (Lindblad-Toh et al., 2005, Sutter et al., 2004) (Figure 1B), resembling observations from inbred mouse strains (Mouse Genome Sequencing Consortium et al., 2002, Kirby et al.,

2010). In contrast, across breeds, short-range LD of tens of kilobases is observed (Figure 1B), mimicking more of the human ancestral haplotypes (Lander et al., 2001, Gabriel et al., 2002, International HapMap Consortium, 2003).

As a result of the genetic characteristics, gene mapping is facilitated in dogs for several reasons. These include the observed long-range LD within breeds, which enables the mapping of trait-associated chromosomal regions using genotyping arrays with remarkably lower marker densities than those required in human studies (Karlsson et al., 2007). Short-range LD across breeds, on the other hand, offers possibilities to narrow down the associated locus efficiently (Lindblad-Toh et al., 2005). In addition, smaller sample sizes are needed for genetic discoveries in Mendelian trait mapping with successful examples reported using samples from only 10 cases and 10 controls (Karlsson et al., 2007).

1.1.2 Development of genomic tools and resources

The unique genome architecture of the domestic dog has made it an important research subject, not only to promote canine health but also to understand major biological concepts such as mechanisms of evolution in general. During the past 10 years, variants in more than 250 canid genes have been identified for Mendelian and complex traits (www.OMIA.org, www.MyBreedData.com). The discovery rate is expected to remain high, as different available resources, together with the unique genome structure, facilitate gene mapping in dogs.

When the CanFam 1.0 and 2.0 annotations for the dog reference sequence were published in 2005 (Lindblad-Toh et al., 2005), comparative genomics with previously sequenced human (Lander et al., 2001), mouse (Mouse Genome Sequencing Consortium et al., 2002) and rat (Gibbs et al., 2004) genomes showed that these four species had a sequence similarity of around 94%. The dog genome is 2.41 Gb in size (Lindblad-Toh et al., 2005) with 20,039 protein-coding genes annotated in the current genome version, the CanFam 3.1 (Hoeppner et al., 2014).

Over the years, several chip arrays with a varying number of single nucleotide polymorphisms (SNPs) have become commercially available, enabling linkage analyses, genome-wide association studies (GWAS) and other methods to map disease and trait-associated loci (van Steenbeek et al., 2016). In 2005, based on the initial haplotype analysis in different dog breeds,

10,000 SNPs in an array was proposed to be sufficient for most mapping purposes (Lindblad-Toh et al., 2005), meaning a required sample number for discoveries is substantially smaller in dogs compared to humans (Karlsson et al., 2007). In the past few years, the CanineHD Whole-Genome Genotyping BeadChip (Illumina, San Diego, CA, USA), with over 170,000 markers, has become the most-used SNP array in canine genetics. This chip was developed in collaboration with the LUPA Consortium, a European–North-American collaborative effort to enhance canine genetics (Lequarré et al., 2011). Recently, the new Axiom Canine Genotyping Array Sets A and B (Applied Biosystems, Waltham, MA, USA), with approximately 1.1 million markers, was released and might replace the CanineHD Whole-Genome Genotyping BeadChip in the near future if proven cost-efficient.

In 2014, the first design of a canine whole-exome sequencing (WES) enrichment assay was published (Broeckx et al., 2014), moving canine genetics into the era of next-generation sequencing. This assembly was already made based on the CanFam 3.1 annotation, although only around 85% of the target regions were covered (Broeckx et al., 2014). In the following year, the Exome-Plus assembly (152 Mb) was released, now also including different non-coding RNA regions such as microRNA, long non-coding RNA and antisense transcripts (Broeckx et al., 2015). As successful variant detection in WES depends completely on the variant being located in the coding region, and as understanding of the importance of the regulatory regions has increased, WES has become less used and replaced by whole-genome sequencing (WGS). However, the widely-used WGS methods in canine genetics do allow for calling only single nucleotide variants (SNVs) and small insertions and deletions (indels), limited by the relatively short read lengths (150 bp) used. Detecting large structural variants requires much longer read lengths, which are provided by newer tools such as the PacBio® Single Molecule, Real-Time (SMRT) sequencing (Eid et al., 2009) and Oxford Nanopore sequencing methods (Mikheyev, Tin, 2014) with long reads of over 10 kb. Reduced read accuracy (Eid et al., 2009, Mikheyev, Tin, 2014) and a substantially higher price compared to short-read WGS have been limiting factors for their use, although long-read sequencing will presumably replace or at least become an important additional method to WGS in the near future. No publications describing either of these methods to be used in dogs are found on PubMed currently, although there are several on-going projects worldwide that use SMRT sequencing in dogs to generate a new genome annotation, CanFam 4.0 (Provisional Program, Conference on Canine and Feline Genetics and Genomics, 2019, Bern, Switzerland).

In addition to available genomic tools, there are also other reasons and resources that have established the dog as an important research subject (summarized in Figure 2). Firstly, dogs are affected with

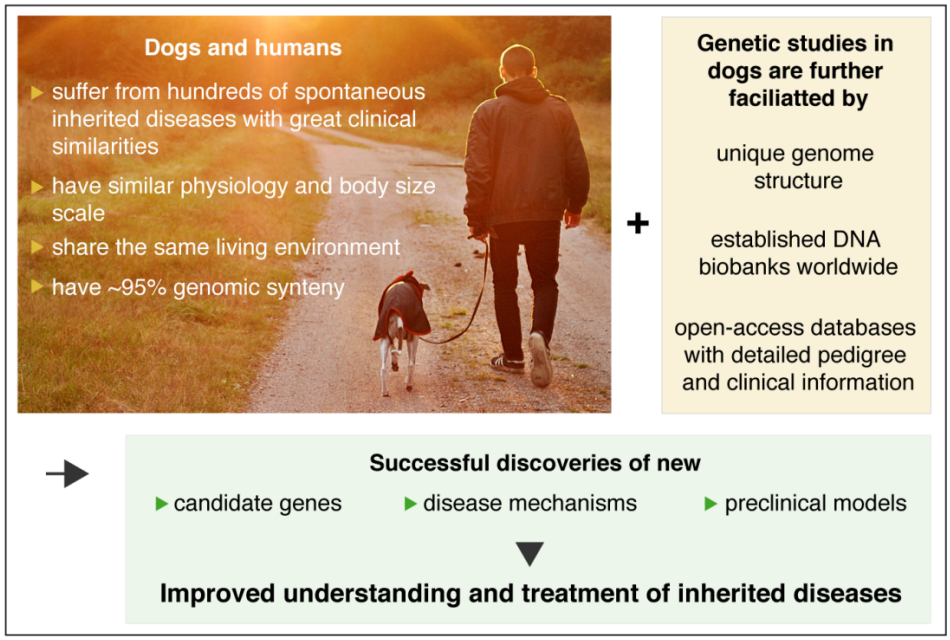

Figure 2 *The dog has become an important model organism to study human diseases and traits due to various physiological, pathological and genetic characteristics. Image source: www.Pixabay.com.*

hundreds of the same diseases as humans (Sargan, 2004), and thus, in addition to purely promoting veterinary medicine, the dog has been used to model human disease genetics, too. Genetic studies have shown that many phenotypically similar diseases in these two species result from mutations in the same causative genes (Zangerl et al., 2006, Ahonen et al., 2014, Everson et al., 2017). In addition, canine studies have also revealed new candidate genes for rare human disorders (Kyöstilä et al., 2015, Hytonen, Lohi, 2016). Dogs, with spontaneous disease occurrence, shared living environment and similar body size and physiology, might serve even better as a model organism for human diseases than the widely-used laboratory animals (e.g., see (Lehtimaki et al., 2018)). In addition, pedigree and health information are readily available for most pure-bred dogs in open-access databases, such as the KoiraNet run by the Finnish Kennel association, facilitating canine disease genetics in a way that would not be possible in humans. Growing canine DNA

biobanks have been set up worldwide (Groeneveld et al., 2016), with one of the world's largest established in Finland in 2006 by Professor Lohi. Currently, this biobank includes DNA samples from over 70,000 dogs, of which 35,000 have been eye examined by veterinary ophthalmologists, offering readily-usable cohorts to study the genetic causes of dozens of hereditary eye diseases.

In this thesis, all the above-mentioned resources and tools were utilized for successful genetic discoveries in the studied blinding eye disorders.

1.2 Healthy canine eye

1.2.1 Anatomy of the canine eye

The ocular globe is a camera-like sensory organ with a very specific anatomical structure, enabling conversion of physical energy (light) into a biological signal (visual sensation). In ophthalmology, unlike in any other medical field, the clinician is able to see into the organ of interest without invasive or complex diagnostic instruments, and many diagnoses are made based on these direct observations. In addition, non-invasive methods, such as optical coherence tomography (OCT), provide opportunities to examine different anatomical parts of the eye in a nearly-histological resolution (Huang et al., 1991).

Several hereditary eye diseases occur spontaneously in different dog breeds, causing disturbed morphology or function in the affected structures. Of the phenotypes studied in this thesis, these targets include development of the ocular globe (study I, microphthalmia (Graw, 2003)), aqueous humor outflow, iridocorneal angle, retinal ganglion cells and optic nerve (study II, glaucoma (Peiffer et al., 1980, Peiffer, Gelatt, 1980, Garcia-Valenzuela et al., 1995, Johnson, 2006, Almasieh et al., 2012)) and retinal morphology and function (study III, progressive retinal atrophy (Parry, 1953)). The overall anatomical structure of the normal canine eye is illustrated in Figure 3, while specific structures and physiological functions affected by the studied three diseases in this thesis are described in more detail in the following chapters.

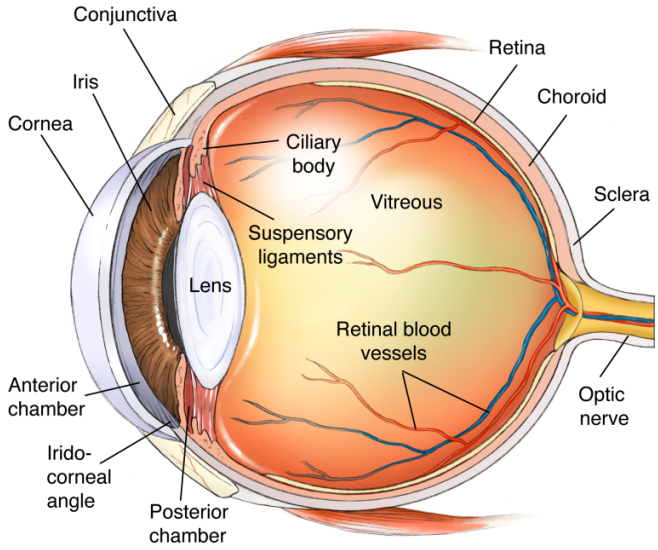

Figure 3 *A schematic view of the normal canine eye. Photo courtesy of Dave Carlson/CarlsonStockArt.com.*

1.2.1.1 The iridocorneal angle

The iridocorneal angle (ICA) is formed anteriorly of the peripheral cornea and the perilimbal sclera and posteriorly of the peripheral iris and anterior ciliary body musculature (Figures 3 and 4A). In dogs, unlike in humans, the anterior iris is further anchored to the inner peripheral cornea with pectinate ligament fibers, which are fine strands composed of collagen that are lined by iridal melanocytes and fibroblasts (Bedford, Grierson, 1986, Simones, De Geest & Lauwers, 1996). These strands are normally slender with an approximate thickness of 100–150 µm (Bedford, Grierson, 1986) and spaces between them, termed the spaces of Fontana, permit uninhibited outflow of the aqueous humor (Bedford, Grierson, 1986, Simones, De Geest & Lauwers, 1996, Van Buskirk, Brett, 1978). The pectinate ligament forms anastomoses with anterior beams of the trabecular meshwork (Bedford, Grierson, 1986), which in turn is further divided into three parts: the cobweblike uveal trabecular meshwork, the lamellated corneoscleral and uveoscleral trabecular meshwork and the nonlamellated juxtacanalicular tissue (Pizzirani, Gong, 2015) (Figure 4B). The trabeculae are formed from collagen and elastin, while each fiber is covered by a single layer of endothelial cells (Bedford, Grierson, 1986, Gong, Trinkaus-Randall & Freddo, 1989). These endothelial cells respond to

mechanical strain and have an important role in regulating intraocular pressure (IOP) (WuDunn, 2009). Macrophages and polymorphonuclear leukocytes in the uveal trabecular meshwork are able to ingest debris, enabling a clearance mechanism to ICA (Samuelson, Gelatt & Gum, 1984).

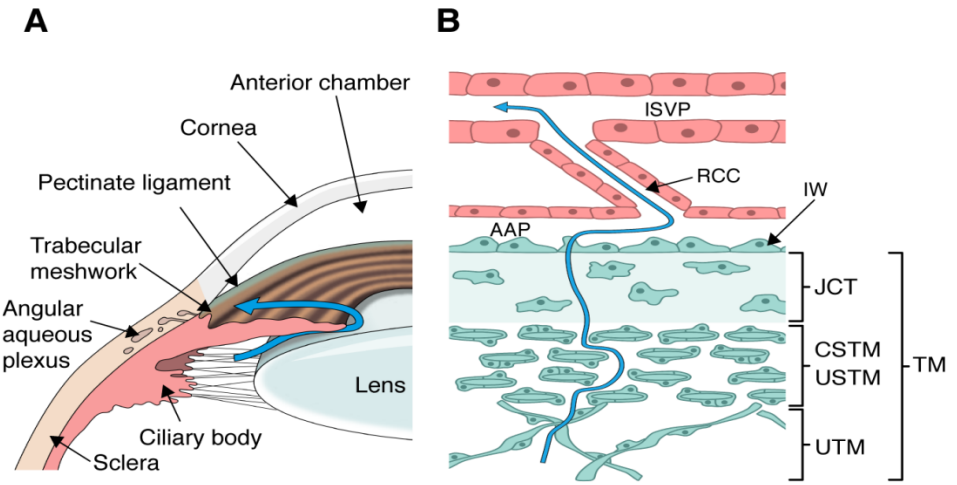

Figure 4 *Schematic representation of [A] the iridocorneal angle and [B] the aqueous humor outflow through the trabecular meshwork, with arrows marking the aqueous humor flow direction. TM = trabecular meshwork, UTM = uveal TM, USTM = uveoscleral TM, CSTM = corneoscleral TM, JCT = juxtacanalicular tissue, AAP = angular aqueous plexus, RCC = radial collector channels, ISVP = intrascleral venous plexus. Figure B adapted from* (Pizzirani, Gong, 2015, Swaminathan et al., 2014). *Photo courtesy of MSc Milla Salonen.*

The ICA is of the utmost importance in the pathology of glaucoma, as aqueous humor drainage occurs largely through ICA and blocked drainage can lead to elevated IOP (Peiffer et al., 1980, Peiffer, Gelatt, 1980), a hallmark feature of glaucoma. The aqueous humor is produced both by passive and active mechanisms, with the latter accounting for at least 80–90% of the production (Green, Pederson, 1972). In the active production, the movement of Na^+ and HCO_3^- from the nonpigmented epithelial cells of the ciliary body into the posterior chamber creates a positive osmotic gradient, drawing fluid along them (BONTING, BECKER, 1964, Cole, 1977). From the posterior chamber, the aqueous humor flows to the anterior chamber while maintaining the physiological IOP and nurturing the avascular ocular tissues, and finally reaches the ICA, where it exits through the trabecular meshwork into the

angular aqueous plexus (Tripathi, 1971, Gong et al., 2002). The angular aqueous plexus is connected to the radial collector channels, through which the aqueous humor finally enters the intrascleral venous plexus and exits the ocular globe (Pizzirani, Gong, 2015, Tripathi, 1971). The aqueous humor outflow through the trabecular meshwork is a passive process and is positively correlated with the IOP gradient (Tamm, 2009). Glycosaminoglycans and their protein complexes, especially in the juxtacanalicular tissue, regulate the outflow (Knepper, Goossens & Palmberg, 1996). The ICA and the structures it is composed of are under constant dynamic changes mediated by different cytokines and growth factors (Pizzirani, Gong, 2015, Rohen, Futa & Lutjen-Drecoll, 1981, Keller, Acott, 2013).

1.2.1.2 The retina

The retina in the ocular fundus consists of multiple layers of highly-specified cell types (Figure 5), accounting for the initiation of the visual sensation. From outermost to innermost, these layers include the retinal pigment epithelium, the photoreceptor, the outer nuclear, the outer plexiform, the inner nuclear, the inner plexiform, the ganglion cell and finally the nerve fiber layer, with the seven innermost forming the inner sensory retina, also termed the neurosensory retina or the neuroretina.

The outermost layer residing in the back of the eye in intimate contact with the neural retina is the retinal pigment epithelium (RPE), which consists of a single layer of polarized epithelial cells located between the choroid and the photoreceptor cells (Rizzolo, 1997). In dogs, the tapetum lucidum, a reflective layer of the inner choroid covering an area of approximately 30% of the superior fundus (Lesiuk, Braekevelt, 1983), is located outside of the RPE. The tapetum lucidum consists of a varying number of layers of tapetal cells packed with membrane-bound reflecting material (Lesiuk, Braekevelt, 1983) that enhances vision in dim light by allowing light that has already passed the retina to be reflected to the photoreceptors again. The RPE forms the outer part of the blood-retina barrier (Rizzolo, 1997), while its other functions include light absorption (Bok, 1993), metabolic end product (Thompson, Gal, 2003), water (Hamann, 2002) and ion transportation (Dornonville de la Cour, 1993), reisomerization of retinal for photoreceptor cells (Besch et al., 2003), phagocytosis of shed photoreceptor outer segments (Bok, 1993, Finnemann, 2003) and secretion of growth factors (Kvanta, 1994, Kannan, Sreekumar & Hinton, 2011) and immunosuppressive factors (Ishida et al., 2003).

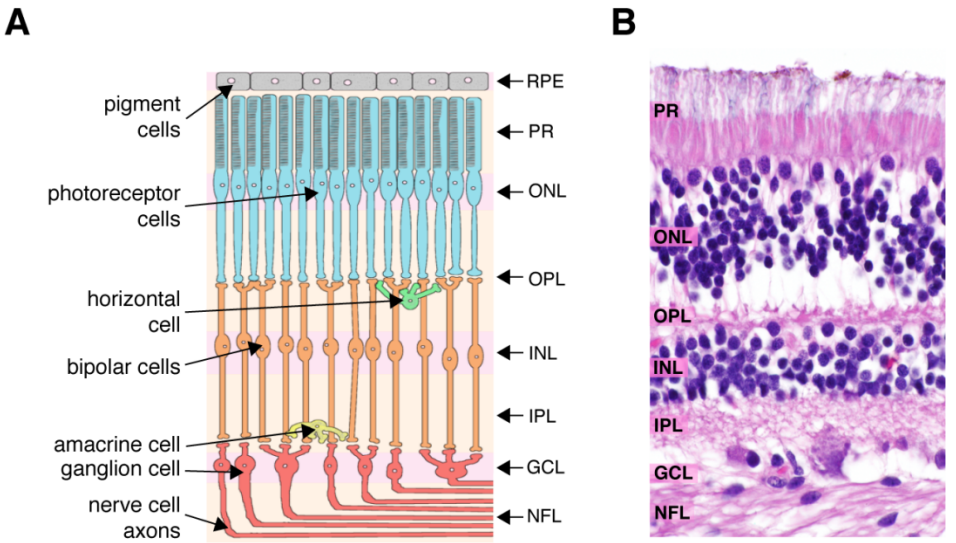

Figure 5 *Normal retina as [A] a schematic illustration and [B] as a H&E stained histological sample. Layers: RPE = retinal pigment epithelium, PR = photoreceptor outer and inner segment layer, ONL = outer nuclear layer, OPL = outer plexiform layer, INL = inner nuclear layer, IPL = inner plexiform layer, GCL = ganglion cell layer, NFL = nerve fiber layer. Image source: Retinal cell layer drawing modified from Wikimedia Commons, Wissenweiß and H&E stained histological image modified from Wikimedia Commons, Librepath.*

Directly below the RPE are the photoreceptor cells, whose cell bodies form the outer nuclear layer. Dogs, like most mammals, have two types of photoreceptor cells, the rods and the cones, which are responsible for vision in dim and bright light conditions, respectively. Different types of photoreceptor cells contain distinct photopigments, which are formed by a protein moiety (G-protein–coupled receptors, opsins) and a chromophore (vitamin A derivative, retinal) and which all have their specific spectral peaks. Opsins are further divided into subfamilies, and scotopsin called rhodopsin is present in the rods (Ovchinnikov, 1982, Hargrave et al., 1983, Palczewski et al., 2000), while different photopsins are found in the cones (Neitz, Geist & Jacobs, 1989). The rods account for over 95% of the photoreceptor cell population in canine retinas (Mowat et al., 2008). Dogs have two distinctive cone subtypes expressing photopigments with spectral peaks of about 429 (blue or S-opsin) and 555 nm (red/green or L/M-opsin) (Neitz, Geist & Jacobs,

1989, Chiao et al., 2000), enabling dichromatic color vision. Dogs, unlike commonly used laboratory rodents (Szel, Rohlich, 1992, Jeon, Strettoi & Masland, 1998), have a cone-dense area in their retina, resembling the human macula and fovea (Mowat et al., 2008, Beltran et al., 2014).

Axons of the photoreceptor cells synapse with dendrites of horizontal and bipolar cells, forming the outer plexiform layer. At this first synaptic layer in the retina, the signal from the photoreceptor cells is conveyed to bipolar cells (Jackman et al., 2011, Thoreson, Mangel, 2012, Chapot, Euler & Schubert, 2017) and shaped by one or multiple horizontal cells (of which dogs have at least two types (Jeon, Jeon, 1998)). The bipolar cells link the outer and inner retina by receiving signals from photon-induced photoreceptor cells and transferring the signal onward (Haverkamp, Grunert & Wassle, 2000, Dowling, Boycott, 1966). There are multiple types of bipolar cells in the mammalian retina, and they can be subdivided for example based on the number and types of photoreceptors they are in contact with (Euler et al., 2014). Stimuli from parallel information pathways modified by the bipolar cells are then passed on to amacrine cells and retinal ganglion cells (Kolb, Famiglietti, 1974, Trexler, Li & Massey, 2005). Amacrine cells, which form the most diverse cell population in the retina, with over 30 distinct types, mainly inhibit the bipolar and retinal ganglion cells as well as each other (MacNeil, Masland, 1998, MacNeil et al., 1999, Lin, Masland, 2006). The soma of the horizontal, bipolar and amacrine cells together form the inner nuclear layer, while the inner plexiform layer is the synaptic region between the bipolar, amacrine and retinal ganglion cells.

Retinal ganglion cell (RCG) bodies, together with neuroglial cells and the inner tips of Müller cells, comprise the ganglion cell layer, while their descending axons form the nerve fiber layer, the optic nerve, the optic chiasm and the optic tract. The main function of the RGCs is to transmit the integrated photoreceptor cell stimuli to the brain, and in more detail, in dogs, to the occipital cortex (Willis et al., 2001) with the corresponding brain region to the area of central vision located at the junction of the marginal and endomarginal gyri in the occipital lobe (Ofri, Dawson & Samuelson, 1995). In addition to this well-known RGC population, a specific subpopulation of RGCs, the intrinsically photosensitive RGCs (ipRGCs), have recently been found and are also present in dog retinas (Yeh et al., 2017). IpRGCs contain a unique photopigment, melanopsin, and are thus able to independently depolarize in response to light (Berson, Dunn & Takao, 2002). The highest density of RGCs in canine retinas is observed in the round central area of the retina and the

lowest outside the central area (Krinke et al., 1981), with breed-specific variation and smaller total count compared to the wolf (Peichl, 1992).

1.2.2 Development of the ocular globe

Eye development is relatively well characterized at the cellular level because of two main reasons: firstly, the outline process is similar across species (Van Cruchten et al., 2017), allowing interspecies comparisons and extrapolations, and secondly, mutation discoveries in individuals with congenital eye defects have shed light on the molecular basis of eye development (Abouzeid et al., 2011, Aldahmesh et al., 2012, Aldahmesh et al., 2013). In dogs, the majority of ocular development happens during the fetal period, although, for example, photoreceptor cell morphology continues to maturate for eight weeks after birth (Gum, Gelatt & Samuelson, 1984), and eyelid fusion breaks at around three weeks in puppies. The normal gestational period in dogs is 64 days on average (Whitney, 1940). It is divided into three phases: the period of the ovum (gestational days GD2–17, from fertilization to implantation of the blastocyst), the period of the embryo (GD19–35, until completion of organogenesis) and the period of the fetus (from GD35 to birth) (Pretzer, 2008).

The first form of the developing eye is the single eye field that is situated centrally in the developing head. Around GD16 in dogs, this single eye field splits into two lateral optic vesicles (Van Cruchten et al., 2017), which develop from the forebrain neural ectoderm, whereas the majority of ocular connective tissue originates from the midbrain neural crest (Johnston et al., 1979). In the optic vesicle, the surface ectoderm invaginates into the underlying neural ectoderm, enabling the formation of the lens vesicle and the optic cup (Figure 6), which in turn give rise to different subparts of the developing eye, as summarized in Table 1. The optic cup is open by optic fissure, which closes by GD25 in dogs (Van Cruchten et al., 2017), allowing IOP establishment.

Eye development is regulated by several genes, which are expressed during early embryogenesis and have been reported to play a role in initiating certain cascades or to regulate cell-lineage commitment. The best-known master control gene in eye development across species is the transcription factor encoding *Paired box gene 6* (*PAX6*). Loss-of-function mutations in *PAX6* leads to an eyeless phenotype in *Drosophila* and severe ocular defects in many mammals (Glaser et al., 1994, Quiring et al., 1994, Halder, Callaerts & Gehring, 1995), whereas its targeted expression induces ectopic eye

development in wings and legs in insects, supporting its putative role in eye field determination (Halder, Callaerts & Gehring, 1995).

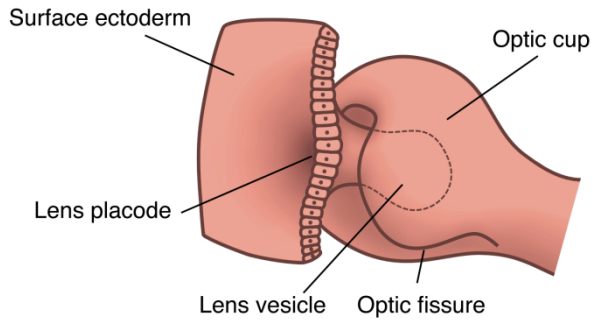

Figure 6 *Schematic representation of the developing eye. Photo courtesy of MSc Milla Salonen.*

Table 1. *Origins of ocular structures.*

Ectoderm		**Mesoderm**
Surface ectoderm	**Neural ectoderm**	
Lens	Retina, neural and pigment	Extraocular muscles
Corneal epithelium	Iris	Vascular endothelium
Conjunctival epithelium	Choroid	
Lacrimal glands	Sclera	
Eyelids	Pupillary muscles	
	Ciliary body	
	Optic nerve	
	Vitreous body	

References: reviewed by Van Cruchten et al., 2017.

1.2.3 Vision

Vision is a multi-step process in which the physical energy of light is transformed into a biological signal. Observable wavelength spectra differ by species based on the degree of light transmission through ocular media and the availability of photopigments in the photoreceptor cells. The spectrum of visible light to humans spans approximately 400 to 700 nm, leaving out the

majority of ultraviolet (UV) wavelengths (Boettner, Wolter, 1962, Lei, Yao, 2006). In contrast, dogs might be able to see UV light as the canine lens has been reported to transmit over 60% of light with wavelengths from 315 to 400 nm (Douglas, Jeffery, 2014). Dogs have their two eyes situated side by side, allowing a considerable portion of the visual field to be seen with binocular vision (Sherman, Wilson, 1975).

Dogs have dichromatic vision as they have two types of cone cells expressing distinctive photopigments. The short wavelength-sensitive cones (S-cones) have a spectral peak of 429 nm (blue), while the long wavelength cones (L-cones, sometimes referred to as long/medium wavelength cones or L/M-cones, too) have a spectral peak of 555 nm (green-yellow) (Neitz, Geist & Jacobs, 1989, Mowat et al., 2008). Color perception might be of greater importance to dogs than conventionally thought, as they have been reported to rely more on color than on brightness cues (Kasparson, Badridze & Maximov, 2013).

1.2.3.1 Retinal light detection

The light detection in the retina initiates a visual sensation that is further processed and interpreted in the central nervous system. Retinal photoreception includes two major processes: the phototransduction cascade in the photoreceptor outer segments and the retinoid cycle in the RPE (Figure 7). In the phototransduction cascade, the absorption of light activates the photopigments by isomerizing the 11-*cis*-retinal chromophore to all-*trans*-retinal (Hubbard, Wald, 1952). Activated photopigments (metarhodopsin II in rods (Dickopf, Mielke & Heyn, 1998)) bind photoreceptor-specific G-protein called transducin (Jager, Palczewski & Hofmann, 1996), which in turn activates cGMP phosphodiesterase (PDE) (Yamazaki et al., 1983, Wensel, Stryer, 1986, Asano, Kawamura & Tachibanaki, 2019). Activated PDE reduces the cytoplasmic concentration of cGMP (Pannbacker, Fleischman & Reed, 1972), closing the cation-selective cGMP-gated channels and ultimately resulting in photoreceptor membrane hyperpolarization (Sunderman, Zagotta, 1999), cessation of glutamate release from the synaptic terminals (Murakami, Otsu & Otsuka, 1972) and, thus, initiation of the visual signal.

After the phototransduction cascade, the retinoid cycle is needed for 11-*cis*-retinal regeneration. First, all-*trans*-retinal is reduced to all-*trans*-retinol by an NADPH-dependent all-*trans*-retinol dehydrogenase (Palczewski et al., 1994, Rattner, Smallwood & Nathans, 2000) and is transferred to RPE. In

RPE, it is esterified by lecithin:retinol acyltransferase (Saari, Bredberg, 1989), converted to 11-*cis*-retinol by retinoid isomerase RPE65 (Jin et al., 2005) and oxidized back to 11-*cis*-retinal by retinol dehydrogenases such as RDH5 (Simon et al., 1999). Finally, 11-*cis*-retinal is transported back to photoreceptor outer segments, where it binds to opsin and is thus available for another phototransduction cascade.

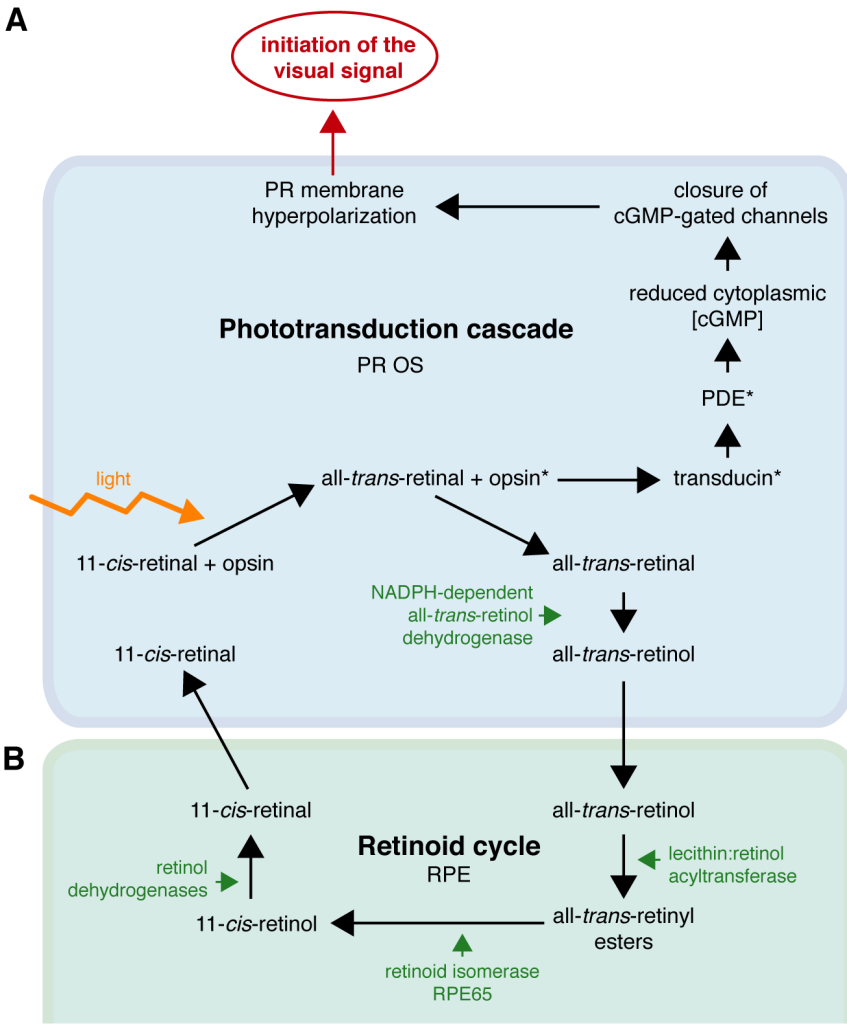

Figure 7 *Schematic representation of the retinal light detection, consisting of the [A] phototransduction cascade in photoreceptor outer segments (PR OS) and [B] the retinoid cycle in RPE. Mutations in genes coding the respective enzymes (e.g. RPE65) have been reported to cause retinal degeneration* (Aguirre et al., 1998). *Activated proteins are marked with an asterisk.*

1.3 Canine hereditary eye diseases

Because of their evolutionary history, purebred dogs suffer from many hereditary diseases as aggressive selection has enriched not only trait-specific but also disease-causing variants in specific dog breeds (Calboli et al., 2008). Currently, OMIA (www.OMIA.org) lists nearly 60 inherited eye diseases in dogs with known genetic causes, while for many, the genetic diagnosis is still lacking.

The most common hereditary eye disease across breeds is hereditary cataract, which affects over 100 dog breeds (Davidson, Nelms & Gelatt, 2007). Interestingly, only one gene, *HSF4*, has been implicated (Mellersh et al., 2006a, Mellersh et al., 2007, Mellersh et al., 2009) despite vigorous attempts to map new loci and causative variants. A great majority of the identified causal variants are breed-specific, although a few, including the variant in *ADAMTS17* causing lens luxation (Farias et al., 2010, Gould et al., 2011) and the variant in *PRCD* causing retinal degeneration (Zangerl et al., 2006, Donner et al., 2018), have been reported to affect several breeds. Below is a review of the previously published literature regarding microphthalmia, glaucoma and progressive retinal atrophy, the three phenotypes studied in this thesis.

1.3.1 Microphthalmia

Microphthalmia refers to abnormally small and underdeveloped ocular globes (Figure 8). Together with anophthalmia (complete lack of eyes) and coloboma (notch-like halos either in the iris, chorioretina or optic nerve head), it forms the MAC spectrum of congenital eye malformations. The general incidence of MAC in dogs is not known, but in humans, it is 1 per 5,300 live births (Morrison et al., 2002). One-third of the affected children have syndromic MAC, while the rest have no extra-ocular manifestations (Verma, FitzPatrick, 2007). Suggested pathological mechanisms include primary failure in optic vesicle growth, optic cup invagination or incomplete closure of the optic fissure (Graw, 2003, Onwochei et al., 2000), although in most cases the etiology is unknown.

Past studies from human MAC patients and induced mice and *Drosophila* have shed light on the genetic causes of the phenotype. In human patients, the most common single-gene defects are dominant *SOX2* loss-of-function variants (Fantes et al., 2003, Gerth-Kahlert et al., 2013). *SOX2*

Figure 8 *Unilateral microphthalmia in a five-week-old Miniature Poodle puppy. Photo courtesy of Marjo Vainio.*

belongs to the sex-determining region Y (SRY) -related high mobility group (HMG) -box transcription factor family and maintains embryonic stem cell pluripotency during early development (Matsushima, Heavner & Pevny, 2011). Restrained *SOX2* expression in the optic cup results in a lack of neural competence and cell fate conversion to the ciliary epithelium (Matsushima, Heavner & Pevny, 2011, Taranova et al., 2006). Other MAC-implicated genes include *PAX6, OTX2* and *STRA6* (Glaser et al., 1994, Ragge et al., 2005, Pasutto et al., 2007). *PAX6* is the best-known master control gene in eye development across species and is required in eye field determination (Glaser et al., 1994); OTX2 is also needed for it (Zuber et al., 2003), but also to RPE specification and photoreceptor cell formation and maintenance (Martínez-Morales et al., 2003, Kole et al., 2018). STRA6 is the cell-surface receptor for retinol uptake (Chen et al., 2016) and is specifically needed for vitamin A homeostasis in the eye (Berry et al., 2013). In addition, multiple environmental factors have been reported for MAC, including maternal dietary vitamin A deficiency (Hornby et al., 2002). Vitamin A is a substrate of retinoic acid, which is an important signaling molecule in the development of many organs, with the developing eye being the most sensitive to its deficiency (Hale, 1935,

Clagett-Dame, Knutson, 2011). During early embryogenesis, retinoic acid regulates transcription factor encoding *PITX2*, which in turn is important to optic fissure closure and anterior eye segment morphogenesis (Lupo et al., 2011). At later stages of eye development, retinoic acid promotes photoreceptor differentiation (Kelley, Turner & Reh, 1994).

In dogs, microphthalmia has been reported in many breeds, including Akitas (Laratta et al., 1985), Miniature Schnauzers (Gelatt et al., 1983) and Portuguese Water Dogs (Shaw, Tse & Miller, 2019). Heredity of the condition in these breeds has been suspected, but no causative variants have been found. Several dog breeds are also affected by a combination of congenital eye diseases termed collectively as collie eye anomaly (CEA). The hallmark features of CEA include choroidal hypoplasia and coloboma, although rare cases of microphthalmia have also been reported. A recessive 7.8-kb deletion in *NHEJ1*, encoding a DNA repair factor, has been proposed to cause CEA (Parker et al., 2007). Part of the reported deletion sequence contains putative binding sites of multiple regulatory proteins, and their prevented interactions were proposed to cause the phenotype (Parker et al., 2007). Recently, the causality of the variant has been questioned because of genotype-phenotype discordance in Danish Rough Collies and Shetland Sheepdogs (Fredholm et al., 2016) and the Nova Scotia Duck Tolling Retrievers (Brown et al., 2018).

1.3.1.1 Microphthalmia in Irish Soft-Coated Wheaten Terriers

Multiple ocular anomalies, including microphthalmia, have been described in Irish Soft-Coated Wheaten Terriers (ISCWTs), a middle-sized terrier breed originally from Ireland (Figure 9). A single case report from 1995 describes two ISCWT litters with microphthalmia and other congenital eye defects (Van der Woerdt et al., 1995). The affected litters were closely related as they had the same sire and the dams were cousins of each other, leading to a suspicion of an inherited disease. In the first affected litter, all 10 puppies presented with lens luxation of varying degrees, while two puppies also had corneal edema and four persistent pupillary membranes. Microphthalmia status for this first affected litter is not clearly stated in the case report, but the authors describe the eyes as too small to be completely examined by indirect ophthalmoscopy. All puppies were euthanized, and necropsies were done on four of them, revealing persistent right aortic arch and hydronephrosis in three puppies, while the fourth had no extra-ocular malformations. Histopathological examinations of the affected eyes confirmed the findings from ophthalmic

examinations and also revealed retinal and optic disk colobomata and choroidal hypoplasia. The second affected litter was born two years later, and eight of the nine puppies were diagnosed with microphthalmia. Other ocular anomalies included colobomata near or in the optic disk, strabismus, distichiasis, corneal dermoid, persistent pupillary membrane and cataract. No extra-ocular malformations were suspected based on clinical examinations. The dams of both litters were unaffected, and no abnormalities were detected during gestation. The sire, common to both litters, was not available for examination (Van der Woerdt et al., 1995).

Figure 9 *The ISCWT is a middle-sized terrier breed originally from Ireland. Image source: www.Pixabay.com.*

Results from any genetic analyses are not described in the original case report, suggesting that such analyses were not undertaken. The study describing the *NHEJ1* variant as the cause of CEA in many breeds (Parker et al., 2007) included samples from affected ISCWTs, but all of them tested negative for the deletion, thus leaving the genetic cause of the phenotype in the breed unknown.

1.3.2 Glaucoma

Glaucomas form a group of progressive optic neuropathies characterized by retinal ganglion cell and optic nerve head damage (Foster et al., 2002, Pizzirani, 2015). Elevated IOP is considered an important risk factor for glaucoma, but is no longer a diagnostic criterion in humans (Foster et al., 2002). In dogs, the definition of glaucoma still includes increased IOP, although its validity has been questioned (Pizzirani, 2015, Strom et al., 2011). Glaucomas are typically categorized based on the suspected cause (primary i.e. hereditary, secondary) and gonioscopic appearance of the drainage angle at disease onset (open, closed). In the absence of any detectable underlying cause, glaucoma is thought to be primary, and they are further subdivided into congenital, closed-angle and open-angle glaucomas (Pizzirani, 2015).

Glaucoma causes irreversible vision loss and, in the case of elevated IOP, severe ocular pain (Pizzirani, 2015). Currently, it is treated with IOP-decreasing medications and surgical interventions, which treat the symptoms instead of the cause (Komáromy et al., 2019). New treatment strategies, including neuroprotective medications and gene therapy, are needed in canine ophthalmology, where glaucoma has remained the most common cause of enucleation (Hamzianpour et al., 2019).

1.3.2.1 Primary congenital glaucoma

Primary congenital glaucoma (PCG) in dogs appears during the first year of life with severe abnormalities in the ICA (Strom et al., 2011). PCG is rare in pure-bred dogs: an epidemiologic study of 5,857 dogs presented to the University of Zurich Ophthalmology Service during 1995–2009 included only four PCG cases, which was substantially less than the number of other primary glaucoma cases (n=123) (Strom et al., 2011). The affected dogs represented four different breeds: the Dogue de Bordeaux, the Jack Russell Terrier, the German Hunting Terrier and the Kooikerhondje (Strom et al., 2011). To date, no genes or loci have been implicated to canine PCG.

PCG in humans accounts for 7–11% of childhood blindness (Gilbert et al., 1994, Tabbara, Badr, 1985). Causative variants in three genes have been reported, with autosomal recessive variants in *CYP1B1* being the most common cause of the disease (Stoilov, Akarsu & Sarfarazi, 1997, Lewis et al., 2017). *CYP1B1* encodes cytochrome P450 1B1, a member of the cytochrome P450 family that consists of membrane-bound oxidase enzymes, which

control hormone and metabolite production during development (Stoilov et al., 2001). The exact pathological mechanism of the *CYP1B1* variants are unknown, but the gene is expressed in the ciliary body and the trabecular meshwork (Stoilov, Akarsu & Sarfarazi, 1997, Stoilov et al., 1998, Zhao et al., 2013), structures that are of fundamental importance to aqueous humor production and outflow, and its reduced activity and stability have been reported in glaucoma (Chavarria-Soley et al., 2008, Jansson et al., 2001). The other two genes implicated in human PCG are TEK receptor tyrosine kinase *(TEK)* (Souma et al., 2016) and latent transforming growth factor beta binding protein 2 (*LTBP2)* (Ali et al., 2009, Narooie-Nejad et al., 2009), variant in which has also been proposed causative for feline PCG (Kuehn et al., 2016).

1.3.2.2 Primary closed-angle glaucoma

Primary closed-angle glaucoma (PCAG) refers to hereditary glaucoma, in which the gonioscopic appearance of the drainage angle is narrow or completely collapsed (Pizzirani, 2015). In dogs, the main risk factor for PCAG is pectinate ligament abnormality (PLA, sometimes called pectinate ligament dysplasia), a condition in which the normally slender strands of collagen with spaces between them (Bedford, Grierson, 1986) become broad sheets, thus inhibiting aqueous humor outflow in the ICA (Wood, Lakhani & Read, 1998, Wood et al., 2001). PLA was previously thought to be congenital (Wood, Lakhani & Read, 1998), but recent studies have shown that gonioscopically normal dogs can develop it later in life, and the severity of the deformity may increase with age (Pearl, Gould & Spiess, 2015, Oliver, Ekiri & Mellersh, 2016b, Oliver, Ekiri & Mellersh, 2016a). Although PLA is considered the most important risk factor for PCAG, not all dogs with PLA develop PCAG during their lifetime (Miller, Bentley, 2015).

The etiology of PCAG is thought to be complex with multiple genetic and environmental factors determining the risk of disease outbreak. Several dog breeds are suspected to suffer from PCAG, and six loci and two genes have been implicated to date (Ahonen et al., 2013, Ahram et al., 2014, Ahram et al., 2015, Oliver et al., 2019a, Oliver et al., 2019b). The first canine PCAG locus was mapped in 2013, when a genome-wide case-control comparison in Dandie Dinmont Terriers indicated a disease-associated chromosomal region in the CFA8 (Ahonen et al., 2013). Studies regarding the genetic cause of PCAG in Basset Hounds have proposed associations to loci in chromosomes 14, 19, 24 and 37 (Ahram et al., 2014, Ahram et al., 2015, Oliver et al., 2019a). A variant

in *NEB,* encoding an actin thin filament-binding protein called nebulin (Littlefield, Fowler, 1998), has been reported to associate with PCAG in the Northern American Basset Hounds (Ahram et al., 2015). However, the pathological role of the *NEB* variant remains elusive, as no differences in immunohistochemical staining intensity in the ciliary body and ciliary cleft were observed when comparing samples from affected and unaffected dogs (Ahram et al., 2015) and because the variant does not segregate with the phenotype in European Basset Hounds (Oliver et al., 2019a). The most recent genetic association for PCAG was reported in early 2019, when a locus on the CFA17 and a variant in *OLFML3,* encoding olfactomedin-like 3 protein, was reported to associate with the phenotype in a world-wide sample collection of affected and unaffected Border Collies (Pugh et al., 2019). In humans, multiple genes and loci have been implicated in PCAG (Wiggs, Pasquale, 2017), but because of the clear anatomical differences in the ICA structure (namely the lack of pectinate ligament in humans), the genetic etiology might be different from that in dogs.

1.3.2.3 Primary open-angle glaucoma

Primary open-angle glaucoma (POAG) refers to hereditary glaucoma with open ICA at disease onset (Pizzirani, 2015). In dogs, POAG is diagnosed less frequently than PCAG (Miller, Bentley, 2015), whereas in humans, it is the most common form of primary glaucoma (Sarfarazi, 1997). The two species also differ in the genetic cause of the disease, as POAG is thought to be complex in humans (Sieving, Collins, 2007), whereas in dogs, it is suspected to result largely from recessive variants (Miller, Bentley, 2015). That being said, variants in contactin 4 (*CNTN4*) (Kaurani et al., 2014), myocilin (*MYOC*) (Wang et al., 2015), neurotrophin 4 (*NTF4*) (Pasutto et al., 2009, Chen et al., 2012), optineurin (*OPTN*) (Rezaie et al., 2002) and WD repeat domain 36 *(WDR36*) (Mookherjee et al., 2011) genes have been implicated in Mendelian forms of the human phenotype, too, but explain only a small percentage of the cases at the population level.

In dogs, prior to the publication of study II in this thesis, POAG with a known genetic cause was reported in only one dog breed, the Beagle, in which the clinical and genetic characteristics have been studied in a research colony. The affected dogs present with elevated IOP at 6–18 months, with open ICA that is later collapsed as the disease progresses (Gelatt et al., 1977, Kuchtey et al., 2011). Ultimately, the disease results in the loss of retinal ganglion cells,

optic nerve head damage and irreversible blindness (Gelatt et al., 1977, Kuchtey et al., 2011). A missense variant (p.G661R) in the ADAM metallopeptidase with thrombospondin type 1 motif, 10 (*ADAMTS10*) is mapped to the disease (Kuchtey et al., 2011, Kuchtey et al., 2013). ADAMTS10 is important in the formation of the extracellular matrix and cytoskeleton (Dagoneau et al., 2004, Kutz et al., 2011), and in dogs, it is preferentially expressed in the trabecular meshwork compared to other ocular tissues (Kuchtey et al., 2011). Mutations in *ADAMTS10* in humans are linked to Weill-Marchesani syndrome, in which glaucoma and other ocular defects are seen along with skeletal abnormalities (Dagoneau et al., 2004, Steinkellner et al., 2015).

1.3.2.4 POAG in Norwegian Elkhounds

The Norwegian Elkhound (NE) is a middle-sized hunting breed originally from Norway (Figure 10). NEs are affected with primary glaucoma originally termed POAG as the affected dogs presented with elevated IOP in the absence of PLA (Ekesten et al., 1997). Clinical findings include optic nerve head atrophy, retinal degeneration, visual deterioration and elevated IOP, which all worsen as the disease progresses (Ekesten et al., 1997). Common findings in the advanced state also include lens luxation, buphthalmos and Haab's striae, and in rare cases, secondary cataract (Ekesten et al., 1997). The clinical presentation resembles the phenotype observed in Beagles (Gelatt et al., 1977, Kuchtey et al., 2011), although the age of onset appears later as POAG is diagnosed in middle-aged or elderly NEs (Ekesten et al., 1997, Gelatt, MacKay, 2004). The phenotype has an estimated prevalence of 2–3% in the Northern American NE population with female dogs slightly overrepresented among the cases (Gelatt, MacKay, 2004).

After the clinical characterization in 1997, histopathological examination of 22 glaucomatous NE eyes showed PLA and/or trabecular meshwork dysplasia (Oshima, Bjerkas & Peiffer Jr, 2004), thus complicating the disease characterization. Discordant results from clinical and histopathological examinations may result from multiple causes: 1) histopathological examinations enable the detection of subtle morphological changes that are undetectable gonioscopically, 2) abnormalities in the ICA appear as the disease progresses and therefore sampling time has a crucial effect on results, or 3) NEs are affected with both POAG and PCAG. The first two reasons are most likely, as the ICA is known to collapse with disease progression (Ekesten

et al., 1997), and the histopathological examinations were conducted with specimens obtained from NEs aged 5.5–8 years, probably representing a moderate or advanced state of the disease (Oshima, Bjerkas & Peiffer Jr, 2004).

Figure 10 *The NE is a middle-sized dog breed originally from Norway. It has been, and still is, used to hunt elk and other game. Image source: www.Pixabay.com.*

1.3.3 Progressive retinal atrophy

A heterogeneous group of inherited retinal diseases with varying ages of onset and rapidity of disease progression affects over 100 dog breeds (Miyadera, Acland & Aguirre, 2012) and are collectively called retinal dystrophies. To date, a genetic cause of the disease has been found in tens of dog breeds, but many still lack molecular diagnosis (Miyadera, 2018). Canine retinal dystrophies can be categorized, for example, based on the primarily affected cell population or the dysplastic or degenerative nature of the disease etiology; however, standardized classification has not been established (Miyadera, Acland & Aguirre, 2012). Canine retinal dystrophies with known genetic causes can be subdivided, for example, into achromatopsias, photoreceptor dysplasias, cone-rod dystrophies and other progressive retinal atrophies (PRA); for the sake of clarity, this is the classification used in this thesis, while the term PRA sometimes refers to all retinal degenerations in which rod loss precedes the one of the cones or is even extended to cover all retinal

degenerations with rod loss regardless of the order of affected cell type. Clinical findings vary between different types of retinal dystrophies, but generally include tapetal hyperreflectivity because of retinal thinning and attenuation of retinal vasculature (Figure 11) (Parry, 1953, Miyadera, Acland & Aguirre, 2012, Petersen-Jones, Komáromy, 2014). Currently, there are no standardized treatment options for any retinal dystrophy and the diseases will lead to impaired vision or even irreversible blindness in many affected individuals.

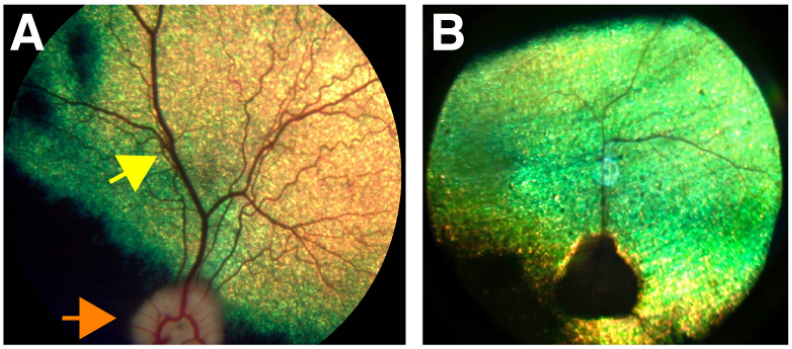

Figure 11 *Fundus images from [A] unaffected dog with normal retinal vasculature (yellow arrow) and optic nerve head (orange arrow) and [B] gPRA affected Nova Scotia Duck Tolling Retriever with advanced retinal thinning and attenuation of retinal vessels. Photo courtesy of DVM Kaisa Wickström.*

Achromatopsias are cone-specific retinal disorders characterized by day blindness, photophobia and normal vision in dim light conditions (Roosing et al., 2014). Currently, four different autosomal recessive variants in two genes have been implicated. A deletion and a missense (p.D262N) variant in *CNGB3*, encoding cyclic nucleotide gated channel subunit beta 3 needed for the cone phototransduction pathway, have been reported as the likely cause in Alaskan Malamutes and German Short-Haired Pointers, respectively (Sidjanin et al., 2002). The first clinical signs include day blindness, which is reported at 8–12 weeks of age, when the affected dogs were still ophthalmoscopically normal (Sidjanin et al., 2002). The deletion variant has been found in Miniature Australian Shepherds, Siberian Huskies and Alaskan Huskies as well (Yeh et al., 2013). Two variants (p.V644del, p.R424W) in *CNGA3* have also been associated with canine achromatopsia and affect Labrador Retrievers and German Shepherds, respectively (Tanaka et al., 2015).

Photoreceptor dysplasias affect photoreceptor cell morphology in very young puppies and can typically be detected, at least in electron microscopy, before the retina has developed into an adult-like state, meaning before the age of eight weeks (Gum, Gelatt & Samuelson, 1984). The disease leads to complete blindness due to degeneration of the dysplastic photoreceptor cells. Rod-cone dysplasias with known genetic causes have been reported in five dog breeds and are summarized in Table 2. The first reported variant causing canine rod-cone dysplasia type 1 in Irish Setters is a nonsense variant in *PDE6B* and causes impaired vision in dim light in puppies 6–8 weeks old, leading to complete blindness by the age of one year (Suber et al., 1993). Notably, a genetic test reporting an insertion variant in *PCARE* found in Gordon Setters and Irish Setters is commercially available as a rod-cone dysplasia type 4 test, but was actually originally described as rod-cone degeneration 4, as it causes very late-onset and slowly progressive retinal degeneration instead of dysplasia in the affected breeds (Downs et al., 2013). Cone-rod dystrophies are characterized by cone photoreceptor loss preceding that of the rods. Five likely causative variants have been reported in dogs and are summarized in Table 3.

Table 2. *Canine rod-cone dysplasias with known genetic cause.*

Name	Gene	Variant	Mode of inheritance	Breed	Reference
rcd1	*PDE6B*	Nonsense	AR	Irish Setter	(Suber et al., 1993)
rcd1a	*PDE6B*	Insertion	AR	Sloughi	(Dekomien et al., 2000)
rcd2	*RD3*	Insertion	AR	Collie, Rough and Smooth	(Kukekova et al., 2009)
rcd3	*PDE6A*	Deletion	AR	Welsh Corgi Cardigan	(Petersen–Jones, Entz & Sargan, 1999)

Rcd = rod-cone dysplasia, AR = autosomal recessive.

In addition to the above-mentioned retinal dystrophies, there is a large group of other PRAs with great clinical importance in many breeds. As stated above, the term PRA is used inconsistently in different sources, and sometimes the rod-cone dysplasias and cone-rod dystrophies are also classified as PRAs. PRAs can also be subdivided into diseases with primary defects in the photoreceptor cells (generalized PRAs or gPRAs) or in the RPE cells (central PRAs or cPRAs). In the gPRAs, according to their name, funduscopic changes are evenly distributed in the affected retina (Figure 11B), whereas in cPRAs (also termed RPE dystrophy or canine multifocal retinopathy), multiple local

subretinal accumulation spots and degenerative areas are observed while the rest of the retina might look normal (Guziewicz et al., 2007). Canine PRAs with known genetic causes falling outside the subtypes already discussed above are summarized in Tables 4 (cPRAs) and 5 (gPRAs).

Table 3. *Canine cone-rod dystrophies with known genetic cause*.

Name	Gene	Variant	Mode of inheritance	Breed	Reference
crd	*NPHP4*	Deletion	AR	Standard Wire-Haired Dachshund	(Wiik et al., 2008)
crd1	*PDE6B*	Deletion	AR	American Staffordshire Terrier	(Goldstein et al., 2013a)
crd2	*IQCB1*	Insertion	AR	Pitbull Terrier	(Goldstein et al., 2013a)
crd3	*ADAM9*	Deletion	AR	Glen of Imaal Terrier	(Goldstein et al., 2010b, Kropatsch et al., 2010)
crd4*	*RPGRIP1*	Insertion	AR	Miniature Long-Haired Dachshund°	(Mellersh et al., 2006b)

Crd = cone-rod dystrophy, AR = autosomal recessive.

*The variant was originally found in a laboratory colony of Miniature Long-Haired Dachshunds (Mellersh et al., 2006b), however causality of the variant was questioned later as in Japanese pet population 16% of the homozygous dogs were unaffected and 20% of the affected dogs were not homozygous for the variant (Miyadera et al., 2009). A strong regulatory locus on the CFA15 was later found to explain the discordant results (Miyadera et al., 2012), which might also be explained by the extensive variability of the age of onset (4 months–15 years) (Miyadera et al., 2009).

°The original variant has been found in Beagles, English Springer Spaniels, French Bulldogs, Labrador Retrievers, Curly Coated Retrievers, Papillons and Phalènes, in which the clinical importance remains elusive (Miyadera et al., 2009).

Table 4. *Canine cPRAs with known genetic cause*.

Name	Gene	Variant	Mode of inheritance	Breed	Reference
cmr1	*BEST1*	p.R25X	AR	Dogue de Bordeaus, English Mastiff, Italian Corso Dog, Pyrenean Mastiff	(Guziewicz et al., 2007)
cmr2	*BEST1*	p.G161D	AR	Coton de Tuléar	(Guziewicz et al., 2007)
cmr3	*BEST1*	p.G493V	AR	Lapponian Herder	(Zangerl et al., 2010)
-	*MERTK*	LINE insertion	AR	Swedish Vallhund	(Ahonen et al., 2014, Everson et al., 2017)
-	*RPE65*	Deletion	AR	Briard	(Aguirre et al., 1998)

Cmr = canine multifocal retinopathy, AR = autosomal recessive.

A similar phenotype to canine PRA, termed retinitis pigmentosa (RP), affects nearly two million people worldwide (Narayan et al., 2016) and has similar genetic etiology (Zangerl et al., 2006). According to the Retinal Information Network RetNet (http://sph.uth.edu/RetNet/), 67 genes and loci have been implicated in non-syndromic RP (Daiger et al., 1998), yet 30–80% of the RP patients still lack genetic diagnoses (Daiger, Sullivan & Bowne, 2013).

Table 5. *Canine gPRAs with known genetic cause.*

Name	Gene	Variant	Mode of inheritance	Breed	Reference
-	*BBS4*	Nonsense	AR	Puli	(Chew et al., 2017)
rcd4	*PCARE*	Insertion	AR	Gordon Setter, Irish Setter	(Downs et al., 2013)
-	*FAM161A*	SINE insertion	AR	Tibetan Spaniel, Tibetan Terrier	(Downs, Mellersh, 2014)
-	*CCDC66*	p.N174X	AR	Schapendoes	(Dekomien et al., 2010)
-	*NECAP1*	p.G182R	AR	Giant Schnauzer	(Hitti et al., 2019)
-	*PRCD*	p.C2Y	AR	Multiple	(Zangerl et al., 2006)
GR-PRA1	*SLC4A3*	Insertion	AR	Golden Retriever	(Downs et al., 2011)
GR-PRA2	*TTC8*	Deletion	AR	Golden Retriever	(Downs et al., 2014)
-	*CNGA1*	Deletion	AR	Shetland Sheepdog	(Wiik et al., 2015)
-	*CNGB1*	Deletion + insertion	AR	Papillon, Phalène	(Ahonen, Arumilli & Lohi, 2013)
-	*SAG*	Non-stop	AR	Basenji	(Goldstein et al., 2013b)
-	*STK38L*	SINE insertion	AR	Norwegian Elkhound	(Goldstein et al., 2010a)
XLPRA 1	*RPGR*	Deletion	XR	Samoyeed, Siberian Husky	(Zhang et al., 2002)
XLPRA 2	*RPGR*	Deletion	XR	Mixed-breed	(Zhang et al., 2002)
-	*RHO*	p.T4A	AD	Bullmastiff, English Mastiff	(Kijas et al., 2002)

AR = autosomal recessive, XR = X-linked recessive, AD = autosomal dominant, GR-PRA = Golden Retriever PRA, XLPRA = X-linked PRA.

1.3.3.1 PRA in Miniature Schnauzers

Miniature Schnauzers (MSs) are small Schnauzer-type dogs (Figure 12) that are affected with PRA with a suspected autosomal recessive mode of inheritance (Parshall et al., 1991, Jeong et al., 2013). Electroretinogram (ERG) recordings from affected North American MSs indicated deficits in puppies as young as eight weeks (Parshall et al., 1991), thus categorizing the disease as photoreceptor dysplasia (Gum, Gelatt & Samuelson, 1984). Ophthalmoscopically, the pathologic changes could not be seen until the age of 2–5 years (Parshall et al., 1991), complicating the diagnosis in routine veterinary ophthalmology. Night blindness and impaired vision in daylight were reported by the age of 3 years and complete blindness by the age of 4–5 years (Parshall et al., 1991). A second clinical report on South Korean MSs, was published in 2013 and described similar findings, although a definitive classification of the phenotype as dysplastic disease could not be made due to a lack of ERG recordings in young puppies (Jeong et al., 2013). While 85% of the affected dogs had clinical symptoms of PRA by the age of five years, some dogs were as old as seven years at presumed disease onset (Jeong et al., 2013). No sex predilection was reported in either study (Parshall et al., 1991, Jeong et al., 2013).

Figure 12 *MSs are small Schnauzer-type dogs originally from Germany. Image source: www.Pixabay.com.*

Over time, several attempts have been made to unravel the genetic cause of the disease in MSs. A candidate gene approach proved unsuccessful (Zhang et al., 1999), whereas a variant in phosducin (*PDC*) encoding gene was proposed as causal (Zhang et al., 1998), but was later refuted (Jeong et al., 2008). Results from the most recent attempt were reported in early 2019, during the course of study III, suggesting causality of a complex structural variant in *PPT1*, a well-known candidate gene for neuronal ceroid lipofuscinosis (NCL) (Murgiano et al., 2018). However, as the reported variant had an alarmingly low penetrance (0.79) for an autosomal recessive disease, and because the PRA-affected MS did not show any neurological symptoms (which are hallmark features in NCL patients), the true causality of the variant remained unresolved.

2 Study aims and hypothesis

The overall aim of this thesis was to identify the genetic cause of microphthalmia in Irish Soft-Coated Wheaten Terriers (study I), primary open-angle glaucoma in Norwegian Elkhounds (study II) and progressive retinal atrophy in Miniature Schnauzers (study III). All three conditions were hypothesized to be hereditary since several diseased dogs were reported in each breed. Therefore, the application of modern genetic approaches should reveal the causative variants and confirm the inheritance models.

To attain the overall goal, the following specific aims were appointed:

1. To establish clinically confirmed study cohorts and pedigrees from affected and unaffected dogs in each breed.

2. To map the disease loci to specific chromosomal regions by genome-wide association studies.

3. To find the causative variants in the associated loci with either whole-genome sequencing (studies I and III) or candidate gene approach (study II).

4. To prioritize the candidate variants by *in silico* analyses and validate them by genetic and functional experiments.

3 Materials and methods

3.1 Ethical statement

All performed experiments were approved by the Animal Ethical Committee of the County Administrative Board of Southern Finland (ESAVI/6054/04.10.03/2012, ESAVI/7482/04.10.07/2015, ESAVI/343/04.10.07/2016) and were performed in accordance with relevant guidelines and regulations and with the owners' consent.

3.2 Study cohorts

3.2.1 Recruitment, pedigrees and sampling

To enable any genetic analysis, well-determined study cohorts are crucial. The cohorts were established from purebred pet dogs, mainly from Finland but also from other countries. Dogs were recruited through breed clubs, advertisements on research group's web pages and on Facebook.

Pedigree information was obtained directly from KoiraNet (http://jalostus.kennelliitto.fi), an open-access database provided by the Finnish Kennel Club or, if not available, from the dogs' registration documents received from the owners. Pedigrees were drawn around the affected dogs using the GenoPro 2.5.4.1 genealogy software (GenoPro, Waterloo, Ontario, Canada).

Peripheral venous blood samples (3 ml) were collected in EDTA-containing tubes from all participating dogs and genomic DNA was extracted from the white blood cells using an automated Chemagen extraction robot (PerkinElmer Chemagen Technologie GmbH, Baesweiler, Germany) following the manufacturer's instructions. DNA concentration and purity were measured using the Qubit fluorometer (Thermo Fisher Scientific, Waltham, Massachusetts, USA), the Nanodrop ND-100 UV/Vis Spectrophotometer (Nanodrop Technologies, Wilmington, Delaware, USA) or the DeNovix DS-11 Spectrophotometer (DeNovix, Wilmington, Delaware, USA). Samples were stored at either –20 °C (stocks) or +4 °C (dilutions).

Altogether, samples from 294 ISCWTs (study I), 596 NEs (study II) and 599 MSs (study III) were utilized in this thesis.

In addition, in study I, serum and urine samples from 17 ISCWTs were collected for functional experiments. Three of the sampled dogs were affected with bilateral microphthalmia, and the rest 14 were unaffected.

In study III, tissue samples from nine dogs were utilized for retinal gene expression experiments. To evaluate general retinal gene expression in healthy canine retina, single-cell tagged reverse transcription (STRT) sequencing was performed using samples from five dogs without the studied phenotype and wild-type for the candidate variant. These dogs included a 3-year-old female Swedish Elkhound, 5- and 6-year-old male Rottweilers, a 6-year-old female Finnish Lapphund and a 6-year-old male Border Collie. The Swedish Elkhound and the Border Collie were euthanized because of epilepsy, the Rottweilers due to gastrointestinal disease and the Finnish Lapphund due to intervertebral hernia. In addition, retinal samples from five dogs were utilized for a case-control comparison of retinal gene expression. These dogs included an 11-year-old PRA-affected male MS, homozygous for the candidate variant, and four controls (the 5-year-old male Rottweiler described above, a 2-year-old female German Pinscher, a 3-year-old female East-European Shepherd and a 5-year-old male Smooth Collie) without the studied phenotype and wild-type for the candidate variant. The MS was euthanized due to congestive heart failure and the German Pinscher, Smooth Collie and East-European Shepherd due to behavioral problems. Retinal samples were collected within 15 minutes after euthanasia and were treated with Invitrogen RNAlater Stabilization Solution (Thermo Fisher Scientific, Waltham, Massachusetts, USA) for 24 hours and then stored at –80 °C. Total RNA was extracted using the RNeasy Mini Kit (Qiagen, Venlo, Netherlands) according to the manufacturer's instructions, and the integrity and concentration of the samples were measured with the Agilent 2100 Bioanalyzer (Agilent Technologies, Santa Clara, California, USA), Qubit fluorometer (Thermo Fisher Scientific, Waltham, Massachusetts, USA) and Nanodrop ND-1000 UV/Vis Spectrophotometer (Nanodrop Technologies, Wilmington, Delaware, USA), respectively.

3.2.2 Clinical phenotyping

Clinical phenotyping was done by veterinary ophthalmologists board-certified by the European or American College of Veterinary Ophthalmologists. First, a basic neuro-ophthalmic examination, including pupillary light reflex,

menace response and dazzle reflex evaluation, were performed. Then, the anterior segment of the eye and adnexa were examined with slit-lamp biomicroscopy and the posterior segment with indirect ophthalmoscopy. Topical tropicamide (Oftan Tropicamid 1%, Santen Tampere, Finland) was applied twice 10 minutes prior to examination to achieve mydriasis. In addition, OCT imaging was performed on 11 ISCWTs in study I and to 1 MS in study III using a Heidelberg Spectralis instrument (Heidelberg Engineering GmbH, Heidelberg, Germany).

In study I, the inclusion criterion for cases was bilateral microphthalmia while controls were completely free of any eye disease. Both cases and controls were examined at the age of 6–10 weeks, as retinal pigmentation may later mask mild CEA changes (Bjerkås, 1991).

In study II, the inclusion criterion for cases was bilateral glaucoma with elevated IOP. No underlying cause for the disease was observed, and thus, their glaucoma was suspected to be primary. Controls were eye examined healthy at the age of eight years or older.

In study III, the inclusion criterion for cases was bilateral severe PRA with hyperreflective tapetum lucidum, vessel attenuation and optic nerve head atrophy. Controls were free of any eye disease and examined at the age of seven years or older.

3.3 Genetic analyses

In each study, genome-wide association studies were performed to map the disease loci, followed by resequencing to find candidate variants within the critical intervals and Sanger sequencing to validate the variants. In addition, KASP and TaqMan genotyping assays were utilized to screen breed cohorts in studies II and III, respectively. The CanFam 3.1 annotation was utilized in all experiments as the reference sequence.

3.3.1 Genome-wide association studies

Genotyping was performed using Illumina Canine HD Bead Chip (Illumina, San Diego, CA, USA) with 173,662 markers at the GeneSeek Laboratory (Neogen Genomics, Lincoln, NE, USA) for 29 ISCWTs, including 12 cases and 17 controls (study I), for 17 NEs, including 8 cases and 9 controls (study II), and to 49 MS, including 16 cases and 33 controls (study III). Samples were

selected based on pedigree information to avoid stratification in the subsequent analysis if possible. The data were stored at the BGGenome 4.4-053 database (BC Platforms, Espoo, Finland).

Prior to association analyses, specific quality control procedures were performed using the PLINK 1.07 software (Purcell et al., 2007). Only individual samples and SNPs with a call rate over 95% and minor allele frequency (MAF) over 5%, were included in the analysis. To exclude SNPs showing significant deviation from the Hardy-Weinberg equilibrium, a threshold value of $p \leq 0.0001$ was determined.

After quality control, differences in allele frequencies between cases and controls were calculated using the PLINK 1.07 software (Purcell et al., 2007). Genomic control corrected p-values were calculated using the estimated genomic inflation factor λ. To correct the genome-wide empirical p-values, 100,000 permutations were applied to the data. In addition, to adjust for population structure, R-package softwares GenABEL with full genomic kinship matrix and GAPIT were utilized to confirm the PLINK results (Aulchenko et al., 2007).

3.3.2 Identification and validation of candidate variants

3.3.2.1 Whole-genome sequencing

In studies I and III, the whole-genome sequencing approach was utilized to find candidate variants in the phenotype-associated chromosomal regions found in GWAS.

In study I, a sample from one affected ISCWT was whole-genome sequenced at the Next Generation Sequencing Platform at the University of Bern using the Illumina HiSeq2500 (Illumina, San Diego, CA, USA) instrument with 15X target coverage and paired-end reads (2x 100 bp).

In study III, samples from two affected, one control and one obligate carrier MSs were sequenced at the Novogene Bioinformatics Institute (Beijing, China) using the Illumina HiSeq X ultra-high-throughput sequencing platform with 30X target coverage and paired-end reads (2x 150 bp).

Mapping the reads to the dog reference genome was performed using the Burrows-Wheeler Aligner (BWA) version 0.5.9 in study I and 0.7.15 in study III, respectively (Li, Durbin, 2009). The duplicate reads were removed and reads were sorted using the Picard tools

(http://sourceforge.net/projects/picard). To reduce erroneous variant calls, post-alignment processing, including local realignment around known INDELs and base quality scores recalibration, was performed (McKenna et al., 2010). Variant calling was done using the HaplotypeCaller in Genome Analysis Tool Kit GATK version 2.6 in study I and 3.7 in study III, respectively. Functional annotation of the variants was performed in ANNOVAR using Ensembl, NCBI and Broad gene databases. Mobile element insertions (MEI) were detected using the Mobile Element Locator Tool (MELT) (Gardner et al., 2017). The Repbase database was utilized as the source of reference sequences of the transposons for MEI discovery (Jurka et al., 2005). The detected variants were stored in the Genotype Query Tools (GQT) variant database (Layer et al., 2015).

Variant filtering was performed using our in-house pipeline. The cases were assumed to be homozygous for the alternative alleles. Data from our previous next-generation sequencing projects and the Dog Biomedical Variant Database Consortium were utilized in filtering as controls. All these dogs were without the studied phenotype and from different breeds than the cases in question. In study I, all the control samples (n=342) were set to be homozygous for the reference allele. In study III, the filtering was performed in two steps: first by comparing only the cases to MS (n=1) and non-MS controls (n=267) and then by applying data from the obligate carrier, too. In study III, 1% of the control dogs were allowed to carry the variant, while 99 % were set to be homozygous for the reference allele. Details of the control dogs can be found as supplementary items in respective studies.

3.3.2.2 Sanger sequencing

Sanger sequencing was utilized to validate candidate variants found in whole-genome sequencing in studies I and III; in study II, as the GWAS locus included a known POAG candidate gene, it was used to examine exonic regions and splice sites in the whole candidate gene. Primers were designed with Primer 3 software (Koressaar, Remm, 2007), and specific primer sequences can be found within supplementary items of each study. PCR amplification was performed with the GC-RICH System Polymerase (Roche Diagnostics GmbH, Mannheim, Germany) in study I and with the Biotools DNA Polymerase (Biotools B&M Labs, S.A., Valle de Tobalina, Madrid, Spain) in studies II and III according to manufacturers' instructions. Exonuclease I and FastAP Thermosensitive Alkaline Phosphatase (Thermo

Fisher Scientific, Waltham, MA, USA) were used to purify the PCR products, which were then capillary sequenced at the Institute for Molecular Medicine Finland (Helsinki, Finland). The Sanger sequencing data were analyzed using the Sequencher 5.1 (Gene Codes Corporation, Ann Arbor, MI, USA) software in studies I and II and the Unipro UGENE 1.31.1 (UniPro, Novosibirsk, Russia) software in study III.

3.3.2.3 Population screening in breed cohorts

To further validate the candidate variants, larger breed cohorts in each specific study were genotyped. In study I, genotyping was performed on 254 ISCWT samples with the Sanger sequencing protocol described above. In study II, the screening was performed on 577 NEs with the KASP by Design genotyping assay (LGC Genomics Ltd, Teddington, UK). In addition, the breed-specificity of the variant was studied by genotyping 71 glaucoma or PLA-/PLD-affected dogs from 17 breeds and 115 unaffected dogs from six breeds (study II, Table S1). Custom TaqMan SNP Genotyping Assay (Thermo Fisher Scientific, Waltham, MA, USA) was utilized to genotype the candidate variant in the breed cohort, including samples from 514 MSs in study III. Specific primer details can be found in supplementary items of the respective study.

3.3.2.4 *In silico* analyses and target gene prioritization

In study III, as the disease-associated variant was not coding, its function as a gene expression regulator was analyzed with multiple *in silico* methods. First, the canine variant site was converted to determine the corresponding human genome position using the UCSC liftOver tool and the GRCh38 as the human reference genome. The JASPAR database was utilized to obtain a HAND1::TCF3 transcription factor binding site (TFBS) motif overlapping the variant site (Khan et al., 2017). Then, motif scanning was performed using the "searchSeq" function of the TFBSTools package (v.1.20) (Tan, Lenhard, 2016) within 500 bps of the transcription start sites of CanFam3.1 Ensembl genes version 94 (Zerbino et al., 2017) to find candidate target genes for HAND1::TCF3. The FANTOM5 and Human Protein Atlas databases (Forrest et al., 2014, Uhlen et al., 2015) were utilized to manually confirm that the candidate target genes were expressed in the retina. STRT RNA sequencing data from canine retinal samples were utilized to confirm expression and to

prioritize the candidate target genes for subsequent validations. The STRT experiment is part of the Dog Genome Annotation (DoGA) Project. A modified STRT method with unique molecular identifiers (Islam et al., 2011, Islam et al., 2014) was utilized for RNA-seq library preparation using 20 ng of RNA for multiplex 48 sample libraries. The applied modifications included longer UMI's of 8 bp, addition of spike-in ERCC control RNA for normalization of expression, and use of Globin lock method (Krjutskov et al., 2016) with LNA primers for canine alpha- and beta-globin genes. Sequencing the libraries was performed using the Illumina NextSeq 500 instrument and read mapping using HISAT1 mapper version 2.1.0 (Pertea et al., 2016). FeatureCounts version 1.6.2 (Love, Huber & Anders, 2014) was used for gene-level quantification, with the counts normalized to the library size and transcript length. Finally, the expression levels of 60 candidate genes (study III/Table S4) were visualized using the ComplexHeatmap package (Gu, Eils & Schlesner, 2016).

3.4 Functional experiments

Several functional experiments were conducted in studies I and III to validate the pathogenicity of the likely causative variants. The following chapters describe the used techniques, plasmid constructs and expression vectors, while canine sample collection is described above in chapter 3.2.

3.4.1 Serum biochemistry

In study I, serum vitamin A was measured in 17 ISCWTs after protein precipitation with U-HPLC chromatography using the Dionex Instrument Rapid Separation LC 3000 unit with the 325-nm array detector (Thermo Fisher Scientific, Waltham, MA, USA). As a control measurement, total protein and albumin were measured using an AU5800 Clinical Chemistry System analyzer (Beckman Coulter, Brea, CA, USA). The measurements were done at the IDEXX Laboratories (Hoofddorp, Netherlands). Student's T-test (two-tailed distribution) was used to assess statistical significance of the differences in serum vitamin A levels of different genotype groups.

3.4.2 Western blotting

To investigate possible changes in protein structure and function in study I, the RBP levels were measured in serum (2 μL) and urine (10 μL) samples from 17 ISCWTs, and HeLa conditioned media (15 μL) and lysates (20 μg) by Western blot analysis, following polyacrylamide gel electrophoresis (SDS-PAGE). All canine samples were transported and stored at –20 °C after collection. Prior to HeLa cell transfection, the secreted portions of wild-type and K12del canine *RBP4* cDNAs (accession XM_534969, GenScript, Piscataway, NJ, USA) were subcloned into the pUS2 vector by PCR and Gibson assembly (Gibson et al., 2009) and were situated downstream of the human *RBP4* signal peptide (MKWVWALLLLAALGSGRA) and HA epitope tag (YPYDVPDYA). The complementary primer sequences can be found in the Supplemental Experimental Procedures of study I. Site-directed mutagenesis (Liu, Naismith, 2008) was utilized to generate orthologous human K12del and E13del pUS2-RBPHA expression plasmids (Chou et al., 2015). Successful plasmid constructions were verified by DNA sequencing.

Prior to transfection, HeLa cells were cultured in Dulbecco's Modified Eagle Medium (DMEM), which was supplemented with 10% fetal bovine serum (FBS), 2 mM glutamine and 100 U/mL penicillin/streptomycin. The cells were incubated at 37 °C in a humidified 10% CO2 atmosphere. Subconfluent cultures were transfected with 6 μg plasmid DNA and 6 μl of Xtremegene HP reagent (Roche Diagnostics GmbH, Mannheim, Germany) per 100 mm dish. The cell media was replaced with 5 mL DMEM after 16 h incubation. After an additional 48 h, conditioned media containing recombinant dog or human HA-RBP was harvested, filtered through 0.22 μm syringe units (Millipore, Billerica, MA, USA) and stored at 4 °C. Adherent cells were collected simultaneously, washed with PBS and frozen. Next, cell pellets were lysed in RIPA buffer (0.1% SDS, 1% NP40, 1% sodium deoxycholate, 150 mM NaCl, 1 mM EDTA, 25 mM Tris pH 7.5) with cOmplete Protease Inhibitor Cocktail (Roche Diagnostics GmbH, Mannheim, Germany) and centrifuged (16000x*g*) to collect lysate supernatants. Human wild-type and stable (A55T) and unstable (G75D, I41N) (Chou et al., 2015) mutant controls were included in the subsequent western analysis.

The Bradford method, using commercial reagents and bovine serum albumin (BSA) standards (Thermo Fisher Scientific, Waltham, MA, USA), was utilized to measure total urinary and cell lysate protein levels. Aliquots were denatured for 10 min at 95 °C in 1X loading buffer (0.5% lithium dodecyl sulfate, 2.5% glycerol, 12 mM EDTA, 62 mM Tris pH 8.5) and

electrophoresed through 4–12% polyacrylamide Bis-Tris gels (NuPAGE, Invitrogen, Carlsbad, CA, USA) in 2-(N-morpholino) ethanesulfonate (MES) running buffer pH 7.3 with 0.1% SDS for 120 min at 25 V/cm. Dithiothreitol (100 mM DTT) or 2-mercaptoethanol (100 mM bME) was added to samples before heating enabling analysis under reducing conditions. Protein gels were electrotransferred to nitrocellulose membranes (GE Life Sciences, Piscataway, NJ, USA) in a Trans-Blot chamber (Biorad, Hercules, CA, USA) for 30V x 16 h at 4 °C in NuPAGE transfer buffer (25 mM Bicine, 25 mM Bis-Tris, 1 mM EDTA, pH 7.2) with 10% methanol. To maximize the detection of native RBP and to fully mobilize proteins and expose epitopes, the nonreducing gels were soaked in a 1X MES running buffer with 300 mM bME 1% SDS for 60 min at 25 °C prior to transfer (Zetterstrom et al., 2007).

For enhanced chemiluminescence (ECL) detection, membranes were washed in Tris-buffered saline (TBS), blocked in TBS 5% BSA 1% non-fat dry milk, and incubated for 16 h at 4 °C with primary antibody. For infrared fluorescence detection, membranes were washed in TBS, blocked in Odyssey-blocking buffer (OBB, LI-COR, Lincoln, NE, USA) and incubated with the primary antibody in a 1:1 mixture of OBB and 0.05% Tween-20 TBS. The primary antibodies were rabbit anti-human RBP4 (1:5000, Dako A0040, Carpinteria, CA, USA), rat anti-HA (1:5000, high affinity monoclonal 3F10, Roche Diagnostics GmbH, Mannheim, Germany), rabbit anti-human TTR (1:5000, Abnova PAB 1221, Walnut, CA, USA) and mouse anti-alpha tubulin (1:2000, monoclonal TU-01, Thermo Fisher Scientific, Waltham, MA, USA). For ECL detection, membranes were rinsed in TBS 0.05% Tween-20 (TBST), incubated at 25 °C for 1 h with horseradish peroxidase (HRP) –conjugated donkey anti-rabbit IgG secondary antibody (1:5000, NA934, GE Amersham, Buckinghamshire, UK) in TBS 5% BSA, and developed using ECL Plus reagents and X-ray film (GE Amersham, Buckinghamshire, UK). For dual wavelength infrared detection, membranes were co-incubated with IR 800CW- and 680LT-conjugated anti-rat, rabbit or mouse IgG secondary antibodies (1:20,000, LI-COR Biotechnology, Lincoln, NE, USA). Densitometry of serial exposures (ImageJ, NIH, Bethesda, MD, USA) was utilized to quantify RBP levels. Signal intensities among ≥4 sample replicates were averaged and results normalized to wild-type mean.

To immunopurify the native HA-RBP complexes from CM, the mouse anti-HA monoclonal IgG –conjugated agarose beads (A2095, Sigma-Aldrich, Saint Louis, MO, USA) and fritted spin columns were used. CM samples (0.5 mL) were incubated with beads for 16 h at 4 °C, and bound proteins were eluted in 200 µL 1X loading buffer for 15 min at 95 °C. The interaction

between secreted HA-RBPs and bovine TTR in the overlying DMEM (10% FBS) was assessed by eluate Western blots (Chou et al., 2015).

3.4.3 Nuclear magnetic resonance

To study the protein structure and function more precisely in study I, a nuclear magnetic resonance (NMR) experiment was conducted. To generate the *E. coli* expression clones, residues 19–201 of wild-type and K12del canine *RBP4* clones (GenScript, Piscataway, NJ, USA) were subcloned into the pET15b vector (Novagen, Billerica, MA, USA) and situated downstream from the GB1 (*Streptococcus sp.* protein G IgG-binding domain) protein coding sequence and the Tobacco Etch Virus (TEV) protease cleavage site. To allow the formation of disulfide bridges in the cytoplasm (De Marco, 2009), 13C, 15N-labeled wild-type and K12del proteins were produced in the Origami B(DE3) *E. coli* strain (Novogen, Merck, Kenilworth, NJ, USA). The clones were grown in M9 minimal media, which were supplemented with 1 g/L 15NH4Cl as the sole nitrogen source, or with 1 g/L 15NH4Cl and 2 g/L 13C-D-glucose as the sole nitrogen and carbon sources, respectively. The bacteria were incubated at 37 °C until an optical density (OD) of 0.4 was reached, and continued thereafter at 16 °C. After OD reached 0.6, the protein production was induced by adding 1 mM isopropyl-β-D-1-thiogalactopyranoside (IPTG). After further incubation (16 °C, 16 h), the cultures were centrifuged and the bacteria collected and disrupted by sonication. The remaining supernatant was clarified by centrifugation (30000x*g*). These supernatants, containing GB1-RBP4 polypeptides, were then applied to 1-mL His GraviTrap columns (GE Healthcare, Wilmington, MA, USA) and eluted according to the manufacturer's instructions. The eluted fusion proteins were filtered against PBS and digested with TEV protease. His GraviTrap columns were utilized to cleave off the polyHis-GB1 N-terminus. The resulting RBP was subsequently eluted in the flow-through fraction, concentrated and subsequently applied to a HiLoad 16/60 Superdex 200 gel filtration column equilibrated with 50 mM NaCl, 20 mM NaPO4 pH 6 (later termed the NMR buffer). Fractions containing purified RBP were pooled and the concentrations set to 0.8 mM (16.8 mg/mL). The ÄKTA Purifier FPLC system (GE Healthcare, Wilmington, MA, USA) was utilized for gel filtration.

The NMR spectra of the *E. coli* strain Origami B(DE3) –expressing recombinant canine wild-type and K12del RBP4 were acquired at 308 °K using a Bruker Avance III HD 800 MHz spectrometer (Bruker, Billerica,

Massachusetts, USA) equipped with a cooled 1H, 13C, 15N TCI cryoprobe. An NMR buffer containing 4% D2O was utilized to dissolve RBP samples. The holoRBP was generated by exposing recombinant RBP to 1 μM all-trans retinol in the NMR buffer. Chemical shifts were determined using Transverse Relaxation-Optimized SpectroscopY (TROSY) based, HN-detected triple resonance experiments HNCACB, CBCA(CO)NH, HNCA and HNCOCA (Muhandiram, Kay, 1994, Sattler, Schleucher & Griesinger, 1999, Permi, Annila, 2004). NMR data processing was performed using the TopSpin 3.5 software (Bruker, Billerica, MA, USA) and was analyzed using the Sparky software (Goddard and Kneller, SPARKY 3, University of California, San Francisco).

3.4.4 Dual luciferase reporter assay

In study III, the candidate variant was situated in a putative silencer region. To confirm the silencer and to examine whether the variant has an effect on its activity, a dual luciferase reporter assay was designed. The utilized plasmids contained the wild-type or mutated canine sequence (CanFam 3.1, 250 bp +/- the variant site) (study III/S3 Table) and were cloned into the pNL3.2[*NlucP*/minP] NanoLuc luciferase vector (Promega, Madison, WI, US). The pGL4.54[luc2/TK] firefly luciferase was used as a co-transfection control vector (Promega, Madison, WI, US). Altogether 60,000 MDCK cells per well were seeded 24 h prior to transfection using the Gibco Advanced MEM medium (Thermo Fisher Scientific, Waltham, Massachusetts, USA) supplemented with 10% FBS, 100 U penicillin/streptomycin and Glutamax. Transfection was performed using Lipofectamine3000 (Invitrogen, Carlsbad, US) according to the manufacturer's instructions. The cells were co-transfected with equal amounts (10 ng) of wild-type, mutated or empty experimental vectors and control vector and 90 ng carrier DNA per well.

The Nano-Glo® Dual-Luciferase® Reporter Assay System (Promega, Madison, WI, US) was used for luciferase activity measurement according to the manufacturer's instructions and luminescence was detected using the Enspire 2300 instrument (PerkinElmer Chemagen Technologie GmbH, Baesweiler, Germany). Observed luminescence values were then normalized by determining the ratio between experimental (NanoLuc) and control (firefly) reporters. Results were analyzed by using one-way ANOVA and Bonferroni approach as post-hoc test with a p-value of less than 0.05

considered significant. The assays were performed twice, with 4 to 6 replicates per treatment.

3.4.5 RT-qPCR

In study III, to examine differences in gene expression levels of *HIVEP3, ENSCAFG00000035604, COL9A2, EDN2, KCNQ4* and *NFYC*, a real-time quantitative PCR (RT-qPCR) method was used. First, equal amounts of total retinal RNA from a case and four controls were reverse transcribed to cDNA using the High Capacity RNA-to-cDNA Kit (Applied Biosystems, Waltham, MA, USA). Primers were designed using the Primer 3 software (Koressaar, Remm, 2007), and corresponding forward and reverse primers were placed in different exons to avoid genomic DNA contamination. The housekeeping genes *GAPDH* and *YWHAZ* were used as normalization controls. Efficiencies of all the primers were determined using a seven-point dilution series. RT-qPCR reactions were performed using the SsoAdvanced Universal SYBR Green Supermix (BioRad Hercules, CA, USA) and the CFX96 Touch Real-Time PCR Detection System (BioRad, Hercules, CA, USA) instrument. The comparative $\Delta\Delta C_T$ method was utilized to determine relative expression (Livak, Schmittgen, 2001). Triplicate samples were used in every experiment. The standard deviation of the mean ΔC_T was calculated to determine error bars and the two-tailed Student's T-test to assess statistical significance.

4 Results

4.1 Single-residue deletion in RBP4 with unique maternal transmission causes congenital eye disease in Irish Soft-Coated Wheaten Terriers

4.1.1 Bilateral microphthalmia and other ocular findings in four closely-related litters of ISCWTs

In 2011, a Finnish ISCWT breeder contacted us after noticing abnormal-looking eyes (Figure 13) in a few puppies from her most recent litter of six. An eye examination of the whole litter revealed bilateral microphthalmia, chorioretinal hypoplasia, scleral folding and retinal colobomas in three puppies, while the other three were normal.

Figure 13 *The external eye phenotype of [A] a healthy and [B] a microphthalmia-affected ISCWT puppy.*

In the following years, three other affected litters were born in Poland and in the Czech Republic. The first Polish litter included eight puppies, of which six were diagnosed with bilateral microphthalmia, and one with chorioretinal hypoplasia and unilateral retinal coloboma while one puppy was normal. Two years later, another litter was born to the same dam but with a different sire.

Of those eight puppies, three were diagnosed with bilateral microphthalmia, chorioretinal coloboma and retinal colobomas, and one with unilateral flat optic nerve head, and four were normal. In the fourth and most recent litter, an affected litter of six puppies was born in the Czech Republic. In this litter, five puppies presented with bilateral microphthalmia and one with chorioretinal hypoplasia.

No extra-ocular findings were detected in any of the affected puppies in general exams. In all four litters, the dams and sires had been normal in eye examinations. The pregnant dams were fed high-quality commercial food and no abnormalities were detected during gestation or labor. All four litters were closely related. Based on pedigree analysis, a recessive mode of inheritance was suspected, as affected puppies were born to unaffected parents.

For genetic analysis, our inclusion criterion for cases was bilateral microphthalmia (n=17, 11 males and 6 females). Control dogs (n=23) were examined healthy at 6–10 weeks of age, as tapetal pigmentation in older dogs might mask mild forms of chorioretinal hypoplasia (Bjerkås, 1991).

4.1.2 Microphthalmia locus maps to canine chromosome 28

To map the disease to a specific chromosomal region, genotyping was performed on 12 cases and 17 controls using the Illumina Canine HD Bead Chip (Illumina, San Diego, CA, USA) with 173,662 markers. After frequency and genotyping pruning, 91,542 informative SNPs remained in the analysis. A comparison of allele frequencies between cases and controls using the PLINK 1.07 software indicated a 15.7-Mb critical region on canine chromosome 28 ($p_{raw}=8.04x10^{-9}$, $p_{genome}=1.00x10^{-5}$, study I/Figure 2A). The locus spanned from 287,714 bp to 16,036,936 bp, and all the genotyped cases shared a homozygous haplotype block that was absent in all the controls (study I/Figure 2B). Analyzing the data with GenABEL using a full genomic kinship matrix to adjust population structure and mixed model approximation confirmed the locus (study I/Figure S1).

4.1.3 Whole-genome sequencing reveals an in-frame deletion in *RBP4*

To find candidate variants in the associated chromosomal region, the whole-genome sequencing approach was utilized for one affected dog that was homozygous for the risk haplotype. In total, 470,800,949 reads were collected,

of which 98.7% mapped to the reference sequence. Over 98% of the reference had >10X coverage, while the mean read depth was 28.7X.

When comparing the sequenced case to the reference genome, 6,497,411 homozygous variants were detected. Of these, 37,291 remained after filtering under a recessive model with 342 controls dogs (study I, Table S2) that were free of the studied phenotype and represented different non-ISCWT breeds. Of the remaining variants, 81 were exonic, of which only one resided in the locus: an in-frame 3-bp deletion variant (c.282_284del) in the retinol-binding protein 4 gene (*RBP4*). The deletion results in the loss of a single lysine residue in a charged segment preceding the lipocalin β-barrel domain (study I, Figure 3). The deleted residue p.K30del is located near the RBP amino terminus, corresponding to K12del in the mature protein as the first 18 amino acids form a signal peptide and are cleaved off. The secreted portions of dog and human RBP have 94.5% sequence similarity and are of the same length, 183 amino acids.

4.1.4 Segregation analysis indicates unique maternal inheritance effect

To validate the candidate variant in *RBP4*, all samples from affected litters and their close relatives (Figure 14) were genotyped by Sanger sequencing. As a result, all the cases (n=17) were homozygous for the variant and all the confirmed controls (n=23) were either wild-type or heterozygous for the variant. Surprisingly, all the dams (n=3) of the affected litters were also homozygotes but had been normal in eye examinations. Their dams were all heterozygotes, suggesting that the disease manifests only if both the dam and the puppy are homozygous for the variant.

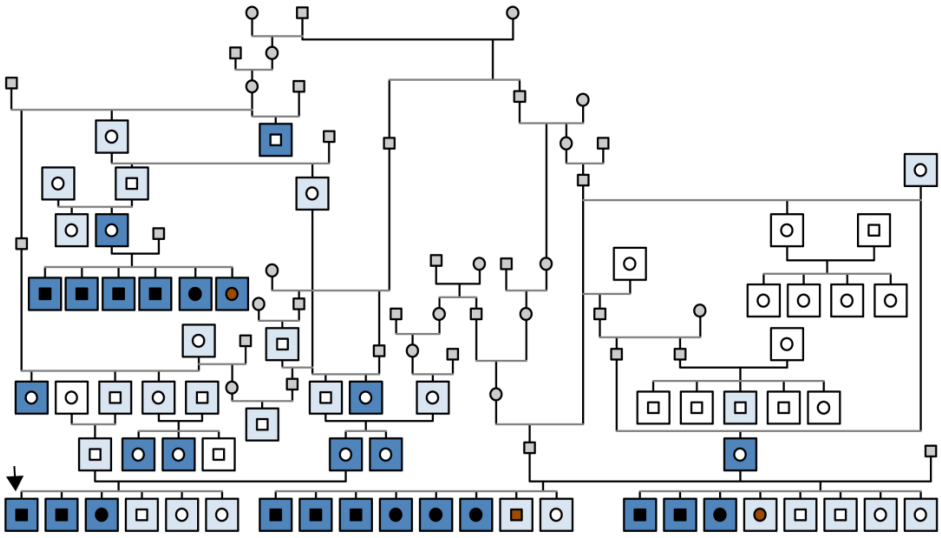

Figure 14 *Schematic representation of the ISCWT pedigree illustrates the four affected litters and their close relatives. Males are presented as squares and females as circles. Microphthalmia-affected dogs are marked with black, chorioretinal hypoplasia with brown and unaffected dogs with white. Dogs that were unavailable for genetic studies are marked with grey. The RBP4 variant status is marked in either dark blue (variant homozygotes), light blue (heterozygotes) or white (wild-types) background and indicates a strong maternal effect on inheritance as bilateral microphthalmia was only observed if both the dam and the offspring were homozygous for the variant. The arrow points to the whole-genome sequenced individual.*

As further validation, all available ISCWT samples in our biobank (n=248) were genotyped by Sanger sequencing. Of these dogs, 185 (74.6%) were wild-type, 55 (22.2%) heterozygous and 8 (3.2%) homozygous for the variant. Of the eight new deletion homozygotes, three had been normal in eye examination done when they were adults, four had been normal and without apparent microphthalmia in general examination, and one had been diagnosed with chorioretinal hypoplasia as a puppy. Maternal genotypes could be determined for seven of the new homozygotes. The dam of the chorioretinal hypoplasia case was homozygous for the deletion, while others were heterozygotes. This breed screening data, together with data from the initial cohort, indicates a strong maternal effect on inheritance ($p<10^{-6}$, Fisher's exact test, *df*=1, study I/Table 1), as the disease manifested only if both the dam and the puppy were homozygous for the deletion (17/18), whereas deletion homozygotes with heterozygous dams all had grossly normal eye anatomy

(9/9). The penetrance of the microphthalmia trait is therefore either 94% or 0%, depending on the dam genotype.

As some of the human *RBP4* alleles have dominant modes of inheritance (Chou et al., 2015), further investigations of the clinical statuses of the deletion carriers were conducted. Of all 71 heterozygotes identified in the both screening cohorts, 46 had been eye examined and, for 37 of these dogs, the dam genotype was known as 12 were wild-type, 11 heterozygous and 14 homozygous for the deletion. None of the dogs presented with microphthalmia, but two had been diagnosed with chorioretinal hypoplasia. These dogs were littermates of the microphthalmia cases (Figure ISCWT_pedigree), and their dams were homozygotes. All other eye examined deletion carriers with homozygote dams were normal, including eight dogs that were examined before 10 weeks of age, allowing for reliable phenotyping (Bjerkås, 1991).

As further validation and investigation of possible mild retinal pathologies, optical coherence tomography imaging was performed on 11 ISCWTs of different genotypes. All the imaged dogs (three wild-types, four heterozygotes and four deletion homozygotes) had been normal in eye or general examinations. Whole-retinal thickness and photoreceptor layer thickness were within normal limits in all individuals, and no statistically significant differences were found when different genotype groups were compared (study I/Figure S2).

To summarize, for offspring to develop the eye disease, the dam has to be a deletion homozygote, while the genotype of the puppy determines the phenotype severity. If the dam was a deletion homozygote, its deletion homozygote puppies presented with bilateral microphthalmia with nearly complete (94%) penetrance and heterozygous puppies with chorioretinal hypoplasia with low (14%) penetrance, whereas offspring of heterozygous dams were all normal, regardless of the offspring genotype.

4.1.5 Dose-dependent decrease in circulating RBP4 and vitamin A *in vivo*

Under normal circumstances, RBP4 circulates in the bloodstream and transports vitamin A from its liver stores to peripheral tissues. During gestation, this is of particular importance as the developing embryo receives vitamin A through the placenta from the hepatic stores of its mother and RBP4 acts as the carrier protein in both individuals. Potentially, the K12 deletion

might lead to disrupted folding, stability or secretion of RBP4, which could then result in altered retinol-binding properties or interaction with its cell-surface receptor, the STRA6 encoded by the stimulated by retinoic acid 6 gene (Kawaguchi et al., 2012). To investigate these, serum and urine samples from 17 ISCWTs were collected and analyzed. The sample cohort included eight variant homozygotes, of which three were affected with bilateral microphthalmia, six were heterozygotes and three were wild-type dogs. Western blotting under reducing conditions showed a dose-dependent decrease in the circulating RBP4 (±SD) as the heterozygotes had roughly half (0.66 ± 0.20) and homozygotes a fourth (0.24 ± 0.10) of the circulating protein amount compared to the wild-type mean (study I/ Figure 4). The observed reduction in circulating RBP4 might result from either reduced secretion or stability of the mutated protein. A western analysis of urinary RBP4 detected protein in only one homozygote and one heterozygote at a level of 1/20th of the mean wild-type serum level (study I/Figure S4), which indicates that the observed decrease in serum is not likely to result from increased renal loss. The two dogs with detectable levels of urinary RBP4 probably have impaired renal function, which should be studied further.

As with serum RBP4, a similar dose-dependent decrease was also observed for the serum vitamin A levels (±SD), as they, too, were severely reduced in homozygotes (0.06 ± 0.02 mg/L, $p<0001$), mildly reduced in heterozygotes (0.34 ± 0.13 mg/L) and normal in wild-type dogs (0.55 ± 0.20 mg/L, normal reference range in dogs 0.3–1.3 mg/L). Interestingly, vitamin A deficiency was seen in both clinically affected and unaffected homozygotes. The observed reduction correlated directly with immunoreactive RBP4 across genotypes (r^2=0.88, study I/Figure 4).

4.1.6 K12del RBP4 circulates as a homodimer *in vivo*

To study the structure of the circulating K12del RBP4 more closely, the western analysis of the ISCWT serum samples was repeated under non-reducing conditions. In the homozygote sera, the protein was observed to migrate as an apparent homodimer of 42 kDa (study I/Figure 4). The mutant protein was also found to be more antigenic than the wild-type monomer, indicating the mutant protein is probably partially unfolded *in vivo*. Analyzing the heterozygote sera indicated that the K12del RBP4 does not significantly dimerize with wild-type protein or reduce its secretion as the dimer/monomer

ratio in these individuals was 0.23 ± 0.04, reflecting the overall reduction in serum RBP4.

4.1.7 K12del RBP4 forms dimers and is poorly secreted from cultured HeLa cells

As further characterization of the K12del RBP4 structure and function, western analyses were conducted. The experiments were performed under reducing and non-reducing conditions on conditioned media (CM) and cell lysates of transfected HeLa cells expressing the canine wild-type and mutated protein and human wild-type and mutated isoforms including the corresponding K12del and E13del mutants as well as stable (A55T) and unstable (G75D, I41N) isoforms (Chou et al., 2015). This showed that 89% of the secreted canine K12del RBP4 fraction appeared as dimers, while 99.3% of the wild-type polypeptide were monomers (study I/Figure 5A, left). Of the human mutant isoforms, the K12del, E13del, G75D and I41N were also predominantly (>85%) secreted as dimers, while dimer fraction in A55T and wild-type were <1% (study I/Figure 5A, left).

To study changes in polypeptide secretion, immunoreactivity of corresponding isoforms was compared in CM and cell lysates. This indicated that both canine K12del and human E13del isoforms accumulated in the cytoplasm as lysate-to-CM ratios were 1.5 and 6.0, respectively (study I/Figure 5C, right). Interestingly, monomers and dimers were equally abundant in K12del and E13del cell lysates, while monomers were sparse (<15%) in CM. In wild-type, monomers account for over 99% of immunoreactive polypeptides in cell lysates and CM. To conclude, these results suggest that the ISCWT mutation causes disrupted folding and reduction in the secretion of RBP4 and support the results obtained from ISCWT serum samples.

4.1.8 K12del protein forms monomers and binds vitamin A *in vitro*

To study K12del folding in the oxidizing cytoplasmic environment, the canine K12del and wild-type proteins were expressed also in *E. coli* Origami B(DE3) and studied with nuclear magnetic resonance (NMR). The isoforms predominated as monomers, although they both had small dimeric peaks at elution volume 82 mL, and the peak was stronger in the K12del

chromatogram. Heteronuclear single quantum coherence spectra indicated uninterrupted folding, while chemical shift perturbations were detected for residues spatially close to the deletion site (study I/Figure 6A–C). The residues C4 and C160 were observed to be oxidized, as their cysteine b-carbon chemical shift values were 38.6 and 40.7 ppm, respectively, and the corresponding value for a reduced cysteine is 28.3 ± 2.2 ppm (Sharma, Rajarathnam, 2000). The oxidized residues can therefore form a wild-type-like disulfide bond within the K12del polypeptide *in vitro*.

The capacity to bind retinol was also studied with NMR spectroscopy, which showed chemical shift perturbations in the same residues in K12del and wild-type isoforms induced by equimolar ratios of vitamin A (study I/Figure 6E). To conclude, unlike *in vivo* experiments and outside the mammalian ER lumen and Golgi network, the K12del isoform seems to fold and bind vitamin A appropriately *in vitro*.

4.2 A novel missense mutation in *ADAMTS10* is associated with primary open-angle glaucoma in Norwegian Elkhounds

4.2.1 Eye examinations reveal severe POAG in NEs

In study II, an initial discovery cohort of 24 NEs from Finland, Norway, Sweden, the United Kingdom and the United States was established to study the genetic cause of POAG in the breed. The inclusion criterion for cases was bilateral glaucoma without any detectable underlying cause. Controls were eye examined healthy at the age of eight years or older. A thorough eye examination of the cohort revealed 16 cases and eight controls. All the cases presented with elevated IOP (25–86 mmHg, normal reference range 10–20 mmHg) and various degrees of optic nerve head atrophy and cupping. Various secondary changes, such as lens luxation, corneal stromal edema and keratitis, were also detected. On average, the dogs were 6.5 years old at the time of diagnosis. Progressive vision loss led to complete blindness within two years after diagnosis. In all affected dogs, response to IOP-reducing medical treatment was either short-term or absent, and bilateral enucleation or euthanasia were conducted to control the pain caused by high IOP.

4.2.2 GWAS maps the disease to a known canine POAG locus

To analyze the mode of inheritance and enable sample choosing for genetic analyses, a pedigree was drawn around the affected NEs (study II/Figure 1). Pedigree analysis suggested an autosomal recessive mode of inheritance, as affected dogs were born to unaffected parents.

To map the disease-associated chromosomal region, genotyping was performed on nine cases and eight controls using the Illumina Canine HD Bead Chip (Illumina, San Diego, CA, USA) with 173,662 markers, of which 89,277 remained in the analysis after quality control procedures. Comparison of allele frequencies between cases and controls indicated a 750-kb locus on the canine chromosome 20 ($p_{raw}=4.93x10^{-6}$, $p_{genome}=0.025$, study II/Figures 2A–B). A mild population stratification was detected ($\lambda=1.1$); however, the association was confirmed with two mixed-model approaches that gave the same results.

The implicated locus spanned from 53,070,684 bp to 53,816,416 bp, and all genotyped cases shared there a homozygous haplotype block that was absent in the controls (study II/Figure 2C). The locus contained 35 genes, one of which, the ADAM metallopeptidase with thrombospondin type 1 motif, 10 (*ADAMTS10*) had previously been implicated in POAG in Beagles (Kuchtey et al., 2011, Kuchtey et al., 2013).

4.2.3 Candidate gene approach reveals a fully-penetrant missense variant in *ADAMTS10*

Because of the previous association to canine POAG, *ADAMTS10* was chosen for candidate gene analysis, and all its coding regions and splice sites were studied for candidate variants in four cases and four controls. Screening identified 10 variants (study II/Table S3) altogether, two of which segregated with the phenotype. The other, a synonymous variant (p.P171P), was not suspected to be in the exonic enhancer region based on ESE-finder results (Smith et al., 2006), whereas the other, a missense variant (p.A387T), was predicted to be pathogenic by Polyphen-2 and SIFT (Ng, Henikoff, 2001, Adzhubei et al., 2010). The p.A387T variant changes a highly conserved residue (study II/Figure S1) in the metalloprotease domain of ADAMTS10 (study II/Figure 3C) and was therefore selected for further validation.

Genotyping of the remaining 12 cases indicated that all but two of the cases were also homozygous for the p.A387T variant. These genetically distinct

cases might represent primary glaucoma from a different genetic cause or might actually have secondary glaucoma misinterpreted as primary in the clinical examinations. A breed screening cohort of 572 NEs randomly selected from our biobank found 420 (73.4%) wild-type NEs, 151 (26.4%) heterozygotes and 1 (0.17%) homozygote. This additional homozygote dog was five years old at the time of the study (2014) and was then unaffected. However, it was later diagnosed with bilateral glaucoma and, thus, the penetrance of the p.A387T variant is complete.

To study the breed-specificity of the variant and as further validation, the variant was screened in 71 glaucoma or PLA cases from 17 breeds and 115 unaffected dogs from six breeds, all of which proved to be wild-type.

4.3 Two new loci and a putative regulatory variant in Miniature Schnauzers affected with progressive retinal atrophy

4.3.1 Clinical examinations suggest multiple different types of PRA in MSs

In study III, an initial discovery cohort of 85 Finnish MSs was established to study the genetic cause of PRA in the breed. The inclusion criteria for cases were bilateral PRA with tapetal hypo- and hyperreflectivity, retinal blood vessel attenuation and pale optic nerve heads. The controls were examined healthy at the age of seven years or older. Phenotyping revealed altogether 18 cases and 67 controls. The age of onset and rate of disease progression seemed to divide the cases into two subtypes as 12 of the affected dogs were diagnosed with severe PRA and total blindness before the age of five years (termed tentatively type 1 cases); the 6 remaining (type 2) cases had distinctively slower disease progression as the average age of onset was seven years, and they still had some visual capacity left at the time of examination. Of the type 1 cases, five were female and seven male, while of the type 2 cases, only one was female and the rest five male, suggesting the type 2 disease might have an X-linked mode of inheritance or other gender-associated disease predisposition.

In addition to regular eye examinations, OCT imaging was performed on one PRA case to study the phenotype in more detail. The studied MS was a four-year-old female that already suffered from total blindness and therefore

most probably represented the type 1 phenotype. OCT imaging revealed total loss of the photoreceptor cell layer (study III/Figure 1), confirming the PRA diagnosis. Unfortunately, no type 2 cases were available for OCT imaging.

The whole study cohort was screened for a variant in *PPT1*, which was published in the course of this study and proposed as a possible genetic cause of autosomal recessive PRA in MSs (Murgiano et al., 2018). As a result, all the type 1 cases were homozygous for the variant, whereas of the type 2 cases, five were wild-type and one heterozygous, suggesting the variant in *PPT1* might indeed replicate in the Finnish sample cohort for the type 1 disease. However, screening of the controls revealed 41 wild-type, 22 heterozygous and 4 homozygous MSs, which accounts for a disease penetrance of only 75%. The discordant cases suggested that the reported *PPT1* variant might actually be in linkage disequilibrium with the true causative variant, which in turn still remained to be uncovered.

4.3.2 GWAS confirms that MSs are affected with at least two genetically distinct types of PRA

To evaluate the mode of inheritance and enable sample selection for genetic analyses, a pedigree was drawn around the 18 affected MSs (study III/Figure 2). As affected dogs were born to unaffected parents and there were multiple affected individuals in some of the diseased litters, a recessive mode of inheritance was suspected. As noted above, if there were indeed multiple genetic forms of the disease, the type 2 phenotype might have an X-linked mode of inheritance, while the type 1 seemed autosomal recessive.

To map the disease to a specific chromosomal region, genotyping was performed in 16 cases and 33 controls using the Illumina Canine HD Bead Chip (Illumina, San Diego, CA, USA) array with 173,662 markers. After quality control procedures, 102,661 SNPs remained in the subsequent analysis and comparison of allele frequencies between cases (regardless of suspected type) and controls suggested an association to the CFA15 ($p_{raw}=4.70x10^{-6}$, $p_{genome}=0.19$, $\lambda=1$). In the best-associated region, 7.2-Mb homozygous haplotype block spanning nucleotides 213,416–7,403,217 bp was observed in all genotyped type 1 cases and was absent in all type 2 cases and 32 controls (Figure 15). Interestingly, the putative risk haplotype was seen in one control dog, which was, like all the other controls, confirmed to be free of PRA at the age of seven years. This suggests the disease-causing variant has either an

incomplete penetrance or such a recent origin that not all the risk haplotype-carrying dogs have it.

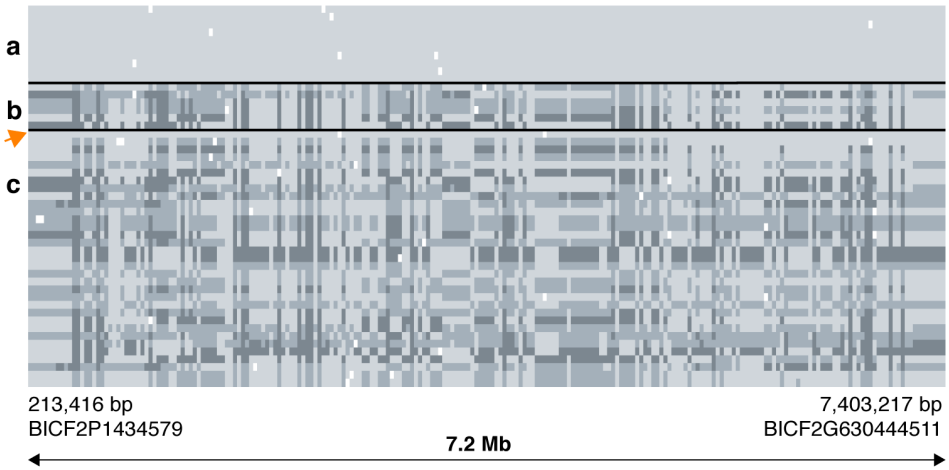

Figure 15 *GWAS analysis with 16 cases and 33 controls indicated a tentative association to CFA15 (p_{raw}=4.70x10^{-6}, p_{genome}=0.19). In the 7.2-Mb critical region, all the earlier onset cases (a) with rapid disease progression (tentatively termed type 1 cases) shared a homozygous haplotype. The later-onset cases (b) with slower disease progression (type 2 cases) did not have the risk haplotype, indicating the two clinically differing types are indeed genetically distinctive. Of the 33 controls (c), 32 were not homozygous for the risk haplotype, while 1 (orange arrow) was. This dog, like all the other controls, was eye examined healthy at the age of seven years, indicating either incomplete penetrance or such a recent origin of the causal variant that not all risk haplotype-carrying dogs have it. Rows represent individual dogs and columns genotyped SNPs. Light gray indicates affected, intermediate heterozygous and dark gray wild-type genotypes.*

Next, the genotyping data were analyzed separately for the two suspected types of PRA. First, GWAS was performed in the type 1 cases (n=10) and controls (n=33). Altogether 100,501 SNPs were included in the analysis after quality control procedures and case-control comparison of the allele frequencies confirmed that the type 1 disease is associated with the above-mentioned chromosomal region on the CFA15 (p_{raw}=2.08x10^{-9}, p_{genome}=2.40x10^{-4}, λ=1.17, study III/Figures 3A–B).

Then, GWAS was performed in the type 2 cases (n=6) and controls (n=33) and with 102,286 SNPs that remained after quality control procedures. This

analysis resulted in a tentative association on the CFAX (p_{raw}=7.06x10^{-7}, p_{genome}=0.17, λ=1.19, study III/Figures 3C–D), thus supporting the hypothesis of an X-linked mode of inheritance for type 2 PRA in MS. In the best-associated region, three of the six cases shared a 15.4-Mb homo-/hemizygous haplotype block from 38,294,920 bp to 53,726,107 bp, which was absent in rest of the cases and all controls. The tentative locus should be confirmed in a larger sample set before any further genetic analyses are performed as the number of cases in this analysis was very limited. The known canine PRA-implicated gene on the CFAX, the *RPGR* (Zhang et al., 2002, Acland et al., 1994, Vilboux et al., 2008, Kropatsch et al., 2016), does not reside in the preliminary locus.

To summarize, GWAS confirmed multiple genetic forms of PRA in MS, which was already suspected based on the distinctive clinical findings such as age of onset and disease progression. Earlier-onset type 1 disease was mapped to a locus on CFA15, where all the type 1 cases shared a homozygous risk haplotype block. In addition, the risk haplotype was also seen in one genotyped control, indicating an incomplete penetrance of the causal variant or such a recent origin that not all the risk haplotype-carrying dogs have it. The later-onset type 2 disease was tentatively mapped to CFAX, which needs to be confirmed prior to any further genetic analyses.

4.3.3 Whole-genome sequencing approach indicates a recent origin for type 1 PRA –specific variant

To find the causative variant for type 1 PRA in MSs, whole-genome sequencing was performed in two cases that were homozygous for the risk haplotype and one control MS with the opposite haplotype. For these three MSs, 467,778,694–512,026,483 reads were collected with 99.5% of them mapping to the reference sequence. The mean read depths were 29–31X and over 97% of the reference had >10X coverage. Filtering was performed under the autosomal recessive model, assuming the cases were homozygous for the alternative allele, and at least 99% of the controls (including the control MS and 267 other dogs (study III/S1 Table) from different breeds and without the studied phenotype) wild-type. Of the control dogs, 141 were whole-genome sequenced enabling their usage as controls in the mobile element insertion (MEI) analysis, whereas the rest were exome-sequenced and were therefore available only for analyzing single nucleotide variants and small insertions and deletions.

The two sequenced MSs shared 2,149,016 homozygous variants altogether, of which 5,235 were left after filtering. Of these, 233 resided in the mapped locus (study III/S2 Table) and 4 (study III/Table 1) were selected for validation based on their predicted effect on amino acid sequence or splicing. The whole initial study cohort of 85 MSs was included in the validation. All the type 1 cases (n=12) were homozygous for all four variants, but so were also the four (for the *DLGAP3* variant) or the two (for the other three variants) control dogs. Therefore, all four variants were associated with the type 1 disease, with a statistical significance 10–100 times stronger than the *PPT1* variant (study III/Table 1) but, again, with incomplete penetrance. Case-specific MEIs or large structural variants were not found.

WGS and GWAS results together indicate that the causal variant most probably has a very recent origin, and not all risk haplotype-carrying dogs have it. Therefore, there will be many variants that are in tight linkage disequilibrium with it, and the validated four WGS and *PPT1* variants most probably represent these rather than any of them being the actual mutation.

After excluding the four WGS variants with predicted effect on either amino acid sequence or splicing, 229 candidate variants without any putative functional effect were left. To reduce the number of potential causal variants, whole-genome sequencing was performed in an obligate carrier MS. To maximize the effect of this additional control on filtering, the sequenced individual was selected to be homozygous for the risk haplotype. This way, the number of variants to be validated in the wet lab was reduced to two: an intergenic 5-bp deletion variant (g.1,887,878_1,887,882del) and an intronic single-nucleotide variant (g.1,432,293G>A) in human immunodeficiency virus type I enhancer binding protein 3 gene (*HIVEP3*, study III/Figures 4A–B) coding a transcription factor. Validation in the study cohort of 85 MSs excluded the intergenic variant from further analyses as 12 of the controls were homozygous for it. In contrast to all previously validated variants, the one in the *HIVEP3* intron had complete penetrance and a very strong association ($p=4.00x10^{-25}$) with the type 1 phenotype as all 12 type 1 cases were homozygous for it and all 67 controls were either wild-type (n=58) or heterozygous (n=9). As further validation, the *HIVEP3* variant was screened in all available MS samples (n=514) from our dog DNA bank. This cohort included three PRA cases and 118 MSs eye examined healthy at the age of five or older. Of this breed screening cohort, 456 (88.7%) were wild-type, 55 (10.7%) heterozygous and three (0.58%) homozygous for the variant. The three identified new homozygotes represented the three PRA cases in the cohort. Combining the results from the initial and breed screening cohorts, the

intronic variant in *HIVEP3* has complete penetrance and a very high association ($p=1.10x10^{-42}$) with the type 1 PRA in MS. The variant seems breed-specific as it was absent in all genomes obtained from dogs (n=735) of different breeds available through the Dog Biomedical Variant Database Consortium.

4.3.4 Type 1 PRA-associated variant lies within a putative silencer with HAND1::TCF3 transcription factor binding motif

As the variant in *HIVEP3* lies within the deep intronic region and is kilobases away from exon-intron boundaries (study III/Figure 4A), its function would be regulatory rather than affecting amino acid sequence or splicing. The variant site also includes a predicted dog-specific long non-coding RNA *ENSCAFG00000035604* that is antisense to *HIVEP3* and could therefore be a negative regulator of it. To study whether the variant affects retinal gene expression in either of these genes, RT-qPCR was performed with retinal samples from a type 1 PRA-affected MS and four control retinal samples from dogs that were wild-type for the variant and without the studied phenotype. As a result, no statistically significant differences were observed. Sanger sequencing of the retinal cDNA of the case revealed no splicing defects for either of the genes.

The sequence surrounding the variant site is ultraconserved among species (study III/Figure 4C), suggesting that the site might still have a regulatory function and contain, for instance, an enhancer or silencer. To examine this, the canine variant site was converted to a corresponding position in the human genome, and on the exact site lies a peak of ENCODE DNaseI hypersensitivity cluster, which indicates an open chromatin environment (Thurman et al., 2012). Predicted transcription factor binding sites (TFBSs) were analyzed for the variant position, and as a result, putative HAND1::TCF3 complex TFBS overlapped exactly the variant site (study III/Figure 4C).

To confirm the enhancer or silencer and study whether the variant has an effect on its activity, a dual luciferase reporter assay was designed. Constructs containing wild-type and mutant canine sequence (500 bp) and an empty vector (study III/S3 Table) were transfected into MDCK cells, and relative luciferase activity was measured. This revealed significantly lower activity in cells transfected with wild-type constructs when compared to empty constructs ($p<0.05$), thus supporting the silencer role. In addition, the type 1 PRA-associated variant seems to disrupt its activity, at least partially (study

III/Figure 5), as cells transfected with the mutant constructs showed significantly higher reporter gene expression compared to the wild-type constructs ($p<0.05$).

4.3.5 Two predicted HAND1::TCF3 target genes, *COL9A2* and *EDN2*, are overexpressed in the case retina

As silencers and promoters of regulated genes share common TFBSs (Andersson et al., 2014), presence of the HAND1::TCF3 motif in the promoters of variant flanking genes (+/- 1.25 MB) in the dog genome were analyzed. This revealed 714 predicted HAND1::TCF3 binding sites in the promoter regions of 60 genes (study III/S4 Table) in close proximity to the variant. Due to limited amount of available retinal RNA from an affected MS, expression analysis of all the 60 genes could not be done. Therefore, the target genes were prioritized based on known retinal expression in FANTOM5 and Human Protein Atlas data (Forrest et al., 2014, Uhlen et al., 2015), motif scanning score and canine retinal STRT data. After prioritization, the four best candidates, the *COL9A2, EDN2, KCNQ4* and *NFYC*, were selected for RT-qPCR conducted with the same sample set described above for *HIVEP3* and *ENSCAFG00000035604*. As a result, retinal expression of *COL9A2* was increased more than 4-fold and *EDN2* more than 16-fold in the case retinas compared to the controls (study III/Figure 4D), accounting for a statistically significant overexpression for both ($p=0.049$ and $p=0.0023$, respectively). *KCNQ4* was increased more than 10-fold in the case retina, but this was not statistically significant ($p=0.065$), as the expression in retinal samples of the right and left eyes of the affected MS differed so much from each other. A significant change in *NFYC* expression was also not observable ($p>0.05$).

5 Discussion

In this doctoral dissertation, new genetic variants, genes and a novel mode of maternal inheritance were discovered for three blinding eye disorders in dogs. The studies were conducted by utilizing the established dog biobank in Finland and by recruiting hundreds of new well-phenotyped dogs. Novel genome wide approaches were used to find candidate variants, which were further studied with various functional tests. New collaborations between basic and clinical researchers were established and new networks created between veterinary and human medical researchers. The results, discussed in the following chapters in detail for each study, have multiple scientific and practical implications in both veterinary and human medicine.

5.1 New mode of maternal inheritance and a novel candidate gene in canine congenital eye disease

In study I, combining careful clinical and genetic analyses, an in-frame deletion in *RBP4* was detected as the cause of microphthalmia in Irish Soft-Coated Wheaten Terriers. The disease manifested only if both the dam and the offspring were homozygotes, indicating a new maternal mode of recessive inheritance. The mutated protein appeared misfolded and dose-dependent decrease in circulating RBP4 and vitamin A were observed *in vivo*.

In normal circumstances, RBP4 circulates in serum and transfers vitamin A from liver stores to peripheral tissues, where STRA6 acts as its receptor (Kawaguchi et al., 2012). During gestation, the developing embryo receives vitamin A through the placenta from the mother, and functional RBP4 on both sides are needed to prevent fetal vitamin A deficiency, a known risk factor for congenital eye defects (Hornby et al., 2002). Mutations in human *RBP4* have previously been implicated in microphthalmia with a dominant mode of inheritance, maternal effect and variable penetrance (Chou et al., 2015), as well as to recessive night blindness in compound heterozygous sisters (Biesalski et al., 1999). In ISCWTs, the maternal genotype determined whether a phenotype manifests in offspring, while the puppy's own genotype determined the severity of the disease. In knock-out mice, a similar recessive mode of inheritance has been observed, but only if the dam is fed a vitamin A –deficient diet during gestation (Quadro et al., 2005). Differences in modes of inheritance and disease manifestation may reflect different mutation types,

species-specific anatomical and functional differences in the placenta, non-RBP4–dependent vitamin A delivery, such as postprandial delivery of retinyl ester in chylomicron particles (D'Ambrosio, Clugston & Blaner, 2011) or direct vitamin A transport via uterine luminal secretion (Suire et al., 2001). It is also possible that the dog, a polyembryonic animal, is more resistant to gestational vitamin A deficiency than humans.

To understand the pathology caused by the discovered mutation, the structure and function of the K12del-RBP4 were studied in canine serum and urine samples as well as in HeLa cells and *E. coli* Origami B(DE3), expressing the recombinant canine mutant and wild-type isoforms. *In vivo*, a dose-dependent decrease in circulating RBP4 and vitamin A were detected. In addition, the mutated polypeptide predominated as a homodimer, while the wild-type was in monomeric form. Experiments with HeLa cells supported these findings as the mutated protein also formed dimers. A reduction in circulating RBP4 may result from either decreased secretion from hepatocytes or increased renal loss. Physiologically, RBP4 binds TTR to increase its molecular weight and to escape glomerular filtration (Vahlquist, Peterson & Wibell, 1973). To detect possible increased renal loss of K12del-RBP4, urinary immunoreactive RBP4 and K12del-RBP4's ability to bind TTR were analyzed. As a result, the observed reduction in circulating RBP4 *in vivo* is more likely to result from reduced secretion than increased renal loss as the mutated protein was found to be more abundant in HeLa cell lysates than in CM, and immunoreactive K12del-RBP4 in urine was detected in only one mutant homozygote dog, even though the K12del polypeptide was evidently unable to bind TTR.

In contrast to *in vivo* and HeLa cell experiment results, *in vitro* studies of K12del-RBP4 indicated uninterrupted folding. These contradictory results most probably reflect differences in protein folding environments in eukaryotes and prokaryotes. In eukaryotes, multiple chaperones facilitate disulfide bond formation to residues C120-C129, C4-C160 and C70-C174, in this order, during oxidative folding of wild-type RBP4 in ER microsomes (Selvaraj, Bhatia & Tatu, 2008). In canine hepatocytes and human cervical carcinoma cells, the K12del-RBP4 misfolded due to one or more failed disulfide bond formations within the ER lumen or during or after translation and signal peptide cleavage, which left some cysteines unpaired. In an oxidizing *E. coli* cytoplasm, the K12del polypeptide was able to fold correctly and form internal disulfide bonds.

Like protein folding, retinol binding capacity also appeared unchanged in K12del-RBP4 *in vitro*, while a dose-dependent decrease in serum vitamin A

was detected *in vivo*. These results indicate that the observed vitamin A deficiency in mutant homozygote dogs either result from a reduced *amount* of circulating K12del-RBP4, or its reduced *capacity* to mobilize retinol. The latter hypothesis is supported by the observed abnormal folding of the mutated protein, which most likely has a harmful effect on its functional properties too (Berni, Formelli, 1992). Formally, this could be distinguished as described before (Chou et al., 2015), although the clinical consequences remain the same.

To our knowledge, this study was the first implication of *RBP4* in canine disease genetics and the first report of a causative mutation for isolated microphthalmia in dogs. The mode of maternal inheritance, distinct from imprinting and oocyte-derived mRNA, highlights the delicate interaction between the mother and the developing embryo and suggests this phenomenon might be more common than suspected in other species too. Conventional assumptions in variant filtering and segregation analyses in an assumed autosomal recessive mode of inheritance would lead to false-negative results, as the clinically unaffected mothers are not obligate carriers. Based on our results, particular attention is called for when studying the genetics of developmental defects, but caution should be exercised for other phenotypes, too.

5.2 A novel missense variant in *ADAMTS10* is associated with canine primary open-angle glaucoma

In study II, a novel recessive missense variant in *ADAMTS10* was discovered as the likely cause of primary open-angle glaucoma in Norwegian Elkhounds. The same gene, but with different mutated residue, has previously been implicated in canine POAG in a laboratory colony of Beagles (Kuchtey et al., 2011, Kuchtey et al., 2013). The NE variant changes a highly conserved residue in the metalloproteinase domain of ADAMTS10, which likely impairs its function and subsequently leads to POAG.

ADAMTS10 belongs to the ADAMTS (a disintegrin and metalloproteinase domain with thrombospondin type-1 motifs) family of zinc-dependent proteases with 18 other genes (Porter et al., 2005). The ADAMTSs are secreted proteins that consist of a signal peptide, pro-, metalloproteinase, disintegrin-like, cysteine-rich and spacer domains, and varying repeats of thrombospondin type 1 motifs, of which ADAMTS10 has five copies (Figure 16) (Porter et al., 2005, Somerville, Jungers & Apte, 2004). Some members

also have other domains, such as the protease and lacunin (PLAC) domain found in the ADAMTS10 carboxyl terminus (Somerville, Jungers & Apte, 2004). In dogs, the ADAMTS10 protein is preferentially expressed in the trabecular meshwork compared to other ocular tissues (Kuchtey et al., 2011). In mice, *Adamts10* is strongly expressed in embryonic ocular tissues, including in the ciliary margin zone, primary lens fibers, lens epithelium, retinal ganglion cells, non-pigmented ciliary epithelium, corneal and scleral cells in the limbal region and cells around Schlemm's canal (Wang et al., 2018). It is also widely expressed in several extra-ocular tissues in humans and mice (Somerville, Jungers & Apte, 2004).

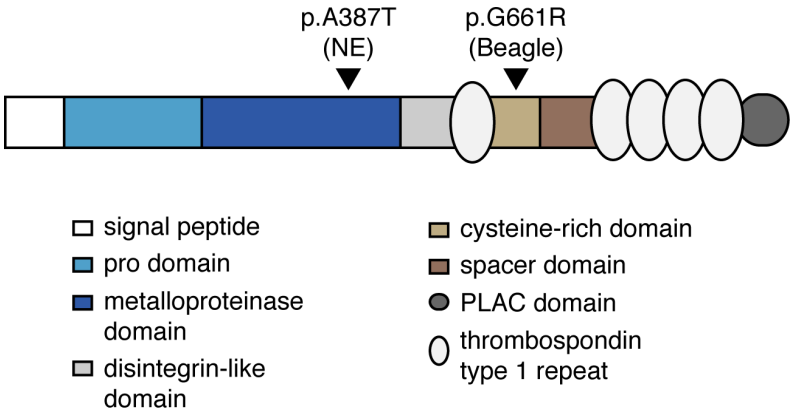

Figure 16 *A schematic representation of the ADAMTS10 polypeptide with a typical ADAMTS family structure. The p.A387T variant is located in the metalloprotease domain, while the previously reported canine variant resides within the cysteine-rich domain.*

ADAMTS10 interacts with fibrillin-1 (FBN1) and promotes its deposition into the extracellular matrix (ECM) (Kutz et al., 2011). Cells with defective ADAMTS10 have impaired focal adhesion and epithelial cell-cell-junction formation (Cain et al., 2016), indicating its important role in ECM composition and dynamics. ADAMTS10 might also participate in the storage and regulation of latent transforming growth factor beta expression (TGFβ) (Ramirez, Rifkin, 2009, Ramirez, Sakai, 2010, Hubmacher, Apte, 2011, Sengle et al., 2012), which is elevated in the glaucomatous aqueous humor (Tripathi et al., 1994).

In humans, several mutations in *ADAMTS10* have been reported to cause Weill-Marchesani syndrome (WMS) (Dagoneau et al., 2004, Steinkellner et al., 2015), which is characterized by short stature, brachydactyly, joint

stiffness and multiple ocular defects, including glaucoma, microspherophakia and ectopia lentis. Fibroblasts derived from WMS patients with *ADAMTS10* mutations have impaired ECM formation and a disorganized cytoskeleton (Dagoneau et al., 2004, Kutz et al., 2011), which is consistent with the known biology of ADAMTS10.

A missense variant (p.G661R) in *ADAMTS10* has previously been implicated in POAG in Beagle dogs (Kuchtey et al., 2011, Kuchtey et al., 2013). The p.G661R variant changes a highly conserved residue in the cysteine-rich domain of the mature protein and is predicted to alter protein folding (Kuchtey et al., 2011). In addition, a splicing variant in *ADAMTS17* has been associated with primary lens luxation but not with glaucoma in several dog breeds (Farias et al., 2010, Gould et al., 2011).

The canine p.A387T variant affecting NEs is located in the metalloproteinase domain, like three of the reported human *ADAMTS10* mutations causing WMS (Dagoneau et al., 2004). However, there are clear differences in the resulting phenotypes, as the p.A387T homozygote dogs, like the p.G661R affected Beagles (Kuchtey et al., 2011), did not present with any of the extra-ocular symptoms reported in the human patients. Primary lens luxation was also absent in the NEs, although lens luxation was diagnosed in several dogs after glaucoma and was thought to be secondary to it. However, now knowing the likely genetic cause of glaucoma in the breed and considering the known function of ADAMTS10 in human ciliary zonules, it might be more probable that lens luxation in NE is actually a direct result of the p.A387T variant. Therefore, lens luxation is primary rather than secondary, even though timewise it is observed after glaucoma has been diagnosed. In contrast, *Adamts10*-knock out mice lack ectopia lentis, while their phenotype otherwise resembles the symptoms observed in WMS patients, as they are smaller in size and have stiff skin (Wang et al., 2018). The absence of lens luxation in mice possibly results from the differences in ciliary zonule composition, as fibrillin-2 predominates fibrillin-1 in mouse zonules (Wang et al., 2018).

The proofed and detailed pathological effect of the p.A387T variant remains to be determined, as we did not have access to tissue samples of any homozygote NEs. Given the location of the variant, it seems that it probably alters the metalloproteinase function of ADAMTS10, which is turn might contribute to the elevation of IOP because of the disorganized ECM structure in the aqueous humor outflow pathway, impaired interaction with FBN1 or activation of TGFβ.

After the study II was published, four different mutations in *ADAMTS17* have been implicated in POAG in Basset Hound, Basset Fauve de Bretagne, Petit Basset Griffon Vendeen and Shar-Pei dog breeds (Oliver et al., 2015, Forman et al., 2015, Oliver et al., 2018), highlighting the importance of the ADAMTS gene family in the pathogenesis of canine glaucoma.

To conclude, in study II a novel recessive missense variant was discovered as the likely cause of POAG in Norwegian Elkhounds. The study establishes a new spontaneous canine model to study ADAMTS10 biology as well as to understand the molecular pathways in glaucoma. The results can be utilized in the future to study therapeutic interventions for glaucoma, and a gene test can be developed for veterinary diagnostics and breeding programs.

5.3 Multiple genetically distinctive types of PRA affect Miniature Schnauzers – a putative silencer variant associated with type 1 disease

In study III, Miniature Schnauzers were found to be affected by multiple clinically and genetically distinct forms of PRA. A putative silencer variant was found to be the likely cause of the earlier-onset type 1 PRA and a tentative locus was mapped for the later-onset type 2 form. The results have multiple important implications in medicine, veterinary medicine and genetics.

Based on the clinical presentation of the cases, multiple genetically distinct types of PRA were suspected to affect MS. Tentatively, two distinctive groups were formed: type 1 cases included a clinically homogenous group of MSs that had clear clinical disease onset at four years of age, classical signs of PRA (Parry, 1953) and became blind within the first year after diagnosis. Type 2 cases, in contrast, had more variable age of onset (with an average of seven years) and disease progression. The type 2 phenotype was predominantly expressed in male dogs, suggesting an X-linked mode of inheritance. GWAS confirmed the two types to be genetically distinct, as the type 1 disease mapped to CFA15, while analyzing the type 2 cases indicated a tentative association to CFAX, concordant with the suspected X-linked mode of inheritance. While the suggestive association in CFAX needs to be replicated in a larger sample set, association of the type 1 PRA in CFA15 was very strong. Haplotype analysis of the locus indicated a 7.2-Mb critical region in CFA15, shared by all the cases and, surprisingly, by one control MS as well. This might result from either incomplete penetrance of the causal variant or

from the fact that the causative variant is so recent that not all risk haplotype-carrying dogs have it.

Analyzing whole-genome sequencing data from cases and controls revealed a number of possibly pathogenic coding variants; however, all of them had incomplete penetrance of 70–80%. Finally, after including sequencing data from an obligate carrier MS homozygous for the risk haplotype, a fully penetrant variant was found for type 1 PRA. This variant resided in a conserved sequence within introns of *HIVEP3* and a dog-specific lncRNA gene (*ENSCAFG00000035604*), albeit kilobases away from exon-intron boundaries. As expected, the variant did not have an effect on splicing. A case-controls comparison of retinal *HIVEP3* and *ENSCAFG00000035604* expression did not show significant changes and, thus, other regulatory functions of the variant site were studied. These revealed a predicted binding site of the HAND1::TCF3 transcription factor complex, suggesting an enhancer or silencer variant. The silencer function, as well as disrupted silencer activity because of the variant, were supported *in vitro* using a dual luciferase reporter assay, although formal confirmation would require further experiments such as chromatin immunoprecipitation analysis, which is ongoing for the revised version of the manuscript. Because of the role of silencers in transcriptional activation, the six most promising retinal HAND1::TCF3 target genes were prioritized for the quantitative retinal expression analysis. As a result, significant overexpression of *COL9A2* and *EDN2* were found in the affected retina, supporting the luciferase assay results of a disrupted silencer leading to a gain-of-function pathology.

Although final conclusions of the disease mechanism are hindered due to limited access of retinal samples from cases, some discussion about the two overexpressed target genes is necessary. A loss-of-function variant in *COL9A2*, encoding the collagen type IX alpha 2 chain, has been associated with autosomal recessive Stickler syndrome, which is characterized by multiple auditory, skeletal, orofacial and ocular abnormalities, including degeneration of the retina (Baker et al., 2011). The PRA-affected MSs were not reported to suffer from any other medical condition; however, upregulation of *COL9A2* could result in a different phenotype compared to the one reported for the loss-of-function variant. *EDN2*, in turn, encodes endothelin-2, which has been associated with angiogenesis, cell migration, cell proliferation, and endothelial activation (Rattner, Nathans, 2005, Bridges et al., 2010, Choi et al., 2011, Howell et al., 2011, Bramall et al., 2013). Retinal overexpression of *Edn2* in mice inhibits the development of retinal vasculature (Rattner et al., 2013), which might also explain the disease etiology in the

affected MS as vascular attenuation is a hallmark feature in canine PRA (Parry, 1953). Alternatively, the observed *EDN2* overexpression might be secondary to PRA, as it has been proposed to be a general stress signal from photoreceptor damage (Rattner, Nathans, 2005, Samardzija et al., 2012). The role of upregulated *COL9A2* and *EDN2*, and other possible retinal target genes including *HIVEP3*, requires additional retinal samples from multiple affected dogs, optimally sampled at disease onset, before definitive conclusions of the disease mechanism can be made.

During the course of this study, a complex structural variant in *PPT1* with incomplete penetrance was reported to cause PRA in MS (Murgiano et al., 2018). That study indicated a suggestive association on the CFA15, where a ~5Mb critical interval was shared by some, but not all, affected dogs. Filtering whole-genome sequencing data from cases and controls found also the same intronic *HIVEP3* variant described here, but its possible functional role was not studied. Instead, the authors turned their focus to a complex structural variant in *PPT1* as some of the cases were homozygous for it, but wild-type or heterozygous for the *HIVEP3* variant. Further screening also revealed that some of the confirmed controls were homozygous for the *PPT1* variant, indicating incomplete penetrance of 79% (Murgiano et al., 2018). In contrast, results from the study III shows that 1) MSs are affected with multiple genetically distinct forms of PRA and that 2) the likely causative variant has such a recent origin that not all risk haplotype-carrying dogs have it. These observations are of fundamental importance as they explain the identification of multiple candidate variants in the locus that seem to associate with the phenotype, but have incomplete penetrance. In study III, only after including whole-genome sequencing data from a healthy obligate carrier that was *homozygous* for the risk haplotype, led to the identification of the fully penetrant variant with 10 billion times stronger association than any of the other seemingly associating coding variants, including that in the *PPT1*. Further analyses indicated putative regulatory role for this variant, which should be used in genetic testing in future instead of the currently offered commercial tests based on the *PPT1* variant.

To our knowledge, in dogs, this is the first report of a putative silencer variant causing PRA (Miyadera, 2018). In humans affected with RP, a single report describing recessive retina-specific cis-regulatory variants in the CRX-binding regions of SAMD7 has been published (Van Schil et al., 2016), underlining the underrepresented number of regulatory variants mapped in disease genetics. Therefore, beyond veterinary medicine, the affected MSs

provide an important spontaneous model to understand retinal gene regulation and the causes of retinal degeneration in other species, too.

In conclusion, in study III, at least two clinically and genetically distinct types of PRA were observed in MS. One confirmed and one tentative locus were mapped, and a likely causative variant for earlier-onset (type 1) PRA was discovered in the predicted binding site of the HAND1::TCF3 TFBS complex with two of its putative target genes, *COL9A2* and *EDN2,* overexpressed in case retina. These results enable accurate gene test development for MSs and establish the breed as a new spontaneous animal model to study the corresponding phenotype, RP, in humans as well as.

6 Conclusions and future prospects

Studies constituting this doctoral thesis were conducted during 2013–2019 and unraveled the likely genetic causes of three canine blinding eye disorders, which currently have no available standardized curative treatment. The studied phenotypes also affect humans, and therefore, the results can be utilized in multiple scientific and translational ways in addition to implementations in veterinary medicine.

As a direct result of this thesis, three new gene tests have already been developed and are utilized worldwide by clinicians, breeders and dog owners. With reliable genetic testing, veterinarians are able to diagnose and treat the conditions earlier and give dog owners accurate information of the diagnosed disease and its prognosis. Breeders, on the other hand, are now able to avoid producing new affected dogs, while simultaneously preventing unnecessary loss of genetic diversity, as they are able to detect the unaffected carriers and combine them only with wild-type dogs. During this doctoral dissertation, genetic tests have become a crucial part of everyday veterinary medicine. In 2013, individual genetic tests were offered, whereas currently utilized panel tests include over a hundred single tests. To respond to the growing need for up-to-date knowledge in genetics, an applied course on clinical veterinary genetics is now offered on a yearly basis at the University of Helsinki as an additional implementation of this doctoral dissertation and other ongoing studies conducted in Finland and worldwide.

Methodologically, studies conducted as parts of this dissertation were performed in a fascinating era, in which candidate gene approaches were largely replaced by next-generation sequencing, which has finally become cost-efficient and computationally feasible. New methods and softwares had to be adopted but are now established and will promote future studies. In addition, due to the discovered peculiarities of the detected variants in the mode of inheritance (study I) and variant type and novelty (study III), the approaches described in this thesis can be utilized as an example for similar future projects. An important methodological implementation in clinical veterinary ophthalmology is also the use of OCT imaging as part of phenotype characterization in studies I and III, as it has not been utilized in Finland for pet animals before, but through the established collaborations here, it is easily available for any future studies. Moreover, all the hundreds of studied dogs in this thesis were privately owned pet dogs of which owners and breeders donated samples voluntarily, illustrating their strong motivation and commitment to promoting canine health. Without their activity, and the

clinicians diagnosing and sampling the dogs, successful biobanking would not be possible. The collected samples here are also available for new studies, thus contributing to the growing resources that enable successful discoveries in the future as well.

Translationally, the obtained results have multiple potential applications as the studied diseases also affect humans. Two of the associated genes, *ADAMTS10* and *RBP4*, have already been implicated in corresponding human diseases, making the affected dogs new spontaneous animal models to study disease pathology and new therapeutic interventions. Eye diseases have long been favorite targets for gene therapies, which will hopefully become standard treatment options for both humans and dogs in the future. In the course of this doctoral dissertation in 2017, the United States Food and Drug Administration (FDA) approved the first gene therapy for a genetic disease. The drug, called Luxturna®, is designed for patients suffering from retinal degeneration termed Leber's congenital amaurosis resulting from recessive *RPE65* defects (Hanein et al., 2006). It contains the human *RPE65* cDNA sequence that is delivered to RPE cells with an adeno-associated virus serotype 2 (AAV2) vector using a subretinal injection. Luxturna® was developed by Spark Therapeutics (Philadelphia, Pennsylvania, USA) and is a result of long-lasting extensive research in which Briard dogs suffering from similar *RPE65* defects were important in the preclinical development of the drug (Narfström et al., 2003, Le Meur et al., 2007). Hopefully, this is only the beginning of a new era and many more human and dog patients suffering from different genetic diseases will have the opportunity for effective gene therapy in the coming years.

Acknowledgments

This doctoral dissertation was carried out at the Department of Veterinary Biosciences, Faculty of Veterinary Medicine and the Department of Medical and Clinical Genetics, Faculty of Medicine, University of Helsinki and the Folkhälsan Research Center under the supervision of Professor Hannes Lohi. The work was financially supported by the Mary and Georg C. Ehnrooth Foundation, the Evald and Hilda Nissi Foundation, the Canine Health Foundation of the American Kennel Club, the Lux Foundation, the Orion Research Foundation, the Finnish Foundation of Veterinary Research, the Canine Health Research Fund and the Doctoral Program in Integrative Life Science, for which I am very grateful.

I would like to express my deepest gratitude to Hannes for his continuous support throughout the project. With your exceptional talent and hard work, you have been able to create one of the world's leading canine genetic groups, and working here has been an honor for me. Thank you for always trusting me and allowing me to put my ideas into action. The whole Lohi group is also warmly thanked for their everyday support. I would especially like to thank Saija from whom I inherited all the inspiring projects. Kaisa, Marjo, Osmo, Meharji, Milla, Sini, Ileana and Inka are also thanked for their kind help and continuous support.

Throughout the whole thesis project, I have also been supported by my thesis committee members, Mari Kaunisto and Eeva-Marja Sankila, for whom I am very thankful. I would also like to thank Professor Danika Bannasch and Adjunct Professor Soile Nymark for their official review of my thesis. Professors Antti Iivanainen and Miia Lindström are warmly thanked for their support during my undergraduate studies and for inspiring me to pursue an academic career.

All my thesis projects were collaborative efforts, and I would like to express my gratitude to all collaborators, with special thanks to Professor Tom Glaser at UC Davis. I would also like to thank all referring veterinarians and especially Kristina Narfström, Sari Jalomäki, Kaisa Wickström and Elina Pietilä for your continuous help and guidance. Breed clubs, dog breeders and dog owners are warmly thanked for providing samples for these projects.

Finally, my warmest thanks go to my family and friends. Your unswerving support means everything to me!

Helsinki, July 2019
Maria Kaukonen

References

Abouzeid, H., Boisset, G., Favez, T., Youssef, M., Marzouk, I., Shakankiry, N., Bayoumi, N., Descombes, P., Agosti, C. & Munier, F.L. 2011, "Mutations in the SPARC-related modular calcium-binding protein 1 gene, SMOC1, cause waardenburg anophthalmia syndrome", *The American Journal of Human Genetics,* vol. 88, no. 1, pp. 92-98.

Acland, G.M., Blanton, S.H., Hershfield, B. & Aguirre, G.D. 1994, "XLPRA: A canine retinal degeneration inherited as an X-linked trait", *American Journal of Medical Genetics Part A,* vol. 52, no. 1, pp. 27-33.

Adzhubei, I.A., Schmidt, S., Peshkin, L., Ramensky, V.E., Gerasimova, A., Bork, P., Kondrashov, A.S. & Sunyaev, S.R. 2010, "A method and server for predicting damaging missense mutations", *Nature methods,* vol. 7, no. 4, pp. 248-249.

Aguirre, G.D., Baldwin, V., Pearce-Kelling, S., Narfström, K., Ray, K. & Acland, G.M. 1998, "Congenital stationary night blindness in the dog: common mutation in the RPE65 gene indicates founder effect", *Molecular vision,* vol. 4, pp. 23.

Ahonen, S.J., Arumilli, M. & Lohi, H. 2013, "A CNGB1 frameshift mutation in Papillon and Phalene dogs with progressive retinal atrophy", *PLoS One,* vol. 8, no. 8, pp. e72122.

Ahonen, S.J., Arumilli, M., Seppälä, E., Hakosalo, O., Kaukonen, M.K., Komáromy, A.M. & Lohi, H. 2014, "Increased expression of MERTK is associated with a unique form of canine retinopathy", *PloS one,* vol. 9, no. 12, pp. e114552.

Ahonen, S.J., Pietilä, E., Mellersh, C.S., Tiira, K., Hansen, L., Johnson, G.S. & Lohi, H. 2013, "Genome-wide association study identifies a novel canine glaucoma locus", *PloS one,* vol. 8, no. 8, pp. e70903.

Ahram, D.F., Grozdanic, S.D., Kecova, H., Henkes, A., Collin, R.W. & Kuehn, M.H. 2015, "Variants in nebulin (NEB) are linked to the development of familial primary angle closure glaucoma in basset hounds", *PloS one,* vol. 10, no. 5, pp. e0126660.

Ahram, D.F., Cook, A.C., Kecova, H., Grozdanic, S.D. & Kuehn, M.H. 2014, "Identification of genetic loci associated with primary angle-closure glaucoma in the basset hound", *Molecular vision,* vol. 20, pp. 497-510.

Aldahmesh, M., Khan, A., Hijazi, H. & Alkuraya, F. 2013, "Mutations in ALDH1A3 cause microphthalmia", *Clinical genetics,* vol. 84, no. 2, pp. 128-131.

Aldahmesh, M.A., Mohammed, J.Y., Al-Hazzaa, S. & Alkuraya, F.S. 2012, "Homozygous null mutation in ODZ3 causes microphthalmia in humans", *Genetics in medicine : official journal of the American College of Medical Genetics,* vol. 14, no. 11, pp. 900-904.

Ali, M., McKibbin, M., Booth, A., Parry, D.A., Jain, P., Riazuddin, S.A., Hejtmancik, J.F., Khan, S.N., Firasat, S. & Shires, M. 2009, "Null mutations in LTBP2 cause primary congenital glaucoma", *The American Journal of Human Genetics,* vol. 84, no. 5, pp. 664-671.

Almasieh, M., Wilson, A.M., Morquette, B., Vargas, J.L.C. & Di Polo, A. 2012, "The molecular basis of retinal ganglion cell death in glaucoma", *Progress in retinal and eye research,* vol. 31, no. 2, pp. 152-181.

Andersson, R., Gebhard, C., Miguel-Escalada, I., Hoof, I., Bornholdt, J., Boyd, M., Chen, Y., Zhao, X., Schmidl, C. & Suzuki, T. 2014, "An atlas of active enhancers across human cell types and tissues", *Nature,* vol. 507, no. 7493, pp. 455.

Asano, T., Kawamura, S. & Tachibanaki, S. 2019, "Transducin activates cGMP phosphodiesterase by trapping inhibitory gamma subunit freed reversibly from the catalytic subunit in solution", *Scientific reports,* vol. 9, no. 1, pp. 7245-019-43675-9.

Aulchenko, Y.S., Ripke, S., Isaacs, A. & van Duijn, C. 2007, "GenABEL: an R library for genome-wide association analysis", *Bioinformatics,* vol. 23, no. 10, pp. 1294-1294.

Baker, S., Booth, C., Fillman, C., Shapiro, M., Blair, M.P., Hyland, J.C. & Ala-Kokko, L. 2011, "A loss of function mutation in the COL9A2 gene causes autosomal recessive Stickler syndrome", *American Journal of Medical Genetics Part A,* vol. 155, no. 7, pp. 1668-1672.

Bedford, P.G. & Grierson, I. 1986, "Aqueous drainage in the dog", *Research in veterinary science,* vol. 41, no. 2, pp. 172-186.

Beltran, W.A., Cideciyan, A.V., Guziewicz, K.E., Iwabe, S., Swider, M., Scott, E.M., Savina, S.V., Ruthel, G., Stefano, F. & Zhang, L. 2014, "Canine retina has a primate fovea-like bouquet of cone photoreceptors which is affected by inherited macular degenerations", *PloS one,* vol. 9, no. 3, pp. e90390.

Berni, R. & Formelli, F. 1992, "In vitro interaction of fenretinide with plasma retinol-binding protein and its functional consequences", *FEBS letters,* vol. 308, no. 1, pp. 43-45.

Berry, D.C., Jacobs, H., Marwarha, G., Gely-Pernot, A., O'Byrne, S.M., DeSantis, D., Klopfenstein, M., Feret, B., Dennefeld, C., Blaner, W.S., Croniger, C.M., Mark, M., Noy, N. & Ghyselinck, N.B. 2013, "The STRA6 receptor is essential for retinol-binding protein-induced insulin

resistance but not for maintaining vitamin A homeostasis in tissues other than the eye", *The Journal of biological chemistry,* vol. 288, no. 34, pp. 24528-24539.

Berson, D.M., Dunn, F.A. & Takao, M. 2002, "Phototransduction by retinal ganglion cells that set the circadian clock", *Science (New York, N.Y.),* vol. 295, no. 5557, pp. 1070-1073.

Besch, D., Jagle, H., Scholl, H.P., Seeliger, M.W. & Zrenner, E. 2003, "Inherited multifocal RPE-diseases: mechanisms for local dysfunction in global retinoid cycle gene defects", *Vision research,* vol. 43, no. 28, pp. 3095-3108.

Biesalski, H.K., Frank, J., Beck, S.C., Heinrich, F., Illek, B., Reifen, R., Gollnick, H., Seeliger, M.W., Wissinger, B. & Zrenner, E. 1999, "Biochemical but not clinical vitamin A deficiency results from mutations in the gene for retinol binding protein", *The American Journal of Clinical Nutrition,* vol. 69, no. 5, pp. 931-936.

Bjerkås, E. 1991, "Collie eye anomaly in the rough collie in Norway", *Journal of Small Animal Practice,* vol. 32, no. 2, pp. 89-92.

Boettner, E.A. & Wolter, J.R. 1962, "Transmission of the ocular media", *Investigative ophthalmology & visual science,* vol. 1, no. 6, pp. 776-783.

Bok, D. 1993, "The retinal pigment epithelium: a versatile partner in vision", *Journal of cell science.Supplement,* vol. 17, pp. 189-195.

Bonting, S.L. & Becker, B. 1964, "Studies on Sodium-Potassium Activated Adenosinetriphosphatase. Xiv. Inhibition of Enzyme Activity and Aqueous Humor Flow in the Rabbit Eye After Intravitreal Injection of Ouabain", *Investigative ophthalmology,* vol. 3, pp. 523-533.

Bramall, A.N., Szego, M.J., Pacione, L.R., Chang, I., Diez, E., D'Orleans-Juste, P., Stewart, D.J., Hauswirth, W.W., Yanagisawa, M. & McInnes, R.R. 2013, "Endothelin-2-mediated protection of mutant photoreceptors in inherited photoreceptor degeneration", *PLoS One,* vol. 8, no. 2, pp. e58023.

Bridges, P.J., Jo, M., Al Alem, L., Na, G., Su, W., Gong, M.C., Jeoung, M. & Ko, C. 2010, "Production and binding of endothelin-2 (EDN2) in the rat ovary: endothelin receptor subtype A (EDNRA)-mediated contraction", *Reproduction, fertility, and development,* vol. 22, no. 5, pp. 780-787.

Broeckx, B.J., Hitte, C., Coopman, F., Verhoeven, G.E., De Keulenaer, S., De Meester, E., Derrien, T., Alfoldi, J., Lindblad-Toh, K. & Bosmans, T. 2015, "Improved canine exome designs, featuring ncRNAs and increased coverage of protein coding genes", *Scientific reports,* vol. 5, pp. 12810.

Broeckx, B.J., Coopman, F., Verhoeven, G.E., Bavegems, V., De Keulenaer, S., De Meester, E., Van Niewerburgh, F. & Deforce, D. 2014, "Development and performance of a targeted whole exome sequencing enrichment kit for the dog (Canis Familiaris Build 3.1)", *Scientific reports,* vol. 4, pp. 5597.

Brown, E.A., Thomasy, S.M., Murphy, C.J. & Bannasch, D.L. 2018, "Genetic analysis of optic nerve head coloboma in the Nova Scotia Duck Tolling Retriever identifies discordance with the NHEJ1 intronic deletion (collie eye anomaly mutation)", *Veterinary ophthalmology,* vol. 21, no. 2, pp. 144-150.

Cain, S.A., Mularczyk, E.J., Singh, M., Massam-Wu, T. & Kielty, C.M. 2016, "ADAMTS-10 and-6 differentially regulate cell-cell junctions and focal adhesions", *Scientific reports,* vol. 6, pp. 35956.

Calboli, F.C., Sampson, J., Fretwell, N. & Balding, D.J. 2008, "Population structure and inbreeding from pedigree analysis of purebred dogs", *Genetics,* vol. 179, no. 1, pp. 593-601.

Chapot, C.A., Euler, T. & Schubert, T. 2017, "How do horizontal cells 'talk' to cone photoreceptors? Different levels of complexity at the cone-horizontal cell synapse", *The Journal of physiology,* vol. 595, no. 16, pp. 5495-5506.

Chavarria-Soley, G., Sticht, H., Aklillu, E., Ingelman-Sundberg, M., Pasutto, F., Reis, A. & Rautenstrauss, B. 2008, "Mutations in CYP1B1 cause primary congenital glaucoma by reduction of either activity or abundance of the enzyme", *Human mutation,* vol. 29, no. 9, pp. 1147-1153.

Chen, L.J., Ng, T.K., Fan, A.H., Leung, D.Y., Zhang, M., Wang, N., Zheng, Y., Liang, X.Y., Chiang, S.W. & Tam, P.O. 2012, "Evaluation of NTF4 as a causative gene for primary open-angle glaucoma", *Molecular vision,* vol. 18, pp. 1763.

Chen, Y., Clarke, O.B., Kim, J., Stowe, S., Kim, Y.K., Assur, Z., Cavalier, M., Godoy-Ruiz, R., von Alpen, D.C., Manzini, C., Blaner, W.S., Frank, J., Quadro, L., Weber, D.J., Shapiro, L., Hendrickson, W.A. & Mancia, F. 2016, "Structure of the STRA6 receptor for retinol uptake", *Science (New York, N.Y.),* vol. 353, no. 6302, pp. 10.1126/science.aad8266.

Chew, T., Haase, B., Bathgate, R., Willet, C.E., Kaukonen, M.K., Mascord, L.J., Lohi, H.T. & Wade, C.M. 2017, "A Coding variant in the gene bardet-biedl syndrome 4 (BBS4) is associated with a novel form of canine progressive retinal atrophy", *G3: Genes, Genomes, Genetics,* vol. 7, no. 7, pp. 2327-2335.

Chiao, C.C., Vorobyev, M., Cronin, T.W. & Osorio, D. 2000, "Spectral tuning of dichromats to natural scenes", *Vision research,* vol. 40, no. 23, pp. 3257-3271.

Choi, D., Kim, E.K., Kim, K., Lee, K., Kang, D., Kim, H.Y., Bridges, P. & Ko, C. 2011, "Expression pattern of endothelin system components and localization of smooth muscle cells in the human pre-ovulatory follicle", *Human reproduction,* vol. 26, no. 5, pp. 1171-1180.

Chou, C.M., Nelson, C., Tarle, S.A., Pribila, J.T., Bardakjian, T., Woods, S., Schneider, A. & Glaser, T. 2015, "Biochemical Basis for Dominant Inheritance, Variable Penetrance, and Maternal Effects in RBP4 Congenital Eye Disease", *Cell,* vol. 161, no. 3, pp. 634-646.

Clagett-Dame, M. & Knutson, D. 2011, "Vitamin A in reproduction and development", *Nutrients,* vol. 3, no. 4, pp. 385-428.

Cole, D.F. 1977, "Secretion of the aqueous humour", *Experimental eye research,* vol. 25 Suppl, pp. 161-176.

D'Ambrosio, D.N., Clugston, R.D. & Blaner, W.S. 2011, "Vitamin A metabolism: an update", *Nutrients,* vol. 3, no. 1, pp. 63-103.

Dagoneau, N., Benoist-Lasselin, C., Huber, C., Faivre, L., Mégarbané, A., Alswaid, A., Dollfus, H., Alembik, Y., Munnich, A. & Legeai-Mallet, L. 2004, "ADAMTS10 mutations in autosomal recessive Weill-Marchesani syndrome", *The American Journal of Human Genetics,* vol. 75, no. 5, pp. 801-806.

Daiger, S., Rossiter, B., Greenberg, J., Christoffels, A. & Hide, W. 1998, "Data services and software for identifying genes and mutations causing retinal degeneration", *Invest Ophthalmol Vis Sci,* vol. 39, pp. S295.

Daiger, S., Sullivan, L. & Bowne, S. 2013, "Genes and mutations causing retinitis pigmentosa", *Clinical genetics,* vol. 84, no. 2, pp. 132-141.

Davidson, M., Nelms, S. & Gelatt, K. 2007, "Veterinary ophthalmology", .

De Marco, A. 2009, "Strategies for successful recombinant expression of disulfide bond-dependent proteins in Escherichia coli", *Microbial cell factories,* vol. 8, no. 1, pp. 26.

Dekomien, G., Vollrath, C., Petrasch-Parwez, E., Boevé, M.H., Akkad, D.A., Gerding, W.M. & Epplen, J.T. 2010, "Progressive retinal atrophy in Schapendoes dogs: mutation of the newly identified CCDC66 gene", *Neurogenetics,* vol. 11, no. 2, pp. 163-174.

Dekomien, G., Runte, M., Godde, R. & Epplen, J.T. 2000, "Generalized progressive retinal atrophy of Sloughi dogs is due to an 8-bp insertion in exon 21 of the PDE6B gene", *Cytogenetics and cell genetics,* vol. 90, no. 3-4, pp. 261-267.

Dickopf, S., Mielke, T. & Heyn, M.P. 1998, "Kinetics of the light-induced proton translocation associated with the pH-dependent formation of the metarhodopsin I/II equilibrium of bovine rhodopsin", *Biochemistry,* vol. 37, no. 48, pp. 16888-16897.

Donner, J., Anderson, H., Davison, S., Hughes, A.M., Bouirmane, J., Lindqvist, J., Lytle, K.M., Ganesan, B., Ottka, C., Ruotanen, P., Kaukonen, M., Forman, O.P., Fretwell, N., Cole, C.A. & Lohi, H. 2018, "Frequency and distribution of 152 genetic disease variants in over 100,000 mixed breed and purebred dogs", *PLoS genetics,* vol. 14, no. 4, pp. e1007361.

Dornonville de la Cour, M. 1993, "Ion transport in the retinal pigment epithelium. A study with double barrelled ion-selective microelectrodes", *Acta ophthalmologica.Supplement,* vol. (209), no. 209, pp. 1-32.

Douglas, R.H. & Jeffery, G. 2014, "The spectral transmission of ocular media suggests ultraviolet sensitivity is widespread among mammals", *Proceedings.Biological sciences,* vol. 281, no. 1780, pp. 20132995.

Dowling, J.E. & Boycott, B.B. 1966, "Organization of the primate retina: electron microscopy", *Proceedings of the Royal Society of London.Series B, Biological sciences,* vol. 166, no. 1002, pp. 80-111.

Downs, L., Bell, J., Freeman, J., Hartley, C., Hayward, L. & Mellersh, C. 2013, "Late-onset progressive retinal atrophy in the G ordon and I rish S etter breeds is associated with a frameshift mutation in C2orf71", *Animal Genetics,* vol. 44, no. 2, pp. 169-177.

Downs, L.M. & Mellersh, C.S. 2014, "An Intronic SINE insertion in FAM161A that causes exon-skipping is associated with progressive retinal atrophy in Tibetan Spaniels and Tibetan Terriers", *PloS one,* vol. 9, no. 4, pp. e93990.

Downs, L.M., Wallin-Håkansson, B., Bergström, T. & Mellersh, C.S. 2014, "A novel mutation in TTC8 is associated with progressive retinal atrophy in the golden retriever", *Canine genetics and epidemiology,* vol. 1, no. 1, pp. 4.

Downs, L.M., Wallin-Håkansson, B., Boursnell, M., Marklund, S., Hedhammar, Å., Truvé, K., Hübinette, L., Lindblad-Toh, K., Bergström, T. & Mellersh, C.S. 2011, "A frameshift mutation in golden retriever dogs with progressive retinal atrophy endorses SLC4A3 as a candidate gene for human retinal degenerations", *PloS one,* vol. 6, no. 6, pp. e21452.

Eid, J., Fehr, A., Gray, J., Luong, K., Lyle, J., Otto, G., Peluso, P., Rank, D., Baybayan, P., Bettman, B., Bibillo, A., Bjornson, K., Chaudhuri, B.,

Christians, F., Cicero, R., Clark, S., Dalal, R., Dewinter, A., Dixon, J., Foquet, M., Gaertner, A., Hardenbol, P., Heiner, C., Hester, K., Holden, D., Kearns, G., Kong, X., Kuse, R., Lacroix, Y., Lin, S., Lundquist, P., Ma, C., Marks, P., Maxham, M., Murphy, D., Park, I., Pham, T., Phillips, M., Roy, J., Sebra, R., Shen, G., Sorenson, J., Tomaney, A., Travers, K., Trulson, M., Vieceli, J., Wegener, J., Wu, D., Yang, A., Zaccarin, D., Zhao, P., Zhong, F., Korlach, J. & Turner, S. 2009, "Real-time DNA sequencing from single polymerase molecules", *Science (New York, N.Y.),* vol. 323, no. 5910, pp. 133-138.

Ekesten, B., Bjerkas, E., Kongsengen, K. & Narfstrom, K. 1997, "Primary glaucoma in the Norwegian Elkhound", *Veterinary and comparative ophthalmology (USA),* .

Euler, T., Haverkamp, S., Schubert, T. & Baden, T. 2014, "Retinal bipolar cells: elementary building blocks of vision", *Nature reviews.Neuroscience,* vol. 15, no. 8, pp. 507-519.

Everson, R., Pettitt, L., Forman, O.P., Dower-Tylee, O., McLaughlin, B., Ahonen, S., Kaukonen, M., Komaromy, A.M., Lohi, H., Mellersh, C.S., Sansom, J. & Ricketts, S.L. 2017, "An intronic LINE-1 insertion in MERTK is strongly associated with retinopathy in Swedish Vallhund dogs", *PloS one,* vol. 12, no. 8, pp. e0183021.

Fantes, J., Ragge, N.K., Lynch, S.A., McGill, N.I., Collin, J.R., Howard-Peebles, P.N., Hayward, C., Vivian, A.J., Williamson, K., van Heyningen, V. & FitzPatrick, D.R. 2003, "Mutations in SOX2 cause anophthalmia", *Nature genetics,* vol. 33, no. 4, pp. 461-463.

Farias, F.H., Johnson, G.S., Taylor, J.F., Giuliano, E., Katz, M.L., Sanders, D.N., Schnabel, R.D., McKay, S.D., Khan, S., Gharahkhani, P., O'Leary, C.A., Pettitt, L., Forman, O.P., Boursnell, M., McLaughlin, B., Ahonen, S., Lohi, H., Hernandez-Merino, E., Gould, D.J., Sargan, D.R. & Mellersh, C. 2010, "An ADAMTS17 splice donor site mutation in dogs with primary lens luxation", *Investigative ophthalmology & visual science,* vol. 51, no. 9, pp. 4716-4721.

Finnemann, S.C. 2003, "Focal adhesion kinase signaling promotes phagocytosis of integrin-bound photoreceptors", *The EMBO journal,* vol. 22, no. 16, pp. 4143-4154.

Forman, O.P., Pettitt, L., Komaromy, A.M., Bedford, P. & Mellersh, C. 2015, "A Novel Genome-Wide Association Study Approach Using Genotyping by Exome Sequencing Leads to the Identification of a Primary Open Angle Glaucoma Associated Inversion Disrupting ADAMTS17", *PloS one,* vol. 10, no. 12, pp. e0143546.

Forrest, A.R., Kawaji, H., Rehli, M., Baillie, J.K., De Hoon, M.J., Haberle, V., Lassmann, T., Kulakovskiy, I.V., Lizio, M. & Itoh, M. 2014, "A

promoter-level mammalian expression atlas", *Nature,* vol. 507, no. 7493, pp. 462.

Foster, P.J., Buhrmann, R., Quigley, H.A. & Johnson, G.J. 2002, "The definition and classification of glaucoma in prevalence surveys", *The British journal of ophthalmology,* vol. 86, no. 2, pp. 238-242.

Frantz, L.A., Mullin, V.E., Pionnier-Capitan, M., Lebrasseur, O., Ollivier, M., Perri, A., Linderholm, A., Mattiangeli, V., Teasdale, M.D., Dimopoulos, E.A., Tresset, A., Duffraisse, M., McCormick, F., Bartosiewicz, L., Gal, E., Nyerges, E.A., Sablin, M.V., Brehard, S., Mashkour, M., Balasescu, A., Gillet, B., Hughes, S., Chassaing, O., Hitte, C., Vigne, J.D., Dobney, K., Hanni, C., Bradley, D.G. & Larson, G. 2016, "Genomic and archaeological evidence suggest a dual origin of domestic dogs", *Science (New York, N.Y.),* vol. 352, no. 6290, pp. 1228-1231.

Fredholm, M., Larsen, R., Jönsson, M., Söderlund, M., Hardon, T. & Proschowsky, H. 2016, "Discrepancy in compliance between the clinical and genetic diagnosis of choroidal hypoplasia in Danish Rough Collies and Shetland Sheepdogs", *Animal Genetics,* vol. 47, no. 2, pp. 250-252.

Gabriel, S.B., Schaffner, S.F., Nguyen, H., Moore, J.M., Roy, J., Blumenstiel, B., Higgins, J., DeFelice, M., Lochner, A., Faggart, M., Liu-Cordero, S.N., Rotimi, C., Adeyemo, A., Cooper, R., Ward, R., Lander, E.S., Daly, M.J. & Altshuler, D. 2002, "The structure of haplotype blocks in the human genome", *Science (New York, N.Y.),* vol. 296, no. 5576, pp. 2225-2229.

Garcia-Valenzuela, E., Shareef, S., Walsh, J. & Sharma, S. 1995, "Programmed cell death of retinal ganglion cells during experimental glaucoma", *Experimental eye research,* vol. 61, no. 1, pp. 33-44.

Gardner, E.J., Lam, V.K., Harris, D.N., Chuang, N.T., Scott, E.C., Pittard, W.S., Mills, R.E., 1000 Genomes Project Consortium & Devine, S.E. 2017, "The Mobile Element Locator Tool (MELT): population-scale mobile element discovery and biology", *Genome research,* vol. 27, no. 11, pp. 1916-1929.

Gelatt, K.N. & MacKay, E.O. 2004, "Prevalence of the breed-related glaucomas in pure-bred dogs in North America", *Veterinary ophthalmology,* vol. 7, no. 2, pp. 97-111.

Gelatt, K.N., Peiffer, R., Gwin, R.M., Gum, G.G. & Williams, L.W. 1977, "Clinical manifestations of inherited glaucoma in the beagle.", *Investigative ophthalmology & visual science,* vol. 16, no. 12, pp. 1135-1142.

Gelatt, K.N., Samuelson, D.A., Bauer, J.E., Das, N.D., Wolf, E.D., Barrie, K.P. & Andresen, T.L. 1983, "Inheritance of congenital cataracts and microphthalmia in the Miniature Schnauzer", *American Journal of Veterinary Research,* vol. 44, no. 6, pp. 1130-1132.

Germonpré, M., Sablin, M.V., Stevens, R.E., Hedges, R.E., Hofreiter, M., Stiller, M. & Després, V.R. 2009, "Fossil dogs and wolves from Palaeolithic sites in Belgium, the Ukraine and Russia: osteometry, ancient DNA and stable isotopes", *Journal of Archaeological Science,* vol. 36, no. 2, pp. 473-490.

Gerth-Kahlert, C., Williamson, K., Ansari, M., Rainger, J.K., Hingst, V., Zimmermann, T., Tech, S., Guthoff, R.F., van Heyningen, V. & Fitzpatrick, D.R. 2013, "Clinical and mutation analysis of 51 probands with anophthalmia and/or severe microphthalmia from a single center", *Molecular Genetics & Genomic Medicine,* vol. 1, no. 1, pp. 15-31.

Gibbs, R.A., Weinstock, G.M., Metzker, M.L., Muzny, D.M., Sodergren, E.J., Scherer, S., Scott, G., Steffen, D., Worley, K.C., Burch, P.E., Okwuonu, G., Hines, S., Lewis, L., DeRamo, C., Delgado, O., Dugan-Rocha, S., Miner, G., Morgan, M., Hawes, A., Gill, R., Celera, Holt, R.A., Adams, M.D., Amanatides, P.G., Baden-Tillson, H., Barnstead, M., Chin, S., Evans, C.A., Ferriera, S., Fosler, C., Glodek, A., Gu, Z., Jennings, D., Kraft, C.L., Nguyen, T., Pfannkoch, C.M., Sitter, C., Sutton, G.G., Venter, J.C., Woodage, T., Smith, D., Lee, H.M., Gustafson, E., Cahill, P., Kana, A., Doucette-Stamm, L., Weinstock, K., Fechtel, K., Weiss, R.B., Dunn, D.M., Green, E.D., Blakesley, R.W., Bouffard, G.G., De Jong, P.J., Osoegawa, K., Zhu, B., Marra, M., Schein, J., Bosdet, I., Fjell, C., Jones, S., Krzywinski, M., Mathewson, C., Siddiqui, A., Wye, N., McPherson, J., Zhao, S., Fraser, C.M., Shetty, J., Shatsman, S., Geer, K., Chen, Y., Abramzon, S., Nierman, W.C., Havlak, P.H., Chen, R., Durbin, K.J., Egan, A., Ren, Y., Song, X.Z., Li, B., Liu, Y., Qin, X., Cawley, S., Worley, K.C., Cooney, A.J., D'Souza, L.M., Martin, K., Wu, J.Q., Gonzalez-Garay, M.L., Jackson, A.R., Kalafus, K.J., McLeod, M.P., Milosavljevic, A., Virk, D., Volkov, A., Wheeler, D.A., Zhang, Z., Bailey, J.A., Eichler, E.E., Tuzun, E., Birney, E., Mongin, E., Ureta-Vidal, A., Woodwark, C., Zdobnov, E., Bork, P., Suyama, M., Torrents, D., Alexandersson, M., Trask, B.J., Young, J.M., Huang, H., Wang, H., Xing, H., Daniels, S., Gietzen, D., Schmidt, J., Stevens, K., Vitt, U., Wingrove, J., Camara, F., Mar Alba, M., Abril, J.F., Guigo, R., Smit, A., Dubchak, I., Rubin, E.M., Couronne, O., Poliakov, A., Hubner, N., Ganten, D., Goesele, C., Hummel, O., Kreitler, T., Lee, Y.A., Monti, J., Schulz, H., Zimdahl, H., Himmelbauer, H., Lehrach, H., Jacob, H.J., Bromberg, S., Gullings-Handley, J., Jensen-Seaman, M.I., Kwitek, A.E., Lazar, J., Pasko, D.,

Tonellato, P.J., Twigger, S., Ponting, C.P., Duarte, J.M., Rice, S., Goodstadt, L., Beatson, S.A., Emes, R.D., Winter, E.E., Webber, C., Brandt, P., Nyakatura, G., Adetobi, M., Chiaromonte, F., Elnitski, L., Eswara, P., Hardison, R.C., Hou, M., Kolbe, D., Makova, K., Miller, W., Nekrutenko, A., Riemer, C., Schwartz, S., Taylor, J., Yang, S., Zhang, Y., Lindpaintner, K., Andrews, T.D., Caccamo, M., Clamp, M., Clarke, L., Curwen, V., Durbin, R., Eyras, E., Searle, S.M., Cooper, G.M., Batzoglou, S., Brudno, M., Sidow, A., Stone, E.A., Venter, J.C., Payseur, B.A., Bourque, G., Lopez-Otin, C., Puente, X.S., Chakrabarti, K., Chatterji, S., Dewey, C., Pachter, L., Bray, N., Yap, V.B., Caspi, A., Tesler, G., Pevzner, P.A., Haussler, D., Roskin, K.M., Baertsch, R., Clawson, H., Furey, T.S., Hinrichs, A.S., Karolchik, D., Kent, W.J., Rosenbloom, K.R., Trumbower, H., Weirauch, M., Cooper, D.N., Stenson, P.D., Ma, B., Brent, M., Arumugam, M., Shteynberg, D., Copley, R.R., Taylor, M.S., Riethman, H., Mudunuri, U., Peterson, J., Guyer, M., Felsenfeld, A., Old, S., Mockrin, S., Collins, F. & Rat Genome Sequencing Project Consortium 2004, "Genome sequence of the Brown Norway rat yields insights into mammalian evolution", *Nature,* vol. 428, no. 6982, pp. 493-521.

Gibson, D.G., Young, L., Chuang, R., Venter, J.C., Hutchison, C.A. & Smith, H.O. 2009, "Enzymatic assembly of DNA molecules up to several hundred kilobases", *Nature methods,* vol. 6, no. 5, pp. 343-345.

Gilbert, C.E., Canovas, R., de Canovas, R.K. & Foster, A. 1994, "Causes of blindness and severe visual impairment in children in Chile", *Developmental Medicine & Child Neurology,* vol. 36, no. 4, pp. 326-333.

Glaser, T., Jepeal, L., Edwards, J.G., Young, S.R., Favor, J. & Maas, R.L. 1994, "PAX6 gene dosage effect in a family with congenital cataracts, aniridia, anophthalmia and central nervous system defects", *Nature genetics,* vol. 7, no. 4, pp. 463-471.

Goldstein, O., Kukekova, A.V., Aguirre, G.D. & Acland, G.M. 2010a, "Exonic SINE insertion in STK38L causes canine early retinal degeneration (erd)", *Genomics,* vol. 96, no. 6, pp. 362-368.

Goldstein, O., Mezey, J.G., Boyko, A.R., Gao, C., Wang, W., Bustamante, C.D., Anguish, L.J., Jordan, J.A., Pearce-Kelling, S.E. & Aguirre, G.D. 2010b, "An ADAM9 mutation in canine cone-rod dystrophy 3 establishes homology with human cone-rod dystrophy 9", *Molecular vision,* vol. 16, pp. 1549.

Goldstein, O., Mezey, J.G., Schweitzer, P.A., Boyko, A.R., Gao, C., Bustamante, C.D., Jordan, J.A., Aguirre, G.D. & Acland, G.M. 2013a, "IQCB1 and PDE6B mutations cause similar early onset retinal

degenerations in two closely related terrier dog breeds", *Investigative ophthalmology & visual science,* vol. 54, no. 10, pp. 7005-7019.

Goldstein, O., Jordan, J.A., Aguirre, G.D. & Acland, G.M. 2013b, "A non-stop S-antigen gene mutation is associated with late onset hereditary retinal degeneration in dogs", *Molecular vision,* vol. 19, pp. 1871-1884.

Gong, H., Ruberti, J., Overby, D., Johnson, M. & Freddo, T.F. 2002, "A new view of the human trabecular meshwork using quick-freeze, deep-etch electron microscopy", *Experimental eye research,* vol. 75, no. 3, pp. 347-358.

Gong, H.Y., Trinkaus-Randall, V. & Freddo, T.F. 1989, "Ultrastructural immunocytochemical localization of elastin in normal human trabecular meshwork", *Current eye research,* vol. 8, no. 10, pp. 1071-1082.

Gould, D., Pettitt, L., McLaughlin, B., Holmes, N., Forman, O., Thomas, A., Ahonen, S., Lohi, H., O'Leary, C., Sargan, D. & Mellersh, C. 2011, "ADAMTS17 mutation associated with primary lens luxation is widespread among breeds", *Veterinary ophthalmology,* vol. 14, no. 6, pp. 378-384.

Graw, J. 2003, "The genetic and molecular basis of congenital eye defects", *Nature Reviews Genetics,* vol. 4, no. 11, pp. 876-888.

Green, K. & Pederson, J.E. 1972, "Contribution of secretion and filtration to aqueous humor formation", *The American Journal of Physiology,* vol. 222, no. 5, pp. 1218-1226.

Groeneveld, L.F., Gregusson, S., Guldbrandtsen, B., Hiemstra, S.J., Hveem, K., Kantanen, J., Lohi, H., Stroemstedt, L. & Berg, P. 2016, "Domesticated animal biobanking: land of opportunity", *PLoS biology,* vol. 14, no. 7, pp. e1002523.

Gu, Z., Eils, R. & Schlesner, M. 2016, "Complex heatmaps reveal patterns and correlations in multidimensional genomic data", *Bioinformatics (Oxford, England),* vol. 32, no. 18, pp. 2847-2849.

Gum, G., Gelatt, K. & Samuelson, D. 1984, "Maturation of the retina of the canine neonate as determined by electroretinography and histology.", *American Journal of Veterinary Research,* vol. 45, no. 6, pp. 1166-1171.

Guziewicz, K.E., Zangerl, B., Lindauer, S.J., Mullins, R.F., Sandmeyer, L.S., Grahn, B.H., Stone, E.M., Acland, G.M. & Aguirre, G.D. 2007, "Bestrophin gene mutations cause canine multifocal retinopathy: a novel animal model for best disease", *Investigative ophthalmology & visual science,* vol. 48, no. 5, pp. 1959-1967.

Halder, G., Callaerts, P. & Gehring, W.J. 1995, "Induction of ectopic eyes by targeted expression of the eyeless gene in Drosophila", *Science (New York, N.Y.),* vol. 267, no. 5205, pp. 1788-1792.

Hale, F. 1935, "The relation of vitamin A to anophthalmos in pigs", *American Journal of Ophthalmology,* vol. 18, no. 12, pp. 1087-1093.

Hamann, S. 2002, "Molecular mechanisms of water transport in the eye", *International review of cytology,* vol. 215, pp. 395-431.

Hamzianpour, N., Smith, K., Dawson, C. & Rhodes, M. 2019, "Bilateral enucleation in dogs: A review of owner perceptions and satisfaction", *Veterinary ophthalmology,* .

Hanein, S., Perrault, I., Gerber, S., Tanguy, G., Rozet, J. & Kaplan, J. 2006, "Leber congenital amaurosis: survey of the genetic heterogeneity, refinement of the clinical definition and phenotype-genotype correlations as a strategy for molecular diagnosis" in *Retinal Degenerative Diseases* Springer, , pp. 15-20.

Hargrave, P.A., McDowell, J.H., Curtis, D.R., Wang, J.K., Juszczak, E., Fong, S.L., Rao, J.K. & Argos, P. 1983, "The structure of bovine rhodopsin", *Biophysics of structure and mechanism,* vol. 9, no. 4, pp. 235-244.

Haverkamp, S., Grunert, U. & Wassle, H. 2000, "The cone pedicle, a complex synapse in the retina", *Neuron,* vol. 27, no. 1, pp. 85-95.

Hitti, R.J., Oliver, J.A., Schofield, E.C., Bauer, A., Kaukonen, M., Forman, O.P., Leeb, T., Lohi, H., Burmeister, L.M. & Sargan, D. 2019, "Whole Genome Sequencing of Giant Schnauzer Dogs with Progressive Retinal Atrophy Establishes NECAP1 as a Novel Candidate Gene for Retinal Degeneration", *Genes,* vol. 10, no. 5, pp. 385.

Hoeppner, M.P., Lundquist, A., Pirun, M., Meadows, J.R., Zamani, N., Johnson, J., Sundström, G., Cook, A., FitzGerald, M.G. & Swofford, R. 2014, "An improved canine genome and a comprehensive catalogue of coding genes and non-coding transcripts", *PloS one,* vol. 9, no. 3, pp. e91172.

Hornby, S.J., Ward, S.J., Gilbert, C.E., Dandona, L., Foster, A. & Jones, R.B. 2002, "Environmental risk factors in congenital malformations of the eye", *Annals of Tropical Paediatrics,* vol. 22, no. 1, pp. 67-77.

Howell, G.R., Macalinao, D.G., Sousa, G.L., Walden, M., Soto, I., Kneeland, S.C., Barbay, J.M., King, B.L., Marchant, J.K., Hibbs, M., Stevens, B., Barres, B.A., Clark, A.F., Libby, R.T. & John, S.W. 2011, "Molecular clustering identifies complement and endothelin induction as early events in a mouse model of glaucoma", *The Journal of clinical investigation,* vol. 121, no. 4, pp. 1429-1444.

Huang, D., Swanson, E.A., Lin, C.P., Schuman, J.S., Stinson, W.G., Chang, W., Hee, M.R., Flotte, T., Gregory, K. & Puliafito, C.A. 1991, "Optical

coherence tomography", *Science (New York, N.Y.),* vol. 254, no. 5035, pp. 1178-1181.

Hubbard, R. & Wald, G. 1952, "Cis-trans isomers of vitamin A and retinene in the rhodopsin system", *The Journal of general physiology,* vol. 36, no. 2, pp. 269-315.

Hubmacher, D. & Apte, S.S. 2011, "Genetic and functional linkage between ADAMTS superfamily proteins and fibrillin-1: a novel mechanism influencing microfibril assembly and function", *Cellular and molecular life sciences : CMLS,* vol. 68, no. 19, pp. 3137-3148.

Hytonen, M.K. & Lohi, H. 2016, "Canine models of human rare disorders", *Rare diseases (Austin, Tex.),* vol. 4, no. 1, pp. e1241362.

International HapMap Consortium 2003, "The International HapMap Project", *Nature,* vol. 426, no. 6968, pp. 789-796.

Ishida, K., Panjwani, N., Cao, Z. & Streilein, J.W. 2003, "Participation of pigment epithelium in ocular immune privilege. 3. Epithelia cultured from iris, ciliary body, and retina suppress T-cell activation by partially non-overlapping mechanisms", *Ocular immunology and inflammation,* vol. 11, no. 2, pp. 91-105.

Islam, S., Kjallquist, U., Moliner, A., Zajac, P., Fan, J.B., Lonnerberg, P. & Linnarsson, S. 2011, "Characterization of the single-cell transcriptional landscape by highly multiplex RNA-seq", *Genome research,* vol. 21, no. 7, pp. 1160-1167.

Islam, S., Zeisel, A., Joost, S., La Manno, G., Zajac, P., Kasper, M., Lonnerberg, P. & Linnarsson, S. 2014, "Quantitative single-cell RNA-seq with unique molecular identifiers", *Nature methods,* vol. 11, no. 2, pp. 163-166.

Jackman, S.L., Babai, N., Chambers, J.J., Thoreson, W.B. & Kramer, R.H. 2011, "A positive feedback synapse from retinal horizontal cells to cone photoreceptors", *PLoS biology,* vol. 9, no. 5, pp. e1001057.

Jager, S., Palczewski, K. & Hofmann, K.P. 1996, "Opsin/all-trans-retinal complex activates transducin by different mechanisms than photolyzed rhodopsin", *Biochemistry,* vol. 35, no. 9, pp. 2901-2908.

Jansson, I., Stoilov, I., Sarfarazi, M. & Schenkman, J.B. 2001, "Effect of two mutations of human CYP1B1, G61E and R469W, on stability and endogenous steroid substrate metabolism", *Pharmacogenetics and Genomics,* vol. 11, no. 9, pp. 793-801.

Jeon, C.J., Strettoi, E. & Masland, R.H. 1998, "The major cell populations of the mouse retina", *The Journal of neuroscience : the official journal of the Society for Neuroscience,* vol. 18, no. 21, pp. 8936-8946.

Jeon, M.H. & Jeon, C.J. 1998, "Immunocytochemical localization of calretinin containing neurons in retina from rabbit, cat, and dog", *Neuroscience research,* vol. 32, no. 1, pp. 75-84.

Jeong, M.B., Park, S.A., Kim, S.E., Park, Y.W., Narfstroem, K. & Kangmoon, S. 2013, "Clinical and Electroretinographic Findings of Progressive Retinal Atrophy in Miniature Schnauzer Dogs of South Korea", *Journal of Veterinary Medical Science,* vol. 75, no. 10, pp. 1303-1308.

Jeong, M., Han, C., Narfstrom, K., Awano, T., Johnson, G., Min, M., Sung, J.K. & Seo, K. 2008, "A phosducin (PDC) gene mutation does not cause progressive retinal atrophy in Korean miniature schnauzers.", *Animal Genetics,* vol. 39, no. 4, pp. 455-456.

Jin, M., Li, S., Moghrabi, W.N., Sun, H. & Travis, G.H. 2005, "Rpe65 is the retinoid isomerase in bovine retinal pigment epithelium", *Cell,* vol. 122, no. 3, pp. 449-459.

Johnson, M. 2006, "What controls aqueous humour outflow resistance?", *Experimental eye research,* vol. 82, no. 4, pp. 545-557.

Johnston, M.C., Noden, D.M., Hazelton, R.D., Coulombre, J.L. & Coulombre, A.J. 1979, "Origins of avian ocular and periocular tissues", *Experimental eye research,* vol. 29, no. 1, pp. 27-43.

Jurka, J., Kapitonov, V.V., Pavlicek, A., Klonowski, P., Kohany, O. & Walichiewicz, J. 2005, "Repbase Update, a database of eukaryotic repetitive elements", *Cytogenetic and genome research,* vol. 110, no. 1-4, pp. 462-467.

Kannan, R., Sreekumar, P.G. & Hinton, D.R. 2011, "VEGF and PEDF secretion in ARPE-19 and fhRPE cells", *Investigative ophthalmology & visual science,* vol. 52, no. 12, pp. 9047-8737.

Karlsson, E.K., Baranowska, I., Wade, C.M., Salmon Hillbertz, N.H., Zody, M.C., Anderson, N., Biagi, T.M., Patterson, N., Pielberg, G.R., Kulbokas, E.J.,3rd, Comstock, K.E., Keller, E.T., Mesirov, J.P., von Euler, H., Kampe, O., Hedhammar, A., Lander, E.S., Andersson, G., Andersson, L. & Lindblad-Toh, K. 2007, "Efficient mapping of mendelian traits in dogs through genome-wide association", *Nature genetics,* vol. 39, no. 11, pp. 1321-1328.

Kasparson, A.A., Badridze, J. & Maximov, V.V. 2013, "Colour cues proved to be more informative for dogs than brightness", *Proceedings.Biological sciences,* vol. 280, no. 1766, pp. 20131356.

Kaurani, L., Vishal, M., Kumar, D., Sharma, A., Mehani, B., Sharma, C., Chakraborty, S., Jha, P., Ray, J. & Sen, A. 2014, "Gene-rich large deletions are overrepresented in POAG patients of Indian and Caucasian

origins", *Investigative ophthalmology & visual science,* vol. 55, no. 5, pp. 3258-3264.

Kawaguchi, R., Zhong, M., Kassai, M., Ter-Stepanian, M. & Sun, H. 2012, "STRA6-catalyzed vitamin A influx, efflux, and exchange", *The Journal of membrane biology,* vol. 245, no. 11, pp. 731-745.

Keller, K.E. & Acott, T.S. 2013, "The Juxtacanalicular Region of Ocular Trabecular Meshwork: A Tissue with a Unique Extracellular Matrix and Specialized Function", *Journal of ocular biology,* vol. 1, no. 1, pp. 3.

Kelley, M.W., Turner, J.K. & Reh, T.A. 1994, "Retinoic acid promotes differentiation of photoreceptors in vitro", *Development,* vol. 120, no. 8, pp. 2091-2102.

Khan, A., Fornes, O., Stigliani, A., Gheorghe, M., Castro-Mondragon, J.A., van der Lee, R., Bessy, A., Cheneby, J., Kulkarni, S.R. & Tan, G. 2017, "JASPAR 2018: update of the open-access database of transcription factor binding profiles and its web framework", *Nucleic acids research,* vol. 46, no. D1, pp. D260-D266.

Kijas, J.W., Cideciyan, A.V., Aleman, T.S., Pianta, M.J., Pearce-Kelling, S.E., Miller, B.J., Jacobson, S.G., Aguirre, G.D. & Acland, G.M. 2002, "Naturally occurring rhodopsin mutation in the dog causes retinal dysfunction and degeneration mimicking human dominant retinitis pigmentosa", *Proceedings of the National Academy of Sciences of the United States of America,* vol. 99, no. 9, pp. 6328-6333.

Kirby, A., Kang, H.M., Wade, C.M., Cotsapas, C., Kostem, E., Han, B., Furlotte, N., Kang, E.Y., Rivas, M., Bogue, M.A., Frazer, K.A., Johnson, F.M., Beilharz, E.J., Cox, D.R., Eskin, E. & Daly, M.J. 2010, "Fine mapping in 94 inbred mouse strains using a high-density haplotype resource", *Genetics,* vol. 185, no. 3, pp. 1081-1095.

Kirkness, E.F., Bafna, V., Halpern, A.L., Levy, S., Remington, K., Rusch, D.B., Delcher, A.L., Pop, M., Wang, W., Fraser, C.M. & Venter, J.C. 2003, "The dog genome: survey sequencing and comparative analysis", *Science (New York, N.Y.),* vol. 301, no. 5641, pp. 1898-1903.

Knepper, P.A., Goossens, W. & Palmberg, P.F. 1996, "Glycosaminoglycan stratification of the juxtacanalicular tissue in normal and primary open-angle glaucoma", *Investigative ophthalmology & visual science,* vol. 37, no. 12, pp. 2414-2425.

Kolb, H. & Famiglietti, E.V. 1974, "Rod and cone pathways in the inner plexiform layer of cat retina", *Science (New York, N.Y.),* vol. 186, no. 4158, pp. 47-49.

Kole, C., Klipfel, L., Yang, Y., Ferracane, V., Blond, F., Reichman, S., Millet-Puel, G., Clérin, E., Aït-Ali, N. & Pagan, D. 2018, "Otx2-

genetically modified retinal pigment epithelial cells rescue photoreceptors after transplantation", *Molecular Therapy,* vol. 26, no. 1, pp. 219-237.

Komáromy, A.M., Bras, D., Esson, D.W., Fellman, R.L., Grozdanic, S.D., Kagemann, L., Miller, P.E., Moroi, S.E., Plummer, C.E. & Sapienza, J.S. 2019, "The future of canine glaucoma therapy", *Veterinary ophthalmology,* .

Koressaar, T. & Remm, M. 2007, "Enhancements and modifications of primer design program Primer3", *Bioinformatics (Oxford, England),* vol. 23, no. 10, pp. 1289-1291.

Krinke, A., Schnider, K., Lundbeck, E. & Krinke, G. 1981, "Ganglionic cell distribution in the central area of the beagle dog retina", *Anatomia, Histologia, Embryologia,* vol. 10, no. 1, pp. 26-35.

Krjutskov, K., Koel, M., Roost, A.M., Katayama, S., Einarsdottir, E., Jouhilahti, E.M., Soderhall, C., Jaakma, U., Plaas, M., Vesterlund, L., Lohi, H., Salumets, A. & Kere, J. 2016, "Globin mRNA reduction for whole-blood transcriptome sequencing", *Scientific reports,* vol. 6, pp. 31584.

Kropatsch, R., Akkad, D.A., Frank, M., Rosenhagen, C., Altmüller, J., Nürnberg, P., Epplen, J.T. & Dekomien, G. 2016, "A large deletion in RPGR causes XLPRA in Weimaraner dogs", *Canine genetics and epidemiology,* vol. 3, no. 1, pp. 7.

Kropatsch, R., Petrasch-Parwez, E., Seelow, D., Schlichting, A., Gerding, W.M., Akkad, D.A., Epplen, J.T. & Dekomien, G. 2010, "Generalized progressive retinal atrophy in the Irish Glen of Imaal Terrier is associated with a deletion in the ADAM9 gene", *Molecular and cellular probes,* vol. 24, no. 6, pp. 357-363.

Kuchtey, J., Kunkel, J., Esson, D., Sapienza, J.S., Ward, D.A., Plummer, C.E., Gelatt, K.N. & Kuchtey, R.W. 2013, "Screening ADAMTS10 in Dog Populations Supports Gly661Arg as the Glaucoma-Causing Variant in Beagles ADAMTS10 Variant in Dog Primary Glaucoma", *Investigative ophthalmology & visual science,* vol. 54, no. 3, pp. 1881-1886.

Kuchtey, J., Olson, L.M., Rinkoski, T., MacKay, E.O., Iverson, T., Gelatt, K.N., Haines, J.L. & Kuchtey, R.W. 2011, "Mapping of the disease locus and identification of ADAMTS10 as a candidate gene in a canine model of primary open angle glaucoma", *PLoS genetics,* vol. 7, no. 2, pp. e1001306.

Kuehn, M.H., Lipsett, K.A., Menotti-Raymond, M., Whitmore, S.S., Scheetz, T.E., David, V.A., O'Brien, S.J., Zhao, Z., Jens, J.K. & Snella,

E.M. 2016, "A mutation in LTBP2 causes congenital glaucoma in domestic cats (Felis catus)", *PloS one,* vol. 11, no. 5, pp. e0154412.

Kukekova, A.V., Goldstein, O., Johnson, J.L., Richardson, M.A., Pearce-Kelling, S.E., Swaroop, A., Friedman, J.S., Aguirre, G.D. & Acland, G.M. 2009, "Canine RD3 mutation establishes rod-cone dysplasia type 2 (rcd2) as ortholog of human and murine rd3", *Mammalian Genome,* vol. 20, no. 2, pp. 109-123.

Kutz, W.E., Wang, L.W., Bader, H.L., Majors, A.K., Iwata, K., Traboulsi, E.I., Sakai, L.Y., Keene, D.R. & Apte, S.S. 2011, "ADAMTS10 protein interacts with fibrillin-1 and promotes its deposition in extracellular matrix of cultured fibroblasts", *The Journal of biological chemistry,* vol. 286, no. 19, pp. 17156-17167.

Kvanta, A. 1994, "Expression and secretion of transforming growth factor-beta in transformed and nontransformed retinal pigment epithelial cells", *Ophthalmic research,* vol. 26, no. 6, pp. 361-367.

Kyöstilä, K., Syrjä, P., Jagannathan, V., Chandrasekar, G., Jokinen, T.S., Seppälä, E.H., Becker, D., Drögemüller, M., Dietschi, E. & Drögemüller, C. 2015, "A missense change in the ATG4D gene links aberrant autophagy to a neurodegenerative vacuolar storage disease", *PLoS Genet,* vol. 11, no. 4, pp. e1005169.

Lander, E.S., Linton, L.M., Birren, B., Nusbaum, C., Zody, M.C., Baldwin, J., Devon, K., Dewar, K., Doyle, M., FitzHugh, W., Funke, R., Gage, D., Harris, K., Heaford, A., Howland, J., Kann, L., Lehoczky, J., LeVine, R., McEwan, P., McKernan, K., Meldrim, J., Mesirov, J.P., Miranda, C., Morris, W., Naylor, J., Raymond, C., Rosetti, M., Santos, R., Sheridan, A., Sougnez, C., Stange-Thomann, Y., Stojanovic, N., Subramanian, A., Wyman, D., Rogers, J., Sulston, J., Ainscough, R., Beck, S., Bentley, D., Burton, J., Clee, C., Carter, N., Coulson, A., Deadman, R., Deloukas, P., Dunham, A., Dunham, I., Durbin, R., French, L., Grafham, D., Gregory, S., Hubbard, T., Humphray, S., Hunt, A., Jones, M., Lloyd, C., McMurray, A., Matthews, L., Mercer, S., Milne, S., Mullikin, J.C., Mungall, A., Plumb, R., Ross, M., Shownkeen, R., Sims, S., Waterston, R.H., Wilson, R.K., Hillier, L.W., McPherson, J.D., Marra, M.A., Mardis, E.R., Fulton, L.A., Chinwalla, A.T., Pepin, K.H., Gish, W.R., Chissoe, S.L., Wendl, M.C., Delehaunty, K.D., Miner, T.L., Delehaunty, A., Kramer, J.B., Cook, L.L., Fulton, R.S., Johnson, D.L., Minx, P.J., Clifton, S.W., Hawkins, T., Branscomb, E., Predki, P., Richardson, P., Wenning, S., Slezak, T., Doggett, N., Cheng, J.F., Olsen, A., Lucas, S., Elkin, C., Uberbacher, E., Frazier, M., Gibbs, R.A., Muzny, D.M., Scherer, S.E., Bouck, J.B., Sodergren, E.J., Worley, K.C., Rives, C.M., Gorrell, J.H., Metzker, M.L., Naylor, S.L.,

Kucherlapati, R.S., Nelson, D.L., Weinstock, G.M., Sakaki, Y., Fujiyama, A., Hattori, M., Yada, T., Toyoda, A., Itoh, T., Kawagoe, C., Watanabe, H., Totoki, Y., Taylor, T., Weissenbach, J., Heilig, R., Saurin, W., Artiguenave, F., Brottier, P., Bruls, T., Pelletier, E., Robert, C., Wincker, P., Smith, D.R., Doucette-Stamm, L., Rubenfield, M., Weinstock, K., Lee, H.M., Dubois, J., Rosenthal, A., Platzer, M., Nyakatura, G., Taudien, S., Rump, A., Yang, H., Yu, J., Wang, J., Huang, G., Gu, J., Hood, L., Rowen, L., Madan, A., Qin, S., Davis, R.W., Federspiel, N.A., Abola, A.P., Proctor, M.J., Myers, R.M., Schmutz, J., Dickson, M., Grimwood, J., Cox, D.R., Olson, M.V., Kaul, R., Raymond, C., Shimizu, N., Kawasaki, K., Minoshima, S., Evans, G.A., Athanasiou, M., Schultz, R., Roe, B.A., Chen, F., Pan, H., Ramser, J., Lehrach, H., Reinhardt, R., McCombie, W.R., de la Bastide, M., Dedhia, N., Blocker, H., Hornischer, K., Nordsiek, G., Agarwala, R., Aravind, L., Bailey, J.A., Bateman, A., Batzoglou, S., Birney, E., Bork, P., Brown, D.G., Burge, C.B., Cerutti, L., Chen, H.C., Church, D., Clamp, M., Copley, R.R., Doerks, T., Eddy, S.R., Eichler, E.E., Furey, T.S., Galagan, J., Gilbert, J.G., Harmon, C., Hayashizaki, Y., Haussler, D., Hermjakob, H., Hokamp, K., Jang, W., Johnson, L.S., Jones, T.A., Kasif, S., Kaspryzk, A., Kennedy, S., Kent, W.J., Kitts, P., Koonin, E.V., Korf, I., Kulp, D., Lancet, D., Lowe, T.M., McLysaght, A., Mikkelsen, T., Moran, J.V., Mulder, N., Pollara, V.J., Ponting, C.P., Schuler, G., Schultz, J., Slater, G., Smit, A.F., Stupka, E., Szustakowki, J., Thierry-Mieg, D., Thierry-Mieg, J., Wagner, L., Wallis, J., Wheeler, R., Williams, A., Wolf, Y.I., Wolfe, K.H., Yang, S.P., Yeh, R.F., Collins, F., Guyer, M.S., Peterson, J., Felsenfeld, A., Wetterstrand, K.A., Patrinos, A., Morgan, M.J., de Jong, P., Catanese, J.J., Osoegawa, K., Shizuya, H., Choi, S., Chen, Y.J., Szustakowki, J. & International Human Genome Sequencing Consortium 2001, "Initial sequencing and analysis of the human genome", *Nature,* vol. 409, no. 6822, pp. 860-921.

Laratta, L.J., Riis, R.C., Kern, T.J. & Koch, S.A. 1985, "Multiple congenital ocular defects in the Akita dog", *The Cornell veterinarian,* vol. 75, no. 3, pp. 381-392.

Layer, R.M., Kindlon, N., Karczewski, K.J., Quinlan, A.R. & Exome Aggregation Consortium 2015, "Efficient genotype compression and analysis of large genetic-variation data sets", *Nature methods,* vol. 13, no. 1, pp. 63.

Le Meur, G., Stieger, K., Smith, A., Weber, M., Deschamps, J., Nivard, D., Mendes-Madeira, A., Provost, N., Pereon, Y. & Cherel, Y. 2007, "Restoration of vision in RPE65-deficient Briard dogs using an AAV

serotype 4 vector that specifically targets the retinal pigmented epithelium", *Gene therapy,* vol. 14, no. 4, pp. 292.

Lehtimaki, J., Sinkko, H., Hielm-Bjorkman, A., Salmela, E., Tiira, K., Laatikainen, T., Makelainen, S., Kaukonen, M., Uusitalo, L., Hanski, I., Lohi, H. & Ruokolainen, L. 2018, "Skin microbiota and allergic symptoms associate with exposure to environmental microbes", *Proceedings of the National Academy of Sciences of the United States of America,* vol. 115, no. 19, pp. 4897-4902.

Lei, B. & Yao, G. 2006, "Spectral attenuation of the mouse, rat, pig and human lenses from wavelengths 360 nm to 1020 nm", *Experimental eye research,* vol. 83, no. 3, pp. 610-614.

Lequarré, A., Andersson, L., André, C., Fredholm, M., Hitte, C., Leeb, T., Lohi, H., Lindblad-Toh, K. & Georges, M. 2011, "LUPA: a European initiative taking advantage of the canine genome architecture for unravelling complex disorders in both human and dogs", *The Veterinary Journal,* vol. 189, no. 2, pp. 155-159.

Lesiuk, T.P. & Braekevelt, C.R. 1983, "Fine structure of the canine tapetum lucidum", *Journal of anatomy,* vol. 136, no. Pt 1, pp. 157-164.

Lewis, C.J., Hedberg-Buenz, A., DeLuca, A.P., Stone, E.M., Alward, W.L. & Fingert, J.H. 2017, "Primary congenital and developmental glaucomas", *Human molecular genetics,* vol. 26, no. R1, pp. R28-R36.

Li, H. & Durbin, R. 2009, "Fast and accurate short read alignment with Burrows-Wheeler transform", *Bioinformatics (Oxford, England),* vol. 25, no. 14, pp. 1754-1760.

Lin, B. & Masland, R.H. 2006, "Populations of wide-field amacrine cells in the mouse retina", *The Journal of comparative neurology,* vol. 499, no. 5, pp. 797-809.

Lindblad-Toh, K., Wade, C.M., Mikkelsen, T.S., Karlsson, E.K., Jaffe, D.B., Kamal, M., Clamp, M., Chang, J.L., Kulbokas, E.J. & Zody, M.C. 2005, "Genome sequence, comparative analysis and haplotype structure of the domestic dog", *Nature,* vol. 438, no. 7069, pp. 803-819.

Littlefield, R. & Fowler, V. 1998, "Defining actin filament length in striated muscle: rulers and caps or dynamic stability?", *Annual Review of Cell and Developmental Biology,* vol. 14, no. 1, pp. 487-525.

Liu, H. & Naismith, J.H. 2008, "An efficient one-step site-directed deletion, insertion, single and multiple-site plasmid mutagenesis protocol", *BMC biotechnology,* vol. 8, no. 1, pp. 91.

Livak, K.J. & Schmittgen, T.D. 2001, "Analysis of relative gene expression data using real-time quantitative PCR and the 2– ΔΔCT method", *methods,* vol. 25, no. 4, pp. 402-408.

Love, M.I., Huber, W. & Anders, S. 2014, "Moderated estimation of fold change and dispersion for RNA-seq data with DESeq2", *Genome biology,* vol. 15, no. 12, pp. 550-014-0550-8.

Lupo, G., Gestri, G., O'Brien, M., Denton, R.M., Chandraratna, R.A., Ley, S.V., Harris, W.A. & Wilson, S.W. 2011, "Retinoic acid receptor signaling regulates choroid fissure closure through independent mechanisms in the ventral optic cup and periocular mesenchyme", *Proceedings of the National Academy of Sciences,* vol. 108, no. 21, pp. 8698-8703.

MacNeil, M.A., Heussy, J.K., Dacheux, R.F., Raviola, E. & Masland, R.H. 1999, "The shapes and numbers of amacrine cells: matching of photofilled with Golgi-stained cells in the rabbit retina and comparison with other mammalian species", *The Journal of comparative neurology,* vol. 413, no. 2, pp. 305-326.

MacNeil, M.A. & Masland, R.H. 1998, "Extreme diversity among amacrine cells: implications for function", *Neuron,* vol. 20, no. 5, pp. 971-982.

Martínez-Morales, J.R., Dolez, V., Rodrigo, I., Zaccarini, R., Leconte, L., Bovolenta, P. & Saule, S. 2003, "OTX2 activates the molecular network underlying retina pigment epithelium differentiation", *Journal of Biological Chemistry,* vol. 278, no. 24, pp. 21721-21731.

Matsushima, D., Heavner, W. & Pevny, L.H. 2011, "Combinatorial regulation of optic cup progenitor cell fate by SOX2 and PAX6", *Development (Cambridge, England),* vol. 138, no. 3, pp. 443-454.

McKenna, A., Hanna, M., Banks, E., Sivachenko, A., Cibulskis, K., Kernytsky, A., Garimella, K., Altshuler, D., Gabriel, S., Daly, M. & DePristo, M.A. 2010, "The Genome Analysis Toolkit: a MapReduce framework for analyzing next-generation DNA sequencing data", *Genome research,* vol. 20, no. 9, pp. 1297-1303.

Mellersh, C.S., McLaughlin, B., Ahonen, S., Pettitt, L., Lohi, H. & Barnett, K.C. 2009, "Mutation in HSF4 is associated with hereditary cataract in the Australian Shepherd", *Veterinary ophthalmology,* vol. 12, no. 6, pp. 372-378.

Mellersh, C.S., Pettitt, L., Forman, O.P., Vaudin, M. & Barnett, K.C. 2006a, "Identification of mutations in HSF4 in dogs of three different breeds with hereditary cataracts", *Veterinary ophthalmology,* vol. 9, no. 5, pp. 369-378.

Mellersh, C., Boursnell, M., Pettitt, L., Ryder, E., Holmes, N., Grafham, D., Forman, O., Sampson, J., Barnett, K. & Blanton, S. 2006b, "Canine RPGRIP1 mutation establishes cone–rod dystrophy in miniature longhaired dachshunds as a homologue of human Leber congenital amaurosis", *Genomics,* vol. 88, no. 3, pp. 293-301.

Mellersh, C.S., Graves, K.T., McLaughlin, B., Ennis, R.B., Pettitt, L., Vaudin, M. & Barnett, K.C. 2007, "Mutation in HSF4 associated with early but not late-onset hereditary cataract in the Boston Terrier", *The Journal of heredity,* vol. 98, no. 5, pp. 531-533.

Mikheyev, A.S. & Tin, M.M. 2014, "A first look at the Oxford Nanopore MinION sequencer", *Molecular ecology resources,* vol. 14, no. 6, pp. 1097-1102.

Miller, P.E. & Bentley, E. 2015, "Clinical Signs and Diagnosis of the Canine Primary Glaucomas", *The Veterinary clinics of North America.Small animal practice,* vol. 45, no. 6, pp. 1183-212, vi.

Miyadera, K. 2018, "Mapping of Canine Models of Inherited Retinal Diseases" in *Retinal Degenerative Diseases* Springer, , pp. 257-264.

Miyadera, K., Acland, G.M. & Aguirre, G.D. 2012, "Genetic and phenotypic variations of inherited retinal diseases in dogs: the power of within-and across-breed studies", *Mammalian Genome,* vol. 23, no. 1-2, pp. 40-61.

Miyadera, K., Kato, K., Aguirre-Hernandez, J., Tokuriki, T., Morimoto, K., Busse, C., Barnett, K., Holmes, N., Ogawa, H., Sasaki, N., Mellersh, C.S. & Sargan, D.R. 2009, "Phenotypic variation and genotype-phenotype discordance in canine cone-rod dystrophy with an RPGRIP1 mutation", *Molecular vision,* vol. 15, pp. 2287-2305.

Miyadera, K., Kato, K., Boursnell, M., Mellersh, C.S. & Sargan, D.R. 2012, "Genome-wide association study in RPGRIP1(-/-) dogs identifies a modifier locus that determines the onset of retinal degeneration", *Mammalian genome : official journal of the International Mammalian Genome Society,* vol. 23, no. 1-2, pp. 212-223.

Mookherjee, S., Chakraborty, S., Vishal, M., Banerjee, D., Sen, A. & Ray, K. 2011, "WDR36 variants in East Indian primary open-angle glaucoma patients", *Molecular vision,* vol. 17, pp. 2618.

Morrison, D., FitzPatrick, D., Hanson, I., Williamson, K., van Heyningen, V., Fleck, B., Jones, I., Chalmers, J. & Campbell, H. 2002, "National study of microphthalmia, anophthalmia, and coloboma (MAC) in Scotland: investigation of genetic aetiology", *Journal of medical genetics,* vol. 39, no. 1, pp. 16-22.

Mouse Genome Sequencing Consortium, Waterston, R.H., Lindblad-Toh, K., Birney, E., Rogers, J., Abril, J.F., Agarwal, P., Agarwala, R., Ainscough, R., Alexandersson, M., An, P., Antonarakis, S.E., Attwood, J., Baertsch, R., Bailey, J., Barlow, K., Beck, S., Berry, E., Birren, B., Bloom, T., Bork, P., Botcherby, M., Bray, N., Brent, M.R., Brown, D.G., Brown, S.D., Bult, C., Burton, J., Butler, J., Campbell, R.D., Carninci, P., Cawley, S., Chiaromonte, F., Chinwalla, A.T., Church, D.M., Clamp, M., Clee, C., Collins, F.S., Cook, L.L., Copley, R.R.,

Coulson, A., Couronne, O., Cuff, J., Curwen, V., Cutts, T., Daly, M., David, R., Davies, J., Delehaunty, K.D., Deri, J., Dermitzakis, E.T., Dewey, C., Dickens, N.J., Diekhans, M., Dodge, S., Dubchak, I., Dunn, D.M., Eddy, S.R., Elnitski, L., Emes, R.D., Eswara, P., Eyras, E., Felsenfeld, A., Fewell, G.A., Flicek, P., Foley, K., Frankel, W.N., Fulton, L.A., Fulton, R.S., Furey, T.S., Gage, D., Gibbs, R.A., Glusman, G., Gnerre, S., Goldman, N., Goodstadt, L., Grafham, D., Graves, T.A., Green, E.D., Gregory, S., Guigo, R., Guyer, M., Hardison, R.C., Haussler, D., Hayashizaki, Y., Hillier, L.W., Hinrichs, A., Hlavina, W., Holzer, T., Hsu, F., Hua, A., Hubbard, T., Hunt, A., Jackson, I., Jaffe, D.B., Johnson, L.S., Jones, M., Jones, T.A., Joy, A., Kamal, M., Karlsson, E.K., Karolchik, D., Kasprzyk, A., Kawai, J., Keibler, E., Kells, C., Kent, W.J., Kirby, A., Kolbe, D.L., Korf, I., Kucherlapati, R.S., Kulbokas, E.J., Kulp, D., Landers, T., Leger, J.P., Leonard, S., Letunic, I., Levine, R., Li, J., Li, M., Lloyd, C., Lucas, S., Ma, B., Maglott, D.R., Mardis, E.R., Matthews, L., Mauceli, E., Mayer, J.H., McCarthy, M., McCombie, W.R., McLaren, S., McLay, K., McPherson, J.D., Meldrim, J., Meredith, B., Mesirov, J.P., Miller, W., Miner, T.L., Mongin, E., Montgomery, K.T., Morgan, M., Mott, R., Mullikin, J.C., Muzny, D.M., Nash, W.E., Nelson, J.O., Nhan, M.N., Nicol, R., Ning, Z., Nusbaum, C., O'Connor, M.J., Okazaki, Y., Oliver, K., Overton-Larty, E., Pachter, L., Parra, G., Pepin, K.H., Peterson, J., Pevzner, P., Plumb, R., Pohl, C.S., Poliakov, A., Ponce, T.C., Ponting, C.P., Potter, S., Quail, M., Reymond, A., Roe, B.A., Roskin, K.M., Rubin, E.M., Rust, A.G., Santos, R., Sapojnikov, V., Schultz, B., Schultz, J., Schwartz, M.S., Schwartz, S., Scott, C., Seaman, S., Searle, S., Sharpe, T., Sheridan, A., Shownkeen, R., Sims, S., Singer, J.B., Slater, G., Smit, A., Smith, D.R., Spencer, B., Stabenau, A., Stange-Thomann, N., Sugnet, C., Suyama, M., Tesler, G., Thompson, J., Torrents, D., Trevaskis, E., Tromp, J., Ucla, C., Ureta-Vidal, A., Vinson, J.P., Von Niederhausern, A.C., Wade, C.M., Wall, M., Weber, R.J., Weiss, R.B., Wendl, M.C., West, A.P., Wetterstrand, K., Wheeler, R., Whelan, S., Wierzbowski, J., Willey, D., Williams, S., Wilson, R.K., Winter, E., Worley, K.C., Wyman, D., Yang, S., Yang, S.P., Zdobnov, E.M., Zody, M.C. & Lander, E.S. 2002, "Initial sequencing and comparative analysis of the mouse genome", *Nature,* vol. 420, no. 6915, pp. 520-562.

Mowat, F.M., Petersen-Jones, S.M., Williamson, H., Williams, D.L., Luthert, P.J., Ali, R.R. & Bainbridge, J.W. 2008, "Topographical characterization of cone photoreceptors and the area centralis of the canine retina", *Molecular vision,* vol. 14, pp. 2518-2527.

Muhandiram, D. & Kay, L.E. 1994, "Gradient-enhanced triple-resonance three-dimensional NMR experiments with improved sensitivity", *Journal of Magnetic Resonance, Series B,* vol. 103, no. 3, pp. 203-216.

Murakami, M., Otsu, K. & Otsuka, T. 1972, "Effects of chemicals on receptors and horizontal cells in the retina", *The Journal of physiology,* vol. 227, no. 3, pp. 899-913.

Murgiano, L., Becker, D., Torjman, D., Niggel, J.K., Milano, A., Cullen, C., Feng, R., Wang, F., Jagannathan, V., Pearce-Kelling, S., Katz, M.L., Leeb, T. & Aguirre, G.D. 2018, "Complex Structural PPT1 Variant Associated with Non-syndromic Canine Retinal Degeneration", *G3 (Bethesda, Md.),* .

Narayan, D.S., Wood, J.P., Chidlow, G. & Casson, R.J. 2016, "A review of the mechanisms of cone degeneration in retinitis pigmentosa", *Acta Ophthalmologica,* vol. 94, no. 8, pp. 748-754.

Narfström, K., Bragadóttir, R., Redmond, T.M., Rakoczy, P.E., van Veen, T. & Bruun, A. 2003, "Functional and structural evaluation after AAV. RPE65 gene transfer in the canine model of Leber's congenital amaurosis" in *Retinal Degenerations* Springer, , pp. 423-430.

Narooie-Nejad, M., Paylakhi, S.H., Shojaee, S., Fazlali, Z., Rezaei Kanavi, M., Nilforushan, N., Yazdani, S., Babrzadeh, F., Suri, F. & Ronaghi, M. 2009, "Loss of function mutations in the gene encoding latent transforming growth factor beta binding protein 2, LTBP2, cause primary congenital glaucoma", *Human molecular genetics,* vol. 18, no. 20, pp. 3969-3977.

Neitz, J., Geist, T. & Jacobs, G.H. 1989, "Color vision in the dog", *Visual neuroscience,* vol. 3, no. 2, pp. 119-125.

Ng, P.C. & Henikoff, S. 2001, "Predicting deleterious amino acid substitutions", *Genome research,* vol. 11, no. 5, pp. 863-874.

Ofri, R., Dawson, W. & Samuelson, D. 1995, "Mapping of the cortical area of central vision in two dog breeds", *Ophthalmic Literature,* vol. 1, no. 48, pp. 61.

Oliver, J., Ekiri, A. & Mellersh, C. 2016a, "Prevalence and progression of pectinate ligament dysplasia in the Welsh springer spaniel", *Journal of Small Animal Practice,* vol. 57, no. 8, pp. 416-421.

Oliver, J.A., Ekiri, A. & Mellersh, C.S. 2016b, "Prevalence of pectinate ligament dysplasia and associations with age, sex and intraocular pressure in the Basset hound, Flatcoated retriever and Dandie Dinmont terrier", *Canine genetics and epidemiology,* vol. 3, no. 1, pp. 1.

Oliver, J.A., Forman, O.P., Pettitt, L. & Mellersh, C.S. 2015, "Two independent mutations in ADAMTS17 are associated with primary open

angle glaucoma in the Basset Hound and Basset Fauve de Bretagne breeds of dog", *PloS one,* vol. 10, no. 10, pp. e0140436.

Oliver, J.A., Ricketts, S.L., Kuehn, M.H. & Mellersh, C.S. 2019a, "Primary closed angle glaucoma in the Basset Hound: Genetic investigations using genome-wide association and RNA sequencing strategies", *Molecular vision,* vol. 25, pp. 93.

Oliver, J.A., Wright, H., Massidda, P.A., Burmeister, L.M. & Mellersh, C.S. 2019b, "A variant in OLFML3 is associated with pectinate ligament abnormality and primary closed-angle glaucoma in Border Collies from the United Kingdom", *Veterinary ophthalmology,* .

Oliver, J.A.C., Rustidge, S., Pettitt, L., Jenkins, C.A., Farias, F.H.G., Giuliano, E.A. & Mellersh, C.S. 2018, "Evaluation of ADAMTS17 in Chinese Shar-Pei with primary open-angle glaucoma, primary lens luxation, or both", *American Journal of Veterinary Research,* vol. 79, no. 1, pp. 98-106.

Onwochei, B.C., Simon, J.W., Bateman, J.B., Couture, K.C. & Mir, E. 2000, "Ocular colobomata", *Survey of ophthalmology,* vol. 45, no. 3, pp. 175-194.

Oshima, Y., Bjerkas, E. & Peiffer Jr, R.L. 2004, "Ocular histopathologic observations in Norwegian Elkhounds with primary open-angle, closed-cleft glaucoma", *Veterinary ophthalmology,* vol. 7, no. 3, pp. 185-188.

Ovchinnikov, Y. 1982, "Rhodopsin and bacteriorhodopsin: structure-function relationships", *FEBS letters,* vol. 148, no. 2, pp. 179-191.

Palczewski, K., Jager, S., Buczylko, J., Crouch, R.K., Bredberg, D.L., Hofmann, K.P., Asson-Batres, M.A. & Saari, J.C. 1994, "Rod outer segment retinol dehydrogenase: substrate specificity and role in phototransduction", *Biochemistry,* vol. 33, no. 46, pp. 13741-13750.

Palczewski, K., Kumasaka, T., Hori, T., Behnke, C.A., Motoshima, H., Fox, B.A., Le Trong, I., Teller, D.C., Okada, T., Stenkamp, R.E., Yamamoto, M. & Miyano, M. 2000, "Crystal structure of rhodopsin: A G protein-coupled receptor", *Science (New York, N.Y.),* vol. 289, no. 5480, pp. 739-745.

Pannbacker, R.G., Fleischman, D.E. & Reed, D.W. 1972, "Cyclic nucleotide phosphodiesterase: high activity in a mammalian photoreceptor", *Science (New York, N.Y.),* vol. 175, no. 4023, pp. 757-758.

Parker, H.G., Kukekova, A.V., Akey, D.T., Goldstein, O., Kirkness, E.F., Baysac, K.C., Mosher, D.S., Aguirre, G.D., Acland, G.M. & Ostrander, E.A. 2007, "Breed relationships facilitate fine-mapping studies: a 7.8-kb deletion cosegregates with Collie eye anomaly across multiple dog breeds", *Genome research,* vol. 17, no. 11, pp. 1562-1571.

Parry, H.B. 1953, "Degenerations of the dog retina. II. Generalized progressive atrophy of hereditary origin", *The British journal of ophthalmology,* vol. 37, no. 8, pp. 487-502.

Parshall, C.J., Wyman, M., Nitroy, S., Acland, G.M. & Aguirre, G.D. 1991, "Photoreceptor dysplasia: an inherited progressive retinal atrophy of miniature schnauzer dogs", *Progress in Veterinary & Comparative Ophthalmology,* vol. 1, no. 3, pp. 187.

Pasutto, F., Matsumoto, T., Mardin, C.Y., Sticht, H., Brandstätter, J.H., Michels-Rautenstrauss, K., Weisschuh, N., Gramer, E., Ramdas, W.D. & van Koolwijk, L.M. 2009, "Heterozygous NTF4 mutations impairing neurotrophin-4 signaling in patients with primary open-angle glaucoma", *The American Journal of Human Genetics,* vol. 85, no. 4, pp. 447-456.

Pasutto, F., Sticht, H., Hammersen, G., Gillessen-Kaesbach, G., FitzPatrick, D.R., Nürnberg, G., Brasch, F., Schirmer-Zimmermann, H., Tolmie, J.L. & Chitayat, D. 2007, "Mutations in STRA6 cause a broad spectrum of malformations including anophthalmia, congenital heart defects, diaphragmatic hernia, alveolar capillary dysplasia, lung hypoplasia, and mental retardation", *The American Journal of Human Genetics,* vol. 80, no. 3, pp. 550-560.

Pearl, R., Gould, D. & Spiess, B. 2015, "Progression of pectinate ligament dysplasia over time in two populations of Flat-Coated Retrievers", *Veterinary ophthalmology,* vol. 18, no. 1, pp. 6-12.

Peichl, L. 1992, "Topography of ganglion cells in the dog and wolf retina", *The Journal of comparative neurology,* vol. 324, no. 4, pp. 603-620.

Peiffer, J.R., Gum, G., Grimson, R. & Gelatt, K. 1980, "Aqueous humor outflow in beagles with inherited glaucoma: constant pressure perfusion.", *American Journal of Veterinary Research,* vol. 41, no. 11, pp. 1808-1813.

Peiffer, R.L.,Jr & Gelatt, K.N. 1980, "Aqueous humor outflow in Beagles with inherited glaucoma: gross and light microscopic observations of the iridocorneal angle", *American Journal of Veterinary Research,* vol. 41, no. 6, pp. 861-867.

Permi, P. & Annila, A. 2004, "Coherence transfer in proteins", *Progress in Nuclear Magnetic Resonance Spectroscopy,* vol. 44, no. 1, pp. 97-137.

Pertea, M., Kim, D., Pertea, G.M., Leek, J.T. & Salzberg, S.L. 2016, "Transcript-level expression analysis of RNA-seq experiments with HISAT, StringTie and Ballgown", *Nature protocols,* vol. 11, no. 9, pp. 1650-1667.

Petersen–Jones, S.M., Entz, D.D. & Sargan, D.R. 1999, "cGMP phosphodiesterase-α mutation causes progressive retinal atrophy in the Cardigan Welsh corgi dog", *Investigative ophthalmology & visual science,* vol. 40, no. 8, pp. 1637-1644.

Petersen-Jones, S.M. & Komáromy, A.M. 2014, "Dog models for blinding inherited retinal dystrophies", *Human Gene Therapy Clinical Development,* vol. 26, no. 1, pp. 15-26.

Pizzirani, S. 2015, "Definition, classification, and pathophysiology of canine glaucoma", *Veterinary Clinics: Small Animal Practice,* vol. 45, no. 6, pp. 1127-1157.

Pizzirani, S. & Gong, H. 2015, "Functional Anatomy of the Outflow Facilities", *The Veterinary clinics of North America.Small animal practice,* vol. 45, no. 6, pp. 1101-26, v.

Porter, S., Clark, I.M., Kevorkian, L. & Edwards, D.R. 2005, "The ADAMTS metalloproteinases", *The Biochemical journal,* vol. 386, no. Pt 1, pp. 15-27.

Pretzer, S.D. 2008, "Canine embryonic and fetal development: a review", *Theriogenology,* vol. 70, no. 3, pp. 300-303.

Pugh, C.A., Farrell, L.L., Carlisle, A.J., Bush, S.J., Ewing, A., Trejo-Reveles, V., Matika, O., de Kloet, A., Walsh, C. & Bishop, S.C. 2019, "Arginine to glutamine variant in olfactomedin like 3 (OLFML3) is a candidate for severe goniodysgenesis and glaucoma in the Border Collie dog breed", *G3: Genes, Genomes, Genetics,* vol. 9, no. 3, pp. 943-954.

Purcell, S., Neale, B., Todd-Brown, K., Thomas, L., Ferreira, M.A., Bender, D., Maller, J., Sklar, P., De Bakker, P.I. & Daly, M.J. 2007, "PLINK: a tool set for whole-genome association and population-based linkage analyses", *The American Journal of Human Genetics,* vol. 81, no. 3, pp. 559-575.

Quadro, L., Hamberger, L., Gottesman, M.E., Wang, F., Colantuoni, V., Blaner, W.S. & Mendelsohn, C.L. 2005, "Pathways of vitamin A delivery to the embryo: insights from a new tunable model of embryonic vitamin A deficiency", *Endocrinology,* vol. 146, no. 10, pp. 4479-4490.

Quiring, R., Walldorf, U., Kloter, U. & Gehring, W.J. 1994, "Homology of the eyeless gene of Drosophila to the Small eye gene in mice and Aniridia in humans", *Science (New York, N.Y.),* vol. 265, no. 5173, pp. 785-789.

Ragge, N.K., Brown, A.G., Poloschek, C.M., Lorenz, B., Henderson, R.A., Clarke, M.P., Russell-Eggitt, I., Fielder, A., Gerrelli, D., Martinez-Barbera, J.P., Ruddle, P., Hurst, J., Collin, J.R., Salt, A., Cooper, S.T., Thompson, P.J., Sisodiya, S.M., Williamson, K.A., Fitzpatrick, D.R.,

van Heyningen, V. & Hanson, I.M. 2005, "Heterozygous mutations of OTX2 cause severe ocular malformations", *American Journal of Human Genetics,* vol. 76, no. 6, pp. 1008-1022.

Ramirez, F. & Rifkin, D.B. 2009, "Extracellular microfibrils: contextual platforms for TGFbeta and BMP signaling", *Current opinion in cell biology,* vol. 21, no. 5, pp. 616-622.

Ramirez, F. & Sakai, L.Y. 2010, "Biogenesis and function of fibrillin assemblies", *Cell and tissue research,* vol. 339, no. 1, pp. 71-82.

Rattner, A. & Nathans, J. 2005, "The genomic response to retinal disease and injury: evidence for endothelin signaling from photoreceptors to glia", *Journal of Neuroscience,* vol. 25, no. 18, pp. 4540-4549.

Rattner, A., Smallwood, P.M. & Nathans, J. 2000, "Identification and characterization of all-trans-retinol dehydrogenase from photoreceptor outer segments, the visual cycle enzyme that reduces all-trans-retinal to all-trans-retinol", *The Journal of biological chemistry,* vol. 275, no. 15, pp. 11034-11043.

Rattner, A., Yu, H., Williams, J., Smallwood, P.M. & Nathans, J. 2013, "Endothelin-2 signaling in the neural retina promotes the endothelial tip cell state and inhibits angiogenesis", *Proceedings of the National Academy of Sciences of the United States of America,* vol. 110, no. 40, pp. E3830-9.

Rezaie, T., Child, A., Hitchings, R., Brice, G., Miller, L., Coca-Prados, M., Héon, E., Krupin, T., Ritch, R. & Kreutzer, D. 2002, "Adult-onset primary open-angle glaucoma caused by mutations in optineurin", *Science,* vol. 295, no. 5557, pp. 1077-1079.

Rizzolo, L.J. 1997, "Polarity and the development of the outer blood-retinal barrier", *Histology and histopathology,* vol. 12, no. 4, pp. 1057-1067.

Rohen, J.W., Futa, R. & Lutjen-Drecoll, E. 1981, "The fine structure of the cribriform meshwork in normal and glaucomatous eyes as seen in tangential sections", *Investigative ophthalmology & visual science,* vol. 21, no. 4, pp. 574-585.

Roosing, S., Thiadens, A.A., Hoyng, C.B., Klaver, C.C., den Hollander, A.I. & Cremers, F.P. 2014, "Causes and consequences of inherited cone disorders", *Progress in retinal and eye research,* vol. 42, pp. 1-26.

Saari, J.C. & Bredberg, D.L. 1989, "Lecithin:retinol acyltransferase in retinal pigment epithelial microsomes", *The Journal of biological chemistry,* vol. 264, no. 15, pp. 8636-8640.

Sablin, M. & Khlopachev, G. 2002, "The earliest Ice Age dogs: evidence from Eliseevichi", *Current anthropology,* vol. 43, no. 5, pp. 795-799.

Samardzija, M., Wariwoda, H., Imsand, C., Huber, P., Heynen, S.R., Gubler, A. & Grimm, C. 2012, "Activation of survival pathways in the degenerating retina of rd10 mice", *Experimental eye research,* vol. 99, pp. 17-26.

Samuelson, D.A., Gelatt, K.N. & Gum, G.G. 1984, "Kinetics of phagocytosis in the normal canine iridocorneal angle", *American Journal of Veterinary Research,* vol. 45, no. 11, pp. 2359-2366.

Sarfarazi, M. 1997, "Recent advances in molecular genetics of glaucomas", *Human molecular genetics,* vol. 6, no. 10, pp. 1667-1677.

Sargan, D.R. 2004, "IDID: inherited diseases in dogs: web-based information for canine inherited disease genetics", *Mammalian genome : official journal of the International Mammalian Genome Society,* vol. 15, no. 6, pp. 503-506.

Sattler, M., Schleucher, J. & Griesinger, C. 1999, "Heteronuclear multidimensional NMR experiments for the structure determination of proteins in solution.", *Progress in Nuclear Magnetic Resonance Spectroscopy,* vol. 34, pp. 93-158.

Savolainen, P., Zhang, Y.P., Luo, J., Lundeberg, J. & Leitner, T. 2002, "Genetic evidence for an East Asian origin of domestic dogs", *Science (New York, N.Y.),* vol. 298, no. 5598, pp. 1610-1613.

Selvaraj, S.R., Bhatia, V. & Tatu, U. 2008, "Oxidative folding and assembly with transthyretin are sequential events in the biogenesis of retinol binding protein in the endoplasmic reticulum", *Molecular biology of the cell,* vol. 19, no. 12, pp. 5579-5592.

Sengle, G., Tsutsui, K., Keene, D.R., Tufa, S.F., Carlson, E.J., Charbonneau, N.L., Ono, R.N., Sasaki, T., Wirtz, M.K., Samples, J.R., Fessler, L.I., Fessler, J.H., Sekiguchi, K., Hayflick, S.J. & Sakai, L.Y. 2012, "Microenvironmental regulation by fibrillin-1", *PLoS genetics,* vol. 8, no. 1, pp. e1002425.

Sharma, D. & Rajarathnam, K. 2000, "13C NMR chemical shifts can predict disulfide bond formation", *Journal of Biomolecular NMR,* vol. 18, no. 2, pp. 165-171.

Shaw, G.C., Tse, M.P.Y. & Miller, A.D. 2019, "Microphthalmia With Multiple Anterior Segment Defects in Portuguese Water Dogs", *Veterinary pathology,* vol. 56, no. 2, pp. 269-273.

Sherman, S.M. & Wilson, J.R. 1975, "Behavioral and morphological evidence for binocular competition in the postnatal development of the dog's visual system", *Journal of Comparative Neurology,* vol. 161, no. 2, pp. 183-195.

Sidjanin, D.J., Lowe, J.K., McElwee, J.L., Milne, B.S., Phippen, T.M., Sargan, D.R., Aguirre, G.D., Acland, G.M. & Ostrander, E.A. 2002, "Canine CNGB3 mutations establish cone degeneration as orthologous to the human achromatopsia locus ACHM3", *Human molecular genetics,* vol. 11, no. 16, pp. 1823-1833.

Sieving, P.A. & Collins, F.S. 2007, "Genetic ophthalmology and the era of clinical care", *JAMA,* vol. 297, no. 7, pp. 733-736.

Simon, A., Romert, A., Gustafson, A.L., McCaffery, J.M. & Eriksson, U. 1999, "Intracellular localization and membrane topology of 11-cis retinol dehydrogenase in the retinal pigment epithelium suggest a compartmentalized synthesis of 11-cis retinaldehyde", *Journal of cell science,* vol. 112 (Pt 4), no. Pt 4, pp. 549-558.

Simones, P., De Geest, J.P. & Lauwers, H. 1996, "Comparative morphology of the pectinate ligaments of domestic mammals, as observed under the dissecting microscope and the scanning electron microscope", *The Journal of veterinary medical science,* vol. 58, no. 10, pp. 977-982.

Smith, P.J., Zhang, C., Wang, J., Chew, S.L., Zhang, M.Q. & Krainer, A.R. 2006, "An increased specificity score matrix for the prediction of SF2/ASF-specific exonic splicing enhancers", *Human molecular genetics,* vol. 15, no. 16, pp. 2490-2508.

Somerville, R.P., Jungers, K.A. & Apte, S.S. 2004, "Discovery and characterization of a novel, widely expressed metalloprotease, ADAMTS10, and its proteolytic activation", *The Journal of biological chemistry,* vol. 279, no. 49, pp. 51208-51217.

Souma, T., Tompson, S.W., Thomson, B.R., Siggs, O.M., Kizhatil, K., Yamaguchi, S., Feng, L., Limviphuvadh, V., Whisenhunt, K.N. & Maurer-Stroh, S. 2016, "Angiopoietin receptor TEK mutations underlie primary congenital glaucoma with variable expressivity", *The Journal of clinical investigation,* vol. 126, no. 7, pp. 2575-2587.

Steinkellner, H., Etzler, J., Gogoll, L., Neesen, J., Stifter, E., Brandau, O. & Laccone, F. 2015, "Identification and molecular characterisation of a homozygous missense mutation in the ADAMTS10 gene in a patient with Weill–Marchesani syndrome", *European Journal of Human Genetics,* vol. 23, no. 9, pp. 1186.

Stoilov, I., Jansson, I., Sarfarazi, M. & Schenkman, J.B. 2001, "Roles of cytochrome p450 in development", *Drug metabolism and drug interactions,* vol. 18, no. 1, pp. 33-56.

Stoilov, I., Akarsu, A.N., Alozie, I., Child, A., Barsoum-Homsy, M., Turacli, M.E., Or, M., Lewis, R.A., Ozdemir, N. & Brice, G. 1998, "Sequence analysis and homology modeling suggest that primary congenital glaucoma on 2p21 results from mutations disrupting either the hinge

region or the conserved core structures of cytochrome P4501B1", *The American Journal of human genetics,* vol. 62, no. 3, pp. 573-584.

Stoilov, I., Akarsu, A.N. & Sarfarazi, M. 1997, "Identification of three different truncating mutations in cytochrome P4501B1 (CYP1B1) as the principal cause of primary congenital glaucoma (Buphthalmos) in families linked to the GLC3A locus on chromosome 2p21", *Human molecular genetics,* vol. 6, no. 4, pp. 641-647.

Strom, A.R., Hässig, M., Iburg, T.M. & Spiess, B.M. 2011, "Epidemiology of canine glaucoma presented to University of Zurich from 1995 to 2009. Part 1: Congenital and primary glaucoma (4 and 123 cases)", *Veterinary ophthalmology,* vol. 14, no. 2, pp. 121-126.

Suber, M.L., Pittler, S.J., Qin, N., Wright, G.C., Holcombe, V., Lee, R.H., Craft, C.M., Lolley, R.N., Baehr, W. & Hurwitz, R.L. 1993, "Irish setter dogs affected with rod/cone dysplasia contain a nonsense mutation in the rod cGMP phosphodiesterase beta-subunit gene.", *Proceedings of the National Academy of Sciences,* vol. 90, no. 9, pp. 3968-3972.

Suire, S., Stewart, F., Beauchamp, J. & Kennedy, M.W. 2001, "Uterocalin, a lipocalin provisioning the preattachment equine conceptus: fatty acid and retinol binding properties, and structural characterization", *The Biochemical journal,* vol. 356, no. Pt 2, pp. 369-376.

Sunderman, E.R. & Zagotta, W.N. 1999, "Sequence of events underlying the allosteric transition of rod cyclic nucleotide-gated channels", *The Journal of general physiology,* vol. 113, no. 5, pp. 621-640.

Sutter, N.B., Eberle, M.A., Parker, H.G., Pullar, B.J., Kirkness, E.F., Kruglyak, L. & Ostrander, E.A. 2004, "Extensive and breed-specific linkage disequilibrium in Canis familiaris", *Genome research,* vol. 14, no. 12, pp. 2388-2396.

Swaminathan, S.S., Oh, D.J., Kang, M.H. & Rhee, D.J. 2014, "Aqueous outflow: segmental and distal flow", *Journal of cataract and refractive surgery,* vol. 40, no. 8, pp. 1263-1272.

Szel, A. & Rohlich, P. 1992, "Two cone types of rat retina detected by anti-visual pigment antibodies", *Experimental eye research,* vol. 55, no. 1, pp. 47-52.

Tabbara, K.F. & Badr, I.A. 1985, "Changing pattern of childhood blindness in Saudi Arabia", *The British journal of ophthalmology,* vol. 69, no. 4, pp. 312-315.

Tamm, E.R. 2009, "The trabecular meshwork outflow pathways: structural and functional aspects", *Experimental eye research,* vol. 88, no. 4, pp. 648-655.

Tan, G. & Lenhard, B. 2016, "TFBSTools: an R/bioconductor package for transcription factor binding site analysis", *Bioinformatics,* vol. 32, no. 10, pp. 1555-1556.

Tanaka, N., Dutrow, E.V., Miyadera, K., Delemotte, L., MacDermaid, C.M., Reinstein, S.L., Crumley, W.R., Dixon, C.J., Casal, M.L. & Klein, M.L. 2015, "Canine CNGA3 gene mutations provide novel insights into human achromatopsia-associated channelopathies and treatment", *PloS one,* vol. 10, no. 9, pp. e0138943.

Taranova, O.V., Magness, S.T., Fagan, B.M., Wu, Y., Surzenko, N., Hutton, S.R. & Pevny, L.H. 2006, "SOX2 is a dose-dependent regulator of retinal neural progenitor competence", *Genes & development,* vol. 20, no. 9, pp. 1187-1202.

Thalmann, O., Shapiro, B., Cui, P., Schuenemann, V.J., Sawyer, S.K., Greenfield, D.L., Germonpre, M.B., Sablin, M.V., Lopez-Giraldez, F., Domingo-Roura, X., Napierala, H., Uerpmann, H.P., Loponte, D.M., Acosta, A.A., Giemsch, L., Schmitz, R.W., Worthington, B., Buikstra, J.E., Druzhkova, A., Graphodatsky, A.S., Ovodov, N.D., Wahlberg, N., Freedman, A.H., Schweizer, R.M., Koepfli, K.P., Leonard, J.A., Meyer, M., Krause, J., Paabo, S., Green, R.E. & Wayne, R.K. 2013, "Complete mitochondrial genomes of ancient canids suggest a European origin of domestic dogs", *Science (New York, N.Y.),* vol. 342, no. 6160, pp. 871-874.

Thompson, D.A. & Gal, A. 2003, "Genetic defects in vitamin A metabolism of the retinal pigment epithelium", *Developments in ophthalmology,* vol. 37, pp. 141-154.

Thoreson, W.B. & Mangel, S.C. 2012, "Lateral interactions in the outer retina", *Progress in retinal and eye research,* vol. 31, no. 5, pp. 407-441.

Thurman, R.E., Rynes, E., Humbert, R., Vierstra, J., Maurano, M.T., Haugen, E., Sheffield, N.C., Stergachis, A.B., Wang, H. & Vernot, B. 2012, "The accessible chromatin landscape of the human genome", *Nature,* vol. 489, no. 7414, pp. 75.

Trexler, E.B., Li, W. & Massey, S.C. 2005, "Simultaneous contribution of two rod pathways to AII amacrine and cone bipolar cell light responses", *Journal of neurophysiology,* vol. 93, no. 3, pp. 1476-1485.

Tripathi, R.C. 1971, "Ultrastructure of the exit pathway of the aqueous in lower mammals:(A preliminary report on the “angular aqueous plexus”)", *Experimental eye research,* vol. 12, no. 3, pp. 311-314.

Tripathi, R.C., Li, J., Chan, W.F. & Tripathi, B.J. 1994, "Aqueous humor in glaucomatous eyes contains an increased level of TGF-beta 2", *Experimental eye research,* vol. 59, no. 6, pp. 723-727.

Uhlen, M., Fagerberg, L., Hallstrom, B.M., Lindskog, C., Oksvold, P., Mardinoglu, A., Sivertsson, A., Kampf, C., Sjostedt, E., Asplund, A., Olsson, I., Edlund, K., Lundberg, E., Navani, S., Szigyarto, C.A., Odeberg, J., Djureinovic, D., Takanen, J.O., Hober, S., Alm, T., Edqvist, P.H., Berling, H., Tegel, H., Mulder, J., Rockberg, J., Nilsson, P., Schwenk, J.M., Hamsten, M., von Feilitzen, K., Forsberg, M., Persson, L., Johansson, F., Zwahlen, M., von Heijne, G., Nielsen, J. & Ponten, F. 2015, "Proteomics. Tissue-based map of the human proteome", *Science (New York, N.Y.),* vol. 347, no. 6220, pp. 1260419.

Vahlquist, A., Peterson, P. & Wibell, L. 1973, "Metabolism of the vitamin A transporting protein complex", *European journal of clinical investigation,* vol. 3, no. 4, pp. 352-362.

Van Buskirk, E.M. & Brett, J. 1978, "The canine eye: in vitro studies of the intraocular pressure and facility of aqueous outflow", *Investigative ophthalmology & visual science,* vol. 17, no. 4, pp. 373-377.

Van Cruchten, S., Vrolyk, V., Perron Lepage, M., Baudon, M., Voute, H., Schoofs, S., Haruna, J., Benoit-Biancamano, M., Ruot, B. & Allegaert, K. 2017, "Pre-and postnatal development of the eye: A species comparison", *Birth defects research,* vol. 109, no. 19, pp. 1540-1567.

Van der Woerdt, A., Stades, F., Van der Linde-Sipman, J. & Boeve, M. 1995, "Multiple ocular anomalies in two related litters of Soft Coated Wheaten Terriers", *Veterinary and comparative ophthalmology (USA),* vol. 5, no. 2, pp. 78.

Van Schil, K., Karlstetter, M., Aslanidis, A., Dannhausen, K., Azam, M., Qamar, R., Leroy, B.P., Depasse, F., Langmann, T. & De Baere, E. 2016, "Autosomal recessive retinitis pigmentosa with homozygous rhodopsin mutation E150K and non-coding cis-regulatory variants in CRX-binding regions of SAMD7", *Scientific reports,* vol. 6, pp. 21307.

van Steenbeek, F.G., Hytonen, M.K., Leegwater, P.A. & Lohi, H. 2016, "The canine era: the rise of a biomedical model", *Animal Genetics,* vol. 47, no. 5, pp. 519-527.

Wang, F., Li, Y., Lan, L., Li, B., Lin, L., Lu, X. & Li, J. 2015, "Ser341Pro MYOC gene mutation in a family with primary open-angle glaucoma", *International journal of molecular medicine,* vol. 35, no. 5, pp. 1230-1236.

Wang, L.W., Kutz, W.E., Mead, T.J., Beene, L.C., Singh, S., Jenkins, M.W., Reinhardt, D.P. & Apte, S.S. 2018, "Adamts10 inactivation in mice leads to persistence of ocular microfibrils subsequent to reduced fibrillin-2 cleavage", *Matrix Biology,* .

Wensel, T.G. & Stryer, L. 1986, "Reciprocal control of retinal rod cyclic GMP phosphodiesterase by its gamma subunit and transducin", *Proteins,* vol. 1, no. 1, pp. 90-99.

Verma, A.S. & FitzPatrick, D.R. 2007, "Anophthalmia and microphthalmia", *Orphanet journal of rare diseases,* vol. 2, no. 1, pp. 47.

Whitney, L. 1940, "The gestation period in the bitch.", *Veterinary Medicine,* vol. 35, pp. 59-60.

Wiggs, J.L. & Pasquale, L.R. 2017, "Genetics of glaucoma", *Human molecular genetics,* vol. 26, no. R1, pp. R21-R27.

Wiik, A., Ropstad, E., Ekesten, B., Karlstam, L., Wade, C. & Lingaas, F. 2015, "Progressive retinal atrophy in S hetland sheepdog is associated with a mutation in the CNGA 1 gene", *Animal Genetics,* vol. 46, no. 5, pp. 515-521.

Wiik, A.C., Wade, C., Biagi, T., Ropstad, E., Bjerkås, E., Lindblad-Toh, K. & Lingaas, F. 2008, "A deletion in nephronophthisis 4 (NPHP4) is associated with recessive cone-rod dystrophy in standard wire-haired dachshund", *Genome research,* vol. 18, no. 9, pp. 1415-1421.

Vila, C., Savolainen, P., Maldonado, J.E., Amorim, I.R., Rice, J.E., Honeycutt, R.L., Crandall, K.A., Lundeberg, J. & Wayne, R.K. 1997, "Multiple and ancient origins of the domestic dog", *Science (New York, N.Y.),* vol. 276, no. 5319, pp. 1687-1689.

Vilboux, T., Chaudieu, G., Jeannin, P., Delattre, D., Hedan, B., Bourgain, C., Queney, G., Galibert, F., Thomas, A. & André, C. 2008, "Progressive retinal atrophy in the Border Collie: A new XLPRA", *BMC veterinary research,* vol. 4, no. 1, pp. 10.

Willis, C.K., Quinn, R.P., McDonell, W.M., Gati, J., Partlow, G. & Vilis, T. 2001, "Functional MRI activity in the thalamus and occipital cortex of anesthetized dogs induced by monocular and binocular stimulation", *Canadian journal of veterinary research = Revue canadienne de recherche veterinaire,* vol. 65, no. 3, pp. 188-195.

Wood, J.L., Lakhani, K.H., Mason, I.K. & Barnett, K.C. 2001, "Relationship of the degree of goniodysgenesis and other ocular measurements to glaucoma in Great Danes", *American Journal of Veterinary Research,* vol. 62, no. 9, pp. 1493-1499.

Wood, J., Lakhani, K. & Read, R. 1998, "Pectinate ligament dysplasia and glaucoma in Flat Coated Retrievers. II. Assessment of prevalence and heritability", *Veterinary ophthalmology,* vol. 1, no. 2-3, pp. 91-99.

WuDunn, D. 2009, "Mechanobiology of trabecular meshwork cells", *Experimental eye research,* vol. 88, no. 4, pp. 718-723.

Yamazaki, A., Stein, P.J., Chernoff, N. & Bitensky, M.W. 1983, "Activation mechanism of rod outer segment cyclic GMP phosphodiesterase. Release of inhibitor by the GTP/GTP-binding protein", *The Journal of biological chemistry,* vol. 258, no. 13, pp. 8188-8194.

Yeh, C.Y., Goldstein, O., Kukekova, A.V., Holley, D., Knollinger, A.M., Huson, H.J., Pearce-Kelling, S.E., Acland, G.M. & Komaromy, A.M. 2013, "Genomic deletion of CNGB3 is identical by descent in multiple canine breeds and causes achromatopsia", *BMC genetics,* vol. 14, pp. 27-2156-14-27.

Yeh, C.Y., Koehl, K.L., Harman, C.D., Iwabe, S., Guzman, J.M., Petersen-Jones, S.M., Kardon, R.H. & Komaromy, A.M. 2017, "Assessment of Rod, Cone, and Intrinsically Photosensitive Retinal Ganglion Cell Contributions to the Canine Chromatic Pupillary Response", *Investigative ophthalmology & visual science,* vol. 58, no. 1, pp. 65-78.

Zangerl, B., Goldstein, O., Philp, A.R., Lindauer, S.J., Pearce-Kelling, S.E., Mullins, R.F., Graphodatsky, A.S., Ripoll, D., Felix, J.S. & Stone, E.M. 2006, "Identical mutation in a novel retinal gene causes progressive rod–cone degeneration in dogs and retinitis pigmentosa in humans", *Genomics,* vol. 88, no. 5, pp. 551-563.

Zangerl, B., Wickström, K., Slavik, J., Lindauer, S.J., Ahonen, S., Schelling, C., Lohi, H., Guziewicz, K.E. & Aguirre, G.D. 2010, "Assessment of canine BEST1 variations identifies new mutations and establishes an independent bestrophinopathy model (cmr3)", *Molecular vision,* vol. 16, pp. 2791.

Zerbino, D.R., Achuthan, P., Akanni, W., Amode, M.R., Barrell, D., Bhai, J., Billis, K., Cummins, C., Gall, A. & Girón, C.G. 2017, "Ensembl 2018", *Nucleic acids research,* vol. 46, no. D1, pp. D754-D761.

Zetterstrom, P., Stewart, H.G., Bergemalm, D., Jonsson, P.A., Graffmo, K.S., Andersen, P.M., Brannstrom, T., Oliveberg, M. & Marklund, S.L. 2007, "Soluble misfolded subfractions of mutant superoxide dismutase-1s are enriched in spinal cords throughout life in murine ALS models", *Proceedings of the National Academy of Sciences of the United States of America,* vol. 104, no. 35, pp. 14157-14162.

Zhang, Q., Acland, G.M., Wu, W.X., Johnson, J.L., Pearce-Kelling, S., Tulloch, B., Vervoort, R., Wright, A.F. & Aguirre, G.D. 2002, "Different RPGR exon ORF15 mutations in Canids provide insights into photoreceptor cell degeneration", *Human molecular genetics,* vol. 11, no. 9, pp. 993-1003.

Zhang, Q., Acland, G.M., Parshall, C.J., Haskell, J., Ray, K. & Aguirre, G.D. 1998, "Characterization of canine photoreceptor phosducin cDNA and

identification of a sequence variant in dogs with photoreceptor dysplasia", *Gene,* vol. 215, no. 2, pp. 231-239.

Zhang, Q., Baldwin, V.J., Acland, G.M., Parshall, C.J., Haskel, J., Aguirre, G.D. & Ray, K. 1999, "Photoreceptor dysplasia (pd) in miniature schnauzer dogs: evaluation of candidate genes by molecular genetic analysis", *The Journal of heredity,* vol. 90, no. 1, pp. 57-61.

Zhao, Y., Wang, S., Sorenson, C.M., Teixeira, L., Dubielzig, R.R., Peters, D.M., Conway, S.J., Jefcoate, C.R. & Sheibani, N. 2013, "Cyp1b1 mediates periostin regulation of trabecular meshwork development by suppression of oxidative stress", *Molecular and cellular biology,* vol. 33, no. 21, pp. 4225-4240.

Zuber, M.E., Gestri, G., Viczian, A.S., Barsacchi, G. & Harris, W.A. 2003, "Specification of the vertebrate eye by a network of eye field transcription factors", *Development,* vol. 130, no. 21, pp. 5155-5167.

Article

Cell Reports

Maternal Inheritance of a Recessive RBP4 Defect in Canine Congenital Eye Disease

Graphical Abstract

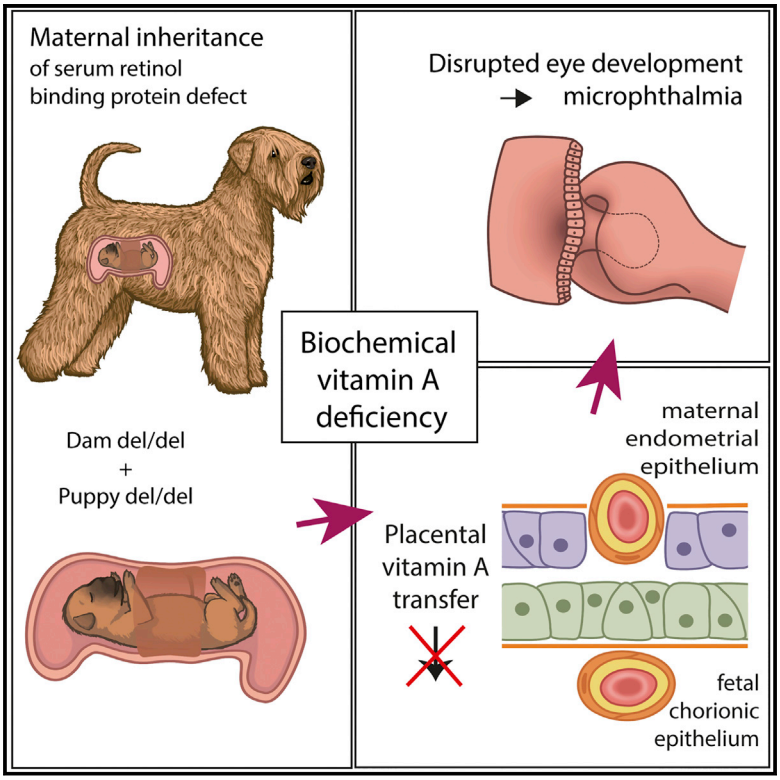

Highlights

- Recessive RBP4 defect with maternal transmission causes congenital eye disease
- Disease manifests only if both the dam and the offspring carry homozygous mutation
- Mutation disrupts RBP4 folding *in vivo* and results in protein hypomorph
- Biochemical serum vitamin A deficiency leads to disrupted fetal eye development

Authors

Maria Kaukonen, Sean Woods, Saija Ahonen, ..., Perttu Permi, Tom Glaser, Hannes Lohi

Correspondence

tmglaser@ucdavis.edu (T.G.), hannes.lohi@helsinki.fi (H.L.)

In Brief

Maternal inheritance distinctive from imprinting and oocyte-derived mRNA mechanisms has been regarded as a rare exception unique to humans. Kaukonen et al. describe a canine model with a recessive maternally transmitted RBP4 defect, suggesting that this mechanism is more common in developmental defects.

Kaukonen et al., 2018, Cell Reports *23*, 2643–2652
May 29, 2018
https://doi.org/10.1016/j.celrep.2018.04.118

CellPress

Cell Reports
Article

Maternal Inheritance of a Recessive RBP4 Defect in Canine Congenital Eye Disease

Maria Kaukonen,[1,2,3] Sean Woods,[4] Saija Ahonen,[1,2,3] Seppo Lemberg,[5] Maarit Hellman,[6] Marjo K. Hytönen,[1,2,3] Perttu Permi,[6,7] Tom Glaser,[4,*] and Hannes Lohi[1,2,3,8,*]

[1]Department of Veterinary Biosciences, University of Helsinki, 00014 Helsinki, Finland
[2]Research Programs Unit, Molecular Neurology, University of Helsinki, 00014 Helsinki, Finland
[3]The Folkhälsan Institute of Genetics, 00290 Helsinki, Finland
[4]Department of Cell Biology and Human Anatomy, University of California, Davis School of Medicine, Davis, CA 95616, USA
[5]Department of Eye Diseases, Helsinki University Hospital, 00029 The Hospital District of Helsinki and Uusimaa, Finland
[6]Department of Chemistry, Nanoscience Center, University of Jyväskylä, 40014 Jyväskylä, Finland
[7]Department of Biological and Environmental Science, Nanoscience Center, University of Jyväskylä, 40014 Jyväskylä, Finland
[8]Lead Contact
*Correspondence: tmglaser@ucdavis.edu (T.G.), hannes.lohi@helsinki.fi (H.L.)
https://doi.org/10.1016/j.celrep.2018.04.118

SUMMARY

Maternally skewed transmission of traits has been associated with genomic imprinting and oocyte-derived mRNA. We report canine congenital eye malformations, caused by an amino acid deletion (K12del) near the N terminus of retinol-binding protein (*RBP4*). The disease is only expressed when both dam and offspring are deletion homozygotes. RBP carries vitamin A (retinol) from hepatic stores to peripheral tissues, including the placenta and developing eye, where it is required to synthesize retinoic acid. Gestational vitamin A deficiency is a known risk factor for ocular birth defects. The K12del mutation disrupts RBP folding *in vivo*, decreasing its secretion from hepatocytes to serum. The maternal penetrance effect arises from an impairment in the sequential transfer of retinol across the placenta, via RBP encoded by maternal and fetal genomes. Our results demonstrate a mode of recessive maternal inheritance, with a physiological basis, and they extend previous observations on dominant-negative *RBP4* alleles in humans.

INTRODUCTION

The microphthalmia, anophthalmia, and coloboma (MAC) spectrum of congenital eye malformations are important causes of childhood blindness (Hornby et al., 2000). Anophthalmia refers to the complete absence and microphthalmia to reduced size of the ocular globe. Colobomas are notch-like defects in the iris, chorioretina, and/or optic nerve head that result from incomplete closure of the axial optic fissure during development (Onwochei et al., 2000). MAC disease has a worldwide incidence of 1 per 5,300 live births (Morrison et al., 2002). Most cases are isolated, with defects limited to the eye, but in one-third of patients the eye malformations occur as part of a syndrome (Verma and Fitzpatrick, 2007). Potential mechanisms include primary failure of optic vesicle growth, optic cup invagination or lens induction, or secondary degeneration of optic anlagen in utero (Graw, 2003). In most cases, the etiology is unknown. Recent reports implicate *SOX2*, *OTX2*, *STRA6*, and *PAX6* (Fantes et al., 2003; Ragge et al., 2005; Pasutto et al., 2007; Glaser et al., 1994), with dominant *SOX2* loss-of-function alleles being the most common single-gene defect (Gerth-Kahlert et al., 2013). Apart from gene mutations, various environmental risk factors have been reported for human MAC disease, most notably vitamin A deficiency (VAD) (Hornby et al., 2002). Vitamin A (retinol) is a substrate for synthesis of retinoic acid (RA), a potent paracrine-signaling molecule needed for proper development of the vertebrate eye and other tissues (Hale, 1935; See and Clagett-Dame, 2009). The eye is most sensitive among organs to reduced RA levels during embryogenesis.

In recent years, the domestic dog has emerged as a powerful model for study of simple and complex mammalian traits, due to its unique genetic architecture and abundant genomic tools (Lindblad-Toh et al., 2005). The canine eye more closely resembles the human eye, anatomically and physiologically, than do mouse or rabbit eyes and spontaneous hereditary eye diseases are common (Vaquer et al., 2013). Microphthalmia has been reported in several dog breeds, including Irish soft-coated wheaten terriers (ISCWTs), in which microphthalmia, retinal coloboma, hypoplasia of the choroid, and severe visceral malformations were reported (Van der Woerdt et al., 1995). The ocular phenotypes resemble the most severe features of collie eye anomaly (CEA), but they are genetically distinct (Parker et al., 2007).

In this study, we report a retinol-binding protein (*RBP4*) defect in a canine developmental eye disease; characterize its clinical, genetic, and biochemical properties; and consider the physiological implications of this unique recessive maternal penetrance effect.

RESULTS

Microphthalmia and Other Developmental Eye Defects in ISCWTs

An ISCWT breeder in Finland contacted us in 2011 after noticing abnormally small eyes in three pups in a litter of six. Eye exams

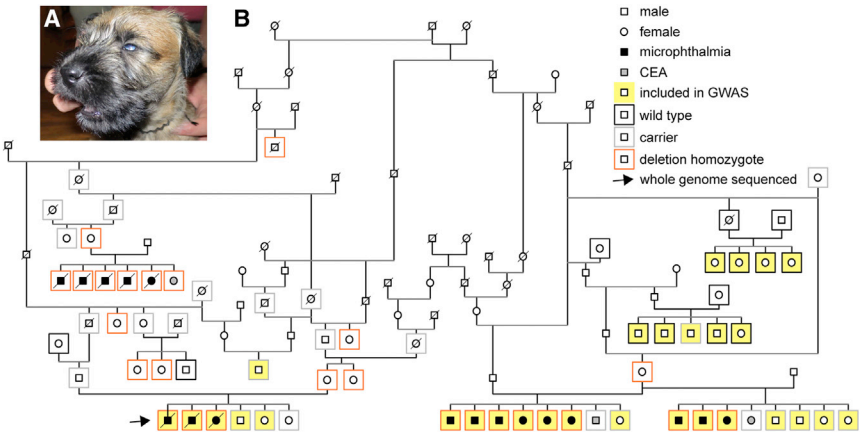

Figure 1. Autosomal Recessive Microphthalmia in ISCWT Dogs

(A) External eye phenotype, showing microphthalmia.

(B) Pedigree diagram showing lineage relationships among diseased dogs, clinical eye findings, *RBP4* genotypes, and the maternal penetrance effect. Phenotypes and confirmed DNA genotypes (n = 67) are indicated by inner and outer symbols, respectively, as described in the inset legend. Dogs included in the GWAS are highlighted in yellow (12 cases and 17 controls). All 17 microphthalmic dogs (■ ●) and their dams are *RBP4* deletion homozygotes (del/del). One deletion homozygote with a homozygous dam had eyes of normal size, with chorioretinal hypoplasia. Ten dogs without microphthalmia (□ ○) were also genotyped as homozygous (del/del), but they had heterozygous (del/+, n = 9) or untyped (del/−, n = 1) dams.

See also Figure S2 and Table S1.

before 10 weeks of age revealed bilateral microphthalmia with scleral folding, chorioretinal hypoplasia, and retinal colobomas in the affected dogs (Figure 1A; Table S1). A second affected litter of eight was subsequently born in Poland. Eye exams confirmed bilateral microphthalmia in six pups and chorioretinal hypoplasia in one pup and unilateral retinal coloboma. Then 2 years later, another litter was born to the same dam with a different sire. Three of eight pups had bilateral microphthalmia, chorioretinal hypoplasia, and retinal colobomas; one had a unilateral flat optic nerve head; and four were unaffected. In a fourth litter, born in the Czech Republic, five of six pups had bilateral microphthalmia and one had chorioretinal hypoplasia. The dam and sire of each litter had normal eye exams. The dams were fed high-quality commercial chow and no abnormalities were noted during gestation.

For genetic analysis, our inclusion criteria for subject dogs (cases) was bilateral microphthalmia (n = 17, with 11 males and 6 females). Normal control dogs (n = 23), ascertained from the same large ISCWT pedigree, were carefully examined by a veterinary ophthalmologist before 10 weeks of age, as tapetal pigmentation in older dogs can mask milder forms of chorioretinal hypoplasia (Bjerkås, 1991).

Genetic Analysis Reveals an In-Frame 3-bp Deletion in RBP4

The four affected litters are related in a single pedigree, with a transmission pattern suggesting an autosomal recessive mode of inheritance as several affected pups in different litters were born to unaffected parents (Figure 1B). To map the disease locus, we performed a genome-wide association study (GWAS) with 12 cases, 17 controls, and 172,963 SNP markers. Statistical analysis of genotype data by PLINK indicated a 15.7-Mb critical region on canine chromosome 28 ($p_{raw} = 8.04 \times 10^{-9}$, $p_{genome} = 1.00 \times 10^{-5}$), spanning nucleotides 287,714 to 16,036,936 bp (CanFam 3.1), in which all cases shared a single homozygous haplotype block (Figure 2). The localization was confirmed by GenABEL analysis, using a full genomic kinship matrix to adjust population structure and mixed model approximation (Figure S1).

To identify the causative variant, we sequenced the entire genome of one affected dog. A total of 470,800,949 reads were collected, of which 98.7% were mapped to the reference genome (CanFam 3.1). The mean read depth was 28.7× and 98.3% of mapped reads had >10× coverage. We identified 6,497,411 homozygous variants compared to the reference sequence, and 37,291 of these remained after filtering variants from 342 control dogs of breeds that lack the studied phenotype (Table S2). Among the remaining variants, 81 were exonic, but only one of these was located in the CFA28 critical region. This variant is a 3-bp deletion (c.282_284del) in the gene encoding *RBP4* gene, resulting in the loss of a single lysine (AAG codon) near the RBP amino terminus (p.K30del), in a charged segment preceding the lipocalin β-barrel domain (Figure 3). This is the 12th amino acid in the mature protein (K12del), after cleavage of the signal peptide, and it is highly conserved among vertebrates. The secreted portions of dog and human RBP are the same length (183 amino acids) and have 94.5% sequence identity.

Maternal Inheritance Effect

To confirm that the *RBP4* variant segregates with the disease trait, we genotyped all available dogs (n = 46) from affected litters and their close relatives (Figure 1B). As expected, the 17 cases were homozygous for the K12 deletion, and the 23 clinically confirmed controls were wild-type (WT) (+/+) or heterozygous (del/+). However, the three dams of the four affected litters were also homozygous for the deletion yet had normal eye exams. Notably, *their* dams were heterozygous. These results suggest a recessive mode of inheritance with reduced penetrance and a potential maternal genotype effect (Figure 1B).

To further evaluate the maternal effect on inheritance, we genotyped all available ISCWT samples in our biobank (n = 248). This analysis revealed 185 WT dogs (74.6%), 55 carriers (22.2%), and 8 homozygotes (3.2%), consistent with Hardy-Weinberg equilibrium (p = 0.32, χ^2 test, *df* = 2). Among these eight new K12del homozygotes, three had normal fundus eye exams as adults, four had normal general exams with no clinically apparent microphthalmia, and one suffered from chorioretinal hypoplasia.

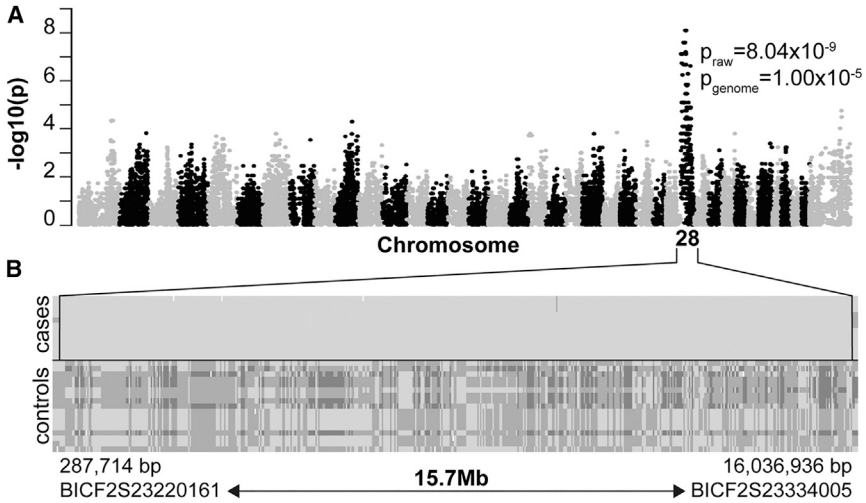

Figure 2. Mapping the ISCWT Microphthalmia Locus

(A) Summary of GWAS data. Manhattan plot of a genome-wide case-control association analysis, with 12 cases and 17 controls, shows localization of microphthalmia trait on CFA28, with a corrected probability value $P_{genome} = 1.00 \times 10^{-5}$.

(B) Genotype data showing a shared haplotype block in microphthalmic dogs (cases). Each row represents a single animal, with the genotypes at each SNP locus (columns) indicated by dark (AA), intermediate (AB), or light (BB) shading, in relation to the affected haplotype (BB). Every affected dog is homozygous within this segment. The 15.7-Mb critical region spans approximately 38% of CFA28, near the centromere, and it is delimited by SNP markers BICF2S23220161 (centromeric) and BICF2S23334005 (telomeric).

See also Figure S1.

Maternal genotypes are known for seven of these dogs; in each case, the dam was heterozygous, except for the dog with chorioretinal hypoplasia, whose dam was an *RBP4* deletion homozygote. These data demonstrate a striking maternal transmission effect on inheritance (Table 1; $p < 10^{-4}$, Fisher's exact test, $df = 1$). Accordingly, the microphthalmia trait is manifest only when *both* dam and offspring are homozygous for the deletion (17/18). If the dam is heterozygous, her homozygous offspring have grossly normal eye anatomy (9/9). The penetrance of the microphthalmia trait in del/del dogs is thus 94% or 0%, respectively, depending on the dam genotype.

Because some human *RBP4* alleles have dominant phenotypes (Chou et al., 2015), we investigated the clinical status of del/+ carriers in detail. Among 71 heterozygotes in our study cohort, 46 had thorough eye exams. Dam genotypes, determined for 37 of these 46 carriers, were as follows: 14 homozygous (del/del), 11 heterozygous (del/+), and 12 WT (+/+). Two carriers did have CEA-like findings (chorioretinal hypoplasia) but no microphthalmia. These 2 dogs were littermates of affected pups (Figure 1B) and their dams were deletion homozygotes. All other del/+ carriers examined were normal. In particular, 8 of these 12 unaffected carriers born to del/del dams had fundus exams before 10 weeks of age to reliably assess choroidal anatomy (Bjerkås, 1991).

To exclude mild retinal pathology in dogs born to heterozygous dams, we performed OCT (optical coherence tomography) imaging on 11 ISCWTs with different genotypes (3 +/+, 4 del/+, and 4 del/del). Whole retinal thickness (WRT) and photoreceptor layer thickness (PRT) were within normal limits in every dog, and no statistically significant difference was found between genotype groups (Figure S2). Thus, for offspring to manifest eye disease, the dam must be an *RBP4* deletion homozygote, with phenotypic severity depending on the offspring genotype ($p < 10^{-6}$, Fisher's exact test, $df = 1$). Deletion homozygotes had microphthalmia with nearly complete penetrance (17/18) or chorioretinal hypoplasia (1/18), whereas heterozygotes had a milder condition, such as chorioretinal hypoplasia, with low penetrance (2/14).

Dose-Dependent Decrease in Serum RBP and Vitamin A Levels

RBP circulates in blood and transports vitamin A from hepatic stores to peripheral tissues, such as the developing eye. In principle, the K12 deletion, near the ligand-binding domain (Figures 3C–3E) may disrupt RBP folding, stability, or secretion; retinol-binding activity; and/or interaction with the STRA6 receptor. To investigate stability and retinol-binding effects, we measured serum RBP and vitamin A levels in 17 adult ISCWTs, including 8 deletion homozygotes (3 with microphthalmia), 6 del/+ carriers, and 3 WT dogs (Figure 4). Serum albumin and total protein were assayed in parallel as a control. RBP levels were assessed by western analysis, following denaturing gel electrophoresis (SDS-PAGE) under reducing conditions, and were normalized to wild-type. Relative RBP levels (±SD) were roughly halved in heterozygotes (0.66 ± 0.20) and greatly reduced in homozygotes (0.24 ± 0.10) compared to WT dogs (1.00 ± 0.39). The mutant protein is thus poorly secreted or rapidly cleared from the bloodstream.

To assess the structure of circulating canine K12del RBP, we performed western analysis on serum samples under non-reducing conditions (Figure 4B). To maximize exposure of epitopes in native globular RBP after electrophoresis, SDS-PAGE gels were treated with β-mercaptoethanol (βME) before transfer (Zetterström et al., 2007). In these experiments, the K12del protein migrated as an apparent homodimer (42 kDa) in homozygote sera, with little or no monomeric RBP. Presumably, the K12del RBP variant folds abnormally in the hepatic endoplasmic reticulum (ER) of mutant dogs, leading to the formation of intermolecular disulfide bonds, which allows progression of the mutant RBP to the Golgi compartment (Kaji and Lodish, 1993). The mutant dimers were more antigenic than wild-type (WT) monomers in non-reducing western blots, reflecting their partially unfolded status *in vivo* (Figure S3). Consequently, the dimer fraction of serum RBP was determined following in-gel reduction. In heterozygous dogs, the ratio of dimers to monomers was 0.23 ± 0.04, consistent with the overall decrease in serum RBP (Figure 4A). These data, and the linear relationship between

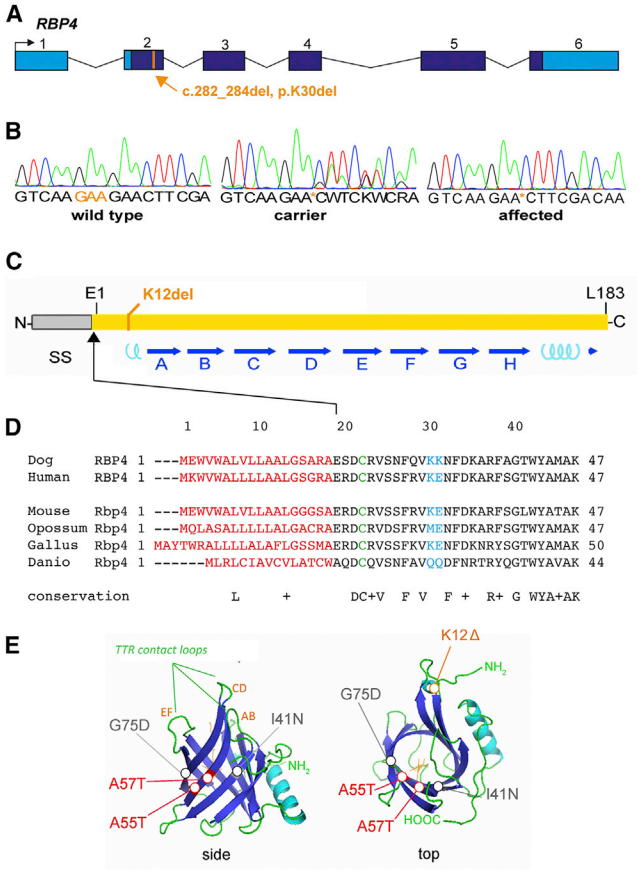

Figure 3. Pathogenic *RBP4* Deletion

(A) p.K30del mutation. Genomic map shows the solitary coding variant identified in the critical region by whole genome sequencing, a 3-bp deletion in exon 2 that removes lysine codon 30 from the RBP precursor. This residue corresponds to K12 in the mature polypeptide, after signal peptide cleavage. Coding (dark blue) and UTR sequences (light blue) are indicated.

(B) Sanger chromatograms showing the DNA sequence of PCR products spanning the *RBP4* deletion in wild-type (WT), carrier, and affected dogs. The deletion removes one of two tandem lysine codons (AAG).

(C) Linear diagram of RBP showing the signal peptide (SS); 8 antiparallel β sheets (A–H, blue arrows), which form the ligand barrel; 2 short α-helical segments (cyan coils); 3 cysteine disulfide bonds, which stabilize the tertiary structure; and the mutated K12 residue.

(D) Alignment of vertebrate RBP sequences showing evolutionary conservation of K12 among eutherians. The signal peptide (red), tandem lysines (K12-K13, blue), and disulfide-linked cysteine (C4, green) are indicated. The N-terminal segment preceding the β-barrel (10 of 21 residues) is highly charged.

(E) Tertiary structure of canine RBP (ribbon views), modeled from human *apo* (1RBP) and *holo* (1BRQ) RBP X-ray data (Cowan et al., 1990; Zanotti et al., 1993a, 1993b), showing K12 near the N terminus, within an α-helical region. By shortening this segment, K12del may limit apposition of C4 and C160 side groups in the ER, preventing formation of one disulfide bond *in vivo* and, consequently, destabilizing the protein.

See also Table S2.

genotype and total RBP levels (Figure 4C), indicate that the K12del protein does not significantly dimerize with WT RBP or interfere with its secretion *in vivo*.

Vitamin A levels (±SD) were severely reduced in all deletion homozygotes (0.06 ± 0.02 mg/L), compared to WT (0.55 ± 0.20 mg/L) and the normal canine reference range (0.3–1.3 mg/L), regardless of phenotype ($p < 0.0001$; Figures 4C and 4D). Vitamin A levels in carriers were 0.34 ± 0.13 mg/L, below (n = 2, 0.19 and 0.21 mg/L) or marginally within (n = 4, 0.31–0.51 mg/L) the reference range. Serum albumin and total protein were normal in 16 of 17 dogs but reduced in one affected dog (Table S1). The vitamin A levels were thus directly correlated with immunoreactive RBP across genotypes ($r^2 = 0.88$; Figure 4D). Collectively, these results suggest that the K12del mutation destabilizes RBP *in vivo*, preventing mobilization of vitamin A from maternal liver stores to the embryo. Moreover, misfolded K12del dimers are unlikely to interact effectively with retinol, transthyretin, or STRA6 *in vivo*, given the behavior of human pathogenic *RBP4* missense alleles *in vitro* (Chou et al., 2015) and steric constraints evident in the X-ray structure of *holo* RBP-TTR_4 (Berni and Formelli, 1992). However, formally the possibility of the direct binding of the K12del mutant to STRA6 could be tested, as described previously (Chou et al., 2015).

Table 1. Eye Phenotypes and Maternal Genotypes of *RBP4* p.K12del Homozygous Offspring

	Microphthalmia in del/del Offspring	
Dam Genotype	Present	Absent
Homozygote (del/del)	17	1[a]
Carrier (del/+)	0	9
Unknown (del/–)	0	1
Total	17	11

Sire genotypes were del/+ for 12 microphthalmic dogs and del/– for 5 dogs. For non-microphthalmic dogs, sire genotypes were del/+ for 7 dogs and del/– for 4 dogs. The skewed distribution of maternal genotypes in this retrospective analysis is highly significant ($p < 10^{-6}$, Fisher's exact test, $df = 1$).

[a]Chorioretinal hypoplasia with normal globe size.

Mutant RBP dimers may be cleared from the bloodstream by megalin (LRP2) or other receptors (Wyatt et al., 2011), but they are unlikely to enter the urine in the absence of renal damage. In normal mammals, *holo* RBP circulates bound to TTR tetramers, which increases its effective molecular weight (>75 kDa) and prevents filtration in the kidneys (Vahlquist et al., 1973). To test this hypothesis, we measured RBP levels in urine (uRBP) samples from the 17 genotyped dogs whose serum data are described above. We detected uRBP in only two samples, a K12del homozygote and a K12del/+ carrier, at approximately 1/20th the mean WT serum level (Figure S4). These two dogs are likely to have impaired renal function, as total urinary protein was also elevated (data not shown).

The K12del Mutation Impairs Secretion of RBP Monomers from Cultured HeLa Cells

As a further test of K12del effects, we compared the abundance and structure of RBP polypeptides secreted into the conditioned media (CMs) and retained in the cytoplasm of transfected HeLa cells and their interactions with transthyretin (Figure 5). Plasmid constructs expressing K12del or WT canine RBP or orthologous human mutants (K12del or E13del) were generated (Table S3) and tested in parallel, with human WT and mutant controls,

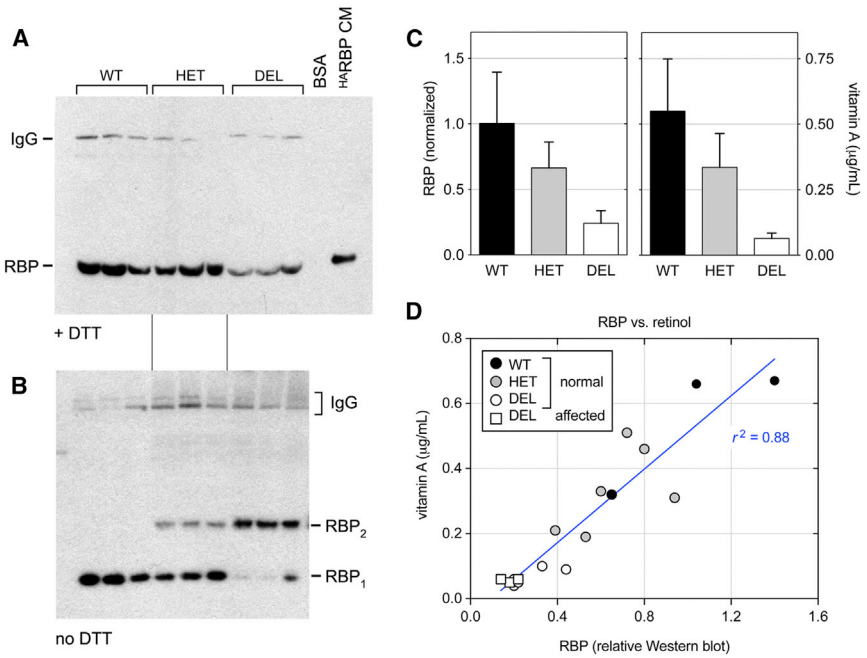

Figure 4. Serum RBP and Vitamin A Analysis

(A) ECL western blot (reducing conditions) showing dog RBP monomers (21 kDa) with human ^{HA}RBP (22 kDa) as a positive control (HeLa-CM). The higher MW signal is dog IgG (150 kDa), which cross-reacts with the secondary reagent (donkey anti-rabbit IgG) and is relatively resistant to DTT (Singh and Whitesides, 1994).

(B) Parallel blot (non-reducing conditions) showing RBP monomers (WT) and homodimers (K12del mutant). Both species are present in heterozygotes, in roughly a 4:1 molar ratio.

(C) Histograms comparing immunoreactive serum RBP and vitamin A (mean ± SD) versus genotype. There is a linear dosage relationship, with heterozygotes having an intermediate level of RBP (0.66 ± 0.20) that is close to the arithmetic mean of del/del and +/+ samples (0.62 ± 0.22).

(D) Scatterplot comparing serum vitamin A (μg/mL, ordinate) and relative RBP (abscissa) for all samples, including WT (black), HET (gray), and DEL (white) dogs with normal eyes (circles) and microphthalmic DEL dogs (white squares). The values are well correlated ($p < 0.0001$, $r^2 = 0.88$); however, the regression line is shifted rightward from the origin, indicating that the K12del protein binds less retinol *in vivo* than WT. The homozygous DEL samples have similar RBP and vitamin A levels, regardless of phenotype (one-way ANOVA, $p = 0.18$ for RBP and $p = 0.45$ for vitamin A, comparing 5 normal and 3 microphthalmic dogs).

See also Tables S1 and S3.

including stable (A55T) and unstable (G75D and I41N) pathogenic isoforms (Chou et al., 2015). Western analysis of CMs and cell lysates, performed under reducing and non-reducing conditions (±βME), showed that secretion of K12del (and E13del) mutants was significantly altered, with a striking predominance of dimers. The dimer fractions for K12del and WT canine RBP in CMs were 0.89 and 0.007, respectively (Figure 5A, left), whereas the total amount of RBP secreted was similar (Figure 5A, right). Likewise, human E13del, K12del, G75D, and I41N mutants were secreted into CMs as >85% dimers, compared to <1% for A55T and WT controls, and secretion of human E13del and K12del was diminished. There were at least two distinct RBP dimer species in CMs, indicated by closely migrating 42-kDa products in the non-reducing western blot (Figure 5A). This conformational heterogeneity is likely to reflect the formation of intermolecular disulfide bonds between different cysteine pairs, with a variable degree of compactness. In a previous study of RBP oxidative folding in HepG2 cells in the presence of DTT, an ensemble of folding intermediates was similarly identified by their heterodisperse migration in non-reducing gels (Kaji and Lodish, 1993).

Western analyses of cell lysates ± βME further showed that dog K12del and human E13del mutant RBPs accumulated in cytoplasm, with normalized lysate-to-CM ratios of 1.5 and 6.0, respectively, compared to WT (ratio = 1.0) (Figure 5C, right). The abundance of RBP monomers in mutant cell lysates was notable, given their paucity in CMs, and these proteins migrated as ≥2 different species (Figure 5C, left). Monomers comprise >50% of RBP in lysates but <15% of RBP secreted into CMs by HeLa cells expressing dog K12del or human E13del mutants. In contrast, monomers comprise >99% of WT RBP in cell lysates and CMs. Together, these data suggest that the ISCWT mutation disrupts the kinetics of RBP folding *in vivo* and slows secretion, with iterative cycles of oxidative refolding or dimerization in the ER as a likely rate-limiting step (Ruggiano et al., 2014).

To further assess mutant RBPs, we tested their interaction with bovine transthyretin (TTR) in CM by immunoprecipitation (Figure 5B). In these experiments, WT and stable mutant RBPs bound TTR, but K12del and other mutants did not. The low levels of serum RBP in mutant dogs may thus arise from decreased hepatic secretion and increased renal or systemic clearance of abnormal RBP dimers.

K12del Protein Can Fold as a Monomer and Bind Vitamin A *In Vitro*

To evaluate how the mutation alters RBP structure more precisely, we expressed recombinant WT and K12del proteins in *E. coli* strain Origami B(DE3), which has an oxidizing cytoplasmic environment allowing disulfide bond formation, and we used gel filtration (size exclusion chromatography [SEC]) as the final purification step (Kawaguchi et al., 2013). WT and K12del RBPs eluted in the same fraction (volume 92 mL) in parallel columns, indicating that both proteins have the same overall size and monomeric form (Figure S5). The chromatograms also showed small dimeric (elution volume 82 mL) and multimeric peaks, which were similar for both variants. The extent of aggregation depended on the concentration of purified proteins: both WT and K12del RBPs were monomeric in concentrations under 0.8 mM but aggregated at higher concentrations, as indicated by an increased nuclear magnetic resonance (NMR) line width.

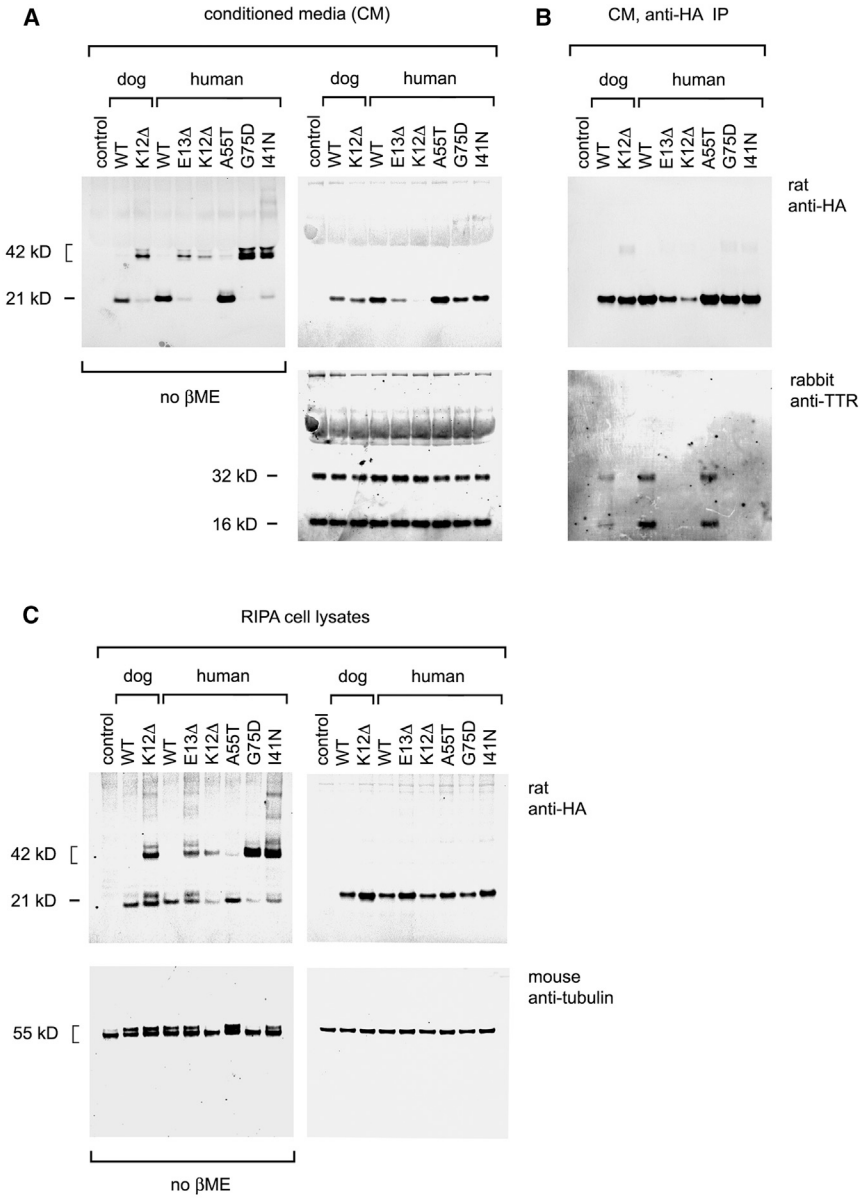

Figure 5. RBP Secretion and Transthyretin Binding *In Vitro*

(A–C) LI-COR western analysis of (A) CM, (B) immunoprecipitates (IP) of CMs, and (C) radioimmunoprecipitation assay buffer (RIPA) lysates from transfected HeLa cells expressing dog (WT and K12del) or human (WT, K12del, E13del, A55T, G75D, and I47N) ^{HA}RBPs, detected using anti-HA antibody. In (A) and (B), parallel gels were electrophoresed under reducing (+βME, right) or non-reducing conditions (no βME, left), with bovine TTR and human α-tubulin as CM and lysate loading controls, respectively.

(A) Recombinant ^{HA}RBPs are secreted as dimers or higher multimers (K12del in both species; human E13del, G75D, and I41N) and monomers (WT in both species, human A55T). The K12del dimers secreted by HeLa cells *in vitro* appear similar to RBP dimers secreted by mutant dogs *in vivo*, and presumably they reflect the exposure of unpaired cysteines, which persist after intramolecular oxidative folding. The A55T, G75D, and I41N proteins behave as previously reported (Chou et al., 2015).

(B) The RBP profiles of transfected cell lysates and CMs generally correspond; however, mutant monomers are notably more abundant (>50%) in cell lysates than in CMs. These abnormal RBPs are presumably retained in the ER and secreted following dimerization.

(C) Co-immunoprecipitation showing that only WT and stable A55T mutant ^{HA}RBPs interact with bovine TTR present in the CMs.

See also Figure S3.

A heteronuclear single quantum coherence (^{15}N-HSQC) spectra of WT and K12del clearly showed that both variants folded *in vitro* and that the deletion did not significantly disrupt the overall structural integrity of RBP (Figures 6A–6D). As expected, chemical shift perturbations (CSPs) between WT and K12del were observed for residues that were spatially close to the deletion site (K12). Chemical shift of cysteine β-carbons is a reliable indicator of cysteine oxidation state (Sharma and Rajarathnam, 2000; Mobli and King, 2010). The observed cysteine β-carbon (Cβ) chemical shift values for residues C4 and C160 were 38.6 and 40.7 ppm, respectively, which are typical values for oxidized cysteine residue. The corresponding chemical shift values for reduced cysteines are 28.3 ± 2.2 ppm (Sharma and Rajarathnam, 2000). These data strongly suggest that C4 and C160 are oxidized and establish a disulfide bond within the recombinant K12del protein, similar to WT.

We also compared retinol binding of WT and K12del proteins using NMR spectroscopy. Retinol induced large CSPs for some residues in the ^{15}N-HSQC spectrum of RBP, making their identification ambiguous, so we reassigned all chemical shifts for retinol-bound RBP (Greene et al., 2006). In this analysis, an equimolar ratio of vitamin A induced CSPs in the same residues of both RBP variants (Figures 6E and 6F). The K12 deletion thus does not alter the intrinsic retinol-binding mechanism or affinity, as WT and K12del RBPs synthesized *in vitro*-bound vitamin A similarly under the conditions studied.

Thus, whereas K12del RBP produced by canine hepatocytes *in vivo* or HeLa cells in culture is misfolded and secreted as abnormal dimers with little or no retinol cargo, NMR data clearly show that K12del RBP synthesized in a heterologous *E. coli* environment, outside the mammalian ER lumen and Golgi network, can fold properly at 16°C and form intramolecular disulfide bridges similar to WT RBP and bind to vitamin A with the same interface and similar affinity as WT RBP (Figure 6F).

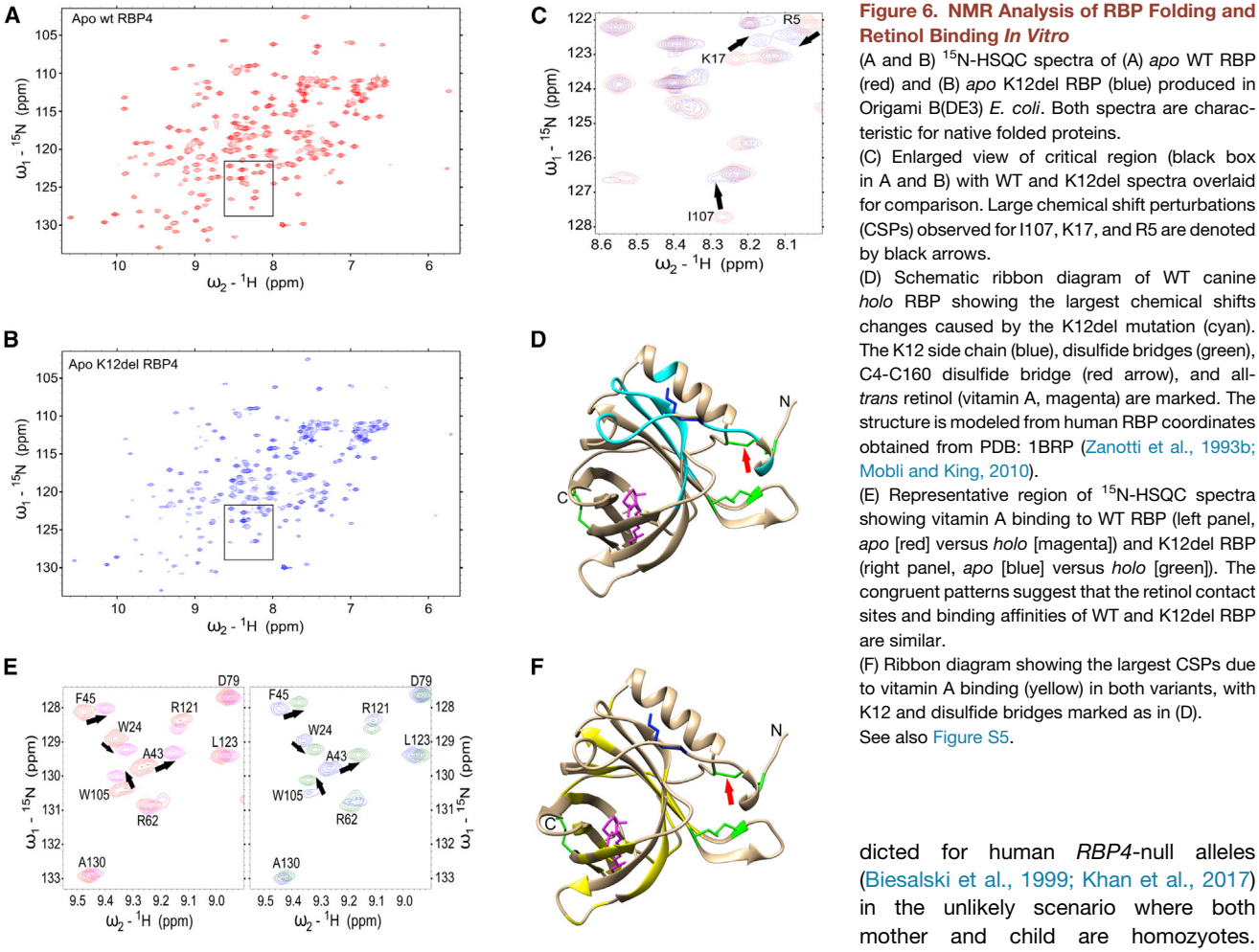

Figure 6. NMR Analysis of RBP Folding and Retinol Binding *In Vitro*

(A and B) ^{15}N-HSQC spectra of (A) *apo* WT RBP (red) and (B) *apo* K12del RBP (blue) produced in Origami B(DE3) *E. coli*. Both spectra are characteristic for native folded proteins.

(C) Enlarged view of critical region (black box in A and B) with WT and K12del spectra overlaid for comparison. Large chemical shift perturbations (CSPs) observed for I107, K17, and R5 are denoted by black arrows.

(D) Schematic ribbon diagram of WT canine *holo* RBP showing the largest chemical shifts changes caused by the K12del mutation (cyan). The K12 side chain (blue), disulfide bridges (green), C4-C160 disulfide bridge (red arrow), and all-*trans* retinol (vitamin A, magenta) are marked. The structure is modeled from human RBP coordinates obtained from PDB: 1BRP (Zanotti et al., 1993b; Mobli and King, 2010).

(E) Representative region of ^{15}N-HSQC spectra showing vitamin A binding to WT RBP (left panel, *apo* [red] versus *holo* [magenta]) and K12del RBP (right panel, *apo* [blue] versus *holo* [green]). The congruent patterns suggest that the retinol contact sites and binding affinities of WT and K12del RBP are similar.

(F) Ribbon diagram showing the largest CSPs due to vitamin A binding (yellow) in both variants, with K12 and disulfide bridges marked as in (D).

See also Figure S5.

DISCUSSION

In this study, we demonstrate that deletion of a single amino acid from the canine serum RBP causes severe congenital eye malformations in ISCWTs using segregation, clinical, and molecular data. The phenotype is transmitted as an autosomal recessive trait with penetrance determined by the maternal genotype. This unusual inheritance pattern is caused by the disruption of vitamin A transport from maternal hepatic stores to the developing fetal eye, in situations where functional RBP is absent on *both* sides of the placenta. In WT mammals, RBP transfers fat-soluble retinol bidirectionally, to (influx) *and* from (efflux) cells at the materno-fetal interface, respectively, via the STRA6 receptor (Kawaguchi et al., 2012). The resulting deficiency of vitamin A in affected ISCWT embryos presumably limits RA signaling during critical stages of eye development. Two hits, maternal *and* fetal homozygous *RBP4* mutations, are evidently needed to reduce vitamin A levels below the threshold for phenotypic expression in offspring. A genetically similar recessive maternal effect has been noted in *Rbp4*-knockout mice, but only when the dam is maintained on a VAD diet after conception (Quadro et al., 2005), and it is predicted for human *RBP4*-null alleles (Biesalski et al., 1999; Khan et al., 2017) in the unlikely scenario where both mother and child are homozyotes. Maternally skewed expression of *RBP4* defects has been reported in human MAC pedigrees, but with dominant transmission and incomplete penetrance (Chou et al., 2015).

The difference in severity of *Rbp4* and *Stra6* phenotypes between species has been puzzling. In particular, the relatively mild developmental effects observed in mutant mice (Quadro et al., 1999) compared to humans (Pasutto et al., 2007; Chou et al., 2015) has led some to assert that the RBP-STRA6 pathway is relatively unimportant for vitamin A homeostasis, apart from retinal physiology (Berry et al., 2013). These discordant phenotypes may reflect differences among mammals in placental anatomy and function, relative dependence on tonic RBP-mediated vitamin A transport versus postprandial delivery of retinyl ester in chylomicron particles (D'Ambrosio et al., 2011), or direct transfer of vitamin A via uterine lumenal secretions (Suire et al., 2001). The canine model confirms the importance of RBP and STRA6 for mobilizing vitamin A during fetal development and further illuminates this pathway. Notably, the ISCWT phenotype manifests without dietary restriction. While the exact cellular interface for materno-fetal vitamin A transfer is poorly defined (Marceau et al., 2007), the placentae of rodents and primates are hemochorial, with direct contact between maternal blood and trophoblast layers, whereas carnivores such as dogs have

endotheliochorial placentae, with greater histocompartmental separation between maternal and fetal circulation (Wooding and Burton, 2008).

To fully understand the molecular effects of the ISCWT mutation, we analyzed K12del RBP4 at three levels: as recombinant protein purified from bacteria, as protein secreted in the CMs of cultured HeLa cells, and as canine sera *in vivo*. When K12del RBP is expressed in the Origami B(DE3) *E. coli* strain under favorable conditions at 16°C, in an oxidizing cytoplasm created by double thioredoxin (*trxB*) and glutaredoxin reductase (*gor*) mutations, it folds correctly, forms internal disulfide bonds, and binds retinol similar to WT, with altered residue positions but no obvious molecular strain. In contrast, when K12del RBP is expressed by eukaryotic cells, both canine hepatocytes and HeLa cervical carcinoma cells, it misfolds, such that one or more internal disulfide bonds does not form within the ER lumen, during or after translation and signal peptide cleavage, leaving unpaired cysteines. The misfolded polypeptides with exposed thiol groups are presumably retained and destroyed via the ERAD (ER-associated protein degradation) pathway, following abortive refolding cycles (Ruggiano et al., 2014), or they are linked to other misfolded RBPs via intermolecular cysteine disulfide bridge(s), passed by ER quality control (Vembar and Brodsky, 2008), and secreted as homodimers. During oxidative folding of WT RBP in ER microsomes, facilitated by multiple chaperones, the C120-C129 disulfide bond forms first and is most critical to stability; the large C4-C160 and C70-C174 loops form subsequently (Selvaraj et al., 2008). Assuming K12del and WT alleles are transcribed and translated with equal efficiency, our quantitative western analyses of dog sera suggest that most K12del protein is degraded prior to secretion or rapidly cleared from the bloodstream.

These disparate results are instructive. K12del folding must be *thermodynamically* favored, as it occurs readily, in a heterologous *E. coli* environment. However, the folding funnel must have altered topology, compared to WT (Dill and Chan, 1997). As noted by Cowan et al. in their original RBP X-ray crystal structure report, "residues which contribute to the formation of the retinol-containing barrel start at residue 12. The methylene groups of the lysine side chain of K12 help close off the barrel... " (Cowan et al., 1990). Consequently, K12del folding within the mammalian ER lumen may be kinetically compromised; it proceeds too slowly to escape the ERAD pathway and allow secretion of K12del RBP monomers. Misfolding occurs in K12del mutant dogs *in vivo*, despite the presence of ample hepatic retinol, which acts as a molecular chaperone to stimulate correct RBP folding and co-secretion of the *holo* RBP-TTR complex (Kawaguchi et al., 2013; Bellovino et al., 1996).

We believe the eukaryotic data best explain the clinical findings and are most relevant and that the K12del mutation acts as a null allele. Indeed, WT *apo* RBP, expressed in reducing *E. coli* strains (e.g., BL21) and oxidized randomly *in vitro* with glutathione (GSSG/GSH), exists as an ensemble of conformers, including several products with non-native disulfide bonds, and it must be further purified for biochemical assays (Kawaguchi et al., 2013). Moreover, an engineered RBP expressed in *E. coli* with six cysteine-to-serine substitutions can fold correctly *in vitro* and bind vitamin A in the absence of stabilizing disulfide bonds (Reznik et al., 2003), whereas similar mutant RBPs expressed in isolated dog microsomes cannot (Selvaraj et al., 2008). Finally, in a previous study of recessive human *RBP4* alleles, G75D and I41N proteins expressed in *E. coli* were reported to fold correctly, bind TTR and retinol, with reduced stability of the *holo* RBP complex (Folli et al., 2005), yet these proteins were undetectable in patient serum (Biesalski et al., 1999) and are secreted as aggregates from transfected HeLa cells (Chou et al., 2015).

Together, our findings highlight a unique type of autosomal recessive inheritance in mammals, a maternal effect on penetrance with a physiological basis in nutrient transport across the placenta. Our study establishes a large animal model to investigate RBP4 function and pathology and enables novel treatment options.

EXPERIMENTAL PROCEDURES

Further details and an outline of resources used in this work can be found in the Supplemental Experimental Procedures.

The Canine Study Cohort

The study cohort was established from privately owned purebred ISCWTs with their owners' consent and included 17 cases (11 males and 6 females) from 4 closely related litters and 23 controls (9 males and 14 females). All dogs were 6–10 weeks old at the time of clinical examinations, as described in the Supplemental Experimental Procedures. DNA analysis was also performed on 254 ISCWTs (111 males and 143 females) of different ages to evaluate the carrier frequency of the mutation in the breed. Sample collection and clinical studies were performed with approval from the Animal Ethical Committee of the County Administrative Board for Southern Finland (ESAVI/6054/04.10.03/2012), and all experiments were performed in accordance with relevant guidelines and regulations.

Genetic Analyses

A GWAS and whole-genome sequencing were performed to map the disease locus and to identify the causative variant followed by a population screening by Sanger sequencing, as described in the Supplemental Experimental Procedures.

Biochemical Studies

Serum and urine samples for RBP and vitamin A assays were collected from 17 dogs and vitamin A was measured. To assess the protein structure and function immunoblot analysis of native canine RBPs and recombinant ^{HA}RBPs expressed by cultured HeLa cells as well as structural NMR studies in *E. coli* were performed. Details of the biochemical studies are described in the Supplemental Experimental Procedures.

Statistical Methods

Parametric tests and exact n values are provided in the respective Experimental Procedures and Results sections. Statistical significance was evaluated in relation to a threshold p value of 0.05 (for GWAS after 100,000 permutations).

DATA AND SOFTWARE AVAILABILITY

The accession number for the whole-genome sequencing data from an affected ISCWT reported in this paper is NCBI Short Read Archive: SRP126148.

SUPPLEMENTAL INFORMATION

Supplemental Information includes Supplemental Experimental Procedures, five figures, and three tables and can be found with this article online at https://doi.org/10.1016/j.celrep.2018.04.118.

ACKNOWLEDGMENTS

We thank referring veterinarians, dog owners, and breeders for canine samples; the Next Generation Sequencing Platform at the University of Bern for whole-genome sequencing experiments; MSc Meharji Arumilli for bioinformatics; and the Institute for Molecular Medicine Finland (FIMM) for Sanger sequencing. We are grateful to the Dog Biomedical Variant Database Consortium for the whole-genome variants from control dogs. We thank Christopher Chou for technical advice on RBP assays, Ed Pugh for helpful discussions, Danika Bannasch for canine serum samples, and Milla Ahola for digital drawings in the graphical abstract. This work was supported by funds from the Mary and Georg C. Ehnrooth Foundation, the Evald and Hilda Nissi Foundation, the Academy of Finland, the Jane and Aatos Erkko Foundation, the Finnish Foundation of Veterinary Research, Genoscoper Oy, Wisdom Health, and the NIH (EY19497).

AUTHOR CONTRIBUTIONS

H.L. and M.K. developed and conceived the idea. H.L., T.G., P.P., and M.K. designed the experiments. M.K., S.W., S.A., S.L., and M.H. performed the experiments. M.K., S.W., M.H., P.P., and T.G. analyzed the data. H.L., T.G., M.K.H., and P.P. contributed reagents/materials/analysis tools. M.K., H.L., T.G., and M.H. wrote the manuscript. All authors read and approved the final manuscript.

DECLARATION OF INTERESTS

A canine *RBP4* genetic test will be available from Genoscoper Laboratories Ltd., which was partly owned by H.L. during this study. H.L. continues as a paid consultant of the company. The authors declare no other competing interests.

Received: November 9, 2017
Revised: April 16, 2018
Accepted: April 26, 2018
Published: May 29, 2018

REFERENCES

Bellovino, D., Morimoto, T., Tosetti, F., and Gaetani, S. (1996). Retinol binding protein and transthyretin are secreted as a complex formed in the endoplasmic reticulum in HepG2 human hepatocarcinoma cells. Exp. Cell Res. *222*, 77–83.

Berni, R., and Formelli, F. (1992). In vitro interaction of fenretinide with plasma retinol-binding protein and its functional consequences. FEBS Lett. *308*, 43–45.

Berry, D.C., Jacobs, H., Marwarha, G., Gely-Pernot, A., O'Byrne, S.M., DeSantis, D., Klopfenstein, M., Feret, B., Dennefeld, C., Blaner, W.S., et al. (2013). The STRA6 receptor is essential for retinol-binding protein-induced insulin resistance but not for maintaining vitamin A homeostasis in tissues other than the eye. J. Biol. Chem. *288*, 24528–24539.

Biesalski, H.K., Frank, J., Beck, S.C., Heinrich, F., Illek, B., Reifen, R., Gollnick, H., Seeliger, M.W., Wissinger, B., and Zrenner, E. (1999). Biochemical but not clinical vitamin A deficiency results from mutations in the gene for retinol binding protein. Am. J. Clin. Nutr. *69*, 931–936.

Bjerkås, E. (1991). Collie eye anomaly in the rough collie in Norway. J. Small Anim. Pract. *32*, 89–92.

Chou, C.M., Nelson, C., Tarlé, S.A., Pribila, J.T., Bardakjian, T., Woods, S., Schneider, A., and Glaser, T. (2015). Biochemical Basis for Dominant Inheritance, Variable Penetrance, and Maternal Effects in RBP4 Congenital Eye Disease. Cell *161*, 634–646.

Cowan, S.W., Newcomer, M.E., and Jones, T.A. (1990). Crystallographic refinement of human serum retinol binding protein at 2A resolution. Proteins *8*, 44–61.

D'Ambrosio, D.N., Clugston, R.D., and Blaner, W.S. (2011). Vitamin A metabolism: an update. Nutrients *3*, 63–103.

Dill, K.A., and Chan, H.S. (1997). From Levinthal to pathways to funnels. Nat. Struct. Biol. *4*, 10–19.

Fantes, J., Ragge, N.K., Lynch, S.A., McGill, N.I., Collin, J.R., Howard-Peebles, P.N., Hayward, C., Vivian, A.J., Williamson, K., van Heyningen, V., and FitzPatrick, D.R. (2003). Mutations in SOX2 cause anophthalmia. Nat. Genet. *33*, 461–463.

Folli, C., Viglione, S., Busconi, M., and Berni, R. (2005). Biochemical basis for retinol deficiency induced by the I41N and G75D mutations in human plasma retinol-binding protein. Biochem. Biophys. Res. Commun. *336*, 1017–1022.

Gerth-Kahlert, C., Williamson, K., Ansari, M., Rainger, J.K., Hingst, V., Zimmermann, T., Tech, S., Guthoff, R.F., van Heyningen, V., and Fitzpatrick, D.R. (2013). Clinical and mutation analysis of 51 probands with anophthalmia and/or severe microphthalmia from a single center. Mol. Genet. Genomic Med. *1*, 15–31.

Glaser, T., Jepeal, L., Edwards, J.G., Young, S.R., Favor, J., and Maas, R.L. (1994). PAX6 gene dosage effect in a family with congenital cataracts, aniridia, anophthalmia and central nervous system defects. Nat. Genet. *7*, 463–471.

Graw, J. (2003). The genetic and molecular basis of congenital eye defects. Nat. Rev. Genet. *4*, 876–888.

Greene, L.H., Wijesinha-Bettoni, R., and Redfield, C. (2006). Characterization of the molten globule of human serum retinol-binding protein using NMR spectroscopy. Biochemistry *45*, 9475–9484.

Hale, F. (1935). The relation of vitamin A to anophthalmos in pigs. Am. J. Ophthalmol. *18*, 1087–1093.

Hornby, S.J., Gilbert, C.E., Rahi, J.K., Sil, A.K., Xiao, Y., Dandona, L., and Foster, A. (2000). Regional variation in blindness in children due to microphthalmos, anophthalmos and coloboma. Ophthalmic Epidemiol. *7*, 127–138.

Hornby, S.J., Ward, S.J., Gilbert, C.E., Dandona, L., Foster, A., and Jones, R.B. (2002). Environmental risk factors in congenital malformations of the eye. Ann. Trop. Paediatr. *22*, 67–77.

Kaji, E.H., and Lodish, H.F. (1993). Unfolding of newly made retinol-binding protein by dithiothreitol. Sensitivity to retinoids. J. Biol. Chem. *268*, 22188–22194.

Kawaguchi, R., Zhong, M., Kassai, M., Ter-Stepanian, M., and Sun, H. (2012). STRA6-catalyzed vitamin A influx, efflux, and exchange. J. Membr. Biol. *245*, 731–745.

Kawaguchi, R., Zhong, M., and Sun, H. (2013). Real-time analyses of retinol transport by the membrane receptor of plasma retinol binding protein. J. Vis. Exp. *71*, e50169.

Khan, K.N., Carss, K., Raymond, F.L., Islam, F., Moore, A.T., Michaelides, M., and Arno, G.; Nihr BioResource-Rare Diseases Consortium (2017). Vitamin A deficiency due to bi-allelic mutation of RBP4: There's more to it than meets the eye. Ophthalmic Genet. *38*, 465–466.

Lindblad-Toh, K., Wade, C.M., Mikkelsen, T.S., Karlsson, E.K., Jaffe, D.B., Kamal, M., Clamp, M., Chang, J.L., Kulbokas, E.J., 3rd, Zody, M.C., et al. (2005). Genome sequence, comparative analysis and haplotype structure of the domestic dog. Nature *438*, 803–819.

Marceau, G., Gallot, D., Lemery, D., and Sapin, V. (2007). Metabolism of retinol during mammalian placental and embryonic development. Vitam. Horm. *75*, 97–115.

Mobli, M., and King, G.F. (2010). NMR methods for determining disulfide-bond connectivities. Toxicon *56*, 849–854.

Morrison, D., FitzPatrick, D., Hanson, I., Williamson, K., van Heyningen, V., Fleck, B., Jones, I., Chalmers, J., and Campbell, H. (2002). National study of microphthalmia, anophthalmia, and coloboma (MAC) in Scotland: investigation of genetic aetiology. J. Med. Genet. *39*, 16–22.

Onwochei, B.C., Simon, J.W., Bateman, J.B., Couture, K.C., and Mir, E. (2000). Ocular colobomata. Surv. Ophthalmol. *45*, 175–194.

Parker, H.G., Kukekova, A.V., Akey, D.T., Goldstein, O., Kirkness, E.F., Baysac, K.C., Mosher, D.S., Aguirre, G.D., Acland, G.M., and Ostrander, E.A. (2007). Breed relationships facilitate fine-mapping studies: a 7.8-kb deletion cosegregates with Collie eye anomaly across multiple dog breeds. Genome Res. *17*, 1562–1571.

Pasutto, F., Sticht, H., Hammersen, G., Gillessen-Kaesbach, G., Fitzpatrick, D.R., Nürnberg, G., Brasch, F., Schirmer-Zimmermann, H., Tolmie, J.L., Chitayat, D., et al. (2007). Mutations in STRA6 cause a broad spectrum of malformations including anophthalmia, congenital heart defects, diaphragmatic hernia, alveolar capillary dysplasia, lung hypoplasia, and mental retardation. Am. J. Hum. Genet. *80*, 550–560.

Quadro, L., Blaner, W.S., Salchow, D.J., Vogel, S., Piantedosi, R., Gouras, P., Freeman, S., Cosma, M.P., Colantuoni, V., and Gottesman, M.E. (1999). Impaired retinal function and vitamin A availability in mice lacking retinol-binding protein. EMBO J. *18*, 4633–4644.

Quadro, L., Hamberger, L., Gottesman, M.E., Wang, F., Colantuoni, V., Blaner, W.S., and Mendelsohn, C.L. (2005). Pathways of vitamin A delivery to the embryo: insights from a new tunable model of embryonic vitamin A deficiency. Endocrinology *146*, 4479–4490.

Ragge, N.K., Brown, A.G., Poloschek, C.M., Lorenz, B., Henderson, R.A., Clarke, M.P., Russell-Eggitt, I., Fielder, A., Gerrelli, D., Martinez-Barbera, J.P., et al. (2005). Heterozygous mutations of OTX2 cause severe ocular malformations. Am. J. Hum. Genet. *76*, 1008–1022.

Reznik, G.O., Yu, Y., Tarr, G.E., and Cantor, C.R. (2003). Native disulfide bonds in plasma retinol-binding protein are not essential for all-trans-retinol-binding activity. J. Proteome Res. *2*, 243–248.

Ruggiano, A., Foresti, O., and Carvalho, P. (2014). Quality control: ER-associated degradation: protein quality control and beyond. J. Cell Biol. *204*, 869–879.

See, A.W., and Clagett-Dame, M. (2009). The temporal requirement for vitamin A in the developing eye: mechanism of action in optic fissure closure and new roles for the vitamin in regulating cell proliferation and adhesion in the embryonic retina. Dev. Biol. *325*, 94–105.

Selvaraj, S.R., Bhatia, V., and Tatu, U. (2008). Oxidative folding and assembly with transthyretin are sequential events in the biogenesis of retinol binding protein in the endoplasmic reticulum. Mol. Biol. Cell *19*, 5579–5592.

Sharma, D., and Rajarathnam, K. (2000). 13C NMR chemical shifts can predict disulfide bond formation. J. Biomol. NMR *18*, 165–171.

Singh, R., and Whitesides, G.M. (1994). Reagents for rapid reduction of native disulfide bonds in proteins. Bioorg. Chem. *22*, 109–115.

Suire, S., Stewart, F., Beauchamp, J., and Kennedy, M.W. (2001). Uterocalin, a lipocalin provisioning the preattachment equine conceptus: fatty acid and retinol binding properties, and structural characterization. Biochem. J. *356*, 369–376.

Vahlquist, A., Peterson, P., and Wibell, L. (1973). Metabolism of the vitamin A transporting protein complex. I. Turnover studies in normal persons and in patients with chronic renal failure. Eur. J. Clin. Invest. *3*, 352–362.

Van der Woerdt, A., Stades, F., Van der Linde-Sipman, J., and Boeve, M. (1995). Multiple ocular anomalies in two related litters of Soft Coated Wheaten Terriers. Vet. Comp. Ophthalmol. *5*, 78.

Vaquer, G., Rivière, F., Mavris, M., Bignami, F., Llinares-Garcia, J., Westermark, K., and Sepodes, B. (2013). Animal models for metabolic, neuromuscular and ophthalmological rare diseases. Nat. Rev. Drug Discov. *12*, 287–305.

Vembar, S.S., and Brodsky, J.L. (2008). One step at a time: endoplasmic reticulum-associated degradation. Nat. Rev. Mol. Cell Biol. *9*, 944–957.

Verma, A.S., and Fitzpatrick, D.R. (2007). Anophthalmia and microphthalmia. Orphanet J. Rare Dis. *2*, 47.

Wooding, P., and Burton, G. (2008). Comparative placentation: structures, functions and evolution (Springer-Verlag Berlin Heidelberg).

Wyatt, A.R., Yerbury, J.J., Berghofer, P., Greguric, I., Katsifis, A., Dobson, C.M., and Wilson, M.R. (2011). Clusterin facilitates in vivo clearance of extracellular misfolded proteins. Cell. Mol. Life Sci. *68*, 3919–3931.

Zanotti, G., Berni, R., and Monaco, H.L. (1993a). Crystal structure of liganded and unliganded forms of bovine plasma retinol-binding protein. J. Biol. Chem. *268*, 10728–10738.

Zanotti, G., Ottonello, S., Berni, R., and Monaco, H.L. (1993b). Crystal structure of the trigonal form of human plasma retinol-binding protein at 2.5 A resolution. J. Mol. Biol. *230*, 613–624.

Zetterström, P., Stewart, H.G., Bergemalm, D., Jonsson, P.A., Graffmo, K.S., Andersen, P.M., Brännström, T., Oliveberg, M., and Marklund, S.L. (2007). Soluble misfolded subfractions of mutant superoxide dismutase-1s are enriched in spinal cords throughout life in murine ALS models. Proc. Natl. Acad. Sci. USA *104*, 14157–14162.

OPEN ACCESS Freely available online

PLOS ONE

A Novel Missense Mutation in *ADAMTS10* in Norwegian Elkhound Primary Glaucoma

Saija J. Ahonen[1,2], Maria Kaukonen[1,2], Forrest D. Nussdorfer[3], Christine D. Harman[3], András M. Komáromy[3,4], Hannes Lohi[1,2]*

1 Department of Veterinary Biosciences and Research Programs Unit, Molecular Neurology, University of Helsinki, Helsinki, Finland, **2** The Folkhälsan Institute of Genetics, Helsinki, Finland, **3** Department of Small Animal Clinical Sciences, College of Veterinary Medicine, Michigan State University, East Lansing, Michigan, United States of America, **4** Department of Clinical Studies, School of Veterinary Medicine, University of Pennsylvania, Philadelphia, Pennsylvania, United States of America

Abstract

Primary glaucoma is one of the most common causes of irreversible blindness both in humans and in dogs. Glaucoma is an optic neuropathy affecting the retinal ganglion cells and optic nerve, and elevated intraocular pressure is commonly associated with the disease. Glaucoma is broadly classified into primary open angle (POAG), primary closed angle (PCAG) and primary congenital glaucoma (PCG). Human glaucomas are genetically heterogeneous and multiple loci have been identified. Glaucoma affects several dog breeds but only three loci and one gene have been implicated so far. We have investigated the genetics of primary glaucoma in the Norwegian Elkhound (NE). We established a small pedigree around the affected NEs collected from Finland, US and UK and performed a genome-wide association study with 9 cases and 8 controls to map the glaucoma gene to 750 kb region on canine chromosome 20 ($p_{raw} = 4.93 \times 10^{-6}$, $p_{genome} = 0.025$). The associated region contains a previously identified glaucoma gene, *ADAMTS10*, which was subjected to mutation screening in the coding regions. A fully segregating missense mutation (p.A387T) in exon 9 was found in 14 cases and 572 unaffected NEs ($p_{Fisher} = 3.5 \times 10^{-27}$) with a high carrier frequency (25.3%). The mutation interrupts a highly conserved residue in the metalloprotease domain of ADAMTS10, likely affecting its functional capacity. Our study identifies the genetic cause of primary glaucoma in NEs and enables the development of a genetic test for breeding purposes. This study establishes also a new spontaneous canine model for glaucoma research to study the *ADAMTS10* biology in optical neuropathy.

Citation: Ahonen SJ, Kaukonen M, Nussdorfer FD, Harman CD, Komáromy AM, et al. (2014) A Novel Missense Mutation in *ADAMTS10* in Norwegian Elkhound Primary Glaucoma. PLoS ONE 9(11): e111941. doi:10.1371/journal.pone.0111941

Editor: Michael G. Anderson, University of Iowa, United States of America

Received June 5, 2014; **Accepted** October 2, 2014; **Published** November 5, 2014

Data Availability: The authors confirm that all data underlying the findings are fully available without restriction. All relevant data are within the paper and its Supporting Information files. The GWAS data have been uploaded to Figshare: http://dx.doi.org/10.6084/m9.figshare.1199862.

Funding: This work was partly supported by the Jane and Aatos Erkko Foundation, Biocentrum Helsinki, Academy of Finland, the Sigrid Juselius Foundation, the National Institutes of Health (K12-EY015398) and Michigan State University faculty startup funds. The funders had no role in study design, data collection and analysis, decision to publish, or preparation of the manuscript.

Competing Interests: The authors have declared that no competing interests exist.

* Email: hannes.lohi@helsinki.fi

Introduction

Glaucoma is an optic neuropathy affecting the retinal ganglion cells and optic nerve. Elevated intraocular pressure (IOP) is commonly associated with the disease. However, normal tension glaucoma is diagnosed as well [1]. Human glaucomas form a heterogeneous group of diseases, which are broadly classified into primary open-angle (POAG), primary closed-angle (PCAG) and primary congenital glaucoma (PCG) [2]. POAG is the most common form in humans [2]. In POAG, the iridocorneal angle (ICA) is open with an elevated IOP, which is considered as a significant risk factor for the disease. PCAG results from the collapse of the ICA structures, elevated IOP and subsequent death of the retinal cells [3]. Elevated IOP is caused by the blockage of the aqueous humor outflow due to a shallow anterior chamber combined with the obstruction of the iris-trabecular meshwork in the iridocorneal angle of the eye, [4]. PCG occurs within the first few years of life and is characterized by abnormalities in the anterior chamber angle and elevated IOP [4].

In human, several loci [5–6] and several genes including, *contactin 4* (*CNTN4*) [7], *myocilin (MYOC)* [8], *neurotrohin 4 (NTF4)* [9], *optineurin (OPTN)* [10] and *WD repeat domain 36 (WDR36)* [11] have been associated with POAG. Three loci [6] and the two genes *cytochrome P450 1B1 (CYP1B1)* [12] and *latent transforming growth factor beta binding protein 2 (LTBP2)* [13] have been associated with PCG. Three loci have been associated with PCAG, in which separate markers showed significant association after replication on human chromosomes 1, 8 and 11 [14]. Only one causative gene *ATP-binding cassette, sub-family C (CFTR/MRP), member 5* (*ABCC5*) has been associated with PCAG [15]. Furthermore, multiple genes and loci have been associated with syndromes and other ocular conditions accompanied by glaucoma [6]. However, glaucoma is considered a multifactorial disease and although several variants have been identified for familial cases, the glaucoma genetics remains controversial [16–17].

In dogs, POAG and PCAG have been described in several breeds [18]. Clinical features resemble human glaucoma, including loss of the retinal ganglion cells and elevated IOP. Abnormalities in the pectinate ligament (PL) structure are considered as a risk factor in canine PCAG [19–24]. The

pectinate ligament forms the internal boundary of the canine ICA and is presented as pillar of tissue. It project from the base of iris to the peripheral Descemet's membrane. It provides support for the iris to the posterior cornea [25]. Although structural abnormalities are considered a risk for the disease, not all dogs affected with PLD develop glaucoma, suggesting other genetic risk factors.

Despite the presence of glaucoma in many breeds the genetic etiology of glaucoma is almost completely unknown in dogs. A novel locus was mapped in Dandie Dinmont Terriers [19] and two loci were suggested for the Basset Hound [26] with PCAG. In a research colony of Beagles a recessive mutation (p.G661R) in the *ADAM metallopeptidase with thrombospondin type 1 motif*, 10 (*ADAMTS10*), has been found in a research colony of Beagles with POAG has been suggested as causative [27]. The early clinical signs in the affected Beagles include open ICA that narrows as the disease progresses, gradual increase in IOP that eventually leads to retinal ganglion cell death, optic nerve atrophy, and irreversible blindness [28]. The age of onset in Beagles varies from 8 to 16 months [29].

In addition to Beagles, Norwegian Elkhounds are also affected with POAG [30–31]. Unlike the Beagle, the disease in NEs is commonly diagnosed in middle-aged or elderly dogs when it starts to affect the dogs hunting capabilities [30]. However, the actual disease onset may be much earlier. Early clinical signs in NEs include a slightly elevated IOP with a normal opening of the ciliary cleft [30]. The peripheral vision is commonly affected. At the later stages of the disease, the narrowing of the ciliary cleft contributes to the elevation of IOP. This may lead to secondary subluxation of the lenses in some cases. The vision deterioration continues to expand due to optic nerve atrophy and cupping. The retina appears funduscopically normal until the late stages of the disease. Other clinical signs include Haabs striae, cataract, and buphthalmos [30].

We aimed to find the genetic cause of primary glaucoma in NEs in this study to better understand the molecular pathogenesis, to establish a large, spontaneous canine model for POAG research, and to develop a genetic test for breeding purposes. We discovered a novel missense mutation in the *ADAMTS10* gene.

Materials and Methods

Study cohort

Blood samples from 596 NEs, including 16 glaucoma affected dogs from Finland, Norway, Sweden, United Kingdom and United States were collected to the canine DNA bank at the University of Helsinki, Finland with owners consent and under the permission of the Animal Ethical Committee of County Administrative Board of Southern Finland (ESAVI/6054/04.10.03/2012). All affected dogs were examined by a certified veterinary ophthalmologist. The clinical diagnoses indicated bilateral primary glaucoma with significantly elevated IOP, between 25–86 mmHg (normal 10–20 mmHg), and no detectable underlying cause. In addition, various degrees of optic nerve atrophy and cupping were reported. In addition, a progressive vision loss was detected in the affected dogs leading to complete blindness. Other, secondary clinical signs included lens luxation, corneal stromal edema, Haabs striae, keratitis, vitreal syneresis and retinal degeneration. The average age at the time of diagnosis was 6.5 years.

Genomic DNA was extracted from EDTA blood using Chemagic Magnetic Separation Module I (MSM I) (Chemagen Biopolymer-Technologie AG, Baeswieler, Germany) according to the manufacturer's instructions. DNA from buccal swabs (Eurotubo Cytobrush, sterile, 200 mm, Danlab, Helsinki, Finland) was extracted using QIAamp DNA Mini Kit (Qiagen).

Genome wide association study

A genome-wide association study (GWAS) was performed using Illumina's CanineHD BeadChip array (San Diego, CA, USA) with 9 cases and 8 controls (**Fig. 1**). The control dogs were at least 8 years of age without any clinical signs of glaucoma. Genotyping was performed at the Geneseek (Lincoln, NE, USA) and the genotyping data was analyzed using PLINK 1.07 analysis software. A total of 173,662 markers were initially included for the analysis. No individual were removed for low genotyping success of 95%. Missingness test of 95% removed 17,484 SNPs. A total of 72,715 SNPs had minor allele frequency of less than 5% and were removed. None of the SNPs deviated from Hardy-Weinberg equilibrium based of HWE test of $P <= 0.0001$. After frequency and genotyping pruning, 89,277 SNPs remained in the analysis. A case-controls association test was performed using PLINK software to compare the allele frequencies between cases and controls (**Fig. 2A**). Identity-by-state (IBS) clustering and CMH meta-analysis (PLINK) were used to adjust for population stratification. Genome-wide corrected empirical p-values were determined applying 100,000 permutations to the data. Besides PLINK the data was analyzed with compressed mixed linear model [32] implemented in the GAPIT R package [33] and with R-implemented GenABEL [34] software (data not shown). The GWAS data is publicly available at dbSNP database (http://www.ncbi.nlm.nih.gov/projects/SNP/).

Candidate gene sequencing

The coding regions of the best candidate gene in the associated region, *ADAMTS10,* were first sequenced in four NE cases, in four NE controls (unaffected >8 years) and in one unaffected Rough Collie samples. The identified candidate mutation was then validated in 596 NEs, including 7 additional cases. In addition, the mutation was studied in 71 dogs from 17 other breeds affected with POAG, PCAG or PLD and in 115 unaffected dogs from 6 breeds (**Table S1**).

Primer pairs (**Table S2**) were designed for the ADAMTS10 gene to amplify the coding regions and splice sites by standard PCR (**Table S2**). PCRs were carried out in 12 µl reactions consisting of 1.2 U Biotools DNA Polymerase (Biotools, Madrid, Spain), 1.5 mM $MgCl_2$ (Biotools, Madrid, Spain), 200 µM dNTPs (Finnzymes, Espoo, Finland), 1 x Biotools PCR buffer without $MgCl_2$ (Biotools, Madrid, Spain), 0.83 µM forward and reverse primer (Sigma Aldrich, St. Louis, USA) and 10 ng template genomic DNA. Reaction mixtures were subjected to a thermal cycling program of 95°C for 10 min, followed by 35 cycles of 95°C for 30 s, 30 s at the annealing temperature and 72°C for 60 s and a final elongation stage of 72°C for 10 min. ExoSap purified PCR fragments were Sanger sequenced in our core facility the FIMM Technology Center using ABI 3730xl DNA analyzer (Applied Biosystems, Foster City, California, USA). Sequence data analysis was performed using the Sequencher software (Gene Codes, Ann Arbor, MI, USA). Build 3.1 of the canine genome reference sequence was applied in the study.

Results

We established a global sample cohort including glaucoma affected (n = 16) and unaffected NEs (>570) to map the disease locus, to identify the causative gene and to validate the segregation of the mutation. We performed a GWAS in a small pedigree of 9 cases and 8 controls. Statistical analyses revealed a 750 kb locus on CFA20 with 23 most highly associated SNPs between 53070684 bp to 53816416 bp ($p_{raw} = 4.93 \times 10^{-06}$, $p_{genome} = 0.025$) (**Fig. 2B, C**). A mild population stratification was identified

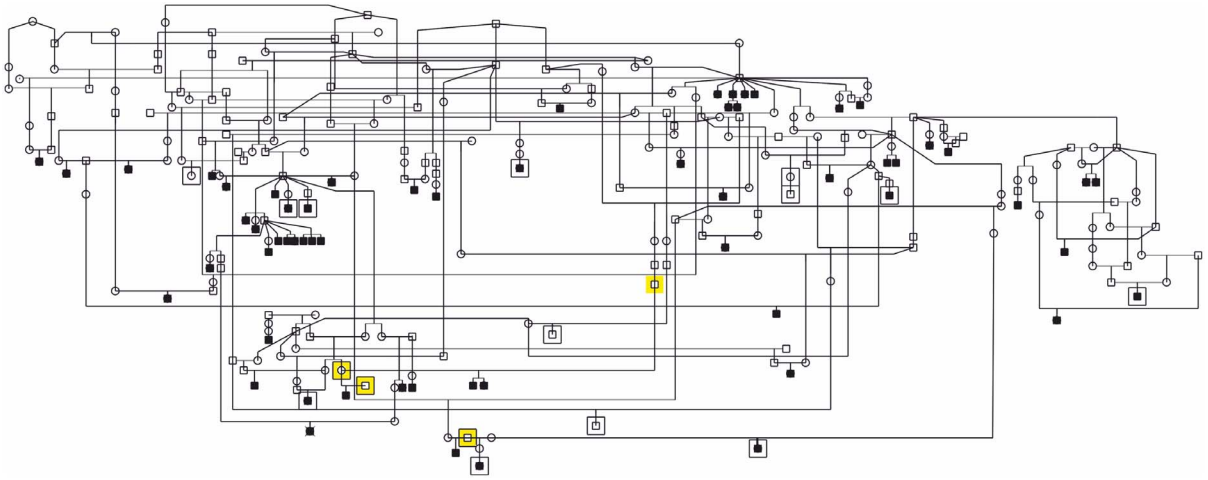

Figure 1. Pedigree of glaucoma affected Norwegian Elkhounds. The pedigree constructed around affected dogs indicates a likely recessive mode of inheritance as the affected dogs are born to unaffected parents and there are multiple affected littermates in some litter. The squared dogs were included in the GWAS. Individuals marked with yellow background were genotyped as obligatory carriers and were all heterozygous for the mutation.
doi:10.1371/journal.pone.0111941.g001

in the study cohort by genome wide IBS clustering (genomic inflation factor $\lambda = 1.1$) (**Fig. S2**), but it did not affect the result as two mixed model approaches (GenABEL and GAPIT) that better control for population stratification, gave the same results (data not shown).

A pedigree constructed around the affected dogs using GenoPro genealogy software (http://www.genopro.com) suggested a recessive mode of inheritance as the affected dogs are born to unaffected parents and there are multiple affected littermates in some litters.

The identified locus contains 35 genes including a known canine POAG gene, *ADAMTS10* (**Fig. 2D**). It was selected for mutation screening in the coding regions and splice sites in four affected and five control dogs. Sequencing identified altogether ten variants; a non-synonymous variant c.1441G>A, p.A387T in the exon 9 (**Fig. 3A, B**), five synonymous and four non-coding variants (**Table S3**). Only one out of the five synonymous variants, p.P171P, co-segregated with the non-synonymous variant. However, it was not suspected to be in the exonic enhancer region when analyzed by the ESE-finder [35]. Instead, the non-synonymous variant was predicted to be pathogenic based on the bioinformatics prediction tools Polyphen2 [36] and SIFT [37]. The mutation affects a highly conserved residue (present in 75 species, **Fig. S1**) in the metalloprotease domain of ADAMTS10 protein (**Fig. 3C**).

To gather further evidence for the p.A387T segregation, we genotyped seven additional NE primary glaucoma cases and four obligatory carriers (**Fig. 1**) and 572 randomly selected unaffected NEs. All but two of the cases were homozygous for the mutation. Unfortunately, we have a limited access to the health records and history of these two affected dogs and they may have had a secondary glaucoma with a primary underlying cause such as inflammation being missed at the end stage of disease when the animals were presented to the veterinary ophthalmologist. All four obligatory carriers were heterozygous. Genotyping of the 572 NEs indicated a 25.3% carrier frequency (151/596) and revealed one additional homozygous dog. This genetically affected dog is now 5 years old without signs of glaucoma yet but needs to be followed up since the average age of diagnosis in the breed is at 6.5 years of age. Collectively, these results support a segregation of a mutation in clinically confirmed primary glaucoma cases with a highly significant association between the mutation and disease when comparing genotyped genetically affected dogs ($n = 16$) and unaffected using Fisher's exact test ($P_{Fisher} = 3.5 \times 10^{-27}$). The breed-specificity of the p.A387T mutation was indicated by excluding it from 71 glaucoma or PLD affected dogs from 17 breeds and from 115 unaffected dogs from six breeds.

Discussion

Our study has identified a novel recessive mutation in the *ADAMT10* gene in the NEs affected with primary glaucoma using genome wide association analysis and candidate sequencing strategies. We mapped the disease to a known canine POAG locus including the *ADAMTS10* candidate gene and subsequently identified a missense mutation in the exon 9 of the *ADAMTS10* gene. This is consistent with the previously reported POAG phenotype of primary glaucoma in this breed [30–31]. The recessively segregating mutation results in an alanine to threonine change (p.A387T) in a highly conserved functional metalloprotease domain of the protein (**Fig. 3C**), which likely impairs ADAMTS10 function, leading to POAG in the homozygous dogs.

ADAMTS10 is a secreted glycoprotein [38] and belongs to a family of metalloproteinases that contribute to the dynamics of the extracellular matrix (ECM) composition and microfibril function [38–40]. It may have a role in the storage and activation of latent transforming growth factor beta (TGF_β), which regulates the collagen turnover [41–43] as well as in the remodeling of the mesenchymal and basement membranes [44].

The members of the ADAMTS family share the same structural organization including catalytic metalloprotease domain, followed by a disintegrin-like, and cysteine-rich domains, a thrombospondin repeat and a spacer region (**Fig. 3C**). ADAMTS10 differs from the others having five thrombospondin type 1 repeats and a PLAC domain in the C-terminal [44].

ADAMTS10 interacts with fibrillin-1 and localized to fibrillin-1 microfibril bundles [39]. It maintains the lens in its position via lens ligaments, which are comprised primarily from fibrillin-1 [43]. Microfibrils localize and activate TGF_β [45]. Fibrillin-1 is expressed in the outflow pathway of the aqueous humor and

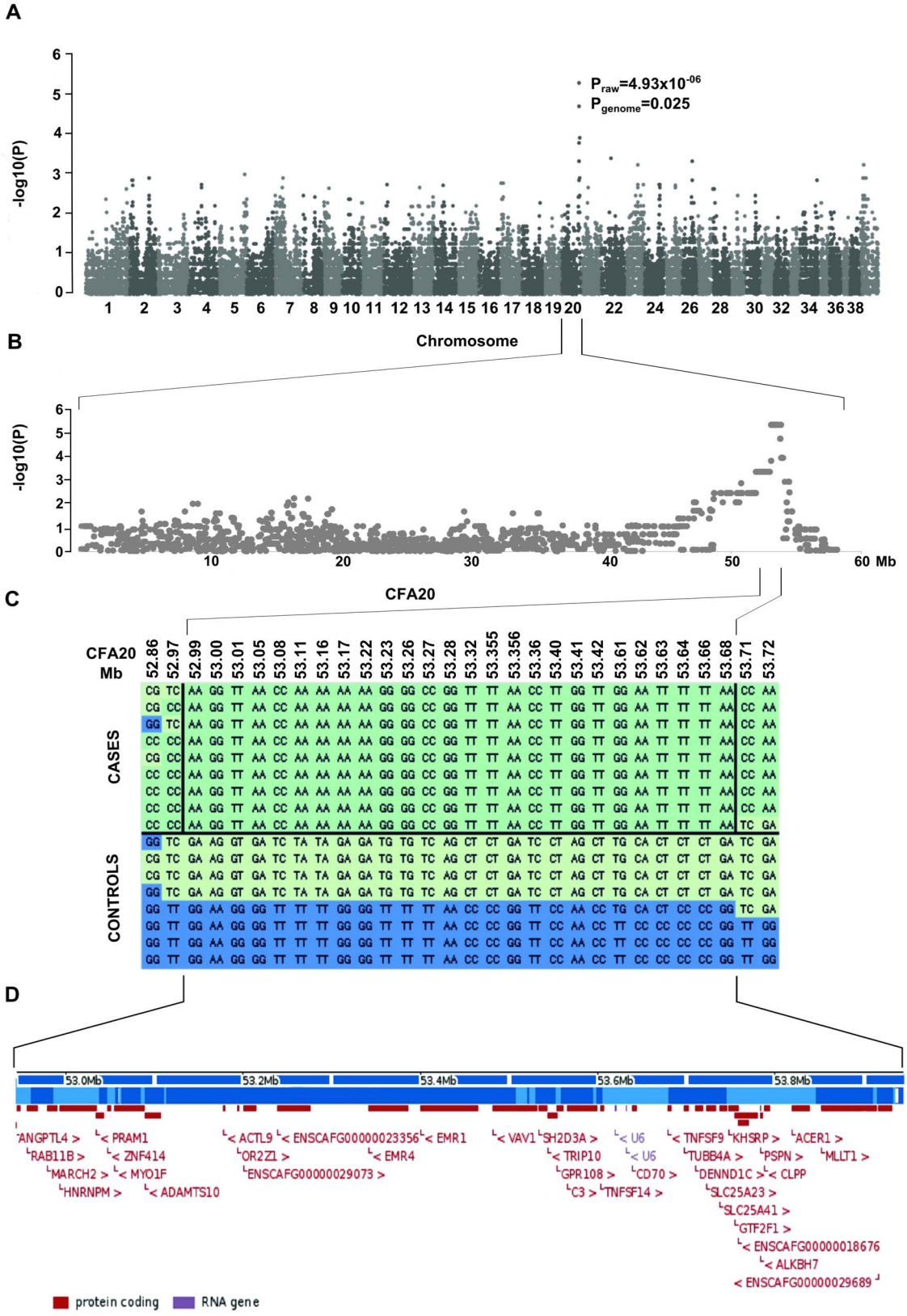

Figure 2. Genome wide association study. A) A Manhattan plot of genome-wide case-control association analysis with 8 cases and 9 controls indicate the most highly associated region in CFA20. **B**) The glaucoma associated region on chromosome 20 spans from 53.1 Mb to 53.8 Mb. **C**) Genotypes at the associated region on CFA20. All cases share a 750 kb homozygous block. **D**) The associated region harbors 35 genes of which only *ADAMTS10* has been associated with POAG.
doi:10.1371/journal.pone.0111941.g002

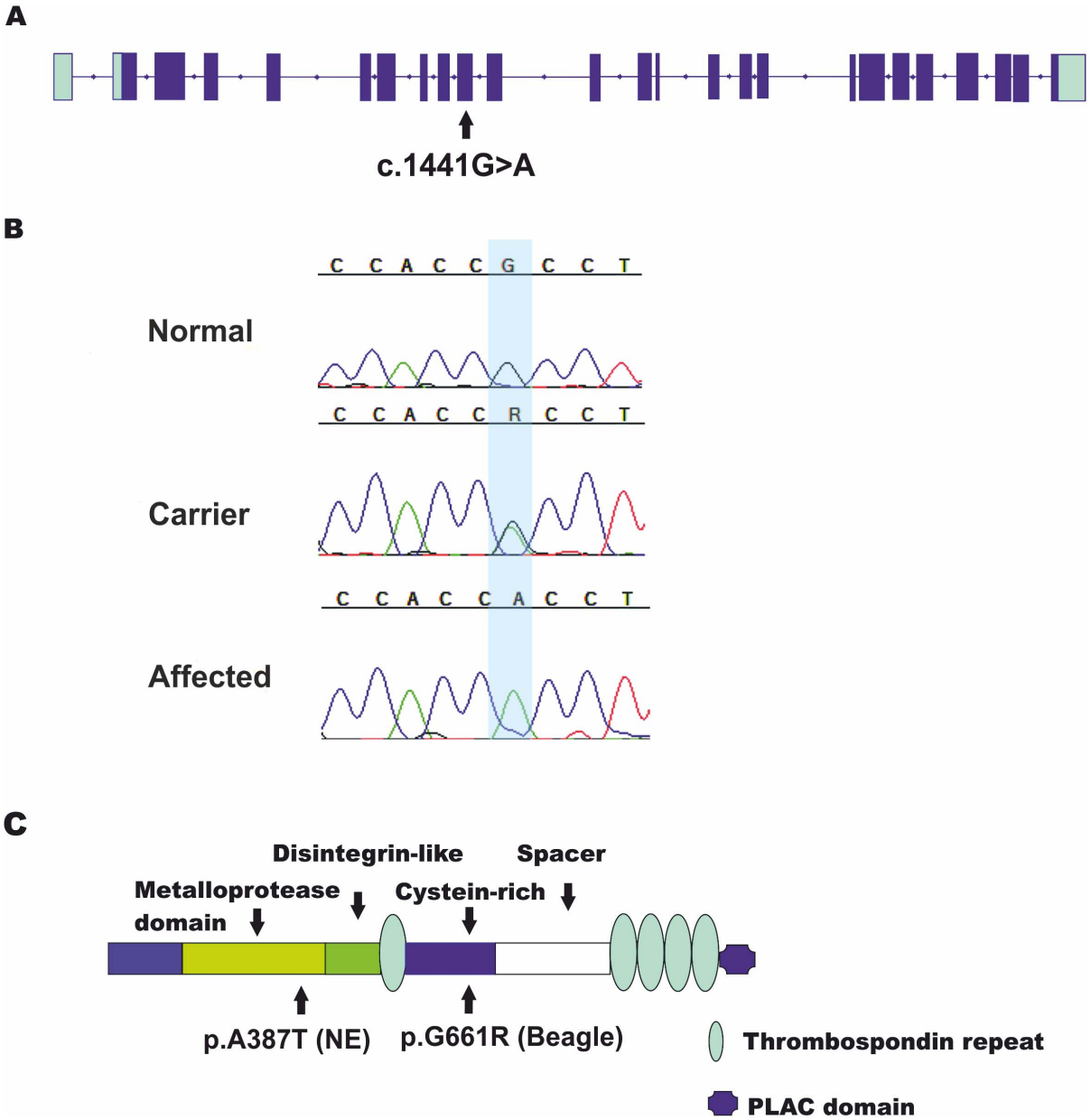

Figure 3. A missense mutation in the *ADAMTS10*. **A**) A schematic representation of the *ADAMTS10* gene structure. The gene is composed of 24 coding exons (dark blue) and the c.1441G>A variant is positioned in the exon 9 (not in scale). **B**) Chromatograms of the non-synonymous variant position in an affected, a carrier and a wild-type dog. **C**) The p.A387T variant is positioned in the catalytic metalloprotease domain.
doi:10.1371/journal.pone.0111941.g003

defect in the fibrillin-1 may lead to impaired aqueous humor flow [46–48].

In dogs, a missense mutation (p.G661R) in the *ADAMTS10* gene has been previously associated with POAG in a research colony of Beagles. The Beagle mutation is positioned in the cysteine rich domain and is hypothesized to disrupt protein folding leading to instability [27].

The NE mutation is different from the Beagles and may result in a different pathogenesis. NE mutation changes a highly conserved residue in the metalloprotease domain, which plays a role in the remodeling of the connective tissue (**Fig. 3C**) [44]. Human metalloprotease domain mutations have revealed abnormalities in the cellular cytoskeleton [44], suggesting abnormal interactions with the ECM. These abnormalities may eventually result in defective microfibrils and glaucoma through alterations in biomechanical properties of tissue and/or through effects on signaling through TGF_{β}, which is known to be elevated in the aqueous humor of glaucoma patients [49]. Unfortunately, we did not have access to any tissue samples from the affected dogs to further investigate the functional consequences of the mutation for *ADAMTS10* and its pathway. Secondary lens luxation diagnosed in the affected NEs may be due to abnormal fibrillin-1 functions as the ADAMTS10 and fibrillin-1 interaction may be impaired causing disruption of the lens ligaments.

Dagoneau et al. identified three causative mutations in the metalloprotease domain of *ADAMTS10* in human WMS patients [44]. When studying patient fibroblasts they noted that abnormally large bundles of actin were present, which were reflection of

cytoskeleton abnormalities as a result of impaired connections between cytoskeleton and ECM [44].

Mutations in *ADAMTS10* [44], [50], *ADAMTS17* [50] and in *fibrillin 1* (*FBN1*) [51] have been associated with a Weill-Marchesani syndrome (WMS) (OMIM 277600). WMS is a connective tissue disorder and characterized by several eye defects including glaucoma, myopia, ectopia lentis, microspherophakia and other features such as short stature, brachydactyly, joint stiffness in the hands, restricted articular movements and some facial features [52]. Glaucoma is diagnosed in WMS patients, but ectopia lentis is the more prevalent clinical sign [53]. In WMS patients the ectopia lentis and dysgenesis of the lens ligament is suspected to be caused by abnormal biogenesis of fibrillin-1 [39]. The same is likely true for *ADAMTS17*-mutant dogs [54] and *ADAMTS10*-mutant Beagles [27]. Interestingly, none of our affected NE dogs presented with signs of primary lens luxation, although this should be expected. Histologic analyses of the lens zonules would be very helpful to identify possible signs of zonular dysplasia. Another difference in the affected NE dogs relates to the lack of severe non-ocular signs, which are commonly present in the WMS patients with mutation in the *ADAMTS10* and *ADAMTS17* genes. Further studies are warranted to investigate whether the observed breed- and species–specific differences are due to alternate mutations in the metalloproteinase domains or possible other factors.

In summary, we have discovered the genetic cause of primary glaucoma in the NEs by identifying a missense mutation in *ADAMTS10*. This study implicates the significant role of ADAMTS10 in canine POAG by identifying the second mutation in the same gene in dogs. Our affected dogs establish a new model to study *ADAMTS10* biology in the microfibrillin theory of the glaucoma [49]. Importantly, given the high frequency of the mutation in the NE breed, our study is a breakthrough for the NE breeders, who will benefit from the genetic test to reduce the disease frequency in future populations.

Supporting Information

Figure S1 ADAMTS10 protein alignments. ADAMTS10 sequence alignment between different species. The mutation is located in a highly conserved region across 75 species. The arrow marks the mutated alanine residue.
(ZIP)

Figure S2 Q-Q plots. Identity-by-state (IBS) clustering and CMH meta-analysis (PLINK) were used to adjust for population stratification (A). A mild population stratification was identified in the study cohort by genome wide IBS clustering (adjusted genomic inflation factor $\lambda = 1.1$) (B).
(TIF)

Table S1 Dogs affected with glaucoma of PLD (71 dogs in 17 breeds) and healthy dog (115 dogs in six breeds) were sequenced for the *ADAMTS10* mutation.
(XLSX)

Table S2 Primers used for PCR amplification and sequencing of canine ADAMTS10 coding regions.
(XLSX)

Table S3 A total of 10 variants were in the coding and splice site regions of *ADAMTS10*.
(XLSX)

Acknowledgments

The authors thank the NE owners and veterinarians for providing phenotype information, blood samples, and pedigrees. Special thanks go to Drs. Vanessa J. Kuonen Cavens and Terah E.R. Webb (MedVet Medical and Cancer Centers for Pets, Columbus and Cincinnati, Ohio), Thomas Sullivan (Animal Eye Clinic, Inc., Seattle, Washington), and Christi Warren (Animal Eye Doctors, Estero, Florida). We also thank Jessica S. Rowlan, Ann E. Cooper (University of Pennsylvania), Ranja Eklund, Sini Karjalainen and Minna Virta (University of Helsinki) for sample processing. This work was partly supported by the Jane and Aatos Erkko Foundation, Biocentrum Helsinki, Academy of Finland, the Sigrid Juselius Foundation, the National Institutes of Health (K12-EY015398) and Michigan State University faculty startup funds.

Author Contributions

Conceived and designed the experiments: SA MK AK HL. Performed the experiments: SA MK FN CH. Analyzed the data: SA MK. Contributed reagents/materials/analysis tools: SA MK FN CH AK HL. Contributed to the writing of the manuscript: SA MK AK HL.

References

1. Lee BL, Bathija R, Weinreb RN (1998) The definition of normal-tension glaucoma. J Glaucoma 7: 366–371.
2. Sarfarazi M (1997) Recent advances in molecular genetics of glaucomas. Hum Mol Genet 6: 1667–1677.
3. Casson RJ, Chidlow G, Wood JPM, Crowston JG, Goldberg I (2012) Definition of glaucoma: Clinical and experimental concepts. Clin Experiment Ophthalmol 40: 341–349.
4. Liu Y, Allingham R (2011) Molecular genetics in glaucoma. Exp Eye Res 93: 331–339.
5. Gemenetzi M, Yang Y, Lotery A (2011) Current concepts on primary open-angle glaucoma genetics: A contribution to disease pathophysiology and future treatment. Eye 26: 355–369.
6. Fuse N (2010) Genetic bases for glaucoma. Tohoku J Exp Med 221: 1–10.
7. Kaurani L, Vishal M, Kumar D, Sharma A, Mehani B, et al. (2014) Gene rich large deletions are overrepresented in POAG patients of Indian and Caucasian origins. Invest Ophthalmol Vis Sci 24: 3258–3264.
8. Stone EM, Fingert JH, Alward WL, Nguyen TD, Polansky JR, et al. (1997) Identification of a gene that causes primary open angle glaucoma. Science 275: 668–670.
9. Pasutto F, Matsumoto T, Mardin CY, Sticht H, Brandstatter JH, et al. (2009) Heterozygous *NTF4* mutations impairing neurotrophin-4 signaling in patients with primary open-angle glaucoma. Am J Hum Genet 85: 447–456.
10. Rezaie T, Child A, Hitchings R, Brice G, Miller L, et al. (2002) Adult-onset primary open-angle glaucoma caused by mutations in *optineurin*. Science 295: 1077–1079.
11. Monemi S, Spaeth G, DaSilva A, Popinchalk S, Ilitchev E, et al. (2005) Identification of a novel adult-onset primary open-angle glaucoma (POAG) gene on 5q22.1. Hum Mol Genet 14: 725–733.
12. Stoilov I, Akarsu AN, Sarfarazi M (1997) Identification of three different truncating mutations in *cytochrome P4501B1* (*CYP1B1*) as the principal cause of primary congenital glaucoma (buphthalmos) in families linked to the GLC3A locus on chromosome 2p21. Hum Mol Genet 6: 641–647.
13. Ali M, McKibbin M, Booth A, Parry DA, Jain P, et al. (2009) Null mutations in *LTBP2* cause primary congenital glaucoma. Am J Hum Genet 84: 664–671.
14. Vithana EN, Khor CC, Qiao C, Nongpiur ME, George R, et al. (2012) Genome-wide association analyses identify three new susceptibility loci for primary angle closure glaucoma. Nat Genet 44: 1142–1146.
15. Nongpiur ME, Khor CC, Jia H, Cornes BK, Chen L, et al. (2014) *ABCC5*, a gene that influences the anterior chamber depth, is associated with primary angle closure glaucoma. PLoS genetics 10: e1004089.
16. Takamoto M, Araie M (2014) Genetics of primary open angle glaucoma. Jpn J Ophthalmol 58: 1–15.
17. Ojha P, Wiggs JL, Pasquale LR (2013) The genetics of intraocular pressure. Semin Ophthalmol 28: 301–305.
18. Strom AR, Hässig M, Iburg TM, Spiess BM (2011) Epidemiology of canine glaucoma presented to university of Zürich from 1995 to 2009. part 1: Congenital and primary glaucoma (4 and 123 cases). Vet Ophthalmol 14: 121–126.
19. Ahonen SJ, Pietilä E, Mellersh CS, Tiira K, Hansen L, et al. (2013) Genome-wide association study identifies a novel canine glaucoma locus. PloS one 8: e70903.
20. Bjerkas E, Ekesten B, Farstad W (2002) Pectinate ligament dysplasia and narrowing of the iridocorneal angle associated with glaucoma in the English Springer Spaniel. Vet Ophthalmol 5: 49–54.
21. Kato K, Sasaki N, Matsunaga S, Mochizuki M, Nishimura R, et al. (2006) Possible association of glaucoma with pectinate ligament dysplasia and

narrowing of the iridocorneal angle in Shiba Inu dogs in Japan. Vet Ophthalmol 9: 71–75.
22. van der Linde-Sipman JS (1987) Dysplasia of the pectinate ligament and primary glaucoma in the Bouvier des Flandres dog. Vet Pathol 24: 201–206.
23. Ekesten B, Narfstrom K (1991) Correlation of morphologic features of the iridocorneal angle to intraocular pressure in Samoyeds. Am J Vet Res 52: 1875–1878.
24. Read RA, Wood JL, Lakhani KH (1998) Pectinate ligament dysplasia (PLD) and glaucoma in Flat Coated Retrievers. I. objectives, technique and results of a PLD survey. Vet Ophthalmol 1: 85–90.
25. Morrison JC, Van Buskirk EM (1982) The canine eye: Pectinate ligaments and aqueous outflow resistance. Invest Ophthalmol Vis Sci 23: 726–732.
26. Ahram DF, Cook AC, Kecova H, Grozdanic SD, Kuehn MH (2014) Identification of genetic loci associated with primary angle-closure glaucoma in the Basset Hound. Molecular vision 20: 497.
27. Kuchtey J, Olson LM, Rinkoski T, Mackay EO, Iverson TM, et al. (2011) Mapping of the disease locus and identification of *ADAMTS10* as a candidate gene in a canine model of primary open angle glaucoma. PLoS Genet 7: e1001306.
28. Gelatt KN, Peiffer RL Jr, Gwin RM, Gum GG, Williams LW (1977) Clinical manifestations of inherited glaucoma in the Beagle. Invest Ophthalmol Vis Sci 16: 1135–1142.
29. Peiffer RL Jr, Gum GG, Grimson RC, Gelatt KN (1980) Aqueous humor outflow in Beagles with inherited glaucoma: Constant pressure perfusion. Am J Vet Res 41: 1808–1813.
30. Ekesten B, Bjerkas E, Kongsengen K, Narfstrom K (1997) Primary glaucoma in the Norwegian Elkhound. Veterinary & Comparative Ophthalmology 7: 14–18.
31. Oshima Y, Bjerkas E, Peiffer RL (2004) Ocular histopathologic observations in Norwegian Elkhounds with primary open-angle, closed-cleft glaucoma. Vet Ophthalmol 7: 185–188.
32. Zhang Z, Ersoz E, Lai C, Todhunter RJ, Tiwari HK, et al. (2010) Mixed linear model approach adapted for genome-wide association studies. Nat Genet 42: 355–360.
33. Lipka AE, Tian F, Wang Q, Peiffer J, Li M, et al. (2012) GAPIT: Genome association and prediction integrated tool. Bioinformatics 28: 2397–2399.
34. Aulchenko Y (2010) GenABEL: an R library for genome-wide association analysis. Bioinformatics 5: 1294–1296.
35. Smith PJ, Zhang C, Wang J, Chew SL, Zhang MQ, et al. (2006) An increased specificity score matrix for the prediction of SF2/ASF-specific exonic splicing enhancers. Hum Mol Genet 15: 2490–2508.
36. Adzhubei IA, Schmidt S, Peshkin L, Ramensky VE, Gerasimova A, et al. (2010) A method and server for predicting damaging missense mutations. Nature methods 7: 248–249.
37. Ng PC, Henikoff S (2001) Predicting deleterious amino acid substitutions. Genome Res 11: 863–874.
38. Somerville RP, Jungers KA, Apte SS (2004) Discovery and characterization of a novel, widely expressed metalloprotease, *ADAMTS10*, and its proteolytic activation. J Biol Chem 279: 51208–51217.
39. Kutz W, Wang L, Bader H, Majors A, Iwata K, et al. (2011) ADAMTS10 protein interacts with fibrillin-1 and promotes its deposition in extracellular matrix of cultured fibroblasts. The Journal of biological chemistry 286: 17156–17167.
40. Porter S, Clark I, Kevorkian L, Edwards D (2005) The ADAMTS metalloproteinases. Biochem J 386: 15–27.
41. Rifkin DB (2005) Latent transforming growth factor-beta (TGF-beta) binding proteins: Orchestrators of TGF-beta availability. J Biol Chem 280: 7409–7412.
42. Isogai Z, Ono RN, Ushiro S, Keene DR, Chen Y, et al. (2003) Latent transforming growth factor beta-binding protein 1 interacts with fibrillin and is a microfibril-associated protein. J Biol Chem 278: 2750–2757.
43. Palko JR, Iwabe S, Pan X, Agarwal G, Komaromy AM, et al. (2013) Biomechanical properties and correlation with collagen solubility profile in the posterior sclera of canine eyes with an *ADAMTS10* mutation. Invest Ophthalmol Vis Sci 54: 2685–2695.
44. Dagoneau N, Benoist-Lasselin C, Huber C, Faivre L, Mégarbané A, et al. (2004) *ADAMTS10* mutations in autosomal recessive Weill-Marchesani syndrome. The American Journal of Human Genetics 75: 801–806.
45. Ramirez F, Rifkin DB (2009) Extracellular microfibrils: Contextual platforms for TGFβ and BMP signaling. Curr Opin Cell Biol 21: 616–622.
46. Kuchtey J, Chang TC, Panagis L, Kuchtey RW (2013) Marfan syndrome caused by a novel *FBN1* mutation with associated pigmentary glaucoma. American Journal of Medical Genetics Part A 161: 880–883.
47. Hann CR, Fautsch MP (2011) The elastin fiber system between and adjacent to collector channels in the human juxtacanalicular tissue. Invest Ophthalmol Vis Sci 52: 45–50.
48. Wheatley HM, Traboulsi EI, Flowers BE, Maumenee IH, Azar D, et al. (1995) Immunohistochemical localization of fibrillin in human ocular tissues: Relevance to the Marfan syndrome. Arch Ophthalmol 113: 103–109.
49. Kuchtey J, Kuchtey RW (2014) The microfibril hypothesis of glaucoma: Implications for treatment of elevated intraocular pressure. Journal of Ocular Pharmacology and Therapeutics 30: 170–180.
50. Morales J, Al-Sharif L, Khalil DS, Shinwari J, Bavi P, et al. (2009) Homozygous mutations in *ADAMTS10* and *ADAMTS17* cause lenticular myopia, ectopia lentis, glaucoma, spherophakia, and short stature. The American Journal of Human Genetics 85: 558–568.
51. Faivre L, Gorlin RJ, Wirtz MK, Godfrey M, Dagoneau N, et al. (2003) In frame *fibrillin-1* gene deletion in autosomal dominant Weill-Marchesani syndrome. J Med Genet 40: 34–36.
52. Faivre L, Mégarbané A, Alswaid A, Zylberberg L, Aldohayan N, et al. (2002) Homozygosity mapping of a Weill-Marchesani syndrome locus to chromosome 19p13. 3-p13. 2. Hum Genet 110: 366–370.
53. Kulkarni M, Venkataramana V, Sureshkumar C (1995) Weill-Marchesani syndrome. Indian Pediatr 32: 923–923.
54. Gould D, Pettitt L, McLaughlin B, Holmes N, Forman O, et al. (2011) *ADAMTS17* mutation associated with primary lens luxation is widespread among breeds. Vet Ophthalmol 14: 378–384.

Full title: A putative regulatory variant in a spontaneous canine model of retinitis pigmentosa

Short title: Putative regulatory variant in canine retinitis pigmentosa model

Maria Kaukonen[1,2,3], Ileana B. Quintero[1,2,3], Abdul Kadir Mukarram[4], Marjo K. Hytönen[1,2,3], Saila Holopainen[1,2,3,5], Kaisa Wickström[6], Kaisa Kyöstilä[1,2,3], Meharji Arumilli[1,2,3], Sari Jalomäki[7], Carsten O. Daub[4,8], Juha Kere[3,4,9], DoGA consortium, Hannes Lohi[1,2,3,*]

[1]Department of Veterinary Biosciences, University of Helsinki, 00014 Helsinki, Finland
[2]Department of Medical and Clinical Genetics, University of Helsinki, 00014 Helsinki, Finland
[3]Folkhälsan Research Center, 00290 Helsinki, Finland
[4]Department of Biosciences and Nutrition, Karolinska Institutet, Huddinge, Sweden
[5]Department of Equine and Small Animal Medicine, University of Helsinki, Helsinki, Finland
[6]Veterinary Clinic Kamu, 90100 Oulu, Finland
[7]Veterinary Clinic Malmin Eläinklinikka Apex, 00700 Helsinki, Finland
[8]Science for Life Laboratory, Karolinska Institutet, Stockholm, Sweden
[9]Stem Cells and Metabolism Research Program STEMM, University of Helsinki, 00014 Helsinki, Finland
[*]Corresponding author
E-mail: hannes.lohi@helsinki.fi, +358 2 941 25085

Abstract

Retinitis pigmentosa (RP) is the leading cause of blindness with nearly two million people affected worldwide. Many genes have been implicated in RP, yet in 30–80% of the RP patients the genetic cause remains unknown. A similar phenotype, progressive retinal atrophy (PRA), affects many dog breeds including the Miniature Schnauzer. We performed clinical, genetic and functional experiments to identify the genetic cause of PRA in the breed. The age of onset and pattern of disease progression suggested that at least two forms of PRA, types 1 and 2 respectively, affect the breed, which was confirmed by genome-wide association study that implicated two distinct genomic loci in chromosomes 15 and X, respectively. Whole-genome sequencing revealed a fully segregating recessive regulatory variant in type 1 PRA. The associated variant has a very recent origin based on haplotype analysis and lies within a regulatory site with the predicted binding site of HAND1::TCF3 transcription factor complex. Luciferase assays suggested that mutated regulatory sequence increases expression. Case-control retinal expression comparison of six best HAND1::TCF3 target genes were analyzed with quantitative reverse-transcriptase PCR assay and indicated overexpression of *EDN2* and *COL9A2* in the affected retina. These results suggested that the regulatory variant disrupts a silencer site but needs to be confirmed in a larger sample set. Defects in both *EDN2* and *COL9A2* have been previously associated with retinal degeneration. In summary, our study describes two genetically different forms of PRA and identifies a fully penetrant variant in type 1 form with a possible regulatory effect. This would be among the first reports of a regulatory variant in retinal degeneration in any species, and establishes a new spontaneous dog model to improve our understanding of retinal biology and gene regulation while the affected breed will benefit from genetic testing.

Author summary

Retinitis pigmentosa (RP) is a blinding eye disease that affects nearly two million people worldwide. Several genes and variants have been associated with the disease, but still 30–80 % of the patients

lack genetic diagnosis. There is currently no standard treatment for RP, and much is expected from gene therapy. A similar disease, called progressive retinal atrophy (PRA), affects many dog breeds. We performed clinical, genetic and functional analyses to find the genetic cause for PRA in Miniature Schnauzers. We discovered two forms of PRA in the breed, named type 1 and 2, and show that they are genetically distinct as they map to different chromosomes, 15 and X, respectively. Further genetic, bioinformatic and functional analyses discovered a fully penetrant recessive variant in a putative silencer region for type 1 PRA. Silencer regions are important for gene regulation and we found that two of its predicted target genes, *EDN2* and *COL9A2*, were overexpressed in the retina of the affected dog. Defects in both *EDN2* and *COL9A2* have been associated with retinal degeneration. This study provides new insights to retinal biology while the genetic test guides better breeding choices.

Introduction

Retinitis pigmentosa (RP) is a heterogeneous group of inherited retinopathies with varying genetic background and highly variable clinical consequences. RP is the leading cause of irreversible blindness in man with a worldwide prevalence of one in 4,000 people [1]. The disease first manifests as impaired vision in dim light (nyctalopia) resulting from progressive loss of the rod photoreceptor cells. As the disease progresses, complete blindness is expected due to cone photoreceptor degeneration accompanied by changes in the retinal pigment epithelium (RPE), the retinal vasculature, the glial cells and neurons of the inner retina. To date, 67 genes and loci have been implicated to nonsyndromic RP according to the Retinal Information Network RetNet (http://sph.uth.edu/retnet/) [2]. In the majority of cases, the mode of inheritance is autosomal recessive, although some autosomal dominant and X-linked RP exist [2]. Despite a large number of implicated genes and variants, 30–80% of the patients have RP of unknown genetic cause and thus many genes remain still to be discovered [3].

RP is incurable at the moment and much is expected from gene therapy to treat this disease. Different eye diseases have been favorite targets of gene therapy for several reasons, including relatively easy access to treat and monitor the target organ. A recent study described patient derived induced pluripotent stem cell (iPSC) treatment with clustered regularly interspersed short palindromic repeats (CRISPR/Cas9) to treat a RP affected patient with an X-linked point mutation in the *retinitis pigmentosa GTPase regulator (RPGR*) gene [4] in addition to other attempts to treat retinal dystrophies. As a known genetic cause of disease is obligatory to any gene therapy and still many RP related genes remain unknown, continuous attempts are needed to discover new causative variants and understand the underlying biology.

The domestic dog (*Canis familiaris*) has emerged as a powerful model to study human inherited diseases as its unique genetic architecture facilitates gene discoveries and many inherited diseases occur spontaneously in different breeds [5]. More than 220 genes have been implicated in various conditions over the past few years (www.OMIA.org) and the discovery rate is expected to remain high due to higher-resolution approaches and available genomic tools combined with the growing canine DNA biobanks worldwide [6,7]. Importantly, the dog presents an excellent model for human eye diseases, as the canine ocular globe bears more resemblance to the human eye, both anatomically and physiologically, than the eyes of the commonly used model organisms such as the mouse (*Mus musculus*) or the rabbit (*Oryctolagus cuniculus*) [8,9].

A similar phenotype to RP affects many dog breeds and is referred to as progressive retinal atrophy (PRA) [10,11]. Clinical findings in PRA include gradual loss of vision, tapetal hyperreflectivity and attenuation of the retinal blood vessels, which result from the degeneration of the photoreceptor layer in the retina – the pathology has great similarities to RP [10,12]. PRA affects over 100 dog breeds and currently 19 genes and 24 variants in 58 dog breeds have been implicated [13]. As with RP, the majority of the PRA related gene variants are autosomal recessive [13], but one dominant [14] and three X-linked variants [15-18] have been reported as well. In many dog breeds the causative variants have remained unknown, including the Miniature Schnauzers (MSs) in which the clinical findings have been previously described while the genetic background is undefined [19-22]. Recently, a genetic association was reported between a variant in *PPT1,* a well-known candidate gene for neuronal ceroid lipofuscinosis (NCL), and PRA in MS [23]. However, as the reported variant had very low penetrance for a recessive disease (0.79) and as the affected MSs did not present with neurological signs seen in the NCL patients [23], the true causality of the variant remains elusive.

With a series of clinical, genetic, bioinformatic and biochemical experiments, we describe here two genetically different forms of retinal degeneration in the MS breed mapping to chromosomes 15 and X. We identify a novel fully penetrant recessive silencer variant in chromosome 15 with a possible gain-of-function effect resulting in overexpression of two retinal target genes, *EDN2* and *COL9A2*. Our results provide a new spontaneous dog model for retinal pathophysiology and insights to retinal biology and gene regulation. The affected breed will benefit from a genetic test for veterinary diagnostics and breeding advice.

Results

Ophthalmologic examinations reveal two types of retinopathy

To examine the PRA status of the study group of 85 MSs, careful eye examinations were performed with inclusion criteria for cases being bilateral PRA findings with tapetal hypo- and hyperreflectivity, vessel attenuation and pale optic nerve heads. The control dogs were free of any eye diseases at the age of seven years or older. This phenotyping approach resulted in a cohort of 18 cases and 67 controls. The clinical findings categorized the affected dogs to two distinctive groups: 12 dogs were diagnosed with severe PRA findings including total blindness before the age of five years (defined as type 1 in this study) while six of the cases had milder symptoms, slower progression with some visual capacity left at the time of examination and an average age of onset seven years. Of the type 1 affected dogs, five were females and seven males. Of the type 2 cases, only one was female while five were males, suggesting a possible sex-predisposition or X-linked mode of inheritance. Control group included 33 female and 34 male MSs.

To evaluate the photoreceptor degeneration more precisely, OCT imaging was performed to a clinically blind, type 1 PRA case. The imaging showed complete loss of the photoreceptor layer (Fig 1) and thus confirmed the diagnosis. The clinical findings and the age of onset of the type 1 cases closely resemble the results of the previous study [22]. Type 2 dogs were not available for the OCT study.

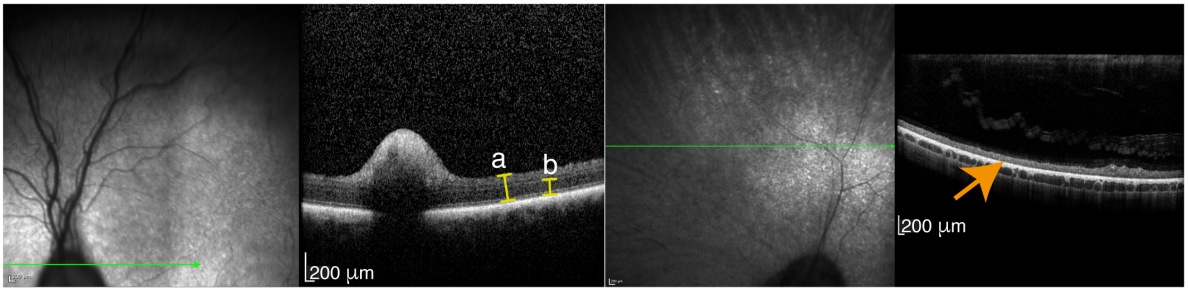

Fig 1. PRA confirmation by optical coherence tomography (OCT). OCT assessment of a healthy control (left hand side) and a four-year-old MS with severe type 1 PRA findings (right hand side). Whole retinal **(a)** and photoreceptor inner and outer segment and outer nuclear layer thickness **(b)** measurement showed total loss of the photoreceptor cell layers in the affected dog (orange arrow).

Genome-wide association study confirms two genetically distinctive types of PRA in MS

A pedigree was drawn around the 18 affected dogs suggesting a recessive mode of inheritance, as affected dogs were born to unaffected parents (Fig 2). To map the disease associated chromosomal region, a genome-wide association study (GWAS) was conducted first with 16 cases (including 10 type 1 and six type 2 cases) and 33 controls. This analysis suggested a PRA locus on the canine chromosome 15 ($p_{raw}=4.70x10^{-6}$, $p_{genome}=0.19$, $\lambda=1$, S1 Fig A). In-depth analysis of the genotypes in the locus showed that all of the type 1 cases shared a homozygous haplotype block of 7.2 Mb from 213,416 bp to 7,403,217 bp that was present neither in the 32 out of 33 control dogs nor in any of the type 2 cases. This result supports the hypothesis of the presence of two genetically distinct types of PRA in the MS breed. Interestingly, the homozygous risk haplotype block was present also in one control dog (S1 Fig B). As all the other control dogs, this one had been eye examined at seven years of age without any clinical signs of PRA, suggesting either incomplete penetrance of the risk haplotype, or that the causative variant is recent and not all the risk haplotype carrying dogs have it.

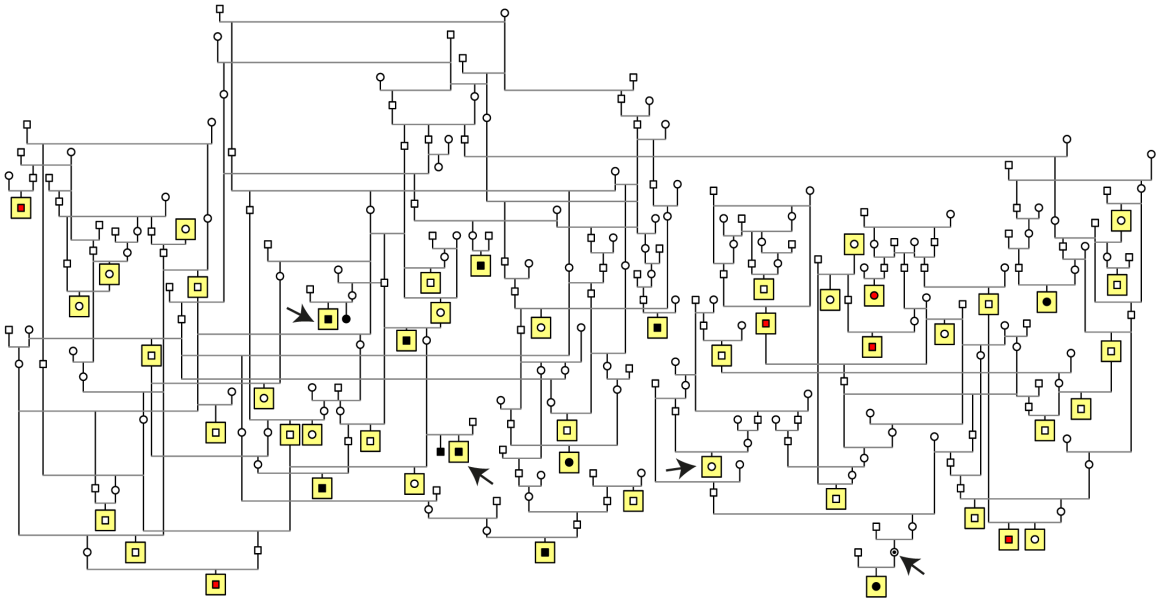

Fig 2. Pedigree of the study cohort. Pedigree analysis suggests a recessive mode of inheritance as affected dogs were born to unaffected parents. Squares indicate males and circles females. Individuals marked with black are type 1 cases, while type 2 cases are marked

with red. Dogs with yellow background were genotyped and included in GWA study. Black arrows mark the whole-genome sequenced dogs.

We then analyzed the genotyping data of the two PRA types separately. When comparing only the type 1 cases (n=10) to the control dogs (n=33), the same CFA15 locus and homozygous haplotype block was associated (Figs 3A and 3B), but with a stronger statistical significance (p_{raw}=2.08x10^{-9}, p_{genome}=2.40x10^{-4}, λ=1.17). In addition, comparison of the type 2 cases (n=6) and controls (n=33) suggested an association to chromosome X (p_{raw}=7.06x10^{-7}, p_{genome}=0.17, λ=1.19), compatible with the suggested X-chromosomal sex pattern. In this locus, three of the six affected dogs shared a homo- or hemizygous haplotype block of 15.4 Mb from 38,294,920 bp to 53,726,107 bp that was absent in the controls and the rest of the type 2 cases (Figs 3C and 3D). As the number of type 2 cases was small, replication of the GWAS result in chromosome X in a larger sample cohort is needed to confirm the locus before further genetic analyses are performed. *RPGR,* the known canine PRA gene in CFAX, is not located in the preliminary locus [15-18].

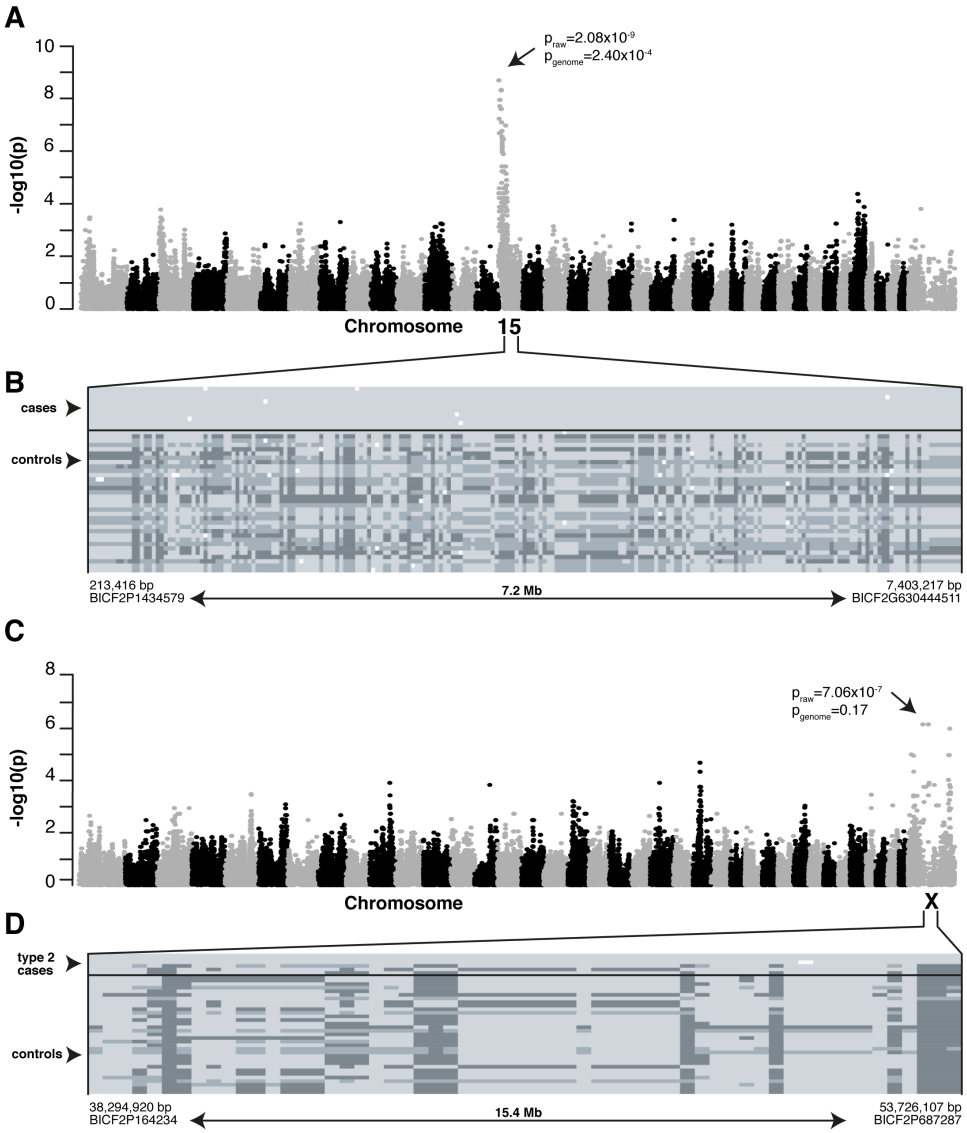

Fig 3. Mapping PRA loci in MSs. (A) Genome-wide comparison of allele frequencies in type 1 cases (n=10) and controls (n=33) indicated a locus on the CFA15 (p_{raw}=2.08x10^{-9}, p_{genome}=2.40x10^{-4}). **(B)** A shared homozygous haplotype block was seen in all the type 1 cases

and one control and absent in 32/33 controls. Each row represents a single animal while genotypes at each SNP (columns) are marked with dark (reference), intermediate (heterozygotes) or light grey (affected haplotype). The critical region of 7.2 Mb spans from 213,416 bp to 7,403,217 bp and upper and lower limits of it were determined by appearance of heterozygous SNPs in the case dogs. **(C)** GWAS in type 2 cases (n=6) and controls (n=33) suggests a locus on CFAX (p_{raw}=7.06x10^{-7}, p_{genome}=0.17). **(D)** A shared homo- or hemizygous haplotype block of 15.4 Mb (spanning nucleotides 38,294,920–53,726,107 bp) is present in 3 out of 6 type 2 cases and absent in the controls and the rest of the type 2 cases.

Whole-genome sequencing reveals four candidate variants

To identify the disease-causing variant in the associated chromosomal region for type 1 PRA in MSs, we performed whole-genome sequencing on three MSs including two type 1 cases with the risk haplotype and one control with opposite haplotype. In total, 467,778,694–512,026,483 reads were collected of which 99.5 % were mapped to the reference sequence. Over 97 % of the reference had >10X coverage while the mean read depths were 29–31. Filtering was done under recessive model, i.e., assuming that the cases were homozygous for the variant and at least 99% of the controls homozygous for the reference allele. The controls included one MS described above and 267 dogs of various breeds and without the studied phenotype (S1 Table). Of the controls, 141 were whole-genome sequenced and available also for a mobile element insertion (MEI) analysis, while 127 where exome-sequenced and therefore available only for analyzing single nucleotide variants and small insertions and deletions.

The two type 1 cases shared 2,149,016 common homozygous variants. After filtering against control dogs, 5,235 variants were left, of which 233 resided in the CFA15 locus (S2 Table). Of these, two were located in exons and two in splice sites (Table 1). These four variants were validated in the study cohort of 18 cases, including 12 type 1 PRA cases, and 67 control MSs. All the type 1 cases were homozygous for all the four variants, indicating association between the variants and the phenotype. However, there were also controls homozygous for the variants (n=4 for the variant in *DLGAP3* and 2 for the other three variants), indicating either incomplete penetrance or that none of these variants are truly causative. We screened also the recently published variant in *PPT1* [23] in the cohort, although it was not caught by filtering. All type 1 cases were homozygous for the variant, while five type 2 cases were wild-type and one heterozygous. Of the 67 control dogs, 41 were wild-type, 22 heterozygous and four homozygous, accounting for an association between the type 1 disease and the *PPT1* variant (p=1.6x10^{-13}). However, this association was 10 to 100 times weaker than that with the other four variants in the same cohort (Table 1). MEI analysis revealed altogether 12 shared homozygous variants in the two cases in the locus, but none of them proved case-specific after filtering. No case-specific large structural variants were detected when analyzing the locus with IGV.

Table 1. Coding or splicing variants resulting from filtering the whole-genome sequencing data did not segregate with the phenotype.

Position (bp)[a]	Ref. allele	Alt. allele	Gene	Variant type	Variant (protein)	Transcript	p-value[b]
603,169	T	C	*C15H1orf50*	nonsynonymous SNV	p.M1V	XM_539558.4	2.1x10^-15
603,940	G	C	*P3H1*	splicing (c.477+13G=C)	-	XM_843477.4	2.1x10^-15
2,064,277	C	T	*SLFNL1*	splicing (c.852+7C=T)	-	XM_022427740.1	2.1x10^-15

7,077,805	CACCAC	del	*DLGAP3*	nonframeshift deletion	p.227_228del	XM_014119248.2	7.0x10^-14

[a]Coordinates refer to the CanFam 3.1 annotation.
[b]Association of the variant with type 1 PRA in initial study cohort of 85 MSs

Sequencing an obligate carrier reveals a fully segregating regulatory variant

The whole-genome sequencing results together with the fact that one of the control dogs in GWAS carried also the homozygous risk haplotype suggested that the causative variant for type 1 PRA in MSs is recent and not all the risk haplotype carrying dogs have it. To test this hypothesis, we performed whole-genome sequencing to an additional control MS, which was homozygous for all the four previously validated variants, but was unaffected still at the age of 10 years. In addition, this dog had a type 1 PRA affected offspring and thus was an obligate carrier for the causative variant (Fig 2). Altogether 456,191,937 reads were collected of which 99.3% were mapped to the reference sequence. Over 97% of the reference had >10X coverage and the mean read depth was 28. Filtering was performed as described above but by defining this sample as an obligate carrier. This approach reduced the case-specific variant list to five candidates including one intronic and four intergenic variants (Table 2). Three of the five variants appeared to be miscalled during validation by Sanger sequencing and IGV visualization. The two variants left, an intergenic 5-bp deletion (g.1,887,878_1,887,882del) and an intronic SNV (g.1,432,293G>A) in the transcription factor encoding the ortholog of *human immunodeficiency virus type I enhancer binding protein 3* gene (*HIVEP3*, Figs 4A and 4B) were validated in the study cohort of 18 cases and 67 controls. Again, all type 1 cases were homozygous for both of the variants. The intergenic 5-bp deletion was found to be homozygous in 12 of the 67 control dogs, thus excluding it from further analysis. The variant in *HIVEP3*, however, indicated complete penetrance as out of the 67 controls, 58 were wild-type, nine heterozygous and none homozygous. Thus, this variant segregated completely with the disease and the association with the type 1 phenotype was more than 10 billion times stronger than any other variants in the region ($p=4.0x10^{-25}$).

Table 2. Applying an obligate carrier to filtering decreased the number of variants to five, of which the intronic variant in *HIVEP3*/*ENSCAFG00000035604* had complete penetrance and strong association with the type 1 PRA in MSs.

Position (bp)[a]	Ref. allele	Alt. allele	Variant type	Gene
223,405	C	del	intergenic*	*ENSCAFG00000039839–ENSCAFG00000002484*
405,398	A	C	intergenic*	*ENSCAFG00000002491–ENSCAFG00000040650*
1,432,293	G	A	intronic	*HIVEP3, ENSCAFG00000035604*
1,887,878	AAAAT	del	intergenic	*ENSCAFG00000038329–SCMH1*
3,716,531	TTTCTT	del	intergenic*	*MACF1–NDUFS5*

[a]Coordinates refer to the CanFam 3.1 annotation.
*Miscalled, excluded by Sanger sequencing and IGV.

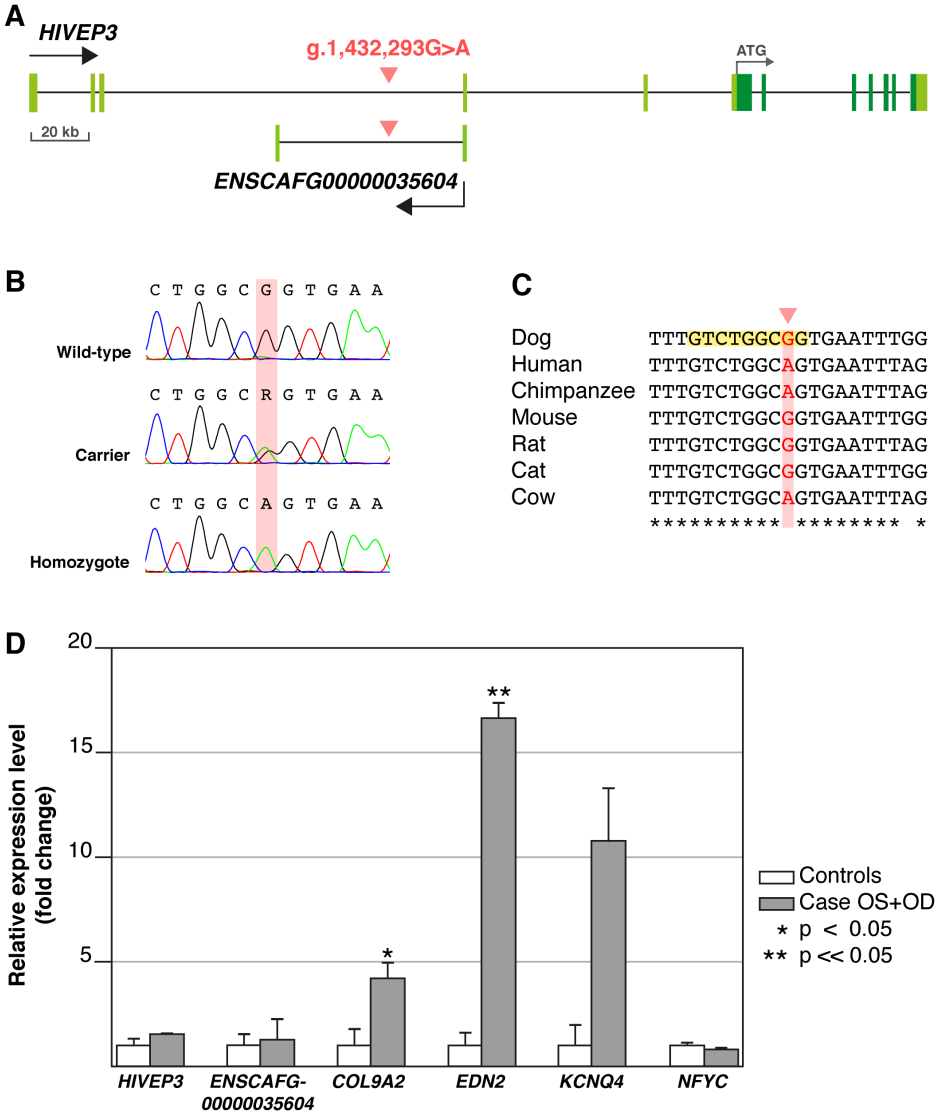

Fig 4. Schematic representation of the variant (g.1,432,293G>A) site and RT-qPCR results of HAND1::TCF3 target genes. **(A)** The *HIVEP3* and *ENSCAFG00000035604* gene structures with coding regions indicated in dark and non-coding in light green. The intronic variant (red) is located kilobases away of the exon-intron boundaries in both genes. **(B)** Sanger chromatograms showing the DNA sequence in wild-type, carrier and homozygous dogs with the mutated nucleotide marked with red background. **(C)** Alignment of different mammalian species showed that the sequence surrounding the variant site is highly conserved, but the variant nucleotide itself (highlighted in red) is not. JASPAR motif scanning indicated that TFBS of HAND1::TCF3 overlaps exactly the variant site (highlighted in yellow). **(D)** RT-qPCR of retinal samples from a type 1 affected MS and four control retinal samples wild-type for the variant and without the studied phenotype showed case-specific over-expression of *EDN2* and *COL9A2*. The comparative $\Delta\Delta C^T$ method was used to determine relative expression [24] and error bars are determined as standard deviation of the mean ΔC^T.

HIVEP3 has been reported to be expressed ubiquitously, including the human retina, but it has not been implicated to retinal disease in any species [25]. The canine *HIVEP3* (XM_003431951.4) spans from 1,302,964 to 1,626,834 bp and includes 12 exons with protein coding sequence in exons 6–12

(Fig 4A). The associated variant in *HIVEP3* is located in the third intron: 105,943 bp downstream to the third and 32,572 bp upstream to the fourth untranslated exon. The surrounding sequence is ultraconserved (Figs 4B and 4C). There is also a predicted dog-specific long non-coding RNA (lncRNA) *ENSCAF00000035604* at the variant locus (Fig 4). This lncRNA is antisense to *HIVEP3* and consists of two exons and an intron. The variant is located 32,566 bp downstream of the first and 42,855 bp upstream to the second exon.

To further validate the intronic variant in *HIVEP3* in the MS breed, we genotyped all the available MS samples (n=514) from our dog DNA bank, including three additional PRA cases and 118 dogs that were examined to have healthy eyes at the age of five or older. Of these, 456 (88.7%) were wild-type, 55 (10.7%) heterozygous and three (0.58%) homozygous for the variant. The identified three homozygotes were the PRA cases in the breed screening cohort and were clinically identical to type 1 cases as described above. These results in the breed screening cohort indicate again a complete penetrance of the intronic variant in *HIVEP3* and strong association with the type 1 phenotype ($p=8.7x10^{-13}$). Combining the results of the initial study cohort and the breed screening cohort resulted in a very strong association ($p=1.1x10^{-42}$) with the type 1 phenotype and was the only one of the validated variants with complete penetrance. The variant was not found from 735 genomes of different breeds available through The Dog Biomedical Variant Database Consortium dataset, which agrees with our hypothesis of a recent variant. No variants in the corresponding position in the human genome have been reported in the Genome Aggregation Database gnomAD [26].

Associated variant is located within a putative silencer with HAND1::TCF3 transcription factor binding motif

The sequence surrounding the variant site is ultraconserved (Fig 4C), suggesting functional importance. The possible effect of the intronic variant on the splicing of the *HIVEP3* and lncRNA *ENSCAFG00000035604* transcripts was investigated by Sanger sequencing the retinal cDNAs from a case dog homozygous for the variant, but indicated no changes compared to the wild-type transcript and thus ruled out splicing defects.

To further explore the functional significance of the associated variant, the syntenic site in the human genome was investigated, revealing that the variant is located in a peak of ENCODE DNaseI hypersensitivity cluster, which indicates an open chromatin environment and a possible regulatory site [27]. To gather further evidence, we next explored the JASPAR database to search for transcription factor binding sites (TFBSs) that could bind the sequence in the variant site. This search resulted in the discovery of a putative HAND1::TCF3 complex TFBS, overlapping exactly the variant location (Fig 4C).

The possible regulatory function was studied by performing a dual luciferase reporter assay in MDCK cells transfected with wild-type, mutant, or empty vector constructs (S3 Table). The wild-type and mutant constructs contained 250 bp of upstream and downstream sequences from the variant site. Relative luciferase activity was significantly lower in cell lines transfected with the wild-type than with the empty vectors ($p<0.05$), thus indicating silencer activity in the variant site. The PRA associated variant seems to disrupt the silencer activity as cells transfected with the mutant constructs showed significantly higher reporter gene expression compared to the wild-type constructs ($p<0.05$).

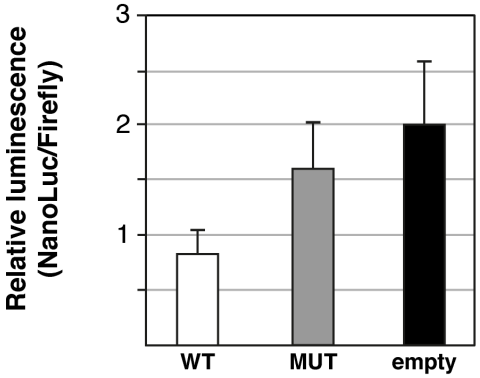

Fig 5. Reporter assay indicates the variant site might be a silencer. Dual luciferase assay with MDCK cells transfected with wild-type (WT), mutant (MT) and empty vectors indicated robust reduction in relative luciferase activity when comparing the wild-type constructs to empty vector, supporting the putative silencer activity ($p<0.05$). Relative luciferase activity was significantly increased in mutant versus wild-type constructs ($p<0.05$), indicating the type 1 PRA associated variant disrupts the putative silencer activity, but might not prevent it completely.

Retinal overexpression of *EDN2* and *COL9A2* in the affected dog

We next investigated whether the silencer variant has any effect on the expression of its target genes. Quantitative reverse-transcriptase PCR (RT-qPCR) with retinal samples from a type 1 PRA case and four unaffected dogs (wild-types for the variant) was performed for a selected set of target genes. As silencers can act from a distance, the presence of the HAND1::TCF3 motif was screened in the promoters of the flanking genes +/- 1.25 Mb from the variant site. Altogether 714 predicted HAND1::TCF3 binding sites were found in the promoter regions in 60 genes (S4 Table). Due to limited amount of available case-specific retinal RNA, six candidate genes were prioritized, including *HIVEP3, lncRNA (ENSCAFG00000035604), COL9A2, EDN2, KCNQ4* and *NFYC*. Prioritization was based on the motif scanning score, known expression in retinal tissues in FANTOM5, Human Protein Atlas data [28,29] and retinal expression data from our STRT sequencing data from five dogs (S2 Fig). The RT-qPCR results indicated that retinal expression of *EDN2* was increased by over 16-fold ($p=0.0023$) and *COL9A2* by over 4-fold ($p=0.049$). Retinal expression of *KCNQ4* was increased by over 10-fold in the case retina, but the change was not statistically significant ($p=0.065$), because of the large differences between retinal samples of the right and left eyes of the affected MS. Retinal *NFYC* expression was also not significantly changed ($p>0.05$).

Discussion

RP is the leading cause of blindness in humans and nearly 70 genes have been implicated in various forms of the disease. However, the genetic origin remains still elusive in many cases [3]. We report here clinical and genetic characterization of a canine RP model (PRA), which provides new insights into the accumulating evidence of regulatory variants in the development of retinal disease.

The key findings of the study have several scientific and medical implications. We demonstrate the presence of at least two clinically and genetically different forms of PRA in the MS breed. The type 1 PRA with a homogeneous onset at 4 years of age mapped to chromosome 15, while the type 2 PRA, with an overrepresentation of affected males and a wider range of age of onset, mapped to chromosome X. While the tentative association in chromosome X needs to be replicated with

additional cases, the association of the type 1 PRA in chromosome 15 was very strong. The origin of the causative variant was suspected to be very recent, since the homozygous risk haplotype was also present in unaffected dogs. Sequence analyses in the 7.2-Mb critical region associated with the type 1 PRA revealed a number of possibly pathogenic coding variants, however, all of them had incomplete penetrance (~80%). The incomplete penetrance of the many coding variants was consistent with the suspected recent origin of the actual causative variant. Indeed, the only fully penetrant variant resided in a conserved sequence within *HIVEP3* and a lncRNA gene, in the predicted binding site of the HAND1::TCF3 TF complex, suggesting a regulatory variant. The silencer function was supported *in vitro* with an increased transcriptional activity of the reporter gene in the mutant recombinant. Finally, given the role of silencers in transcriptional activation, six most promising retinal HAND1::TCF3 target genes within 1.25 Mb distance up- or downstream from the variant site were prioritized for the quantitative measurement of transcripts. Expectedly, overexpression of *EDN2* and *COL9A2* was found in the affected retina, suggesting a gain-of-function variant. Further studies with larger sample sets are needed to confirm the functional aspects of the variant. In addition, to formally confirm the silencer role and the binding repressor(s), chromatin immunoprecipitation and EMSA gel shift assays are required.

Recently, a complex structural variant in *PPT1* was proposed to cause PRA in MS [23]. This study, using lower resolution genotyping array, found a suggestive GWAS signal on the CFA15 with a ~5Mb critical interval that some, but not all, cases shared. Whole-genome sequencing approach identified the same intronic *HIVEP3* variant described here, but its potential functional properties were not studied and the focus was turned to the complex structural variant in *PPT1* as it was homozygous in some of the affected dogs that were wild-type or heterozygous for the *HIVEP3* variant. Additional screening found also some of the controls to be homozygous for the *PPT1* variant, accounting for a penetrance of 79% [23]. In contrast, our data shows that the breed is affected with multiple genetically distinct forms of PRA and that the causative variant has such a recent origin that not all risk haplotype-carrying dogs have it. This leads to the identification of many candidate variants in the critical interval that seem to, misleadingly, associate with the phenotype, but have incomplete penetrance. In contrast, in our cohort, the predicted silencer variant located in the *HIVEP3* intron, has complete penetrance and 10 billion times stronger association with the type 1 PRA.

To our knowledge, this is only the second report of a potential regulatory RP variant in any species and provides an important spontaneous model to understand retinal gene regulation and the causes of RP. Previously, recessive non-coding retina-specific cis-regulatory variants in the CRX-binding regions of SAMD7 have been suggested in human patients with atypical RP [30]. Our risk variant is located in the intron of *HIVEP3* transcription factor and a lncRNA *ENSCAFG00000035604*, however, kilobases away from any predicted splice sites. Interestingly, expression of neither *HIVEP3* nor lncRNA (*ENSCAFG00000035604*) was significantly changed in the affected retina. Instead, two more distant proposed target genes, the *EDN2* and *COL9A2*, were upregulated. Although our conclusions about the disease mechanisms are limited because of access to only one set of affected retinas from an 11-years-old type 1 affected MS, and should be therefore interpreted very cautiously, some discussion about the two target genes is warranted. *EDN2* encodes endothelin-2, which has been implicated in various cellular functions such as angiogenesis, cell migration, cell proliferation, and endothelial activation [31-35]. Overexpression of *Edn2* in the mouse retina inhibits retinal vascular development [36], which might also explain the etiology of the disease in MS type 1 cases as attenuation of retinal vessels is a hallmark feature in canine PRA [10] and was also observed in the cases here. However, *EDN2* overexpression might also function as a general stress signal from

photoreceptor damage, and therefore it cannot be distinguished here, whether the observed overexpression of *EDN2* reflects the primary etiology of the retinal degeneration in type 1 PRA or the secondary stress reaction to the photoreceptor damage [31,37]. A loss-of-function variant in COL9A2 has been associated to autosomal recessive Stickler syndrome, in which vitreoretinal degeneration is one of the symptoms together with other ocular, auditory, skeletal and orofacial abnormalities [38]. To our knowledge, the affected MSs manifested only retinal phenotype, however, upregulation of *COL9A2* could result in a more limited phenotype compared to the loss-of-function variant phenotype. Overall, the role of upregulated *EDN2* and *COL9A2*, and possible other retinal target genes in the type 1 PRA locus including *HIVEP3*, requires additional retinal samples from the affected dogs for further conclusions.

To summarize, we have identified two forms of retinal degeneration in a dog breed and showed that these phenotypes are distinct both clinically and genetically. We mapped two new loci and identified a type 1 disease-specific recessive variant in a putative silencer located in predicted HAND1::TCF3 TFBS with two of its target genes overexpressed in the affected retina sample. These results establish the MS dog breed as a spontaneous large animal model to study human RP and provide a new potential regulatory variant to understand the retina in health and disease. For veterinary medicine, a gene test has been developed to aid diagnostic and breeding programs. This is important since the earlier description of the *PPT1* variant in the breed is not fully penetrant, as opposed to our variant, and its current diagnostic use leads to confusing results to the breeders.

Materials and methods

Ethics statement

All dogs used in this study were privately owned pet dogs. EDTA blood samples (3 ml) from all the dogs and tissue samples from six dogs (euthanized because of severe diseases, described in detail below) donated to research were collected under the permission of animal ethical committee of County Administrative Board of Southern Finland (ESAVI/343/04.10.07/2016) and all experiments were performed in accordance with relevant guidelines and regulations and with owners' written consent.

Study cohort

This study included altogether 599 privately owned purebred MSs, including a discovery cohort of 85 dogs and a population screening cohort of 514 dogs. The discovery cohort included 18 cases and 67 control dogs, which all were eye examined by veterinary ophthalmologists board-certified by the European College of veterinary ophthalmologists. The eye examination included basic neuro-ophthalmic examination, slit-lamp biomicroscopy to evaluate the adnexa and anterior segment and indirect ophthalmoscopy to examine the posterior parts of the eye. Topical tropicamide (Oftan Tropicamid 1%, Santen, Tampere, Finland) was used to achieve mydriasis. Optical coherence tomography, OCT, (Heidelberg's Spectralis, Heidelberg Engineering GmbH, Heidelberg, Germany) was performed to one PRA affected MS. Inclusion criteria for cases were bilateral severe PRA findings. Controls did not show any symptoms of eye disease and were minimum of seven years old at the time of the examination. Population based variant screening was performed in 514 MSs of which three were affected with type 1 PRA and 118 were eye examined healthy at the age five or older by veterinary ophthalmologists as described above. EDTA blood samples (3 ml) from all the dogs and tissue samples from six euthanized dogs donated to research were collected under the permission of animal ethical committee of County Administrative Board of Southern Finland (ESAVI/343/04.10.07/2016) and all experiments were performed in accordance with relevant

guidelines and regulations. Genomic DNA was extracted from the white blood cells using a semi-automated Chemagen extraction robot (PerkinElmer Chemagen Technologie GmbH, Baeswieler, Germany) according to the manufacturer's instructions. DNA concentrations were measured using Qubit fluorometer (Thermo Fisher Scientific, Waltham, Massachusetts, USA) and Nanodrop ND-1000 UV/Vis Spectrophotometer (Nanodrop technologies, Wilmington, Delaware, USA) and samples were stored at –20 °C.

Genome-wide association study

A genome-wide association study, GWAS, was performed using Illumina's CanineHD BeadChip arrays with 172,963 markers (San Diego, CA, USA). Genotyping was performed in GeneSeek Laboratory (Neogen Genomics, Lincoln, NE, USA) to 16 cases and 33 controls. After quality control procedures, only SNPs which conformed to Hardy-Weinberg expectations P<0.0001, had >95% genotyping rate and minor allele frequency of >5 % were included in the analysis, resulting in the total number of 102,661 SNPs when analyzing all the cases and controls and 100,501 and 102,286 when comparing separately the type 1 cases and type 2 cases to controls, respectively. The differences in allele frequency between cases and controls were calculated using the PLINK 1.07 software [39]. Corrected empirical p-values were calculated with 100,000 permutations and genomic control adjusted significance values based on the estimation of the inflation factor.

Whole-genome sequencing

Whole genome sequencing was performed to two cases and two controls using the Illumina HiSeq X ultra-high-throughput sequencing platform with 30X target coverage (paired-end reads, 2x 150 bp) (Novogene Bioinformatics Institute, Beijing, China). Mapping the reads to the dog reference genome (assembly CanFam 3.1) was performed using the Burrows-Wheeler Aligner (BWA) version 0.7.15 [40]. The reads were sorted and duplicate reads marked using the Picard tools (http://sourceforge.net/projects/picard). Post-alignment processing includes local realignment around known INDELs and base quality scores recalibration to reduce erroneous variant calls [41]. Variant calling was done using the HaplotypeCaller in Genome Analysis Tool Kit GATK version 3.7. Functional annotation of the variants was done in ANNOVAR using Ensembl, NCBI and Broad gene databases. Mobile element insertions were detected in the three whole-genome sequenced samples using the Mobile Element Locator Tool (MELT) [42]. The reference sequences of the transposons for MEI discovery were retrieved from Repbase database [43]. The detected variants were stored in Genotype Query Tools (GQT) [44] variant database and variant filtering was performed using our in-house pipeline assuming recessive mode of inheritance, i.e. the cases were homozygous for the alternative alleles. The variant data from whole-exome (n=127) and whole-genome sequenced (n=140) dogs without the studied phenotype and from various breeds were used in filtering as controls (S1 Table). A maximum of 1 % of the controls were allowed to be heterozygotes of the alternative allele, while the rest were set to be homozygous for the reference allele.

Sanger sequencing and TaqMan genotyping

Sanger sequencing was utilized to perform segregation analyses for the variants found in filtering the whole-genome sequencing data. Segregation analysis of the *PPT1* structural variant was performed utilizing the consecutive markers (g.2,872,023_2,872,024del and g.2,872,103G>A) confirmed to be consistent with the actual complex structural variant in the original study [23] and which was also validated in our whole-genome sequenced MS samples. All other variants were directly sequenced. Primers (S5 Table) were designed using the Primer3 program [45] and PCR

products amplified using Biotools DNA Polymerase (Biotools B&M Labs, S.A., Valle de Tobalina, Madrid, Spain). The PCR products were treated with exonuclease I and shrimp alkaline phosphatase and capillary sequenced in the Institute for Molecular Medicine Finland (Helsinki, Finland). The Sanger sequence data were analyzed using Sequencher 5.1 (Gene Codes Corporation, Ann Arbor, MI, USA) and Unipro UGENE 1.31.1 (UniPro, Novosibirsk, Russia). Variant screening in the MS breed cohort with 514 dogs was performed using Custom TaqMan SNP Genotyping Assay (S5 Table) chemistry (ThermoFisher Scientific, Waltham, MA, USA) and CFX96 Touch Real-Time PCR Detection System (BioRad, Hercules, CA, USA).

***In-silico* analysis of transcription factor binding sites and target gene prioritization**

The UCSC liftOver tool was utilized to convert the corresponding variant site in the human genome version GRCh38. The overlapping TFBS motif (HAND1::TCF3) was obtained from the JASPAR database [46]. Motif scanning was done using "searchSeq" function of TFBSTools package (v.1.20) under R programming language [47] on the +/-500 bp regions surrounding the TSSs of CanFam3.1 Ensembl genes version 94 [48]. Target gene prioritization was performed based on motif scanning score and confirming retinal expression in canine STRT sequencing data and in the FANTOM5 [28] and the Human Protein Atlas [29] databases. STRT RNA-sequencing was performed to retinal samples collected from five dogs: a 3-year-old female Swedish Elkhound, 5- and 6-year-old male Rottweilers, a 6-year-old female Finnish Lapphund and a 6-year-old male Border Collie that were all wild-type for the type 1 PRA associated variant and without the studied phenotype. The dogs were privately owned pets. The Swedish Elkhound and the Border Collie were euthanized because of epilepsy, the Rottweilers due to gastrointestinal disease and the Finnish Lapphund due to intervertebral hernia. Samples were collected within 15 minutes after death and treated with Invitrogen RNAlater Stabilization Solution (Thermo Fisher Scientific, Waltham, Massachusetts, USA) for 24 hours and stored in –80 °C. RNA was extracted using the RNeasy Mini Kit (Qiagen, Venlo, Netherlands) according to manufacturer's instructions. Integrity of RNA was evaluated with Agilent 2100 Bioanalyzer (Agilent Technologies, Santa Clara, California, USA) and concentration measured with Qubit fluorometer (Thermo Fisher Scientific, Waltham, Massachusetts, USA) and Nanodrop ND-1000 UV/Vis Spectrophotometer (Nanodrop technologies, Wilmington, Delaware, USA). 20 ng of RNA was used for multiplex 48 sample RNA-seq libraries, which were prepared using modified STRT method with unique molecular identifiers [49,50]. The modifications included longer UMI's of 8 bp, addition of spike-in ERCC control RNA for normalization of expression, and use of Globin lock method [51] with LNA-primers for canine alpha- and betaglobin genes. The libraries were sequenced with Illumina NextSeq 500, High Output (75 cycles). Reads were mapped to CanFam3.1 genome annotation using HISAT1 mapper version 2.1.0 [52]. Gene level quantification was done using featureCounts version 1.6.2 [53] and the counts were then normalized to the library size and transcript length. The expression levels of 60 flanking genes (Table S4) was then visualized using the ComplexHeatmap package [54].

Dual luciferase reporter assay

To verify the predicted silencer role and to study whether the found variant has an effect on its function, constructs containing the wild-type and mutated canine sequence (CanFam 3.1, 250 bp +/- of the variant site) were generated (S3 Table) and cloned into the pNL3.2[*NlucP*/minP] NanoLuc luciferase vector (Promega, Madison, WI, US). The pGL4.54[luc2/TK] firefly luciferase was used as a co-transfection control vector (Promega, Madison, WI, US). For transfection assay, 3 x 10^5 MDCK cells were seeded per well in 96 well cell culture microplate with white walls (CellStar, Greiner bio-one, Germany) 24h prior to transfection, using Gibco Advanced MEM medium (Thermo Fisher

Scientific, Waltham, Massachusetts, USA) supplemented with 10% FBS, 100 U penicillin/streptomycin and Glutamax. Cell transfection was performed using Lipofectamine3000 (Invitrogen, Carlsbad, US) according to manufacturer instructions. The co-transfection was performed using 10 ng wild-type, mutated or empty experimental vector, 10 ng control vector and 90 ng carrier DNA per well. Luciferase activities were measured after 48 h using the Nano-Glo® Dual-Luciferase® Reporter Assay System (Promega, Madison, WI, US) according to the manufacturer's instructions and luminescence was detected using the Enspire 2300 instrument (PerkinElmer Chemagen Technologie GmbH, Baeswieler, Germany). Luminescence values were normalized by calculating the ratio between experimental (NanoLuc) and control (firefly) reporter. Statistical significance of the results was assessed by one-way ANOVA and Bonferroni approach as post-hoc test and p-value < 0.05 was considered significant. The assays were performed twice with 4 to 6 replicates per treatment.

Retinal target gene expression analysis

Retinal samples from both eyes were collected from a 11-year old male MS affected with type 1 PRA and homozygous for the intronic variant in *HIVEP3*. Control retinal samples were collected from a 2-year-old female German Pinscher, a 3-year-old female East-European Shepherd, a 5-year old male Smooth Collie and a 5-year-old male Rottweiler that were all wild-type for the variant and without the studied phenotype. The dogs were privately owned pets. The MS was euthanized because of congestive heart failure, the Rottweiler due to inflammatory bowel disease and the German Pinscher, Smooth Collie and the East-European Shepherd due to behavioral problems. Samples were collected and treated as were the ones used for the STRT experiment described above. Reverse transcription from RNA to cDNA was performed to equal amounts of sample RNA with High Capacity RNA-to-cDNA Kit (Applied Biosystems, Waltham, Massachusetts, USA). Primer3 program [45] was used to design the primers (S4 Table) for the six target genes (*HIVEP3, ENSCAFG00000035604, COL9A2, EDN2, KCNQ4, NFYC*) and the two house-keeping genes (*GAPDH* and *YWHAZ*), that were used as normalization controls. Forward and reverse primers were positioned in different exons to avoid genomic DNA contamination. Primer efficiencies were determined from a seven-point dilution series and the comparative $\Delta\Delta C^T$ method was used to determine relative expression [24]. Real-time quantitative PCR (RT-qPCR) was performed with SsoAdvanced Universal SYBR Green Supermix (BioRad Hercules, CA, USA) and the CFX96 Touch Real-Time PCR Detection System (BioRad, Hercules, CA, USA) according to manufacturer's instructions. Three technical replicates were used for all reactions. Error bars were determined as standard deviation of the mean ΔC^T.

Acknowledgements

We thank all the referring veterinarians, dog owners and breeders for sending canine samples. Seppo Lemberg and the Department of Eye Diseases, Helsinki University Hospital, Hospital District of Helsinki and Uusimaa is thanked for OCT imaging. Institute for Molecular Medicine Finland (FIMM) is thanked for Sanger sequencing core facilities, Biomedicum Functional Genomics Unit (FuGU), University of Helsinki, for STRT library sequencing services and the CSC for computational support in whole-genome sequencing analyses. The Dog Biomedical Variant Database Consortium (Gus Aguirre, Catherine André, Danika Bannasch, Doreen Becker, Brian Davis, Cord Drögemüller, Kari Ekenstedt, Kiterie Faller, Oliver Forman, Steve Friedenberg, Eva Furrow, Urs Giger, Christophe Hitte, Marjo Hytönen, Vidhya Jagannathan, Tosso Leeb, Hannes Lohi, Cathryn Mellersh, Jim Mickelson, Leonardo Murgiano, Anita Oberbauer, Sheila Schmutz, Jeffrey Schoenebeck, Kim Summers, Frank van Steenbeck, Claire Wade) is thanked for providing access to whole-genome variants from control dogs and the Dog Genome Annotation (DoGA) Consortium (Hannes Lohi, Juha

Kere, Carsten Daub, Marjo Hytönen, César L. Araujo, Ileana B. Quintero, Kaisa Kyöstilä, Maria Kaukonen, Meharji Arumilli, Milla Salonen, Riika Sarviaho, Julia Niskanen, Sruthi Hundi, Jenni Puurunen, Sini Sulkama, Sini Karjalainen, Antti Sukura, Pernilla Syrjä, Niina Airas, Henna Pekkarinen, Ilona Kareinen, Anna Knuuttila, Heli Nordgren, Karoliina Hagner, Tarja Pääkkönen, Kaarel Krjutskov, Sini Ezer, Shintaro Katayama, Masahito Yoshihara, Auli Saarinen, Abdul Kadir Mukarram, Matthias Hörtenhuber, Amitha Raman, Irene Stevens) for the retinal STRT data. HL is a HiLIFE Fellow.

Author contributions

Conceived and designed the experiments: HL and MK. Performed the experiments: MK, AKM, IBQ, KW, MA, SJ. Analyzed the data: MK, AKM, IBQ, KK, MA, HL. Contributed to reagents/materials/analysis tools: MK, KW, SJ, KK, COD, JK, DoGA consortium, HL. Wrote the paper: MK and HL with the help from AKM, IBQ, MA and other co-authors. All authors have read and approved the manuscript.

References

1. Narayan DS, Wood JP, Chidlow G, Casson RJ. A review of the mechanisms of cone degeneration in retinitis pigmentosa. Acta Ophthalmol 2016;94(8):748-754.
2. Daiger S, Rossiter B, Greenberg J, Christoffels A, Hide W. Data services and software for identifying genes and mutations causing retinal degeneration. Invest Ophthalmol Vis Sci 1998;39:S295.
3. Daiger S, Sullivan L, Bowne S. Genes and mutations causing retinitis pigmentosa. Clin Genet 2013;84(2):132-141.
4. Bassuk AG, Zheng A, Li Y, Tsang SH, Mahajan VB. Precision Medicine: Genetic Repair of Retinitis Pigmentosa in Patient-Derived Stem Cells. Sci Rep 2016 Jan 27;6:19969.
5. Lindblad-Toh K, Wade CM, Mikkelsen TS, Karlsson EK, Jaffe DB, Kamal M, et al. Genome sequence, comparative analysis and haplotype structure of the domestic dog. Nature 2005;438(7069):803-819.
6. Lequarré A, Andersson L, André C, Fredholm M, Hitte C, Leeb T, et al. LUPA: a European initiative taking advantage of the canine genome architecture for unravelling complex disorders in both human and dogs. The Veterinary Journal 2011;189(2):155-159.
7. Groeneveld LF, Gregusson S, Guldbrandtsen B, Hiemstra SJ, Hveem K, Kantanen J, et al. Domesticated animal biobanking: land of opportunity. PLoS biology 2016;14(7):e1002523.
8. Vaquer G, Dannerstedt FR, Mavris M, Bignami F, Llinares-Garcia J, Westermark K, et al. Animal models for metabolic, neuromuscular and ophthalmological rare diseases. Nature Reviews Drug Discovery 2013;12(4):287-305.
9. Slijkerman RW, Song F, Astuti GD, Huynen MA, van Wijk E, Stieger K, et al. The pros and cons of vertebrate animal models for functional and therapeutic research on inherited retinal dystrophies. Prog Retin Eye Res 2015;48:137-159.
10. Parry HB. Degenerations of the dog retina. II. Generalized progressive atrophy of hereditary origin. Br J Ophthalmol 1953 Aug;37(8):487-502.
11. Zangerl B, Goldstein O, Philp AR, Lindauer SJ, Pearce-Kelling SE, Mullins RF, et al. Identical mutation in a novel retinal gene causes progressive rod–cone degeneration in dogs and retinitis pigmentosa in humans. Genomics 2006;88(5):551-563.
12. Petersen-Jones SM, Komáromy AM. Dog models for blinding inherited retinal dystrophies. Human Gene Therapy Clinical Development 2014;26(1):15-26.
13. Miyadera K, Acland GM, Aguirre GD. Genetic and phenotypic variations of inherited retinal diseases in dogs: the power of within-and across-breed studies. Mammalian Genome 2012;23(1-2):40-61.
14. Kijas JW, Cideciyan AV, Aleman TS, Pianta MJ, Pearce-Kelling SE, Miller BJ, et al. Naturally occurring rhodopsin mutation in the dog causes retinal dysfunction and degeneration mimicking human dominant retinitis pigmentosa. Proc Natl Acad Sci U S A 2002 Apr 30;99(9):6328-6333.
15. Acland GM, Blanton SH, Hershfield B, Aguirre GD. XLPRA: A canine retinal degeneration inherited as an X-linked trait. American Journal of Medical Genetics Part A 1994;52(1):27-33.
16. Zhang Q, Acland GM, Wu WX, Johnson JL, Pearce-Kelling S, Tulloch B, et al. Different RPGR exon ORF15 mutations in Canids provide insights into photoreceptor cell degeneration. Hum Mol Genet 2002;11(9):993-1003.

17. Vilboux T, Chaudieu G, Jeannin P, Delattre D, Hedan B, Bourgain C, et al. Progressive retinal atrophy in the Border Collie: A new XLPRA. BMC veterinary research 2008;4(1):10.
18. Kropatsch R, Akkad DA, Frank M, Rosenhagen C, Altmüller J, Nürnberg P, et al. A large deletion in RPGR causes XLPRA in Weimaraner dogs. Canine genetics and epidemiology 2016;3(1):7.
19. Progressive retinal atrophy in the miniature schnauzer. Proc. Am. Coll. Vet. Ophthalmol; 1985.
20. Zhang Q, Baldwin VJ, Acland GM, Parshall CJ, Haskel J, Aguirre GD, et al. Photoreceptor dysplasia (pd) in miniature schnauzer dogs: evaluation of candidate genes by molecular genetic analysis. J Hered 1999 Jan-Feb;90(1):57-61.
21. Jeong M, Han C, Narfstrom K, Awano T, Johnson G, Min M, et al. A phosducin (PDC) gene mutation does not cause progressive retinal atrophy in Korean miniature schnauzers. Animal Genetics 2008;39(4):455-456.
22. Jeong MB, Park SA, Kim SE, Park YW, Narfstroem K, Kangmoon S. Clinical and Electroretinographic Findings of Progressive Retinal Atrophy in Miniature Schnauzer Dogs of South Korea. Journal of Veterinary Medical Science 2013;75(10):1303-1308.
23. Murgiano L, Becker D, Torjman D, Niggel JK, Milano A, Cullen C, et al. Complex Structural PPT1 Variant Associated with Non-syndromic Canine Retinal Degeneration. G3 (Bethesda) 2018 Dec 12.
24. Livak KJ, Schmittgen TD. Analysis of relative gene expression data using real-time quantitative PCR and the 2−ΔΔCT method. Methods 2001;25(4):402-408.
25. Lizio M, Harshbarger J, Shimoji H, Severin J, Kasukawa T, Sahin S, et al. Gateways to the FANTOM5 promoter level mammalian expression atlas. Genome Biol 2015 Jan 5;16:22-014-0560-6.
26. Lek M, Karczewski KJ, Minikel EV, Samocha KE, Banks E, Fennell T, et al. Analysis of protein-coding genetic variation in 60,706 humans. Nature 2016;536(7616):285.
27. Thurman RE, Rynes E, Humbert R, Vierstra J, Maurano MT, Haugen E, et al. The accessible chromatin landscape of the human genome. Nature 2012;489(7414):75.
28. Forrest AR, Kawaji H, Rehli M, Baillie JK, De Hoon MJ, Haberle V, et al. A promoter-level mammalian expression atlas. Nature 2014;507(7493):462.
29. Uhlen M, Fagerberg L, Hallstrom BM, Lindskog C, Oksvold P, Mardinoglu A, et al. Proteomics. Tissue-based map of the human proteome. Science 2015 Jan 23;347(6220):1260419.
30. Van Schil K, Karlstetter M, Aslanidis A, Dannhausen K, Azam M, Qamar R, et al. Autosomal recessive retinitis pigmentosa with homozygous rhodopsin mutation E150K and non-coding cis-regulatory variants in CRX-binding regions of SAMD7. Scientific reports 2016;6:21307.
31. Rattner A, Nathans J. The genomic response to retinal disease and injury: evidence for endothelin signaling from photoreceptors to glia. Journal of Neuroscience 2005;25(18):4540-4549.
32. Bridges PJ, Jo M, Al Alem L, Na G, Su W, Gong MC, et al. Production and binding of endothelin-2 (EDN2) in the rat ovary: endothelin receptor subtype A (EDNRA)-mediated contraction. Reprod Fertil Dev 2010;22(5):780-787.
33. Choi D, Kim EK, Kim K, Lee K, Kang D, Kim HY, et al. Expression pattern of endothelin system components and localization of smooth muscle cells in the human pre-ovulatory follicle. Human reproduction 2011;26(5):1171-1180.
34. Howell GR, Macalinao DG, Sousa GL, Walden M, Soto I, Kneeland SC, et al. Molecular clustering identifies complement and endothelin induction as early events in a mouse model of glaucoma. J Clin Invest 2011 Apr;121(4):1429-1444.
35. Bramall AN, Szego MJ, Pacione LR, Chang I, Diez E, D'Orleans-Juste P, et al. Endothelin-2-mediated protection of mutant photoreceptors in inherited photoreceptor degeneration. PLoS One 2013;8(2):e58023.
36. Rattner A, Yu H, Williams J, Smallwood PM, Nathans J. Endothelin-2 signaling in the neural retina promotes the endothelial tip cell state and inhibits angiogenesis. Proc Natl Acad Sci U S A 2013 Oct 1;110(40):E3830-9.
37. Samardzija M, Wariwoda H, Imsand C, Huber P, Heynen SR, Gubler A, et al. Activation of survival pathways in the degenerating retina of rd10 mice. Exp Eye Res 2012;99:17-26.
38. Baker S, Booth C, Fillman C, Shapiro M, Blair MP, Hyland JC, et al. A loss of function mutation in the COL9A2 gene causes autosomal recessive Stickler syndrome. American Journal of Medical Genetics Part A 2011;155(7):1668-1672.
39. Purcell S, Neale B, Todd-Brown K, Thomas L, Ferreira MA, Bender D, et al. PLINK: a tool set for whole-genome association and population-based linkage analyses. The American Journal of Human Genetics 2007;81(3):559-575.
40. Li H, Durbin R. Fast and accurate short read alignment with Burrows-Wheeler transform. Bioinformatics 2009 Jul 15;25(14):1754-1760.

41. McKenna A, Hanna M, Banks E, Sivachenko A, Cibulskis K, Kernytsky A, et al. The Genome Analysis Toolkit: a MapReduce framework for analyzing next-generation DNA sequencing data. Genome Res 2010 Sep;20(9):1297-1303.
42. Gardner EJ, Lam VK, Harris DN, Chuang NT, Scott EC, Pittard WS, et al. The Mobile Element Locator Tool (MELT): population-scale mobile element discovery and biology. Genome Res 2017 Nov;27(11):1916-1929.
43. Jurka J, Kapitonov VV, Pavlicek A, Klonowski P, Kohany O, Walichiewicz J. Repbase Update, a database of eukaryotic repetitive elements. Cytogenet Genome Res 2005;110(1-4):462-467.
44. Layer RM, Kindlon N, Karczewski KJ, Quinlan AR, Exome Aggregation Consortium. Efficient genotype compression and analysis of large genetic-variation data sets. Nature methods 2015;13(1):63.
45. Koressaar T, Remm M. Enhancements and modifications of primer design program Primer3. Bioinformatics 2007 May 15;23(10):1289-1291.
46. Khan A, Fornes O, Stigliani A, Gheorghe M, Castro-Mondragon JA, van der Lee R, et al. JASPAR 2018: update of the open-access database of transcription factor binding profiles and its web framework. Nucleic Acids Res 2017;46(D1):D260-D266.
47. Tan G, Lenhard B. TFBSTools: an R/bioconductor package for transcription factor binding site analysis. Bioinformatics 2016;32(10):1555-1556.
48. Zerbino DR, Achuthan P, Akanni W, Amode MR, Barrell D, Bhai J, et al. Ensembl 2018. Nucleic Acids Res 2017;46(D1):D754-D761.
49. Islam S, Kjallquist U, Moliner A, Zajac P, Fan JB, Lonnerberg P, et al. Characterization of the single-cell transcriptional landscape by highly multiplex RNA-seq. Genome Res 2011 Jul;21(7):1160-1167.
50. Islam S, Zeisel A, Joost S, La Manno G, Zajac P, Kasper M, et al. Quantitative single-cell RNA-seq with unique molecular identifiers. Nat Methods 2014 Feb;11(2):163-166.
51. Krjutskov K, Koel M, Roost AM, Katayama S, Einarsdottir E, Jouhilahti EM, et al. Globin mRNA reduction for whole-blood transcriptome sequencing. Sci Rep 2016 Aug 12;6:31584.
52. Pertea M, Kim D, Pertea GM, Leek JT, Salzberg SL. Transcript-level expression analysis of RNA-seq experiments with HISAT, StringTie and Ballgown. Nat Protoc 2016 Sep;11(9):1650-1667.
53. Love MI, Huber W, Anders S. Moderated estimation of fold change and dispersion for RNA-seq data with DESeq2. Genome Biol 2014;15(12):550-014-0550-8.
54. Gu Z, Eils R, Schlesner M. Complex heatmaps reveal patterns and correlations in multidimensional genomic data. Bioinformatics 2016 Sep 15;32(18):2847-2849.

Supporting information captions

S1 Fig. Initial mapping approach for PRA locus in MSs. (A) Genome-wide comparison of allele frequencies in all cases regardless of the disease type (n=16) and controls (n=33) suggested a locus on the CFA15 (p_{raw}=4.70x10^{-6}, p_{genome}=0.19). **(B)** A shared homozygous haplotype block was seen in all the type 1 cases and absent in all the type 2 cases and in 32/33 controls, indicating the two clinically distinct types are indeed genetically different. Interestingly, the risk haplotype was also present in one of the confirmed controls, indicating either incomplete penetrance of the risk haplotype, or that the causative variant is recent and not all the risk haplotype carrying dogs have it. Each row represents a single animal while genotypes at each SNP (columns) are marked with dark (reference), intermediate (heterozygotes) or light grey (affected haplotype). The critical region of 7.2 Mb spans from 213,416 bp to 7,403,217 bp and upper and lower limits of it were determined by appearance of heterozygous SNPs in the case dogs.

S2 Fig. Heat map from the canine retinal STRT sequencing experiment. Retinal samples from five dogs wild-type for the type 1 PRA associated variant and without the studied phenotype were STRT sequenced to examine retinal gene expression of the 60 target genes for HAND1::TCF3 TFBS. Columns indicate individual samples (SE = Swedish Elkhound, RW = Rottweiler, FL = Finnish Lapphund, BC = Border Collie), rows each target gene. Darker green color indicates stronger expression in the retina (TPM = transcripts per million). The six genes prioritized by several factors for RT-qPCR were all expressed in the canine retina (ENSCAFG00000002576, HIVEP3; ENSCAFG00000002827, NFYC; ENSCAFG00000035604, lincRNA; ENSCAFG00000002579, EDN2;

ENSCAFG00000002997, COL9A2; ENSCAFG00000002814, KCNQ4).

S1 Table. Filtering the whole-genome sequencing data: controls. Control dogs used for filtering the whole-genome sequencing data (numbers per breed).

S2 Table. Filtering the whole-genome sequencing data: results. Filtering the whole-genome data from two type 1 PRA cases against 268 controls resulted in 233 variants.

S3 Table. Dual Luciferase reporter assay. The construct sequences used for MDCK cell transfections.

S4 Table. Motif search results. Motif search found 714 predicted HAND1::TCF3 binding sites (Sheet1) in the promoter regions (+/- 500 bp TSS) of 60 genes (Sheet2) flanking the variant site.

S5 Table. Primer sequences. Primer sequences for Sanger sequencing, RT-qPCR and Taqman assay.

Data availability statement

Whole-genome sequences and STRT data can be found in the NCBI Short Read Archive (SRA study accession PRJNA491400 for WGS and [pending] for STRT).

Funding

This study was partly supported by grants from the Jane and Aatos Erkko Foundation (http://jaes.fi), the Academy of Finland (http://www.aka.fi), HiLife (http://www.helsinki.fi/en/helsinki-institute-of-life-science) and Wisdom Health (http://www.wisdompanel.com) to HL, American Kennel Club Canine Health Foundation (02340) (http://www.akcchf.org) to HL and MK, Mary and Georg C. Ehnrooth Foundation (http://www.marygeorg.fi/saatio.html), Evald and Hilda Nissi Foundation (http://www.nissinsaatio.fi), Orion Research Foundation (http://www.orion.fi/en/rd/orion-research-foundation/) and Canine Health Research Fund (http://www.helsinki.fi/en/support-us/funds-and-campaigns-you-can-support/canine-health-research-fund) to MK. The funders had no role in study design, data collection and analysis, decision to publish, or preparation of the manuscript.

Competing interests

We have read the journal's policy and the authors of this manuscript have the following competing interests: HL is a paid consultant to Genoscoper Laboratories Ltd, which will provide a genetic test for the type 1 PRA in MSs.